Turbo Machine

Instruction Manual

- Achyut Paudel
IOE, Thapathali Campus

Preface

This instruction manual on Turbo Machine (IV/I) has been compiled as per the syllabus issued by the Institute of Engineering, Nepal. The course in Turbo Machine is more focused in the use of turbomachinery in aircraft propulsion rather than hydraulic machines, compressors or fans. The basic components of a typical Gas Turbine engine and jet engines is the main essence of this manual. Hence, this course is more of an introductory course in aircraft propulsion.

This manual mainly focuses in developing the conceptual theory and also consists of mathematical relations and very few solved out numerical. Various sources (books, journals, articles, online pages) have been consulted during the building of this manual. Following are the list of books from where the excerpts and figures have been derived.
"Aircraft Propulsion" – Saeed Farokhi , John Wiley and Sons
"The Jet Engines" – Rolls Royce
"Fluid Mechanics and Fundamentals of Turbomachinery" – S.L. Dixon, C.A. Hall
Still there might be many typos and irregularities that may pose difficulties to students while going through this manual. I duly apologize for these incongruities. Any suggestions regarding the improvement of this manual shall be highly appreciated.

Achyut Paudel
Department of Automobile and Mechanical Engineering
Institute of Engineering, Thapathali Campus

Table of Contents

1. Chapter One- Introduction……...……3
2. Chapter Two- Velocity Vector Diagram……..……..11
3. Chapter Three- Gas Turbine Engine……..……19
4. Chapter Four- Gas Turbine Nozzles……..91
5. Chapter Five- Jet Propulsion……115
6. Chapter Six- Variation of Basic Aircraft Cycles…….……132

Chapter One

Introduction to Turbo-machinery

Definition:

The rotary type of machines where energy transfer is brought about by dynamic action, without an impervious boundary that prevents the free flow of a fluid at any time. Such devices are called *turbomachines*.

In a broad definition "*A turbomachine is a device in which energy transfer occurs between a flowing fluid and a rotating element due to dynamic action resulting in a change in pressure and momentum of the fluid*. Mechanical energy transfer occurs into or out of the turbomachine, usually in steady flow. Turbomachines include all those types that produce large-scale power such as turbines and those that produce a *head* or pressure, such as centrifugal pumps and compressors.

The principal components of a turbomachine are: (*i*) A *rotating element carrying vanes* operating in a stream of fluid, (*ii*) A *stationary element* or elements which generally act as guide vanes or passages for the proper control of flow direction and the energy conversion process, (*iii*) an *input* and/or an *output* shaft, and (*iv*) a *housing* as shown in figure.

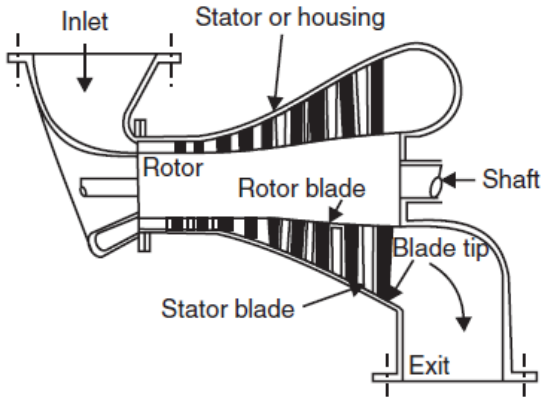

Fig. 1.1. Schematic cross-sectional view of a turbine showing the principal parts of the turbomachine.

If the turbo machine is *power-absorbing*, the enthalpy of the fluid flowing through it increases due to mechanical energy input at the shaft. If the turbomachine is *power-generating*, mechanical energy output is obtained at the shaft due to a decrease in enthalpy of the flowing fluid.

Examples of power-absorbing turbo machines are mixed-flow, axial-flow and centrifugal pumps, fans, blowers and exhausters, centrifugal and axial compressors, etc. Examples of power generating devices are steam, gas and hydraulic turbines. The best known examples of power transmitting turbomachines are fluid-couplings and torque-converters for power transmission used in automobiles, trucks and other industrial applications.

Turbomachines are also categorized by the direction of fluid flow. The flow directions are: (i) axial, (ii) radial and (iii) mixed. In the axial-flow and radial-flow turbomachines, the major flow directions are approximately axial and radial respectively, while in the mixed-flow machine, the flow usually enters the rotor axially and leaves radially or vice versa. Mixed flow may also

involve flow over the surface of a cone. An example of a mixed flow machine is a mixed-flow pump. A radial flow machine may also be classified into *radial inward flow(centripetal) or radial outward flow(centrifugal) types* depending on whether the flow is directed towards or away from the shaft axis.

Basic Thermodynamics in Turbomachinery

In dealing with turbomachines, one is concerned with fluids, often compressible and moving at high speeds exceeding the speed of sound. Even in turbomachines dealing with incompressible fluids where the velocities are relatively low, the kinetic and potential energies of the fluid are often large and constitute major fractions of the total energy available for conversion into work. It is advisable to include two different properties of fluids at two different states, static and total.

Static Properties:

This property refers to the fluid properties taken in an assumption to a static fluid. Suppose the static pressure of a moving fluid refers to the pressure is the fluid is assumed to have been at rest or the relative velocity of the measuring instrument and the fluid is zero. For example, one can consider a
pressure measurement made with a static pressure gauge which is usually fixed to the side of the duct. In this case, the fluid particle and the instrument are *at rest with respect to each other at the point where the measurement is being made*. Hence, the measured pressure is a static pressure. Any measurement made in consonance with this stipulation determines a static property, be it one of pressure, temperature, volume, or any other, as specified. The state of the particle fixed by a set of static properties is called the '*Static State'*.

Stagnation or Total Properties:

The *stagnation state is defined as the terminal state of a fictitious, isentropic, work-free and steady-flow process during which the macroscopic kinetic and potential energies of the fluid particle are reduced to zero*, the initial state for the process being the static state. It means that the flowing fluid has some enthalpy, kinetic and potential energy in it. If the moving fluid is brought to rest isentropically without any loss, the value of the kinetic energy and the potential energy then adds up to the enthalpy of the fluid which is then termed as stagnation enthalpy. By using the definition of a stagnation state, it is possible to obtain expressions for stagnation properties in terms of static properties. Considering any steady-flow process, the First Law of Thermodynamics gives the equation

$$q - w = \Delta h + \Delta ke + \Delta pe, \qquad \ldots(1.1)$$

where, q and w are respectively the energy transfers as heat and work per unit mass flow, h is the static enthalpy and ke and pe are respectively the macroscopic kinetic and potential energies per unit mass. It is known that $ke = V^2/2$, and $pe = gz$, V, being the fluid particle velocity and z, the height of the particle above the datum at the point under consideration.

Since the static state is the initial state in a fictitious isentropic, work-free, steady flow process and the stagnation state is the terminal state where both the kinetic and potential energies are zero, the difference in enthalpies between the stagnation and static states is obtained by setting $q = w = 0$, $\Delta h = ho - hi$, $ke_o = 0$ and $pe_o = 0$ in Eq. (1.1). There is then obtained:

$$h_o - (h_i + ke_i + pe_i) = 0 \text{ or, } h_o = (h + ke + pe), \qquad \ldots(1.2)$$

where the subscript o represents the stagnation state and i represents the initial static state. Equation (1.2) follows from the fact that at the stagnation state, both the kinetic and the potential energies are zero. In the last part of Eq. (1.2), the subscript, i, has been removed and from here onwards, the properties at the static state will be indicated without the subscript as shown. The enthalpy ho in the stagnation state has thus been expressed in terms of three known properties, h, ke and pe of the static state. As stated earlier, it is necessary that the process changing the state from static to stagnation be isentropic, i.e., $s_o = s$, and hence, the entropy in the stagnation state is equal to the entropy in the static state. Thus, two independent stagnation properties, namely the enthalpy ho and the entropy so, have been determined in terms of the known properties at the static state. According to the 'State Postulate', the knowledge of any two independent properties at a specified state is sufficient to fix the state of a simple compressible substance, the stagnation state is totally determined and it should be possible to determine any other required property of the stagnation state in terms of the two known properties, h_o and s_o. Also, according to the Second Law of Thermodynamics, since $T.ds = dh - v.dp$, and the entropy remains constant in the change from static to stagnation state, $ds = 0$ and $dh = v.dp$, $v = 1/\rho$, being the specific volume and ρ, the density. Hence, integration yields for the change from static to stagnation state:

$$h_o - h = \int dh = \int v \cdot dp. \qquad \ldots(1.3)$$

The integration on the right hand side depends on the variation of volume with respect to pressure in an isentropic process. If the p-v property relation is known, the equation above may be integrated and one can determine the stagnation pressure p_o in terms of the static enthalpy h and the static pressure p.

FIRST AND SECOND LAWS OF THERMODYNAMICS APPLIED TO TURBOMACHINES

Assuming there is a single inlet and a single outlet for the turbomachine across the sections of which the velocities, pressures, temperatures and other relevant properties are uniform, one writes the steady flow equation of the First Law of thermodynamics in the form:

$$Q + \dot{m}\,(h_1 + V_1^2/2 + gz_1) = P + \dot{m}\,(h_2 + V_2^2/2 + gz_2). \qquad \ldots(1.10)$$

Here, Q = Rate of energy transfer as heat across the boundary of the control volume,
P = Power output due to the turbomachine, and
m = Mass flow rate.
Since $ho = h + V^2/2 + gz$, (Eq. 1.3), one obtains:
$q - w = \Delta ho$,
where, $\Delta ho = ho2 - ho1$, represents the *change in stagnation enthalpy between the inlet and the outlet of the turbomachine*. Also, $q = Q/m$ and, $w = P/m$ represent respectively, the heat and mass transfer per unit mass flow through the control volume.
Generally, all turbomachines are well-insulated devices. By neglecting q therefore, one can treat a turbomachine like a perfectly insulated device for which:

$$\Delta h_o = -w = -P/\dot{m} \quad \text{or,} \quad dh_o = -\delta w, \qquad \ldots(1.11b)$$

The energy transfer as work is therefore numerically equal to the change in stagnation enthalpy of the fluid between the inlet and the outlet of the turbomachine. In a power-generating turbomachine, w is positive as defined so that Δho is negative, i.e., the stagnation enthalpy at the exit of the machine is less than that at the inlet. The machine puts out work at the shaft. In a power-absorbing turbomachine, Δho is positive. The stagnation enthalpy at the outlet will be greater than that at the inlet and work is done on the flowing fluid due to the rotation of the shaft. As already shown in the example preceding Eq. (1.7), in turbomachines handling compressible fluids, changes in static head cause negligible changes in total enthalpy. For these machines therefore, it is sufficiently accurate to write

$$w = -\Delta h_o = -\Delta(h + V^2/2). \qquad \ldots(1.11c)$$

For a non- power generating or non- power absorbing machines like stator in turbo machines, nozzles etc , $h_{o1} = h_{o2}$. Where suffix 1 and 2 are for inlet and outlet. Depending upon whether the machine is power-generating or power-absorbing. Hence, $h_{o1} > h_{02}$ if the machines develops power and if $ho1 < ho2$, the machine needs a driver and absorbs power. If the system is perfectly reversible and adiabatic with no energy transfer as work, no changes can occur in the stagnation properties (enthalpy, pressure and temperature) between the inlet and the outlet of the machine. All turbo machines exchange work with the fluid and also suffer from frictional as well as other losses. The effect of the losses in a power-generating machine is to reduce the stagnation pressure and to increase entropy so that the net work output is less than that in an ideal process. The corresponding work input is higher in a power-absorbing machine as compared with that in an ideal process. In order to understand how this happens, consider the Second Law equation of state, $T_o ds_o = dh_o - v_o dp_o$. (This is the form of the equation $Tds = dh - vdp$, when applied to stagnation properties.) Also, $dho = -\delta w$, as demonstrated earlier (Eq. 1.11b). Hence,

$$-\delta w = v_o dp_o + T_o ds_o. \qquad \ldots(1.11e)$$

In a power-generating machine, dpo is negative since the flowing fluid undergoes a pressure drop when mechanical energy output is obtained. However, the Clausius inequality requires that $T_o ds_o \geq \delta q$, and as $\delta q \approx 0$, in a turbomachine $T_o ds_o \geq 0$. The sign of equality applies only to a reversible process which has a work output $\Delta w = -v_o dp_o > 0$. In a real machine, $T_o ds_o > 0$, so that $\Delta wi - \Delta w = T_o ds_o > 0$ and represents the decrease in work output due to the irreversibilities in the machine. The reversible power-generating machine therefore exhibits the highest mechanical output of all the machines undergoing a given stagnation pressure change. A similar argument may be used to prove that if the device absorbs power, the work input needed to obtain a specified stagnation pressure rise is a minimum when the device is reversible. In this case, $\Delta wi - \Delta w = T_o ds_o > 0$, so that both the ideal work Δwi and the actual work Δw are negative, the actual work being larger than the ideal work in magnitude.

EFFICIENCY OF TURBOMACHINES

It has been seen above that the performance of a real machine is inferior to that of a frictionless and loss-free ideal machine. A measure of its performance is the *efficiency*, defined differently for power-generating and power-absorbing machines as given by the following equations:

$$\eta_{pg} = \frac{\text{Actual Shaft Work Output}}{\text{Ideal Work Output}} = \frac{w_s}{w_i}, \qquad \ldots(1.12)$$

and,

$$\eta_{pa} = \frac{\text{Ideal Work Input}}{\text{Actual Shaft Work Input}} = \frac{w_i}{w_s}. \qquad \ldots(1.13)$$

In the expressions above, *ws* represents the shaft power output for the power-generating machine and the shaft-power input for the power-absorbing machine. For a loss-free system, the term *wi*, represents the ideal output if the machine generates power and the ideal power input if it absorbs power. The ideal work is calculated on the basis of isentropic processes throughout the system.
Generally speaking, losses occur in turbomachines due to: (*a*) bearing friction, windage, etc. all of which may be classified as *mechanical* losses, (*b*) unsteady flow, friction between the blade and the fluid, etc., which are internal to the system and may be classified as *fluid-rotor losses.* (There are other losses like leakage across blades, labyrinth leakage, etc. in addition to the above losses. These are covered under fluid-rotor losses.) If the mechanical and fluid-rotor losses are separated, the efficiencies written earlier may be rewritten in the following forms:

$$\eta_{pg} = \frac{\text{Fluid-Rotor Work}}{\text{Ideal Work Output}} \times \frac{\text{Shaft Work Output}}{\text{Fluid-Rotor Work}} = \frac{w_r}{w_i} \times \frac{w_s}{w_r}, \qquad \ldots(1.14)$$

and similarly,

$$\eta_{pa} = \frac{\text{Ideal Work Input}}{\text{Rotor-Fluid Work}} \times \frac{\text{Rotor-Fluid Work}}{\text{Shaft-Work Input}} = \frac{w_i}{w_r} \times \frac{w_r}{w_s}. \qquad \ldots(1.15)$$

In Eq. (1.14), *wr* is the energy transfer between the fluid and the rotor and would be the output at the shaft, if there were no mechanical losses due to windage, friction at the bearings etc. The quantity w_r/w_i, is called the *adiabatic*, *isentropic* or *hydraulic* efficiency of the power generating system, since *wi*, is always calculated on the basis of a loss-free isentropic flow.
Hence, *adiabatic efficiency for a power-generating machine* may be rewritten as:

$$\eta_a = \frac{\text{Mechanical Energy Supplied by the Rotor}}{\text{Hydrodynamic Energy Available from the Fluid}}. \qquad \ldots(1.16a)$$

Similarly, for a power-absorbing machine, (Eq. (1.15) with adiabatic efficiency = w_i/w_r, it is seen that:

$$\eta_a = \frac{\text{Hydrodynamic Energy Supplied to the Fluid}}{\text{Mechanical Energy Supplied to the Rotor}}. \qquad \ldots(1.16b)$$

The difference between w_s and w_r is expressed in terms of mechanical efficiency, defined by the equations:

$$\eta_m = \frac{w_s}{w_r} = \frac{\text{Shaft Work Output}}{\text{Fluid-Rotor Work}} \text{ (from Eq. (1.14), } pg \text{ machine).} \qquad \ldots(1.17a)$$

$$\eta_m = \frac{w_s}{w_r} = \frac{\text{Rotor-Fluid Work}}{\text{Actual Work Input to Shaft}} \text{ (from Eq. (1.15), } pa \text{ machine).} \qquad \ldots(1.17b)$$

Then, $\eta_{pg} = \eta_a . \eta_m$ (pg and pa machines, both) ...(1.18)

Usually, mechanical losses in large turbomachines do not exceed 1%. In very large machines dealing with hundreds of megawatts of power, (the kind used in large power stations), these losses may be smaller than 0.5%.

In order to determine the adiabatic efficiency of a turbomachine during a test, it is necessary to specify the ideal work input or output by using the fluid states at the inlet and the outlet respectively. The ideal work based upon static states only or stagnation states only to specify the properties at the inlet and exit will not differ much if the inlet and exit fluid kinetic energies are not large. In modern turbines however, the fluid at the inlet and the exit can be at high velocities and efficiencies based on stagnation properties may be of greater value in judging the performance of these devices. Referring to the *h–s* diagrams Fig. 1.5(a) for power-generating and Fig. 1.5(b) for power absorbing turbomachines, the fluid has initially the static pressure and temperature determined by state 1, with state o1, as the corresponding stagnation state. After passing through the turbomachine, the final static properties of the fluid are determined by state 2, with o2 as the corresponding stagnation state. If the process were reversible, the final fluid static state would be 2', and the stagnation state would be o2'. The dashed-lines 1–2 in static coordinates and *o*1–*o*2 in stagnation coordinates represent the real process in each of the two figures.

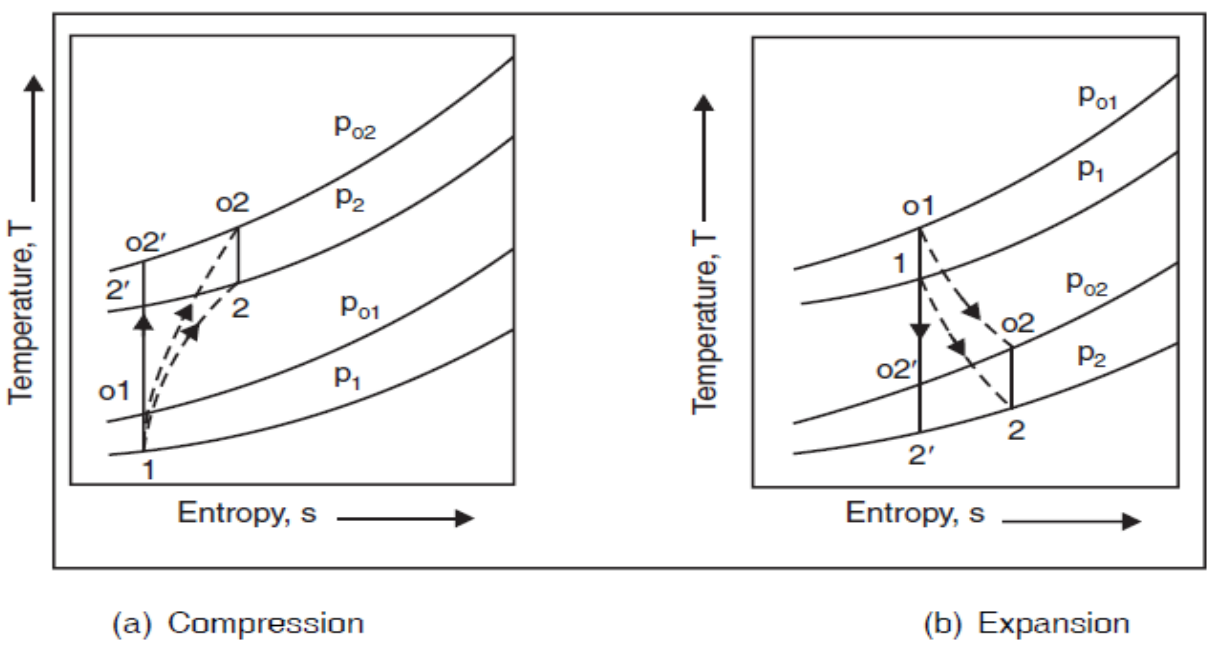

Fig. 1.5. Isentropic and irreversible processes for a perfect gas.

The actual work input or output *w*, is the quantity h_{o1}–h_{o2} whereas the ideal work *wi*, can be calculated by any one of the following four equations:

$$(i)\quad w_{t-t} = h'_{o2} - h_{o1}, \text{ (initial and final states both total)}, \qquad \ldots(1.20)$$

$$(ii)\quad w_{t-s} = h'_{2} - h_{o1}, \text{ (initial state total, final state static)}, \qquad \ldots(1.21)$$

$$(iii)\quad w_{s-t} = h'_{o2} - h_{1}, \text{ (initial state static, final state total)}, \qquad \ldots(1.22)$$

$$(iv)\quad w_{s-s} = h'_{2} - h_{1}. \text{ (initial and final states static)}. \qquad \ldots(1.23)$$

The proper equation for use is to be decided by the conditions of the turbomachine in question. For example, in a turbine, if the kinetic energy of the fluid can be used for the production of mechanical energy somewhere else and the kinetic energy at the inlet *is negligible, one can use the static-to-total definition*, (Eqs. 1.22, 1.24c), *or* the *total-to-total definition* (Eqs. 1.20, 1.24a). The results obtained from both the definitions will be nearly the same and will take account of all the useful energy for the evaluation of efficiency. However, *if the exit kinetic energy is wasted, the appropriate measure will be static-to-static* (Eq. 1.23, 1.24d), to increase the measure of ideal work and show the losses to the system

Based on the calculations of mechanical work presented above, the following efficiencies for power-generating machines may be defined:

$$(i)\quad \eta_{t-t} = (h_{o1} - h_{o2})/(h_{o1} - h_{o2}'). \qquad \ldots(1.24a)$$

$$(ii)\quad \eta_{t-s} = (h_{o1} - h_{o2})/(h_{o1} - h_{2}'). \qquad \ldots(1.24b)$$

$$(iii)\quad \eta_{s-t} = (h_{o1} - h_{o2})/(h_{1} - h_{o2}'). \qquad \ldots(1.24c)$$

$$(iv)\quad \eta_{s-s} = (h_{o1} - h_{o2})/(h_{1} - h_{2}'). \qquad \ldots(1.24d)$$

All the above definitions are applicable to power-generating machines, since the actual work is in the numerator and the denominator contains the ideal work, based on the conditions of the system for which efficiency is being defined.

For power-absorbing machines, the applicable definitions of efficiency are the following:

$$(i)\quad \eta_{t-t} = (h_{o2}' - h_{o1})/(h_{o2} - h_{o1}). \qquad \ldots(1.25a)$$

$$(ii)\quad \eta_{t-s} = (h_{2}' - h_{o1})/(h_{o2} - h_{o1}). \qquad \ldots(1.25b)$$

$$(iii)\quad \eta_{s-t} = (h_{o2}' - h_{1})/(h_{o2} - h_{o1}). \qquad \ldots(1.25c)$$

$$(iv)\quad \eta_{s-s} = (h_{2}' - h_{1})/(h_{o2} - h_{o1}). \qquad \ldots(1.25d)$$

Worked out Example

Air flows through an air turbine where its stagnation pressure is decreased in the ratio 5:1. The total-to-total efficiency is 0.8 and the air flow rate is 5 kg.s–1. If the total power output is 400 kW, find: (*a*) the inlet total temperature, (*b*) the actual exit total temperature, (*c*) the actual exit static temperature if the exit flow velocity is 100 m.s–1 and (*d*) the total-to static efficiency η*t–s* of the device.

Solution: (a) Work output/unit mass flow of air, (c_p = 1.004 kJ·kg^{-1}K^{-1}).

$$w = -\Delta h_o = -c_p(T_{o2} - T_{o1}) = P/\dot{m} = 400/5 = 80 \text{ kJ·kg}^{-1}$$

Thus, $T_{o2} - T_{o1} = -80.0/1.004 = -79.7$ K.

However, since the stagnation pressure ratio is 5 and the total-to-total efficiency is 0.8,

$$T'_{o2}/T_{o1} = (p_{o2}/p_{o1})^{(\gamma-1)/\gamma} = (0.2)^{(0.4/1.4)} = 0.631.$$

$$T_{o1} - T_{o2} = \eta_{t\text{-}t}(T_{o1} - T'_{o2}) = 0.8(1.0 - 0.631)T_{o1} = 79.7.$$

$$\boldsymbol{T_{o1}} = \mathbf{270\ K.}$$

(b) $\boldsymbol{T_{o2}} = T_{o1} - 79.7 = 270 - 79.7 = 190.3$ K.

(c) For the static temperature, we have: $T = T_o - V^2/(2c_p)$, so that:

$$\boldsymbol{T_2} = T_{o2} - V_2^2/(2c_p) = 190.3 - 100^2/[(2)(1004)] = \mathbf{185.3\ K.}$$

(d) From parts (*a*) and (*b*) above,

$$T_{o2}' = 0.631T_{o1} = (0.631)(270) = 170.4 \text{ K.}$$

Hence, $T_2' = T_{o2}' - V_2^2/(2c_p) = 170.4 - 100^2/[(2)(1004)] = 165.4$ K

$$\boldsymbol{\eta_{t\text{-}s}} = (T_{o1} - T_{o2})/(T_{o1} - T_2') = (270 - 190.4)/(270 - 165.4) = \mathbf{0.76}.$$

Chapter Two
Velocity Vector Diagram

Introduction

This chapter will be concerned with the velocity vector diagrams and stage efficiency of axial flow axial flow turbines that are used in a gas turbine engine. A general Euler's turbomachinery equation shall be derived and used to solve related problems.

The Euler's work equation

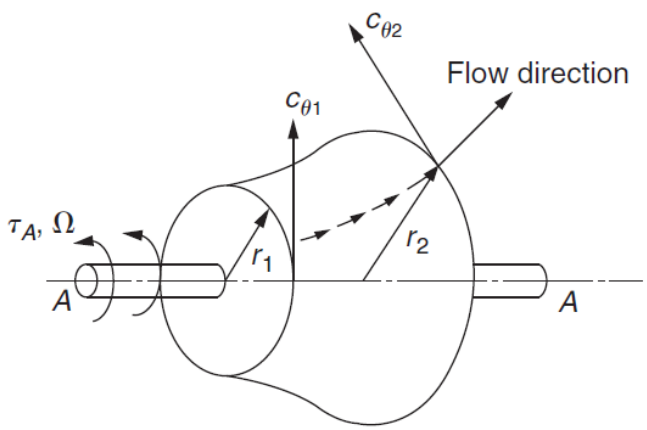

For a system of mass m, the vector sum of the moments of all external forces acting on the system about some arbitrary axis A–A fixed in space is equal to the time rate of change of angular momentum of the system about that axis, i.e.,

$$\tau_A = m\frac{\mathrm{d}}{\mathrm{d}t}(rc_\theta), \qquad (1.17a)$$

where r is distance of the mass centre from the axis of rotation measured along the normal to the axis and c_θ the velocity component mutually perpendicular to both the axis and radius vector r. For a control volume the law of moment of momentum can be obtained. Figure above shows the control volume enclosing the rotor of a generalised turbomachine. Swirling fluid enters the control volume at radius r1 with tangential velocity $c_{\theta 1}$ and leaves at radius r_2 with tangential velocity $c_{\theta 2}$. For onedimensional steady flow,

$$\tau_A = \dot{m}(r_2 c_{\theta 2} - r_1 c_{\theta 1}), \qquad (1.17b)$$

which states that the sum of the moments of the external forces acting on fluid temporarily occupying the control volume is equal to the net time rate of efflux of angular momentum from the control volume. For a pump or compressor rotor running at angular velocity Ω, the rate at which the rotor does work on the fluid is

$$\tau_A \Omega = \dot{m}(U_2 c_{\theta 2} - U_1 c_{\theta 1}), \qquad (1.18a)$$

where the blade speed U = Ω r.
Thus, the work done on the fluid per unit mass or specific work is

$$\Delta W_c = \frac{\dot{W}_c}{\dot{m}} = \frac{\tau_A \Omega}{\dot{m}} = U_2 c_{\theta 2} - U_1 c_{\theta 1} > 0. \qquad (1.18b)$$

This equation is referred to as ***Euler's pump equation.***

For a turbine the fluid does work on the rotor and the sign for work is then reversed. Thus, the specific work is

$$\Delta W_t = \frac{\dot{W}_t}{\dot{m}} = U_1 c_{\theta 1} - U_2 c_{\theta 2} > 0. \qquad (1.18c)$$

Equation (1.18c) is referred to as ***Euler's turbine equation.***
Note that, for any adiabatic turbomachine (turbine or compressor), applying the steady flow energy equation, eqn. (1.13), gives

$$\Delta W_x = (h_{01} - h_{02}) = U_1 c_{\theta 1} - U_2 c_{\theta 2}. \qquad (1.19a)$$

Alternatively, this can be written as

$$\Delta h_0 = \Delta(U c_\theta). \qquad (1.19b)$$

Equations (1.19a) and (1.19b) are the general forms of the Euler work equation. By considering the assumptions used in its derivation, this equation can be seen to be valid for adiabatic flow for any streamline through the blade rows of a turbomachine. It is applicable to both viscous and inviscid flow, since the torque provided by the fluid on the blades can be exerted by pressure forces or frictional forces. It is strictly valid only for steady flow but it can also be applied to time-averaged unsteady flow provided the averaging is done over a long enough time period. In all cases, all of the torque from the fluid must be transferred to the blades. Friction on the hub and casing of a turbomachine can cause local changes in angular momentum that are not accounted for in the Euler work equation. Note that for any stationary blade row, U = 0 and therefore h_0 = constant. This is to be expected since a stationary blade cannot transfer any work to or from the fluid.

Gas turbine blades and vector diagrams

A typical gas turbine blade is an airfoil shaped on its cross section. The blades are twisted from the hub to tip with an angle, by what we call stagger angle. Analysis and description about blades attachment, materials, and shapes are done in more detail in chapter three. Here we, focus mainly on the vector diagrams in turbine blades and the stage efficiency.

The axial turbine stage comprises a row of fixed guide vanes or nozzles (often called a stator row) and a row of moving blades or buckets (a rotor row). Fluid enters the stator with absolute velocity c_1 at angle α_1 and accelerates to an absolute velocity c_2 at angle α_2 (Figure 4.3). All angles are measured from the axial (x) direction. The sign convention is such that angles and velocities as drawn in Figure 4.3 will be taken as positive throughout this chapter. From the velocity diagram, the rotor inlet relative velocity w_2, at an angle β_2, is found by subtracting, vectorially, the blade speed U from the absolute velocity c_2. The relative flow within the rotor accelerates to velocity w_3 at an angle β_3 at rotor outlet; the corresponding absolute flow (c_3, α_3) is obtained by adding, vectorially, the blade speed U to the relative velocity w_3. When drawing the velocity triangles it is always worth sketching the nozzle and rotor rows beside them, as shown in Figure 4.3. This helps prevent errors, since the absolute velocities are roughly aligned with the

inlet and exit angles from the nozzle row and the relative velocities are aligned with the rotor row. Note that, within an axial turbine, the levels of turning are very high and the flow is turned through the axial direction in both the rotors and nozzles. The continuity equation for uniform, steady flow is

$$\rho_1 A_{x1} c_{x1} = \rho_2 A_{x2} c_{x2} = \rho_3 A_{x3} c_{x3}. \tag{4.1}$$

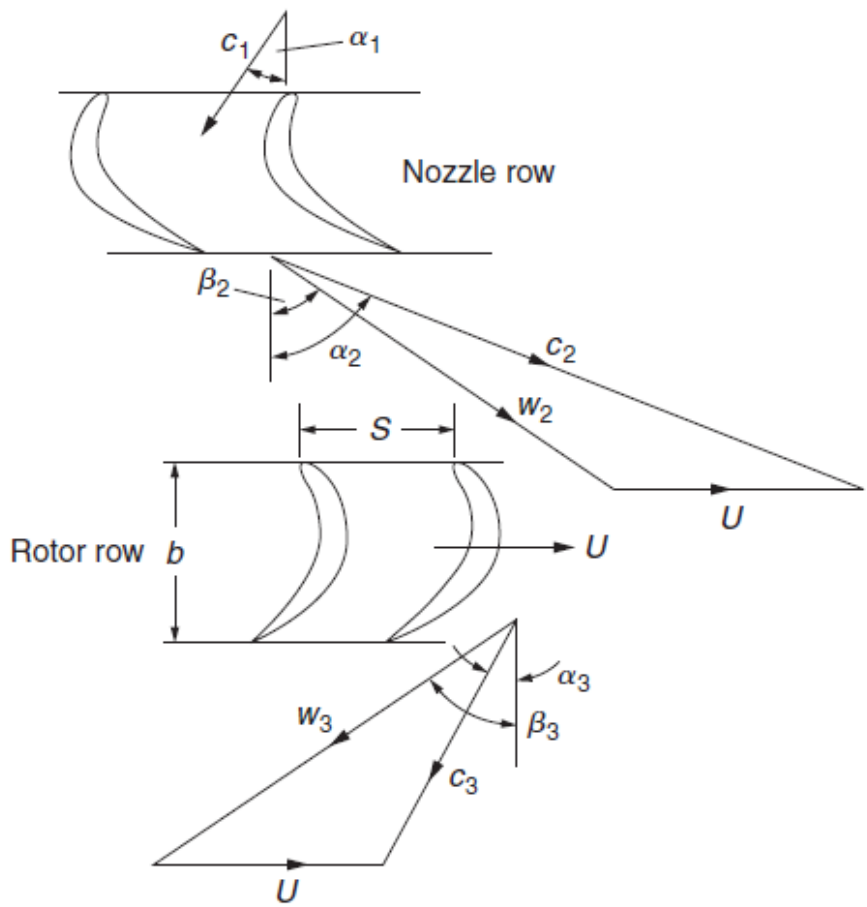

FIGURE 4.3

Turbine Stage Velocity Diagrams

Turbine Stage Design Parameters

Three key non-dimensional parameters are related to the shape of the turbine velocity triangles and are used in fixing the preliminary design of a turbine stage.

Design Flow Coefficient

It is defined as the ratio of the meridional flow velocity to the blade speed, $\Phi = c_m / U$, but in a purely axial flow machine, $\Phi = c_x / U$. The value of Φ for a stage determines the relative flow angles. A stage with a low value of Φ implies highly staggered blades and relative flow angles close to tangential. High values imply low stagger and flow angles closer to axial. For a fixed geometry and fixed rotational speed, the mass flow through the turbine increases with increasing Φ.

Stage Loading Coefficient

The stage loading is defined as the ratio of the stagnation enthalpy change through a stage to the square of the blade speed, $\psi=\Delta h_0 /U^2$. In an adiabatic turbine, the stagnation enthalpy change is equal to the specific work, ΔW, and for a purely axial turbine with constant radius, we can use the Euler work equation to write $\Delta h_0=U\ \Delta c\theta$. The stage loading can therefore be written as

$$\psi = \Delta c_\theta / U, \qquad (4.2)$$

where $\Delta c\theta$ represents the change in the tangential component of absolute velocity through the rotor. Thus, high stage loading implies large flow turning and leads to highly "skewed" velocity triangles to achieve this turning. Since the stage loading is a non-dimensional measure of the work extraction per stage, a high stage loading is desirable because it means fewer stages are needed to produce a required work output. However, as shown in later sections of this chapter, the stage loading is limited by the effects that high stage loadings have on efficiency.

Stage Reaction

The stage reaction is defined as the ratio of the static enthalpy drop in the rotor to the static enthalpy drop across the stage. Thus,

$$R = (h_2 - h_3)/(h_1 - h_3). \qquad (4.3a)$$

Taking the flow through a turbine as nearly isentropic the equation of the second law of thermodynamics, $Tds=dh - dp/\rho$ can be approximated by $dh=dp/\rho$, and ignoring compressibility effects, the reaction can thus be approximated as

$$R \approx (p_2 - p_3)/(p_1 - p_3). \qquad (4.3b)$$

The reaction therefore indicates the drop in pressure across the rotor compared to that for the stage. However, as a design parameter, the reaction is more significant since it describes the asymmetry of the velocity triangles and is therefore a statement of the blade geometries. As will be shown later, a 50% reaction turbine implies velocity triangles that are symmetrical, which leads to similar stator and rotor blade shapes. In contrast, a zero reaction turbine stage implies little pressure change through the rotor. This requires rotor blades that are highly cambered, that do not accelerate the relative flow greatly, and low cambered stator blades that produce highly accelerating flow.

Thermodynamics of the Axial Turbine Stage

The work done on the rotor by unit mass of fluid, the specific work, equals the stagnation enthalpy drop incurred by the fluid passing through the stage (assuming adiabatic flow). From the Euler work equation we can write

$$\Delta W = \dot{W}/\dot{m} = h_{01} - h_{03} = U(c_{\theta 2} + c_{\theta 3}). \qquad (4.4)$$

In eqn. (4.4) the absolute tangential velocity components ($c\theta$) are added, so as to adhere to the agreed sign convention of Figure 4.3. As no work is done in the nozzle row, the stagnation enthalpy across it remains constant and

$$h_{01} = h_{02}. \qquad (4.5)$$

In an axial turbine, the radial component of velocity is small. Writing $h0= h + ½(c^2x+c^2\theta)$ and using eqn. (4.5) in eqn. (4.4) we obtain

$$h_{02} - h_{03} = (h_2 - h_3) + \frac{1}{2}(c_{\theta 2}^2 - c_{\theta 3}^2) + \frac{1}{2}(c_{x2}^2 - c_{x3}^2) = U(c_{\theta 2} + c_{\theta 3}),$$

hence,

$$(h_2 - h_3) + \frac{1}{2}(c_{\theta 2} + c_{\theta 3})[(c_{\theta 2} - U) - (c_{\theta 3} + U)] + \frac{1}{2}(c_{x2}^2 - c_{x3}^2) = 0.$$

It is observed from the velocity triangles of Figure 4.3 that $c_{\theta 2} - U = w_{\theta 2}$, $c_{\theta 3} + U = w_{\theta 3}$ and $c_{\theta 2} + c_{\theta 3} = w_{\theta 2} + w_{\theta 3}$. Thus,

$$(h_2 - h_3) + \frac{1}{2}(w_{\theta 2}^2 - w_{\theta 3}^2) + \frac{1}{2}(c_{x2}^2 - c_{x3}^2) = 0.$$

This equation can be reduced to

$$h_2 + \frac{1}{2}w_2^2 = h_3 + \frac{1}{2}w_3^2 \text{ or } h_{02,\text{rel}} = h_{03,\text{rel}}. \qquad (4.6)$$

Thus, the relative stagnation enthalpy, $h_{0\text{rel}} = h + 1/2\ w^2$, remains unchanged through the rotor of a purely axial turbomachine. It is assumed that no radial shift of the streamlines occurs in this flow. In some modern axial turbines the mean flow may have a component of radial velocity, and in this case the more general form of the Euler work equation must be used to account for changes in the blade speed perceived by the flow, see eqn. (1.21a). It is then the *rothalpy* that is conserved through the rotor,

$$h_2 + \frac{1}{2}w_2^2 - \frac{1}{2}U_2^2 = h_3 + \frac{1}{2}w_3^2 - \frac{1}{2}U_3^2 \text{ or } I_2 = I_3 \qquad (4.7)$$

where U_2 and U_3 are the local blade speeds at inlet and outlet from the rotor, $U_2 = r_2\Omega$ and $U_3 = r_3\Omega$. Within the rest of this chapter, the analysis presented is directed at purely axial turbines that have a constant mean flow radius and therefore a single blade speed.

A Mollier diagram showing the change of state through a complete turbine stage, including the effects of irreversibility, is given in Figure 4.4. Through the nozzles, the state point moves from 1 to 2 and the static pressure decreases from p_1 to p_2. In the rotor row, the absolute static pressure reduces (in general) from p_2 to p_3. It is important to note that all the conditions contained in eqns. (4.4) – (4.6) are satisfied in the figure.

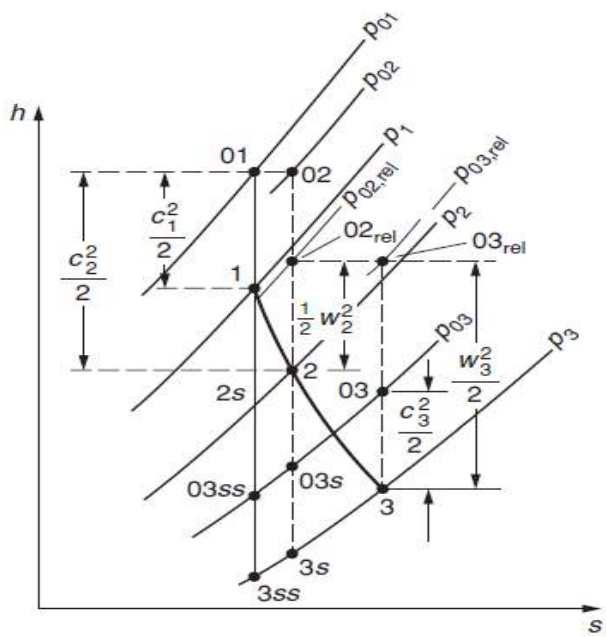

FIGURE 4.4

Mollier Diagram for a Turbine Stage

Repeating Stage Turbines

Aero-engine and power generation applications require turbines with high power output and high efficiency. To achieve this, an axial turbine with multiple stages is required. In these multi-stage axial-flow turbines, the design is often chosen to have identical, or at least very similar, mean velocity triangles for all stages. To achieve this, the axial velocity and the mean blade radius must remain constant throughout the turbine. To allow for the reduction in fluid density that arises as the flow expands through the turbine, the blade height must be continuously increasing between blade rows. Figure 4.5 shows the arrangement of a multi-stage turbine within an aero-engine, showing the increasing blade height and the constant mean radius.

For the velocity diagrams to be the same, the flow angles at exit from each stage must be equal to those at the inlet. The requirements for a repeating stage can therefore be summarized as

$$c_x = \text{constant},\ r = \text{constant},\ \alpha_1 = \alpha_3.$$

Note that a single stage turbine can also satisfy these conditions for a repeating stage. Stages satisfying these requirements are often referred to as normal stages. For this type of turbine, several useful relationships can be derived relating the shapes of the velocity triangles to the flow coefficient, stage loading, and reaction parameters. These relationships are important for the preliminary design of the turbine.

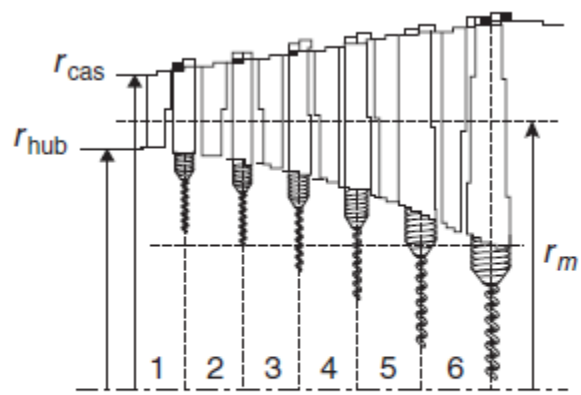

FIGURE 4.5

General Arrangement of a Repeating Six-Stage Turbine

Starting with the definition of reaction,

$$R = (h_2 - h_3)/(h_1 - h_3) = 1 - (h_1 - h_2)/(h_{01} - h_{03}). \qquad (4.8)$$

Note that h_{01}-h_{03}=h_1-h_3 since the inlet and exit velocities for the stage are equal. Through the stator no work is done, so the stagnation enthalpy stays constant across it. Given that the axial velocity is also constant this gives

$$(h_1 - h_2) = (h_{01} - h_{02}) + \frac{1}{2}(c_2^2 - c_1^2) = \frac{1}{2}c_x^2(\tan^2\alpha_2 - \tan^2\alpha_1). \qquad (4.9)$$

From the definition of stage loading,

$$(h_{01} - h_{03}) = U^2\psi. \qquad (4.10)$$

Substituting these in the equations for the reaction (4.3) and by applying the definition of flow coefficient for a purely axial turbine, $\Phi = c_x / U$, the following is obtained:

$$R = 1 - \frac{\phi^2}{2\psi}(\tan^2\alpha_2 - \tan^2\alpha_1). \qquad (4.11)$$

This is true whether or not the exit angle from the stage equals the inlet angle. It shows how the three non-dimensional design parameters are related to the flow angles at inlet and exit from the turbine nozzle. In a repeating stage turbine this relationship can be further simplified, since the stage loading can be written as follows:

$$\psi = \frac{\Delta c_\theta}{U} = \frac{c_x(\tan\alpha_2 + \tan\alpha_3)}{U} = \phi(\tan\alpha_2 + \tan\alpha_1). \qquad (4.12)$$

Substituting this into equation (4.11) we obtain

$$R = 1 - \frac{\phi}{2}(\tan\alpha_2 - \tan\alpha_1). \qquad (4.13a)$$

This can be combined with eqn. (4.12) to eliminate α_2. Adding 2 times eqn. (4.13a) to eqn (4.12) gives the following relationship between stage loading, flow coefficient, and reaction:

$$\psi = 2(1 - R + \phi\tan\alpha_1). \qquad (4.14)$$

This is a very useful result. It also applies to repeating stages of compressors. It shows that, for high stage loading, ψ, the reaction, R, should be low and the inter-stage swirl angle, $\alpha_1=\alpha_3$, should be as large as possible. Equations (4.13a) and (4.14) also show that, once the stage loading, flow coefficient, and reaction are fixed, all the flow angles, and thus the velocity triangles, are fully specified. This is true since eqn. (4.14) gives α_1, and α_2 then follows from eqn. (4.13). The other angles of the velocity triangles are then fixed from the repeating stage condition, $\alpha_1=\alpha_3$, and the relationship between relative and absolute flow angles,

$$\tan\beta_2 = \tan\alpha_2 - \frac{1}{\phi},\ \tan\beta_3 = \tan\alpha_3 + \frac{1}{\phi}. \qquad (4.15)$$

Note that by combining eqn. (4.15) with eqn. (4.13a) another useful equation for the reaction can be formed in terms of the relative flow angles,

$$R = \frac{\phi}{2}(\tan\beta_3 - \tan\beta_2). \qquad (4.13b)$$

In summary, to fix the velocity triangles for a repeating stage a turbine designer can fix Φ, ψ, and R or Φ, ψ, and $\alpha 1$ (or indeed any independent combination of three angles and parameters). Once the velocity triangles are fixed, key features of the turbine design can be determined, such as the turbine blade sizes and the number of stages needed. The expected performance of the turbine can also be estimated. Note also that the choice of the velocity triangles for the turbine (i.e., the choice of Φ, ψ, and R) are largely determined by best practice and previous experience. For a company that has already designed and tested many turbines of a similar style, it will be very challenging to produce a turbine with very different values of Φ, ψ, and R that has as good performance as its previous designs.

Stage losses and efficiency

In Chapter one various definitions of efficiency for complete turbomachines were given. For a turbine stage the total-to-total efficiency is

$$\eta_{tt} = \frac{\text{actual work output}}{\text{ideal work output when operating to same back pressure}} = (h_{01} - h_{03})/(h_{01} - h_{03ss})$$

At the entry and exit of a repeating (or normal) stage, the flow conditions (absolute velocity and flow angle) are identical, i.e., $c_1=c_3$ and $\alpha_1=\alpha_3$. If it is assumed that $c_{3ss}=c_3$, which is a reasonable

approximation for turbines operating with a fairly low pressure ratio, the total-to-total efficiency then becomes

$$\eta_{tt} = (h_1 - h_3)/(h_1 - h_{3ss}) = (h_1 - h_3)/[(h_1 - h_3) + (h_3 - h_{3s}) + (h_{3s} - h_{3ss})]. \qquad (4.16)$$

Now the slope of a constant pressure line on a Mollier diagram is (∂h / ∂s)p=T, obtained from eqn. (1.28). Thus, for a finite change of enthaply in a constant pressure process, Δh = TΔs and, therefore,

$$h_{3s} - h_{3ss} \cong T_3(s_{3s} - s_{3ss}), \qquad (4.17a)$$

$$h_2 - h_{2s} \cong T_2(s_2 - s_{2s}). \qquad (4.17b)$$

Noting, from graph, that s_{3s} -s_{3ss}=s_2- s_{2s}, the last two equations can be combined to give

$$h_{3s} - h_{3ss} = (T_3/T_2)(h_2 - h_{2s}). \qquad (4.18)$$

The effects of irreversibility through the stator and rotor are expressed by the differences in static enthalpies, (h_2 -h_{2s}) and (h_3- h_{3s}), respectively. Non-dimensional enthalpy "loss" coefficients can be defined in terms of the exit kinetic energy from each blade row. Thus, for the nozzle row,

$$h_2 - h_{2s} = \frac{1}{2} c_2^2 \zeta_N. \qquad (4.19a)$$

For the rotor row,

$$h_3 - h_{3s} = \frac{1}{2} w_3^2 \zeta_R. \qquad (4.19b)$$

Where ζ_N and ζ_R are enthalpy loss coefficient for nozzle and rotor. Combining eqns. (4.19a) and (4.19b) with eqn. (4.16) gives

$$\eta_{tt} = \left[1 + \frac{\zeta_R w_3^2 + \zeta_N c_2^2 T_3/T_2}{2(h_1 - h_3)}\right]^{-1}. \qquad (4.20a)$$

When the exit velocity is not recovered a total to- static efficiency for the stage is used:

$$\eta_{ts} = (h_{01} - h_{03})/(h_{01} - h_{3ss}) = \left[1 + \frac{\zeta_R w_3^2 + \zeta_N c_2^2 T_3/T_2 + c_1^2}{2(h_1 - h_3)}\right]^{-1}, \qquad (4.21a)$$

where, as before, it is assumed that c_1=c_3. In initial calculations or in cases where the static temperature drop through the rotor is not large, the temperature ratio T_3 / T_2 is set equal to unity, resulting in the more convenient approximations:

$$\eta_{tt} = \left[1 + \frac{\zeta_R w_3^2 + \zeta_N c_2^2}{2(h_1 - h_3)}\right]^{-1}, \qquad (4.20b)$$

$$\eta_{ts} = \left[1 + \frac{\zeta_R w_3^2 + \zeta_N c_2^2 + c_1^2}{2(h_1 - h_3)}\right]^{-1}. \qquad (4.21b)$$

Chapter Three

Gas Turbine Engine

Introduction:

The gas turbine engine is essentially a heat engine using air as a working fluid to provide thrust. To achieve this, the air passing through the engine has to be accelerated; this means that the velocity or kinetic energy of the air is increased. To obtain this increase, the pressure energy is first of all increased, followed by the addition of heat energy, before final conversion back to kinetic energy in the form of a high velocity jet efflux.

Gas Turbine and Piston Engine Comparison:

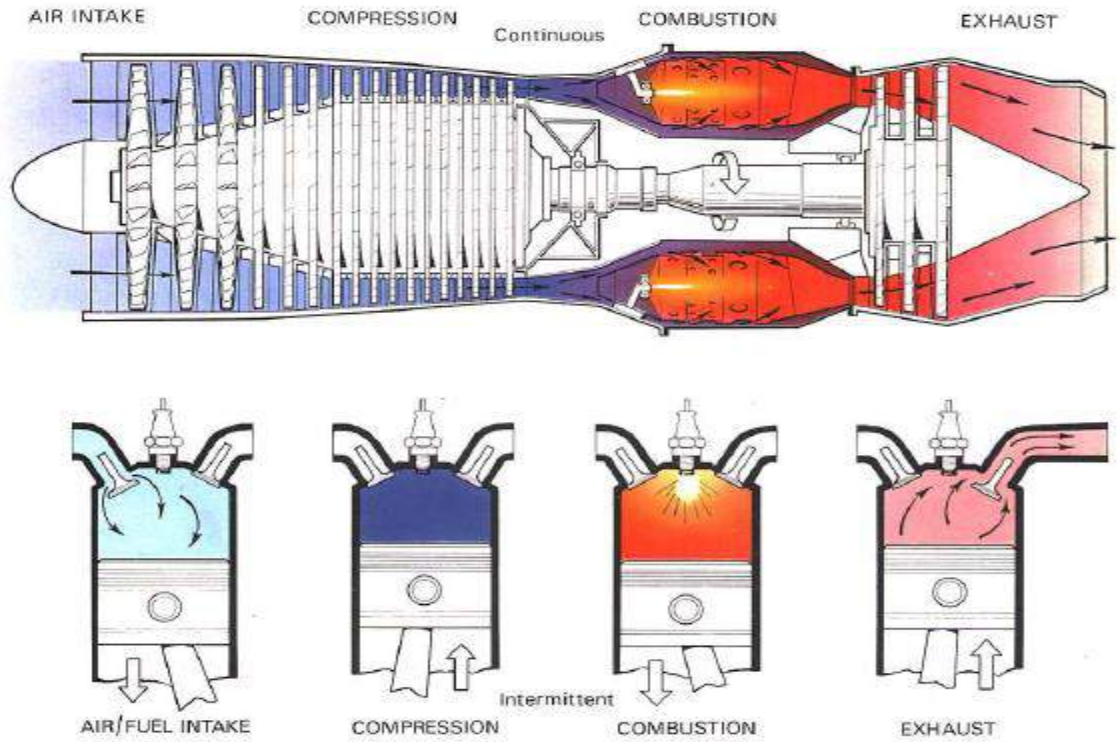

Fig. 2-1 A comparison between the working cycle of a turbo-jet engine and a piston engine.

Air-standard assumptions used in Gas Turbine Analysis:

1.The working fluid is air, which continuously circulates in a closed loop and always behaves as an ideal gas.

2.All the processes that make up the cycle are internally reversible.

3.The combustion process is replaced by a heat-addition process from an external source.

4.The exhaust process is replaced by a heat-rejection process that restores the working fluid to its initial state.

The idealizations and simplifications in the analysis of power cycles:

1.The cycle does not involve any *friction.* Therefore, the working fluid does not experience any pressure drop as it flows in pipes or devices such as heat exchangers.

2.All expansion and compression processes take place in a *quasi-equilibrium* manner.

3.The pipes connecting the various components of a system are well insulated, and *heat transfer* through them is negligible.

Cold-air-standard assumptions: When the working fluid is considered to be air with constant specific heats at room temperature (25°C).

Air-standard cycle: A cycle for which the air-standard assumptions are applicable

Gas Turbine Working Cycle: The Brayton Cycle

The Brayton cycle is the air-standard ideal cycle approximation for the gas-turbine engine. An open system, steady-flow analysis is used to determine the heat transfer and work for the cycle.

The combustion process is replaced by a constant-pressure heat-addition process from an external source, and the exhaust process is replaced by a constant-pressure heat-rejection process to the ambient air.

We assume the working fluid is air and the specific heats are constant and will consider the cold-air-standard cycle.

1-2 Isentropic compression (in a compressor)
2-3 Constant-pressure heat addition (Combustor)
3-4 Isentropic expansion (in a turbine)
4-1 Constant-pressure heat rejection (Exhaust)

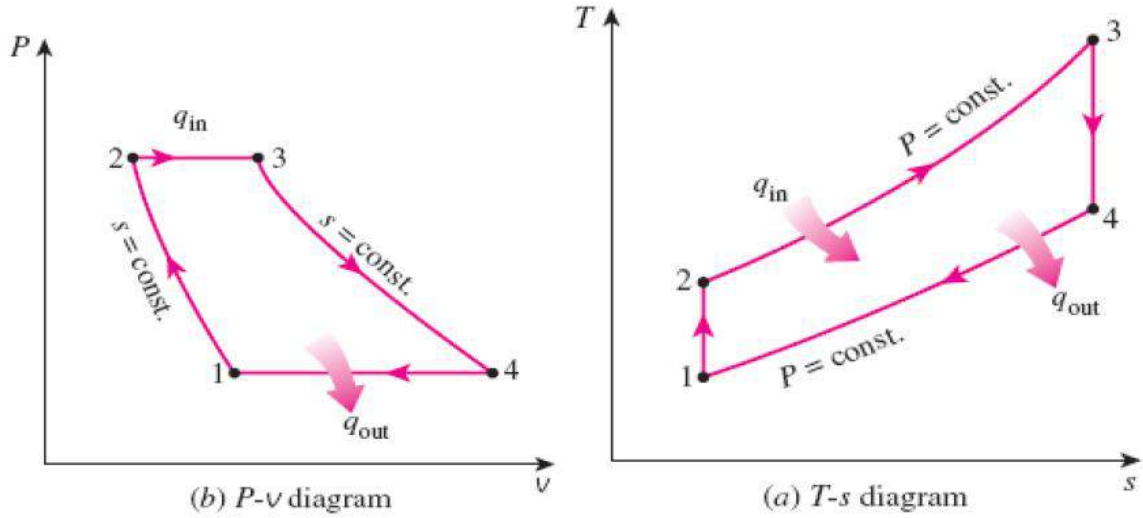

Open and closed gas turbine cycle:

There are two types of Brayton cycles, open to the atmosphere and using internal combustion chamber or closed and using a heat exchanger. Although the Brayton cycle is usually run as an open system i.e. the gases from the exhaust are lost to the ambient and a fresh intake of air is done, it is conventionally assumed for the purposes of thermodynamic analysis that the exhaust gases are reused in the intake, enabling analysis as a closed system. A closed Brayton cycle recirculates the working fluid, the air expelled from the turbine is reintroduced into the compressor, this cycle uses a heat exchanger to heat the working fluid instead of an internal combustion chamber. The closed Brayton cycle is used for example in closed-cycle gas turbine and space power generation.

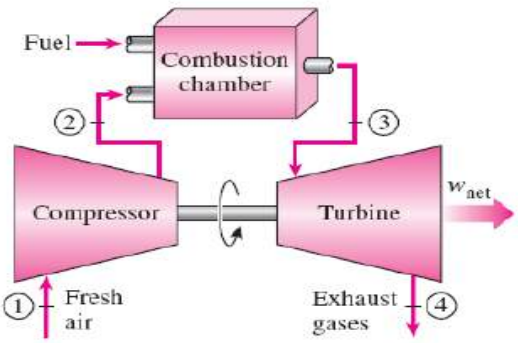

An open-cycle gas-turbine engine.

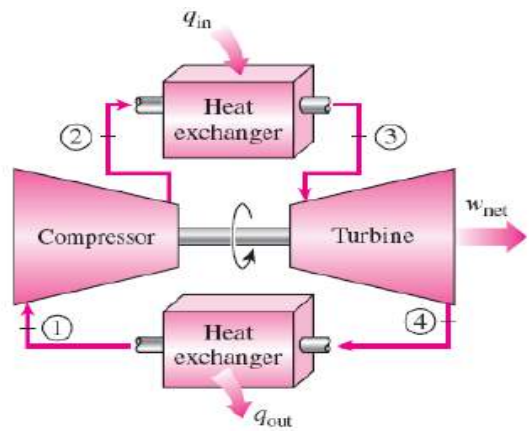

A closed-cycle gas-turbine engine.

Gas Turbine Cycle Analysis:

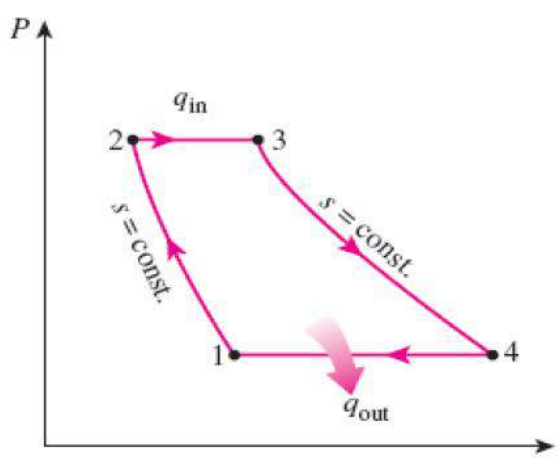

(b) P-v diagram

The 4 ideal processes in the cycle.

1 - 2 Reversible adiabatic (isentropic) compression requiring power input.

$P_{in} = \Delta H/s = m\, c_p\, (T_2 - T_1)$

2 - 3 Constant pressure heating requiring heat input.

$Q_{in} = \Delta H/s = m\ c_p\ (T_3 - T_2)$

3 - 4 Reversible adiabatic (isentropic) expansion producing power output.

$P_{out} = \Delta H/s = m\ c_p\ (T_3 - T_4)$

4 - 1 Constant pressure cooling back to the original state requiring heat removal.

$Q_{out} = \Delta H/s = m\ c_p\ (T_4 - T_1)$

Using first law of thermodynamics for a closed cycle, that is the net head addition(Qin-Qout) is equal to total power developed(Pout-Pin), we can write the efficiency of the Brayton cycle as the ratio of net power developed to the net heat added to the cycle, and deduce efficiency relation as:

$$1 - \frac{mc_p(T_4 - T_1)}{mc_p(T_3 - T_2)} = 1 - \frac{(T_4 - T_1)}{(T_3 - T_2)}$$

It assumed that the mass and the specific heats are the same for the heat addition and heat rejection process. It is easy to show that the temperature ratio for the turbine and compressor are the same.

$$\frac{T_2}{T_1} = \left(\frac{p_2}{p_1}\right)^{1-\frac{1}{\gamma}} = r_p^{1-\frac{1}{\gamma}} \qquad \frac{T_3}{T_4} = \left(\frac{p_3}{p_4}\right)^{1-\frac{1}{\gamma}} = r_p^{1-\frac{1}{\gamma}} \qquad \frac{T_3}{T_4} = \frac{T_2}{T_1}$$

r_p is the pressure compression ratio for the turbine and compressor.

$$\eta_{th} = 1 - \frac{(T_4 - T_1)}{(T_3 - T_2)} = 1 - \frac{\left(\frac{T_3 T_1}{T_2} - T_1\right)}{\left(\frac{T_2 T_4}{T_1} - T_2\right)} = 1 - \frac{T_1\left(\frac{T_3}{T_2} - 1\right)}{T_2\left(\frac{T_4}{T_1} - 1\right)}$$

$$\frac{T_3}{T_2} = \frac{T_4}{T_1} \qquad \frac{T_3}{T_2} - 1 = \frac{T_4}{T_1} - 1$$

$$\eta_{th} = 1 - \frac{T_1}{T_2} = 1 - \frac{T_4}{T_3} = 1 - \frac{1}{r_p^{1-\frac{1}{\gamma}}}$$

Hence from the above relation, it can be noted that the efficiency of an Ideal Brayton cycle is a function of pressure ratio r_p only. The efficiency of the cycle increases with pressure ratio as shown in the graph. The typical range of pressure ratios for a gas turbine cycle lies between 5-20. However, there are practical limits when it comes to increasing the pressure ratio. First of all, increasing the pressure ratio increases the compressor discharge temperature. This can cause the temperature of the gasses leaving the combustor to exceed the metallurgical limits of the turbine. Also, the diameter of the compressor blades becomes progressively smaller in higher pressure stages of the compressor. Because the gap between the blades and the engine casing increases in size as a percentage of the compressor blade height as the blades get smaller in diameter, a greater percentage of the compressed air can leak back past the blades in higher pressure stages.

This causes a drop in compressor efficiency, and is most likely to occur in smaller gas turbines (since blades are inherently smaller to begin with). Finally, as can be seen in figure, the efficiency levels off as pressure ratio increases. Hence, there is little to gain by increasing the pressure ratio further if it is already at a high level.

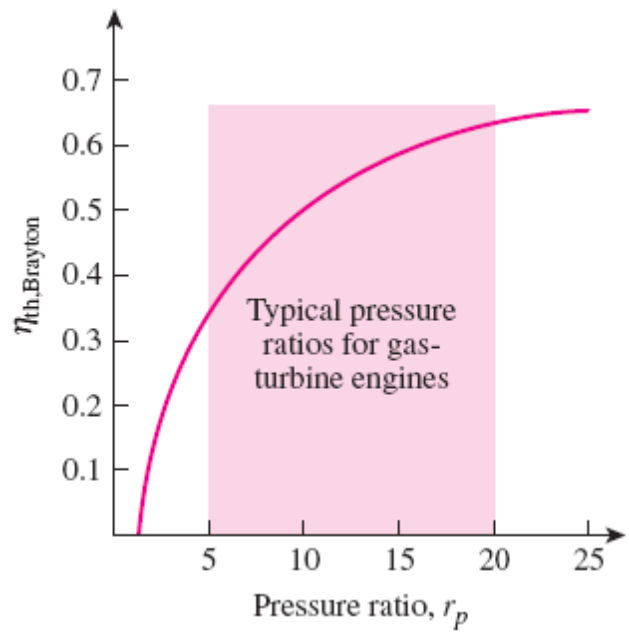

As we can see that the compressor is driven by the power generated from the turbine, the compressor is coupled with the turbine assembly and runs through the shaft power transmitted from the turbine. We can define a term, ***Back Work Ratio*** as the total fraction of power generated by the turbine that is used in running the compressor. Hence it is the ration of the compressor work to the turbine work.

Numerical Example:

The ideal air-standard Brayton cycle operates with air (γ or k =1.4) entering the compressor at 95 kPa, 22 ^{0}C. The pressure ratio r_p is 6:1 and the air leaves the heat addition process at 1100 K. Determine the compressor work and the turbine work per unit mass flow, the cycle efficiency, the back work ratio, and compare the compressor exit temperature to the turbine exit temperature. Assume constant properties.

Solution:

Since the compression is regarded isentropic for an ideal Brayton cycle,

$$\frac{T_2}{T_1} = \left(\frac{P_2}{P_1}\right)^{(k-1)/k} = r_p^{(k-1)/k}$$

$$T_2 = T_1 r_p^{(k-1)/k}$$

$$= (22+273)K(6)^{(1.4-1)/1.4}$$

$$= 492.5\,K$$

Compressor work per unit mass flow

$$w_{comp} = C_p(T_2 - T_1)$$
$$= 1.005\frac{kJ}{kg \cdot K}(492.5 - 295)K$$
$$= 198.15\frac{kJ}{kg}$$

Since process 3-4 is isentropic expansion

$$\frac{T_4}{T_3} = \left(\frac{P_4}{P_3}\right)^{(k-1)/k}$$

Since $P3 = P2$ and $P4 = P1$, we see that

$$\frac{T_4}{T_3} = \left(\frac{1}{r_p}\right)^{(k-1)/k}$$

$$T_4 = T_3\left(\frac{1}{r_p}\right)^{(k-1)/k} = 1100K\left(\frac{1}{6}\right)^{(1.4-1)/1.4} = 659.1K$$

$$w_{turb} = C_p(T_3 - T_4) = 1.005\frac{kJ}{kg \cdot K}(1100 - 659.1)K$$
$$= 442.5\frac{kJ}{kg}$$

Heat supplied to cycle per unit mass flow is given by

$$q_{in} = \frac{\dot{Q}_{in}}{\dot{m}} = h_3 - h_2$$
$$= C_p(T_3 - T_2) = 1.005\frac{kJ}{kg \cdot K}(1100 - 492.5)K$$
$$= 609.6\frac{kJ}{kg}$$

$$w_{net} = w_{turb} - w_{comp}$$
$$= (442.5 - 198.15)\frac{kJ}{kg}$$
$$= 244.3\frac{kJ}{kg}$$

$$\eta_{th,\,Brayton} = \frac{w_{net}}{q_{in}}$$
$$= \frac{244.3\frac{kJ}{kg}}{609.6\frac{kJ}{kg}} = 0.40 \quad or \quad 40\%$$

$$BWR = \frac{w_{in}}{w_{out}} = \frac{w_{comp}}{w_{turb}}$$
$$= \frac{198.15\frac{kJ}{kg}}{442.5\frac{kJ}{kg}} = 0.448$$

Note that $T4$ = 659.1 K > $T2$ = 492.5 K, or the turbine outlet temperature is greater than the compressor exit temperature. This temperature difference can be used to increase the thermal efficiency of the cycle. The heat from the turbine exhaust temperature can be used in an heat exchanger to heat the compressor outlet gas at T2. This reduces the compressor work, which

eventually will increase the cycle efficiency. This type of modified cycle is termed as the ***regenerative gas turbine cycle*** and the process is called ***regeneration*** which we will discuss in detail here.

Regenerative Gas Turbine Cycle: The temperature of the exhaust gases in a simple gas turbine is higher than the temperature of the air after compression process. The η of the Brayton cycle can be increased by utilizing part of the energy of the exhaust gas from the turbine in heating up the air leaving the compression in a heat exchanger called a regenerator, thereby reducing the amount of heat supplied from an external source and also the amount of heat rejected.

Figure shows a single stage regenerative gas turbine cycle

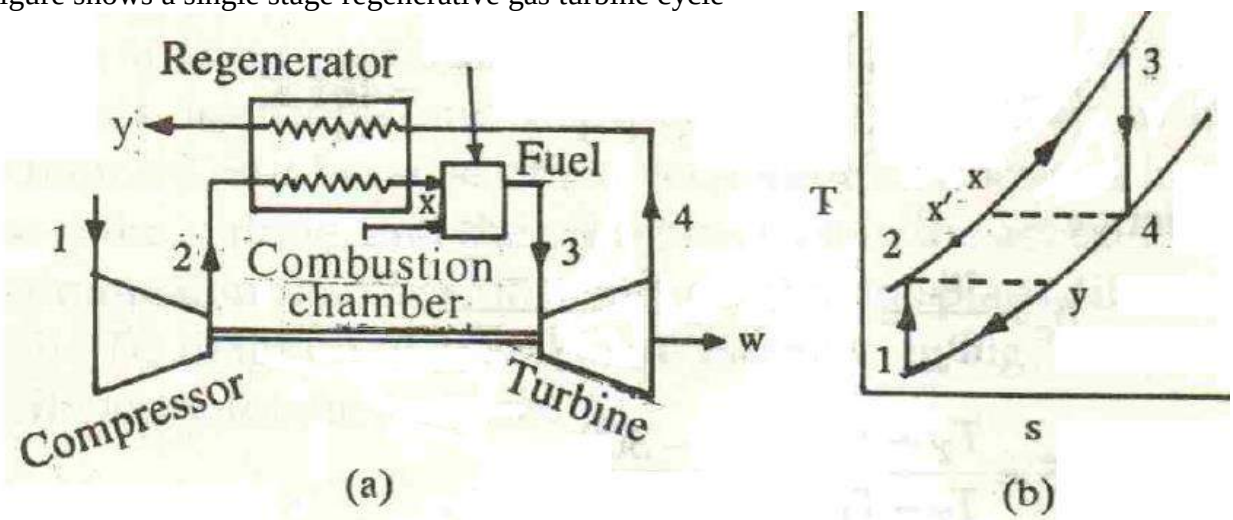

An ideal air standard regenerative gas turbine cycle

Air is drawn from the atmosphere into the compressor and is compressed isentropically to state 2. It is then heated at constant pressure in the regenerator to state x by the hot burnt gases from the gas turbine. Since the temperature of the air increases before it reaches the combustion chamber, less amount of fuel will be required to attain the designed turbine inlet temperature of the products of combustion. After combustion at constant pressure in the combustion chamber, the gas enters the turbine at state 3 and expands isentropically to state 4 in the turbine. It then enters the counter-flow regenerator as stated earlier, where it gives up a portion of its heat energy to the compressed air from the compressor and leaves the regenerator at state y.

In an ideal cycle, the temperature of the air leaving the regenerator is equal to the temperature of the burnt gases leaving the turbine, i.e., Tx = T4. But in practice, the temperature of the air leaving the regenerator is less than Tx. In T-S diagram, Tx1 is the temperature of the air leaving the regenerator in an actual plant.

$\therefore$ Effectiveness of a regenerator is $\varepsilon = \eta_r = \dfrac{T_{x^1} - T_2}{T_x - T_2}$ when C_P is constant.

In an ideal regenerator, heat loss by the burnt gases is equal to the heat gained by the air in the regenerator, i.e., T4 – Ty = Tx – T2, Where Tx = T4 and Ty = T2 and hence □r = 1

$$\eta_{th} = 1 - \frac{Q_L}{Q_H}$$

For an ideal regenerative gas turbine cycle,

$$Q_L = C_P (T_y - T_1) = C_P (T_2 - T_1) \text{ and}$$
$$Q_H = C_P (T_3 - T_x) = C_P (T_3 - T_4)$$

$$\therefore \eta_{th} = 1 - \frac{(T_2 - T_1)}{(T_3 - T_4)} = 1 - \frac{T_1\left[\frac{T_2}{T_1} - 1\right]}{T_3\left[1 - \frac{T_4}{T_3}\right]}$$

Since $\frac{T_2}{T_1} = \left(\frac{P_2}{P_1}\right)^{\frac{r-1}{r}} = R^{\frac{r-1}{r}}$ *and* $\frac{T_4}{T_3} = \left(\frac{P_4}{P_3}\right)^{\frac{r-1}{r}} = \left(\frac{P_1}{P_2}\right)^{\frac{r-1}{r}} = \left(\frac{1}{R}\right)^{\frac{r-1}{r}}$

$$\therefore \eta_{th} = 1 - \frac{1}{t}\frac{\left(R^{\frac{r-1}{r}} - 1\right)}{\left(1 - \frac{1}{R^{\frac{r-1}{r}}}\right)} = 1 - \frac{1}{t}.\quad R^{\frac{r-1}{r}}$$

i.e., $\eta_{th} = 1 - \frac{1}{t} R^{\frac{r-1}{r}}$

It is evident that the ηth of an ideal regenerative gas turbine cycle depends not only on the pressure ratio R but also on the ratio of the two extreme temperatures. For a fixed ratio of T3/T1, the cycle η drops with increasing pressure ratio. In practice the regenerator is costly, heavy and bulky, and causes pressure losses which bring about a decrease in cycle η.

The following graph shows the variation of thermal efficiency of a regenerative gas turbine cycle with increasing pressure ratio. It can be seen that the regenerative cycle is not feasible for higher pressure ratios.

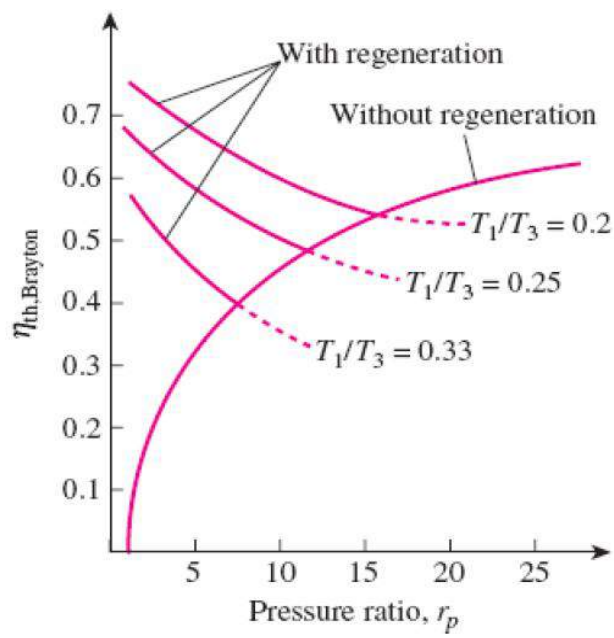

Variation of Actual Gas Turbine Cycle from Ideal Brayton Cycle

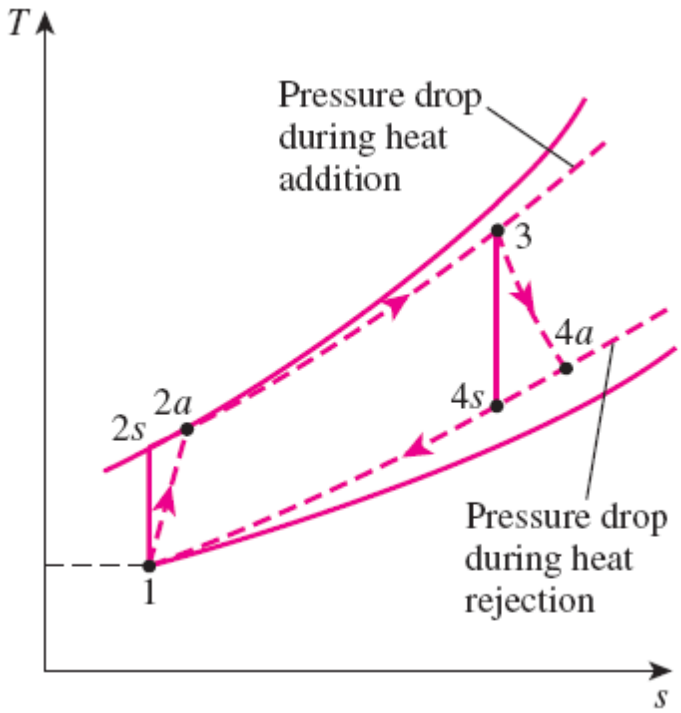

Reasons:

• Some pressure drop in an actual gas turbine cycle during heat addition and heat rejection processes is unavoidable.

• Owing to irreversibility, such as friction and non-quasi equlibrium operation conditions of actual devices, the actual work input of the compressor will be more, and the actual work output from the turbine will be less.

• Irreversibilities in turbine and compressors, pressure drops, heat losses

The efficiency of the turbines and compressors can be approximated by the following relation.

$$\eta_C = \frac{w_s}{w_a} \cong \frac{h_{2s}}{h_{2a}} \eta_T = \frac{w_a}{w_s} \cong \frac{h_3 - h_{4a}}{h_3 - h_{4s}}$$

Numerical

A gas turbine uses a standard Joule cycle but there is friction in the compressor and turbine. The air is drawn into the compressor at 1 bar 15oC and is compressed with an isentropic efficiency of 94% to a pressure of 9 bar. After heating, the gas temperature is 1000 ^{0}C. The isentropic efficiency of the turbine is also 94%. The mass flow rate is 2.1 kg/s. Determine the following.

Ans: 612 kW and 40.4%

Gas Turbine cycle with reheat and multiple expansion

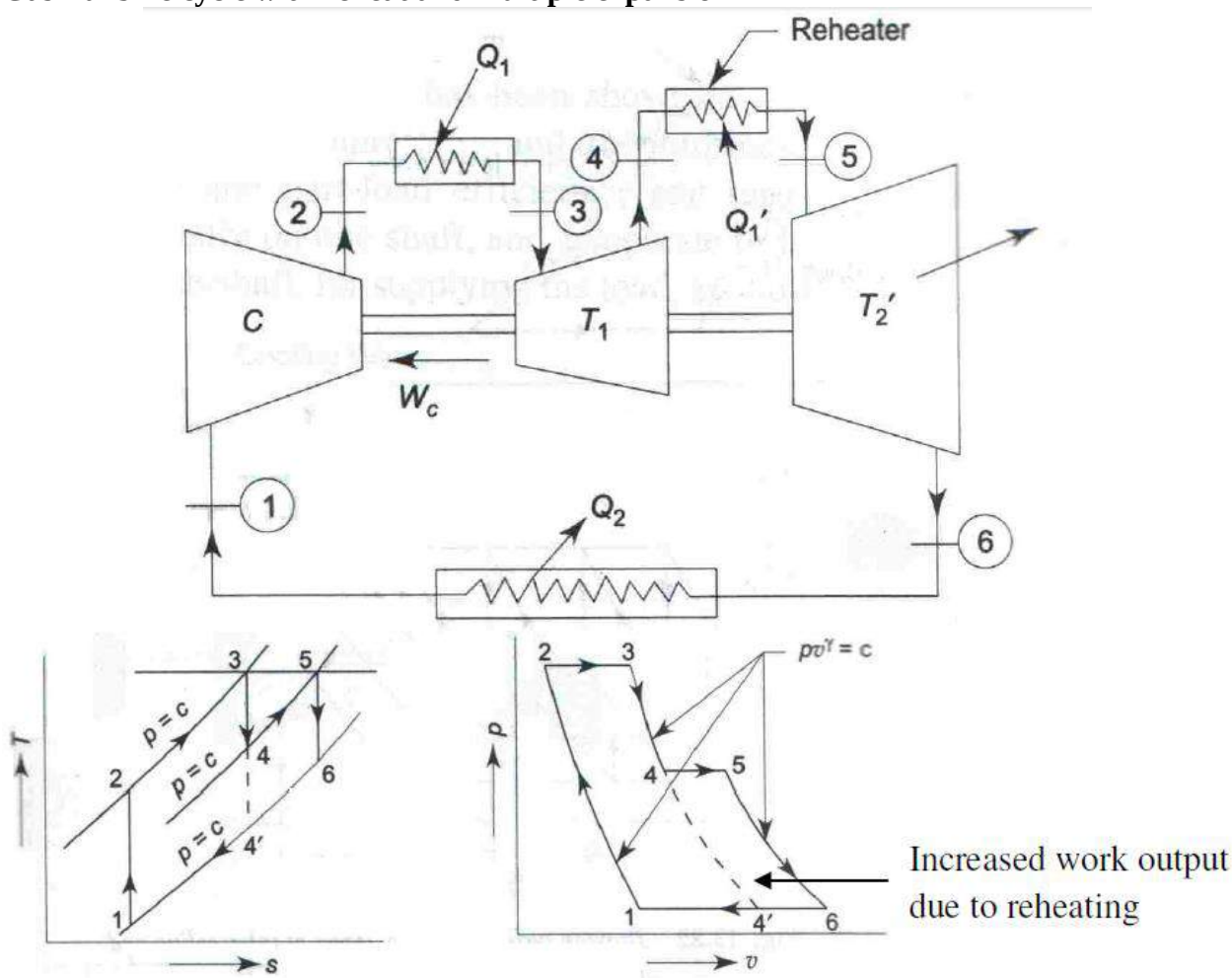

Work output of the turbine is increased by multistage expansion with reheating. In the above illustration, two-stage expansion is done in low pressure (T1) and high pressure (T2
1) turbines with reheating the air in between stages.

Gas turbine cycle with multistage compression with inter cooling in between the stages:

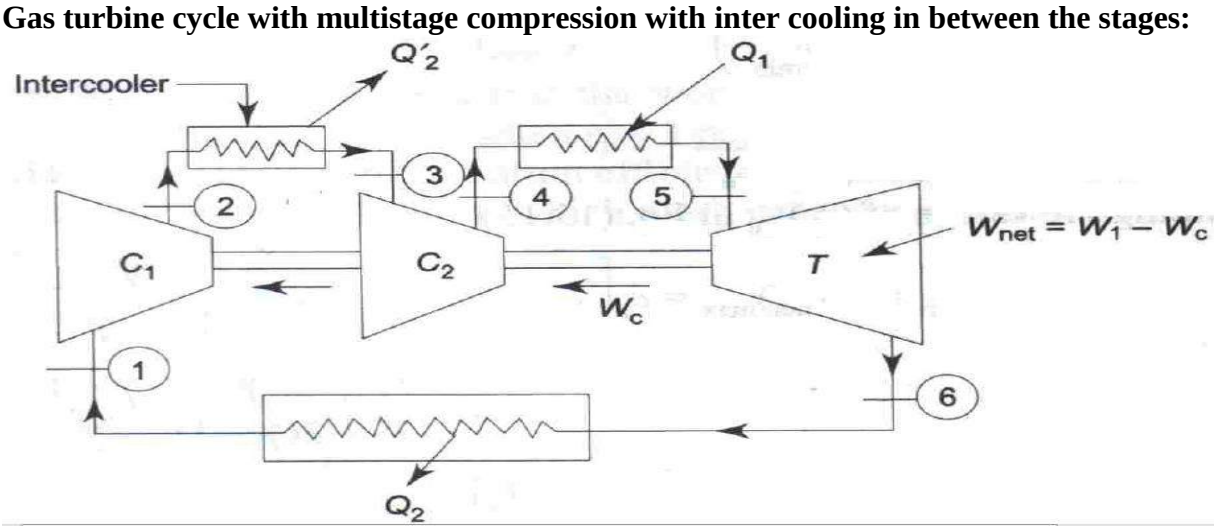

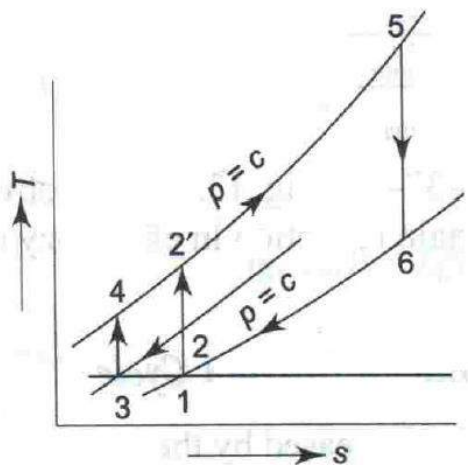

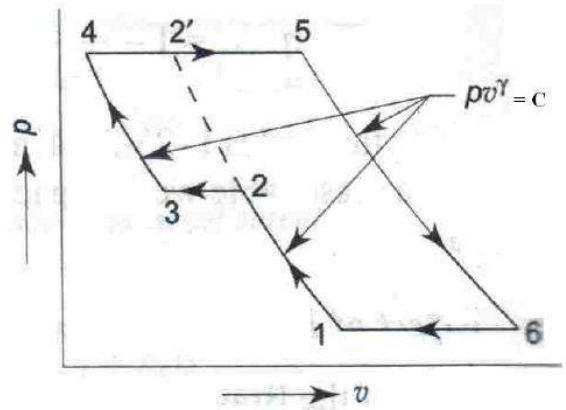

The work output from a simple gas turbine cycle can be increased also by having multistage compression with inter cooling in between the stages. The effect of having two stage compression with inter cooling in between the stages is illustrated on the T-S diagram. It can be seen that, a higher work output has been achieved than that of simple cycle by an amount shown by the shaded area. The disadvantage of it is that more heat has to be supplied to heat the air than that is required for simple cycle. This may reduce the thermal η of the cycle.

Gas turbine cycle with two stage compression two-stage expansion and regenerator:
In multistage compression with inter-cooling, the work required to compress a gas between two specified pressures can be decreased by carrying out the compression process in stages and cooling the gas in between. This keeps the specific volume as low as possible. Whereas in multistage expansion with reheating keeps the specific volume of the working fluid as high as possible during an expansion process, thus maximizing work output.

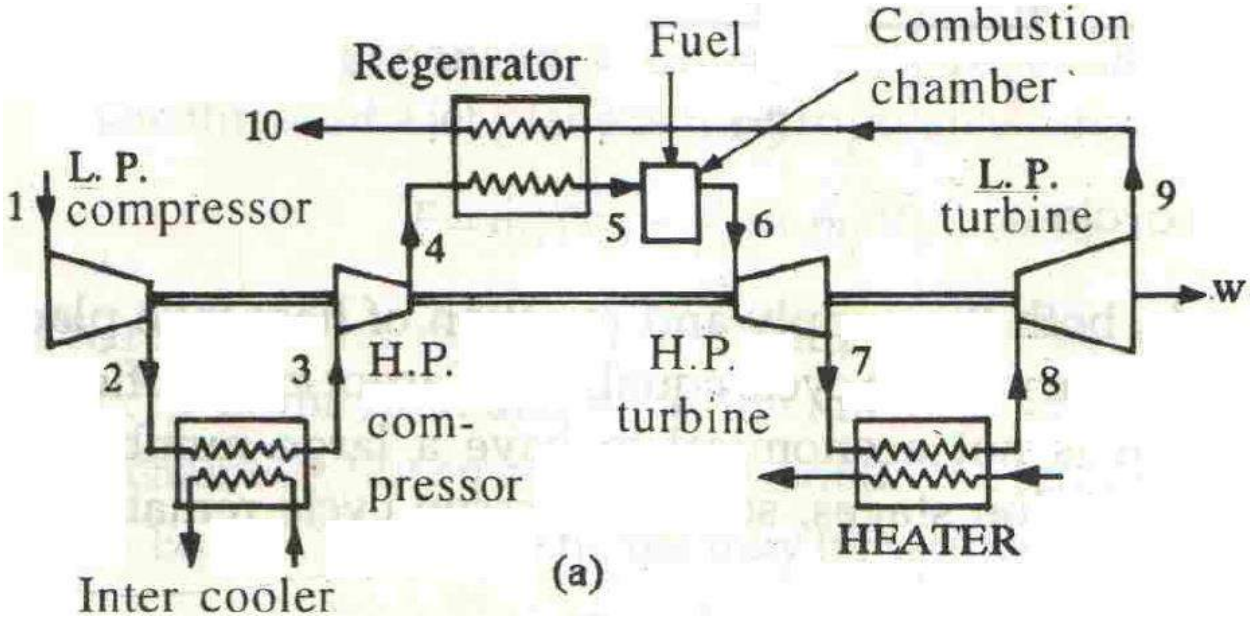

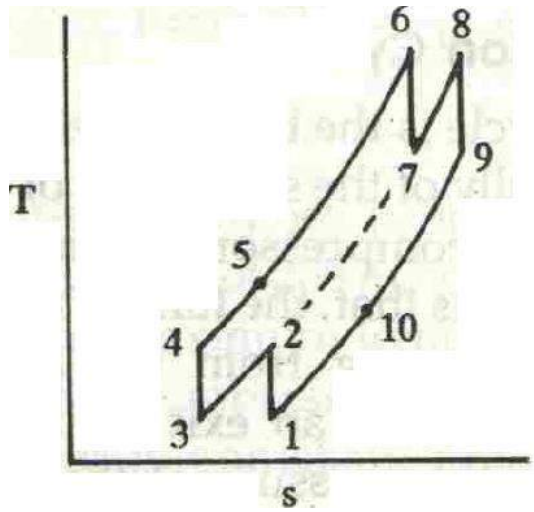

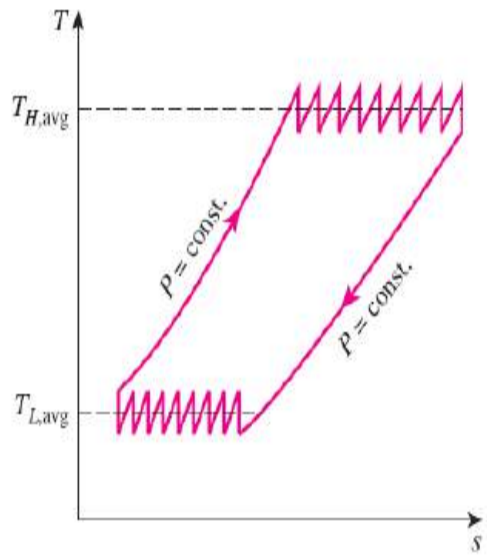

A gas turbine cycle with multiple stages of intercooling and multiple stages of reheating assumes the graph as shown above which is similar to Ericsson cycle. The thermal η of a gas turbine cycle may be improved by incorporating multistage compression with intercooling between the stages and multistage expansion with reheating between the turbines and also providing a regenerator. There is a definite saving of work due to multistage compression with intercooling arrangement between the stages. Similarly, the work output of the turbine is increased by multistage expansion with reheating. As a result, the net work of the plant increases.

Aircraft Gas Turbine Engine Modules and their Thermodynamics:

We will limit our discussions to the following gas turbine engine modules in this manual.

a. Inlet
b. Compressor
c. Combustion Chamber
d. Turbine
e. Exhaust/Nozzle
f. Afterburners

Before we start discussing about the inlet of a gas turbine, it is advisable that you review first the Nozzles chapter in this manual. You should have a basic knowledge about the flow regimes, isentropic relations in terms of Mach no. and basic knowledge of shocks.

Gas Turbine Engine Notations and Station numbers:

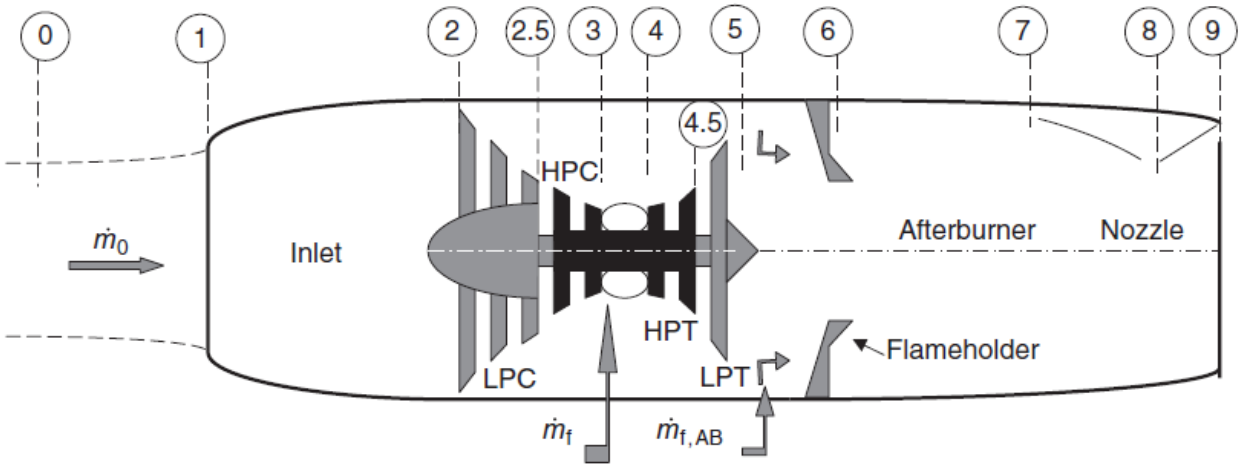

The above figure depicts a twin spool (consisting two sets of compressors and turbines each) turbojet engine with an afterburner.

The air is brought in through the air intake, or inlet, system, where station 0 designates the unperturbed flight condition, station 1 is at the inlet (or cowl) lip, and station 2 is at the exit of the air intake system, which corresponds to the inlet of the compressor (or fan). The compression process from stations 2 to 3 is divided into a low-pressure compressor (LPC) spool and a high-pressure compressor (HPC) spool. The exit of the LPC is designated by station 2.5 and the exit of the HPC is station 3. The HPC is designed to operate at a higher shaft rotational speed than the LPC spool. The compressed gas enters the main or primary burner at 3 and is combusted with the fuel to produce hot high pressure gas at 4 to enter the high-pressure turbine (HPT). Flow expansion through the HPT and the low-pressure turbine (LPT) produces the shaft power for the HPC and LPC, respectively. An afterburner is designated between stations 5 and 7, where an additional fuel is combusted with the turbine discharge flow before it expands in the exhaust nozzle. Station 8 is at the throat of the nozzle and station 9 designates the nozzle exit. Throughout our discussions in this Manual, we will be using the notations as described above.

The Inlet/Intake:

The main requirement of an air inlet is that under all operating conditions, delivery of the air to the engine is achieved with the minimum loss of energy occurring through the duct. To enable the compressor to operate satisfactorily, the air must reach the compressor at a uniform pressure distributed evenly across the whole inlet area.

The ideal air intake for a turbo jet engine fitted to an aircraft flying at subsonic or low supersonic speed is a short, pitot-type circular intake as shown in the figure below. This type of intake makes the fullest use of the ram effect on the air due to forward speed, and suffers the minimum loss of ram pressure with changes of aircraft attitude. However, as sonic speed is approached the efficiency of this type of intake begins to fall because of the formation of shock waves at the intake lip.

At higher supersonic speeds the air flow velocities met are much higher than the compressor can efficiently use, therefore the intake air velocity must be decreased. In this case it is necessary to have an intake that has a variable throat area and spill valves to accommodate and control the changing volume of air as shown in the figure below.

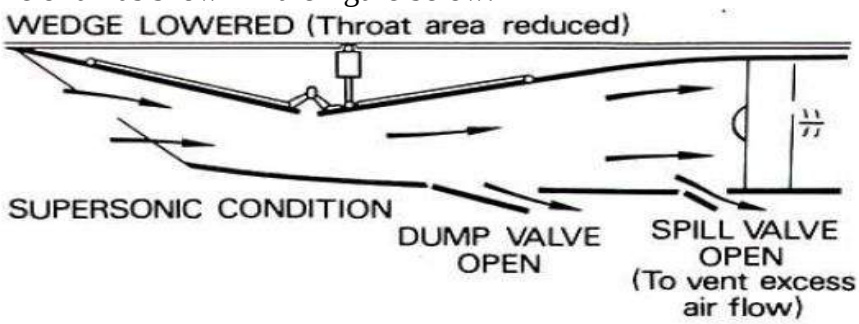

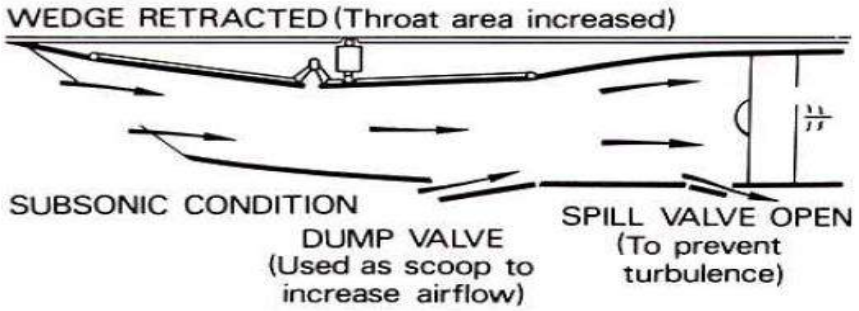

The engine intake is the biggest single source of drag on the aircraft and so designers have to be very careful when deciding where to install engines. Engines that are far from the centre line of the aircraft will impose considerable turning moments on the aircraft when under power or when shut down in flight. Having the engines close to the fuselage is more practicable but gives rise to the possibility of turbulent air entering the intake from the skin of the aircraft. Clearly, the best location is at the nose of the aircraft but, for a four-engined commercial transport aircraft, this is entirely impracticable! Following are the commonly incorporated inlet types in aircrafts.

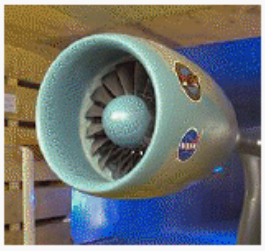

Subsonic

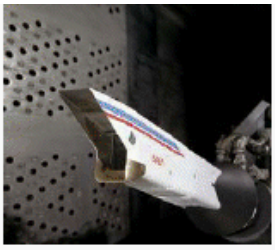

Rectangular Supersonic

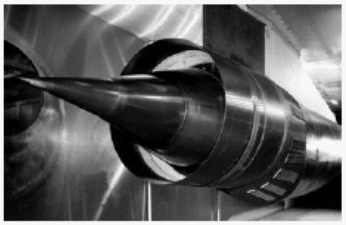

Axisymmetric Supersonic

Inlet Thermodynamics:

The *basic* function of the inlet is to deliver the air to the compressor at the *right* Mach number M_2 and the *right* quality, that is, low distortion. The subsonic compressors are designed for an axial Mach number ofM_2 = 0.5–0.6. Therefore, if the flight Mach number is higher than 0.5 or 0.6, which includes all commercial (fixed wing) transports and military (fixed wing) aircraft, then the inlet is required to *decelerate* the air efficiently. Therefore, the main function of an inlet is to *diffuse or decelerate* the flow, and hence it is also called a diffuser.

An ideal inlet is considered to provide a *reversible and adiabatic*, that is, isentropic, compression of the captured flow to the engine. The adiabatic aspect is actually met in real inlets as well. This requirement says that there is no heat exchange between the captured stream and the ambient air, through the diffuser walls.

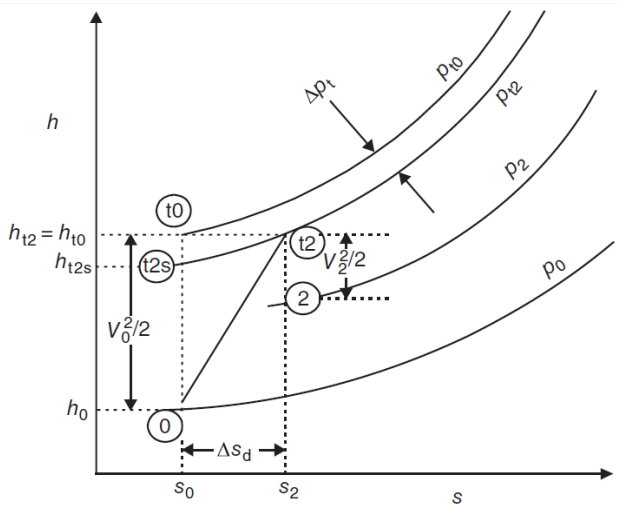

Now, let us describe the information we observe in above figure. First, four isobars are shown on the *h-s* diagram. From the lowest to the highest value, these are p_0, the static pressure at the flight altitude, p_2, the static pressure at the engine face, p_{t2}, the total pressure at the inlet discharge (or compressor face), and p_{t0}, the flight total pressure. We also note five thermodynamic states identified, as the flight static (0), the flight total (t0), the compressor face or inlet discharge static (2), and total (t_2) and a stagnation state (t_{2s}) that does not actually exist! Note, that the first four states, that is, 0, t_0, 2, and t_2, do all in reality exist and are measured. The states 0 and t0 are measured by a pitot-static tube on an aircraft, and the static and total pressures at the engine face are measured by a pressure rake or inlet pitot tubes.We note that the state (t_{2s}) is at the intersection of s_0 and p_{t2}, which is arrived at isentropically from state (0) to a state that shares the same total pressure as that of a real inlet (t_2). We note an entropy rise Δ*s*d across the inlet as well. The total enthalpy of the real inlet h_{t2} is identified to be the same as the total enthalpy of flight h_{t0}. This is based on the earlier assertion that a *real* inlet flow may be considered to be *adiabatic*. It is to be noted that although the total energy of the fluid in a real inlet is not changing, there is an *energy conversion* that takes place in the inlet. The inlet kinetic energy is partially converted to the static pressure (rise) and partially it is dissipated into heat. It is the latter portion, that is, the dissipation, which renders the process irreversible and cause the entropy to rise. The entropy rise in an adiabatic process leads to a total pressure loss Δp_t following the combined first and second law of thermodynamics, that is, Gibbs equation, according to

$$\frac{p_{t2}}{p_{t0}} = e^{-\frac{s_2 - s_0}{R}} = e^{-\frac{\Delta s}{R}}$$

From above figure, we also note that the states (t_0) and (0) are separated *isentropically* by the amount of $V^2_0/2$, as expected from the definition of stagnation state and its relation to the static state. The states (t_{2s}) and (0) are separated isentropically by a kinetic energy amount, which produces p_{t2} as its stagnation state and obviously the rest of the kinetic energy, that is, the gap between the states (t_0) and (t_{2s}), represents the amount of dissipated kinetic energy into heat. Therefore, the smaller the gap between the states (t_{2s}) and (t_0), the more efficient will the diffuser flow process be. Consequently, we use the fictitious state (t_{2s}) in a definition of inlet efficiency (or a figure of merit) known as the *inlet adiabatic efficiency*. Symbolically, the inlet adiabatic efficiency is defined as

$$\eta_d \equiv \frac{h_{t2s} - h_0}{h_{t2} - h_0} = \frac{(V^2/2)_{ideal}}{V_0^2/2} \qquad \textbf{(4.3)}$$

The practical form of the above definition is derived when we divide the numerator and denominator by h_0 to get

$$\eta_d = \frac{\frac{h_{t2s}}{h_0} - 1}{\frac{h_{t2}}{h_0} - 1} = \frac{\frac{T_{t2s}}{T_0} - 1}{\frac{h_{t0}}{h_0} - 1} = \frac{\left(\frac{p_{t2}}{p_0}\right)^{\frac{\gamma-1}{\gamma}} - 1}{\frac{\gamma-1}{2}M_0^2} = \frac{\left(\frac{p_{t2}}{p_0}\right)^{\frac{\gamma-1}{\gamma}} - 1}{\tau_r - 1} \qquad \textbf{(4.4)}$$

where we have used the isentropic relation between the states (t_{2s}) and (0). Note that the only unknown in Equation 4.4 is p_{t2} for a given flight altitude p_0, flight Mach number M_0, and an inlet adiabatic efficiency η_d. We can separate the unknown term p_{t2} and write the following expression:

$$\frac{p_{t2}}{p_0} = \left\{1 + \eta_d \frac{\gamma - 1}{2} M_0^2\right\}^{\frac{\gamma}{\gamma-1}} \qquad \textbf{(4.5)}$$

It is interesting to note that Equation 4.5 recovers the isentropic relation for a 100% efficient inlet or $\eta_d = 1.0$. Another parameter, or a *figure of merit*, that describes the inlet performance is the total pressure ratio between the compressor face and the (total) flight condition. This is given a symbol π_d and is often referred to as the *inlet total pressure recovery*:

$$\pi_d \equiv \frac{p_{t2}}{p_{t0}} \qquad \textbf{(4.6)}$$

As expected, the two figures of merit for an inlet, that is, η_d or π_d, are not independent from each other and we can derive a relationship between η_d and π_d working the left-hand side of Equation 4.5, as follows:

$$\frac{p_{t2}}{p_0} = \frac{p_{t2}}{p_{t0}}\frac{p_{t0}}{p_0} = \left\{1 + \eta_d \frac{\gamma - 1}{2} M_0^2\right\}^{\frac{\gamma}{\gamma-1}} \qquad \textbf{(4.6a)}$$

$$\pi_d = \frac{\left\{1 + \eta_d \frac{\gamma - 1}{2} M_0^2\right\}^{\frac{\gamma}{\gamma-1}}}{\frac{p_{t0}}{p_0}} = \left\{\frac{1 + \eta_d \frac{\gamma - 1}{2} M_0^2}{1 + \frac{\gamma - 1}{2} M_0^2}\right\}^{\frac{\gamma}{\gamma-1}} = \frac{\left[1 + \eta_d \frac{\gamma - 1}{2} M_0\right]^{\frac{\gamma}{\gamma-1}}}{\pi_r} \qquad \textbf{(4.6b)}$$

■ **FIGURE 4.4**
Schematic drawing of an inlet flow at low-speed and/or takeoff flight condition (note: $A_0 > A_2$)

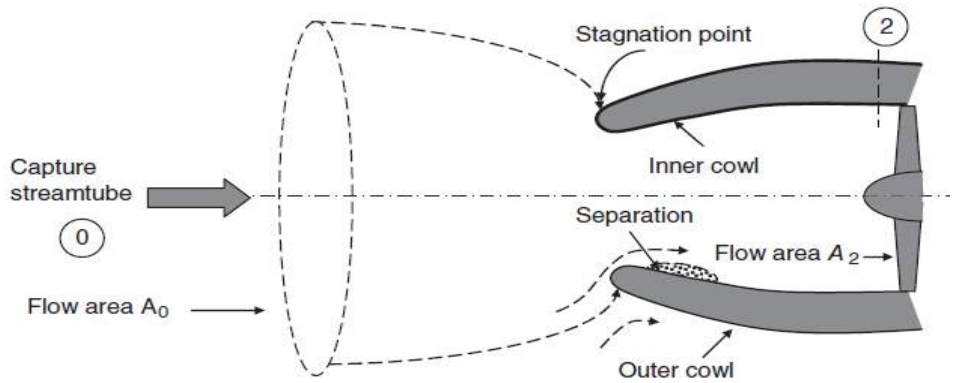

Therefore, Equation 4.6b relates the inlet total pressure recovery π_d to the inlet adiabatic efficiency η_d at any flight Mach number M_0. We note that Equation 4.6b as $\eta_d \to 1$, then $\pi_d \to 1$ as well, as expected. Figure 4.3 also shows the static state 2, which shares the same entropy as the total state t2 and lies below it by the amount of kinetic energy at 2, namely, $V_2^2/2$. Compare the kinetic energy at 2 and at 0, shown in Figure 4.3, and then justify the static pressure rise achieved in the inlet (diffuser), $p_2 - p_0$.

■ **FIGURE 4.5**
Bellmouth inlet guides the flow smoothly into the engine on a static test rig

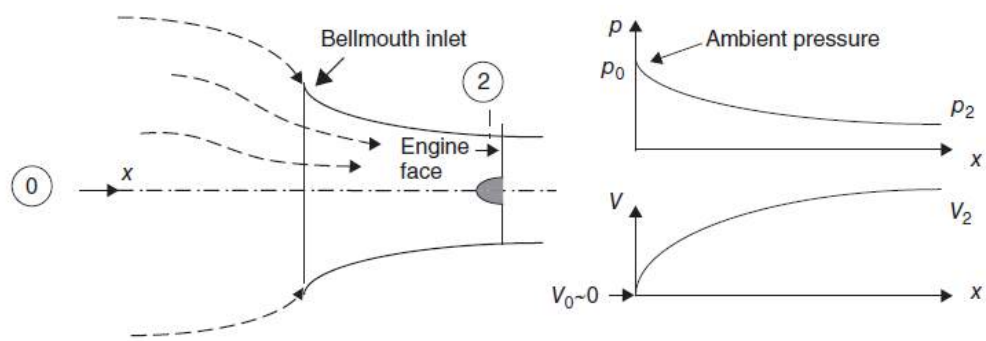

Numerical Example

An aircraft is flying at an altitude where the ambient static pressure is p_0 = 10 kPa and the flight Mach number is M_0 =.85. The total pressure at the engine face is measured to be p_{t2} = 15.88 kPa. Assuming the inlet is adiabatic and γ = 1.4, calculate

(a) the inlet total pressure recovery π_d

(b) the inlet adiabatic efficiency η_d

(c) the nondimensional entropy rise caused by the inlet $\Delta s_d/R$

Solution:

We first calculate the flight total pressure p_{t0}, and from definition of π_d (i.e., Equation 4.6), the inlet total pressure recovery.

$$p_{t0} = p_0[1 + (\gamma - 1)M_0^2/2]^{\frac{\gamma}{\gamma-1}} = 10\,\text{kPa}[1 + 0.2(0.85)^2]^{3.5}$$
$$= 16.04\,\text{kPa}$$
$$\pi_d \equiv p_{t2}/p_{t0} = 15.88/16.04 = 0.990$$

Inlet adiabatic efficiency η_d is calculated from Equation 4.4

$$\eta_d = \left[\left(\frac{p_{t2}}{p_0}\right)^{\frac{\gamma-1}{\gamma}} - 1\right] \Big/ \left(\frac{\gamma-1}{2}M_0^2\right)$$
$$= [(15.88/10)^{0.2857} - 1]/[0.2(0.85)^2] \cong 0.9775$$

The entropy rise is linked to the inlet total pressure loss parameter π_d via Equation 4.2,

$$\Delta s_d/R = -\ln(\pi_d) = -\ln(0.99) \cong 0.010$$

The Compressor:

In the gas turbine engine, compression of the air before expansion through the turbine is effected by one of two basic types of compressor, one giving centrifugal flow and the other axial flow. Both types are driven by the engine turbine and are usually coupled direct to the turbine shaft.

The centrifugal flow compressor (fig. 3-1) is a single or two stage unit employing an impeller to accelerate the air and a diffuser to produce the required pressure rise. The axial flow compressor (fig. 3-7 and fig. 3-8) is a multi-stage unit employing alternate .rows of rotating (rotor) blades and stationary (stator) vanes, to accelerate and diffuse the air until the required pressure rise is obtained. In some cases, particularly on small engines, an axial compressor is used to boost the inlet pressure to the centrifugal. With regard to the advantages and disadvantages of the two types, the centrifugal compressor is usually more robust than the axial compressor and is also easier to develop and manufacture. The axial compressor however consumes far more air than a can be designed to attain much higher pressure ratios. Since the air flow is an important factor in determining the amount of thrust, this means the axial compressor engine will also give more thrust for the same frontal area. This, plus the ability to increase the pressure ratio by addition of extra stages, has led to the adoption of axial compressors in most engine designs. However, the centrifugal compressor is still favoured for smaller engines where its simplicity and ruggedness outweigh any other disadvantages.

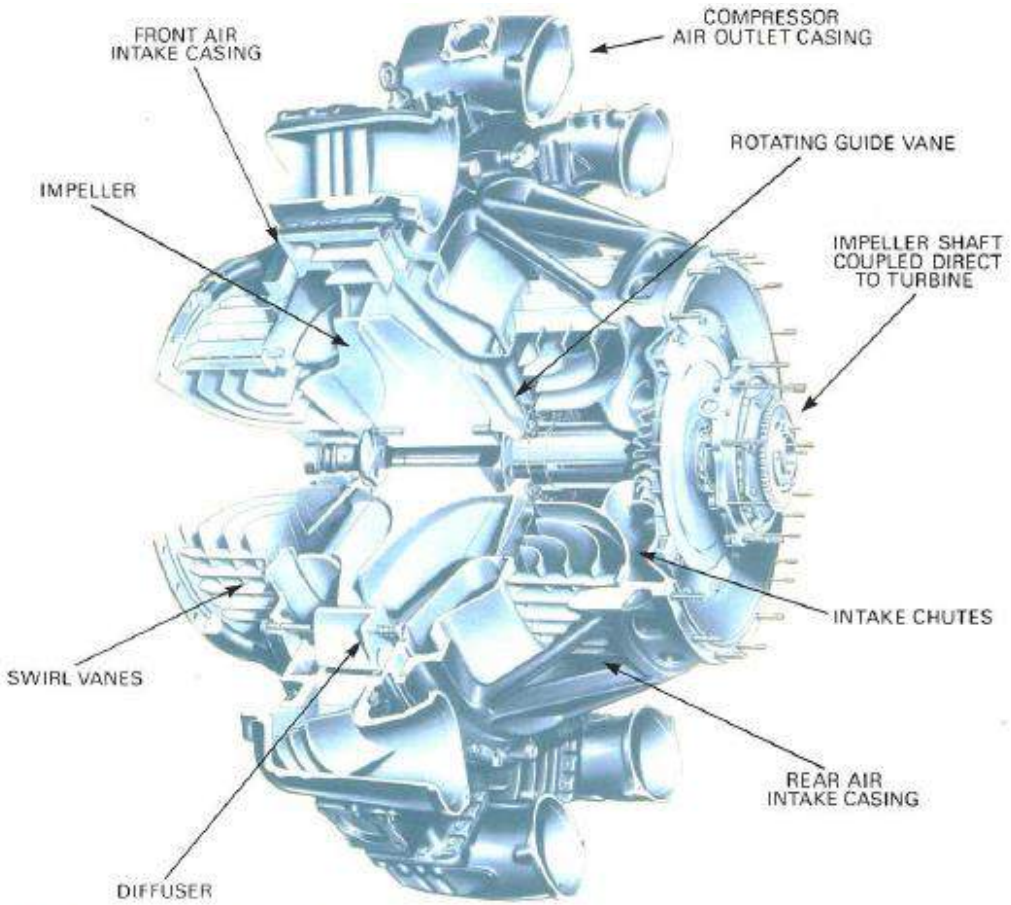

Fig. 3-1 A typical centrifugal flow compressor.

The trend to high pressure ratios which has favoured the adoption of axial compressors is because of the improved efficiency that results, which in turn leads to improved specific fuel consumption for a given thrust, ref. fig. 3-2.

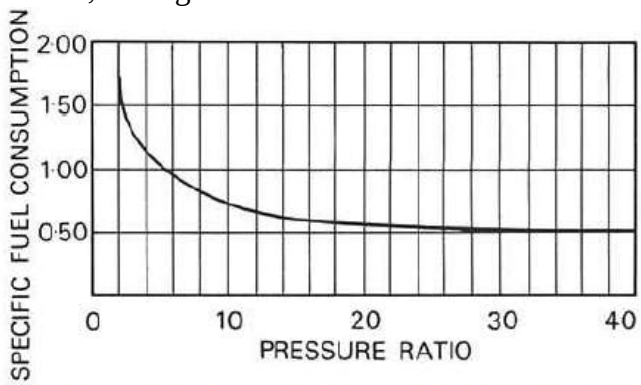

Fig. 3-2 Specific fuel consumption and pressure ratio.

THE CENTRIFUGAL FLOW COMPRESSOR

Centrifugal flow compressors have a single or double-sided impeller and occasionally a two-stage, single sided impeller is used, as on the Rolls-Royce Dart. The impeller is supported in a casing that also contains a ring of diffuser vanes. If a double-entry impeller is used, the airflow to the rear side is reversed in direction and a plenum chamber is required.

Principles of operation

The impeller is rotated at high speed by the turbine and air is continuously induced into the centre of the impeller. Centrifugal action causes it to flow radially outwards along the vanes to the impeller tip, thus accelerating the air and also causing a rise in pressure to occur. The engine intake duct may contain vanes that provide an initial swirl to the air entering the compressor. The air, on leaving the impeller, passes into the diffuser section where the passages form divergent nozzles that convert most of the kinetic energy into pressure energy, as illustrated in fig. 3-3. In practice, it is usual to design the compressor so that about half of the pressure rise occurs in the impeller and half in the diffuser. To maximize the airflow and pressure rise through the compressor requires the impeller to be rotated at high speed, therefore impellers are designed to operate at tip speeds of up to 1,600 ft/s.

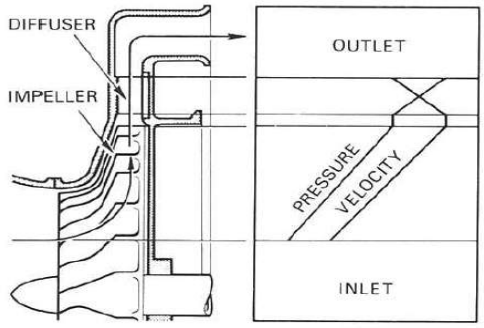

Fig. 3-3 Pressure and velocity changes through a centrifugal compressor.

Construction

The construction of the compressor centres around the impeller, diffuser and air intake system. The impeller shaft rotates in ball and roller bearings and is either common to the turbine shaft or split in the centre and connected by a coupling, which is usually designed for ease of detachment.

Impellers

The impeller consists of a .forged, disc with integral, radially disposed vanes on one or both sides (fig. 3-5) forming convergent passages in conjunction with the compressor casing. The vanes may beswept back, but for ease of manufacture straight radial vanes are usually employed. To ease the air from axial flow in the entry duct on to the rotating impeller, the vanes in the centre of the impeller are curved in the direction of rotation. The curved sections may be integral with the radial vanes or formed separately for easier and more accurate manufacture.

Fig. 3-5 Typical impellers for centrifugal compressors.

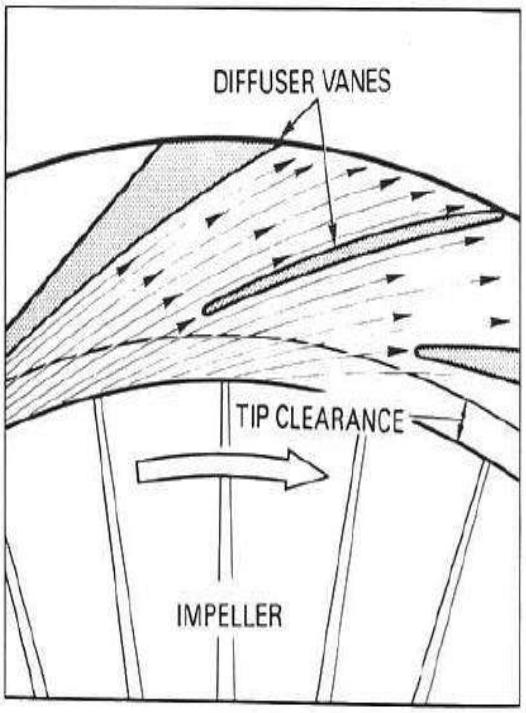

Fig. 3-6 Airflow at entry to diffuser.

Diffusers

The diffuser assembly may be an integral part of the compressor casing or a separately attached assembly. In each instance it consists of a number of vanes formed tangential to the impeller. The vane passages are divergent to convert the kinetic energy into pressure energy and the inner edges of the vanes are in line with the direction of the resultant airflow from the impeller (fig. 3-6). The clearance between the impeller and the diffuser is an important factor, as too small a clearance will set up aerodynamic buffeting impulses that could be transferred to the impeller and create an unsteady airflow and vibration.

THE AXIAL FLOW COMPRESSOR

An axial flow compressor (fig. 3-7 and fig. 3-8) consists of one or more rotor assemblies that carry blades of airfoil section. These assemblies are mounted between bearings in the casings which incorporate the stator vanes. The compressor is a multi-stage unit as the amount of pressure increase by each stage is small; a stage consists of a row of rotating blades followed by a row of stator vanes. Where several stages of compression operate in series on one shaft it becomes necessary to vary the stator vane angle to enable the compressor to operate effectively at speeds below the design condition. As the pressure ratio is increased the incorporation of variable stator vanes ensures that the airflow is directed onto the succeeding stage of rotor blades at an acceptable angle.

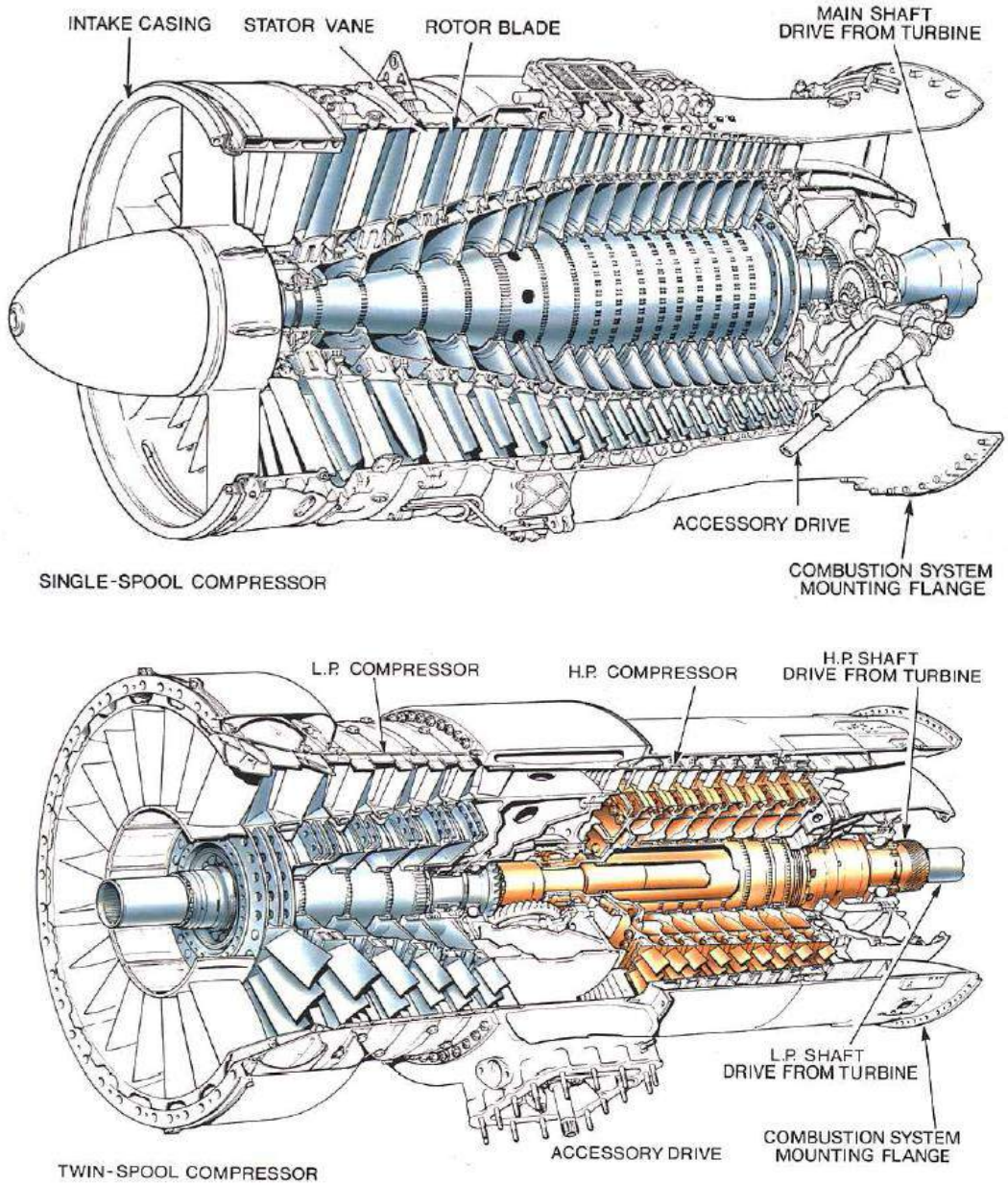

Fig. 3-7 Typical axial flow compressors.

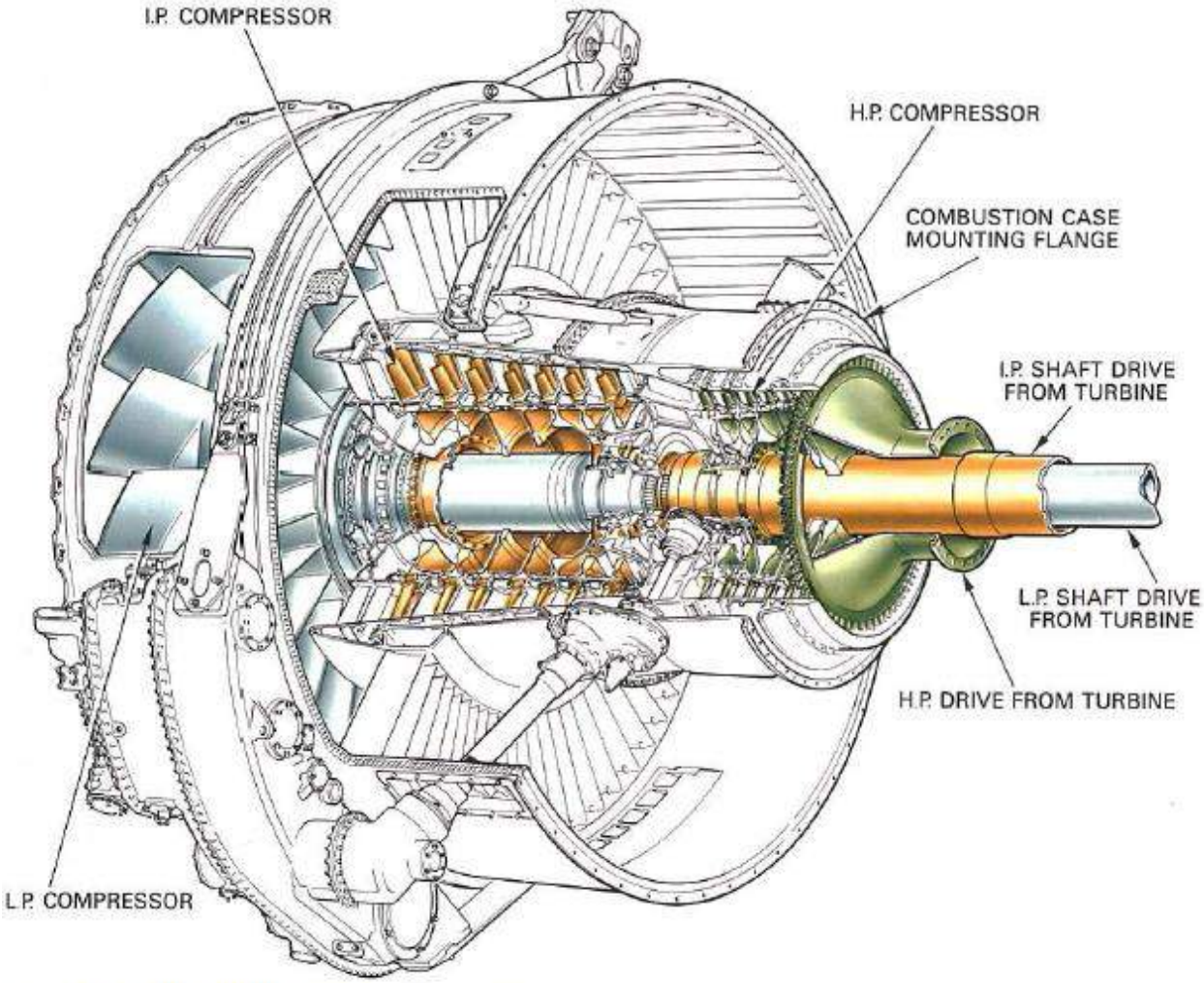

Fig. 3-8 Typical triple spool compressor.

From the front to the rear of the compressor, i.e. from the low to the high pressure end, there is a gradual reduction of the air annulus area between the rotor shaft and the stator casing. This is necessary to maintain a near constant air axial velocity as the density increases through the length of the compressor. The convergence of the air annulus is achieved by the tapering of the casing or rotor. A combination of both is also possible, with the arrangement being influenced by manufacturing problems and other mechanical design factors. A single-spool compressor (fig. 3-7) consists of one rotor assembly and stators with as many stages as necessary to achieve the desired pressure ratio and all the airflow from the intake passes through the compressor. The multi-spool compressor consists of two or more rotor assemblies, each driven by their own turbine at an optimum speed to achieve higher pressure ratios and to give greater operating flexibility.

Although a twin-spool compressor (fig. 3-7) can be used for a pure jet engine, it is most suitable for the by-pass type of engine where the front or low pressure compressor is designed to handle a larger airflow than the high pressure compressor. Only a percentage of the air from the low pressure compressor passes into the high pressure compressor; the remainder of the air, the by-pass flow, is ducted around the high pressure compressor. Both flows mix in the exhaust system before passing to the propelling nozzle. This arrangement

matches the velocity of the jet nearer to the optimum requirements of the aircraft and results in higher propulsive efficiency, hence lower fuel consumption. For this reason the pure jet engine where all the airflow passes through the full compression cycle is now obsolete for all but the highest speed aircraft. With the high by-pass ratio turbo-fan this trend is taken a stage further. The intake air undergoes only one stage of compression in the fan before being split between the core or gas generator system and the by-pass duct in the ratio of approximately one to five (fig. 3-8). This results in the optimum arrangement for passenger and/or transport aircraft flying at just below the speed of sound. The fan may be coupled to the front of a number of core compression stages (two shaft engine) or a separate shaft driven by its own turbine (three shaft engine).

Principles of operation

During operation the rotor is turned at high speed by the turbine so that air is continuously induced into the compressor, which is then accelerated by the rotating blades and swept rearwards onto the adjacent row of stator vanes. The pressure rise results from the energy imparted to the air in the rotor which increases the air velocity. The air is then decelerated (diffused) in the following stator passage and the kinetic energy translated into pressure. Stator vanes also serve to correct the deflection given to the air by the rotor blades and to present the air at the correct angle to the next stage of rotor blades. The last row of stator vanes usually act as air straighteners to remove swirl from the air prior to entry into the combustion system at a reasonably uniform axial velocity. Changes in pressure and velocity that occur in the airflow through the compressor are shown diagrammatically in fig. 3-9. The changes are accompanied by a progressive increase in air temperature as the pressure increases.

Across each stage the ratio of total pressures of outgoing air and inlet air is quite small, being between 1:1 and 1:2. The reason for the small pressure increase through each stage is that the rate of diffusion and the deflection angle of the blades must be limited if losses due to air breakaway at the blades and subsequent blade stall are to be avoided. Although the pressure ratio of each stage is small, every stage increases the exit pressure of the stage that precedes it. So whilst this first stage of a compressor may only increase the pressure by 3 to 4 lb. per sq. in., at the rear of a thirty to one compression system the stage pressure rise can be up to 80 lb, per sq. in, The ability to design multistage axial compressors with controlled air velocities and straight through flow, minimizes losses and results in a high efficiency and hence low fuel consumption. This gives it a further advantage over the centrifugal compressor where these conditions are fundamentally not so easily achieved.

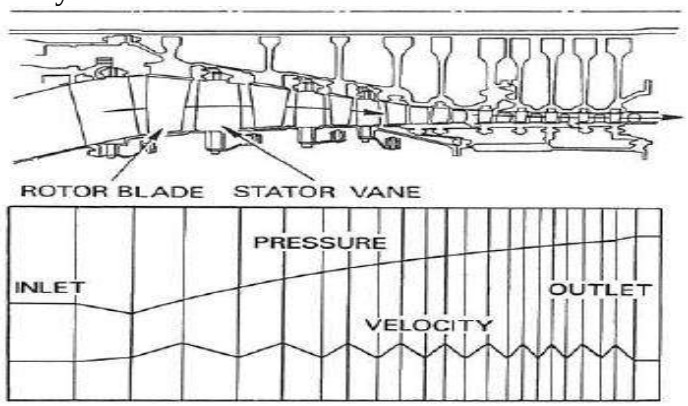

Fig. 3-9 Pressure and velocity changes through an axial compressor.

The more the pressure ratio of a compressor is increased the more difficult it becomes to ensure that it will operate efficiently over the full speed range. This is because the requirement for the ratio of inlet area to exit area, at the high speed case, results in an inlet area that becomes progressively too large relative to the exit area as the compressor speed and hence pressure ratio is reduced. The axial velocity of the inlet air in the front stages thus becomes low relative to the blade speed, this changes the incidence of the air onto the blades and a condition is reached where the flow separates and the compressor flow breaks down. Where high pressure ratios are required from a single compressor this problem can be overcome by introducing variable stator vanes in the front stages of the system. This corrects the incidence of air onto the rotor blades to angles which they can tolerate. An alternative is the incorporation of interstage bleeds, where a proportion of air after entering the compressor is removed at an intermediate stage and dumped into the bypass flow. While this method corrects the axial velocity through the preceding stages, energy is wasted and incorporation of variable stators is preferred.

The fan of the high by-pass ratio turbo-fan is an example of an axial compressor which has been optimized to meet the specific requirements of this cycle. While similar in principle to the core compressor stage, the proportions of design are such that the inner gas path is similar to that of the core compressor that follows it, while the tip diameter is considerably larger. The mass flow passed by the fan is typically six times that required by the core, the remaining five sixths by-pass the core and is expanded through its own coaxial nozzle, or may be mixed with the flow at exit from the core in a common nozzle. To optimize the cycle the by-pass flow has to be raised to a pressure of approximately 1.6 times the inlet pressure. This is achieved in the fan by utilizing very high tip speeds (1500 ft. per sec.) and airflow such that the by-pass section of the blades operate with a supersonic inlet air velocity of up to Mach 1.5 at the tip. The pressure that results is graded from a high value at the tip where relative velocities are highest to the more normal values of 1.3 to 1.4 at the inner radius which supercharges the core where aerodynamic design is more akin to that of a conventional compressor stage. The capability of this type of compressor stage achieves the cycle requirement of high flow per unit of frontal area, high efficiency and high pressure ratio in a single rotating blade row without inlet guide vanes within an acceptable engine diameter. Thus keeping weight and mechanical complexity at an acceptable level.

Construction

The construction of the compressor centres around the rotor assembly and casings. The rotor shaft is supported in ball and roller bearings and coupled to the turbine shaft in a manner that allows for any slight variation of alignment. The cylindrical casing assembly may consist of a number of cylindrical casings with a bolted axial joint between each stage or the casing may be in two halves with a bolted centre line joint. One or other of these construction methods is required in order that the casing can be assembled around the rotor.

Rotor

In compressor designs (fig. 3-10) the rotational speed is such that a disc is required to support the centrifugal blade load. Where a number of discs are fitted onto one shaft they may be coupled and secured together by a mechanical fixing but generally the discs are assembled and welded together, close to their periphery, thus forming an integral drum.

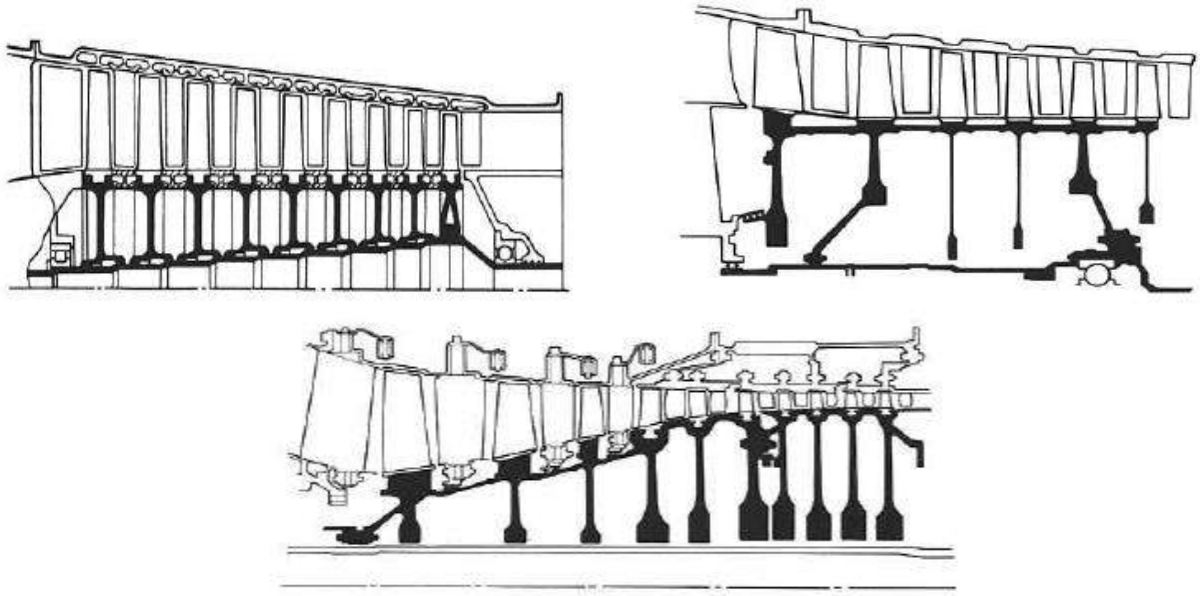

Fig. 3-10 Rotors of drum and disc construction.

Typical methods of securing rotor blades to the disc are shown in fig. 3-11, fixing may be circumferential or axial to suit special requirements of the stage. In general the aim is to design a securing feature that imparts the lightest possible load on the supporting disc thus minimizing disc weight. Whilst most compressor designs have separate blades for manufacturing and maintainability requirements, it becomes more difficult on the smallest engines to design a practical fixing. However this may be overcome by producing blades integral with the disc; the so called ’blisk’.

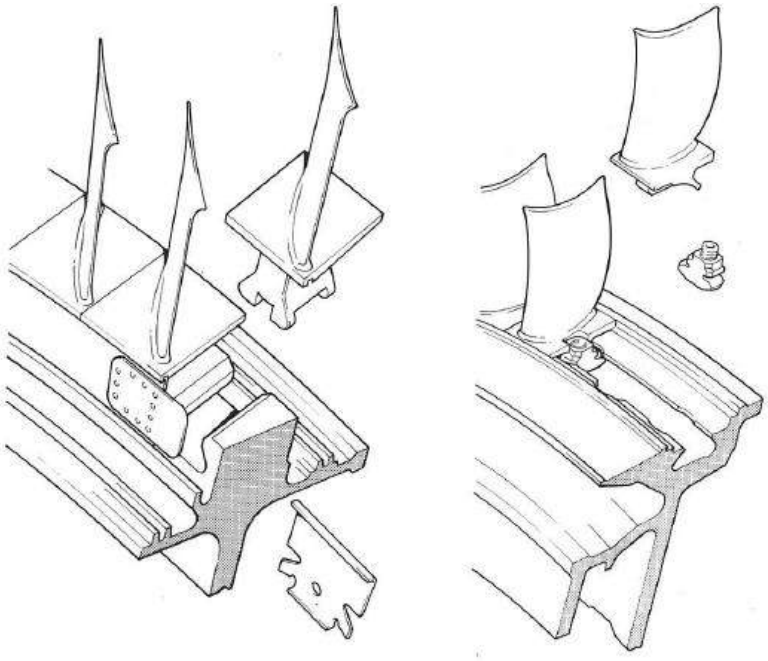

Fig. 3-11 Methods of securing blades to disc.

Rotor blades

The rotor blades are of airfoil section (fig. 3-12) and usually designed to give a pressure gradient along their length to ensure that the air maintains a reasonably uniform axial velocity. The higher pressure towards the tip balances out the centrifugal action of the rotor on the airstream. To obtain these conditions, it is necessary to 'twist' the blade from root to tip to give the correct angle of incidence at each point. Air flowing through a compressor creates two boundary layers of slow to stagnant air on the inner and outer walls. In order to compensate for the slow air in the boundary layer a localized increase in blade camber both at the blade tip and root has been introduced. The blade extremities appear as if formed by bending over each corner, hence the term 'end-bend'. Blades suffer centrifugal, aerodynamic and vibrating forces. Attachment is also important. There are two types of attachment.

- **Swallow tail attachment**: Easy fabrication.
- **Pivot attachment**: No bending stress.

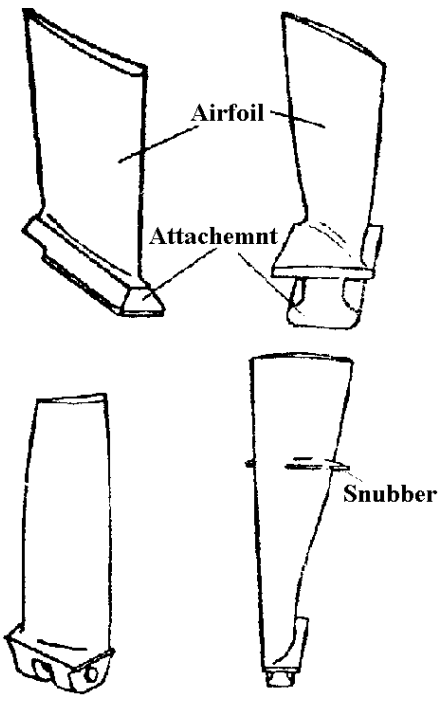

Stator vanes

The stator vanes are again of airfoil section and are secured into the compressor casing or into stator vane retaining rings, which are themselves secured to the casing (fig. 3-13). The vanes are often assembled in segments in the front stages and may be shrouded at their inner ends to minimize the vibrational effect of flow variations on the longer vanes. It is also necessary to lock the stator vanes in such a manner that they will not rotate around the casing.

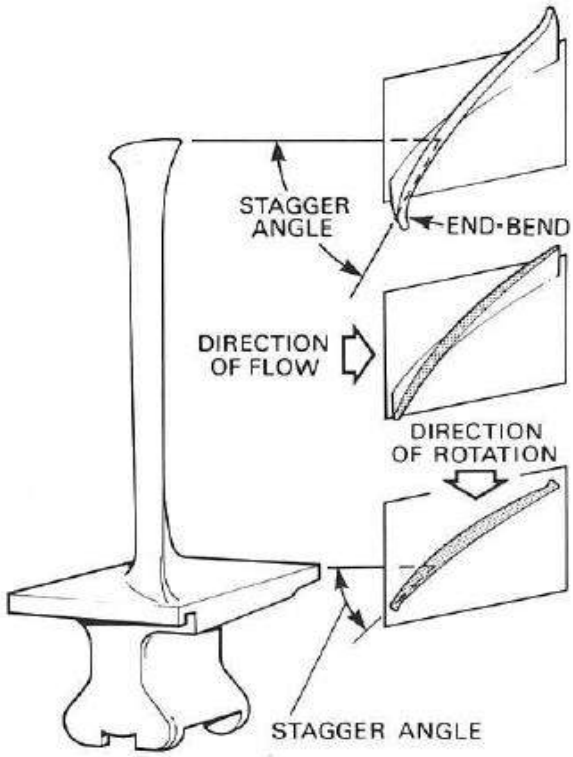

Fig. 3-12 A typical rotor blade showing twisted contour.

Operating Condition

Each stage of a multi-stage compressor possesses certain airflow characteristics that are dissimilar from those of its neighbour; thus to design a workable and efficient compressor, the characteristics of each stage must be carefully matched. This is a relatively simple process to implement for one set of conditions (design mass flow, pressure ratio and rotational speed), but is much more difficult when reasonable matching is to be retained with the compressor operating over a wide range of conditions such as an aircraft engine encounters.

If the operating conditions imposed upon the compressor blade departs too far from the design intention, breakdown of airflow and/or aerodynamically induced vibration will occur. These phenomena may take one of two forms; the blades may stall because the angle of incidence of the air relative to the blade is too high (positive incidence stall) or too low (negative incidence stall). The former is a front stage problem at low speeds and the latter usually affects the rear stages at high speed, either can lead to blade vibration which can induce rapid destruction. If the engine demands a pressure rise from the compressor, which is higher than the blading can sustain, 'surge' occurs. In this case there is an instantaneous breakdown of flow through the machine and the high pressure air in the combustion system is expelled forward through the compressor with a loud 'bang' and a resultant loss of engine thrust. Compressors are designed with adequate margin to ensure that this area of instability (fig. 3-14) is avoided.

In a simple way we can understand that for a given axial compressor, the rpm and mass flow rate are the design parameters that must match in order to produce a designed pressure ratio. At compressor stalling, the mass flow leaving the compressor is greatly reduced and as approximately 60% of this air is used to keep combustion chamber temperature within limits, the

temperature rises and can cause serious damage to the engine. If combustion pressure also increases due to excessive temperature, above compressor outlet pressure, the airflow will reverse in direction and surge forward through the compressor, with possible risk of damage to the engine called compressor stall and compressor surge.
A compressor stall can be recognized by the following: Vibration, Rumbling noise, Inability of the engine to accelerate, Rapid rise in exhaust gas temperature

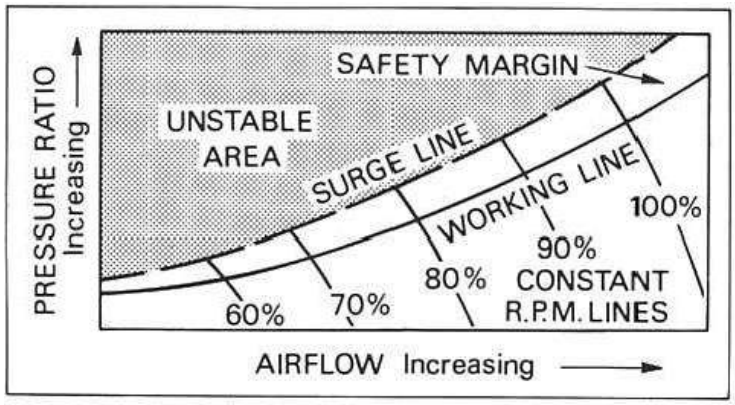

Fig. 3-14 Limits of stable airflow.

Air Flow Control

Where high pressure ratios on a single shaft are required it becomes necessary to introduce airflow control into the compressor design. This may take the form of variable inlet guide vanes for the first stage plus a number of stages incorporating variable stator vanes for the succeeding stages as the shaft pressure ratio is increased (fig. 3-15). As the compressor speed is reduced from its design value these static vanes are progressively closed in order to maintain an acceptable air angle value onto the following rotor blades. Additionally interstage bleed may be provided but its use in design is now usually limited to the provision of extra margin while the engine is being accelerated, because use at steady operating conditions is inefficient and wasteful of fuel.

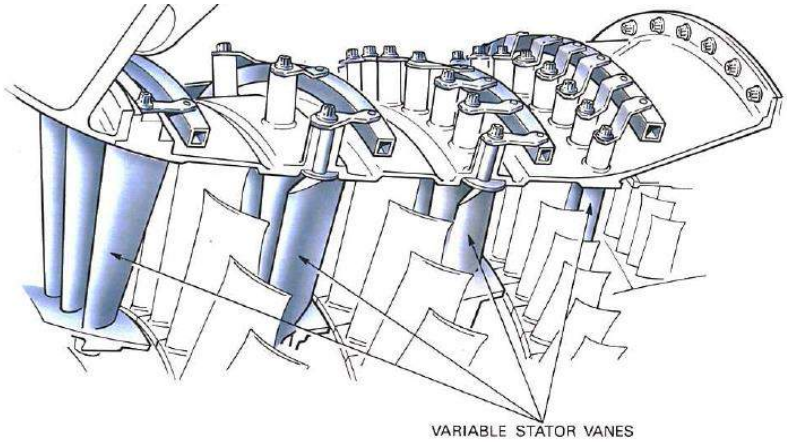

Fig. 3-15 Typical variable stator vanes.

Material

Materials are chosen to achieve the most cost effective design for the components in question, in practice for aero engine design this need is usually best satisfied by the lightest design that technology allows for the given loads and temperatures prevailing. For casing designs the need is for a light but rigid construction enabling blade tip clearances to be accurately maintained ensuring the highest possible efficiency. These needs are achieved by using aluminium at the front of the compression system followed by .alloy steel as compression temperature increases. Whilst for the final stages of the compression system, where temperature requirements possibly exceed the capability of the best steel, nickel based alloys may be required. The use of titanium in .preference to aluminium and steel is now more common; particularly in military engines where its high rigidity to density ratio can result in significant weight reduction. With the development of new manufacturing methods component costs can now be maintained at a more acceptable level in pite of high initial material costs. Stator vanes are normally produced from steel or nickel based alloys, a prime requirement being a high fatigue strength when "notched" by ingestion damage. Earlier designs specified aluminium alloys but because of its inferior ability to withstand damage its use has declined. Titanium may be used for stator vanes in the low pressure area but is unsuitable for the smaller stator vanes further rearwards in the compression system because of the higher pressures and temperatures encountered. Any excessive rub which may occur between rotating and static components as a result of other mechanical failures, can generate sufficient heat from friction to ignite the titanium. This in turn can lead to expensive repair costs and a possible airworthiness hazard. In the design of rotor discs, drums and blades, centrifugal forces dominate and the requirement is for metal with the highest ratio of strength to density. This results in the lightest possible rotor assembly which in turn reduces the forces on the engine structure enabling a further reduction in weight to be obtained. For this reason, titanium even with its high initial cost is the preferred material and has replaced the steel alloys that were favored in earlier designs. As higher temperature titanium alloys are developed and produced they are progressively displacing the nickel alloys for the disc and blades at the rear of the system.

Fig. 3-19 Typical types of fan blades.

The high by-pass ratio fan blade (fig. 3-19) only became a design possibility with the availability of titanium, conventional designs being machined from solid forgings. A low weight fan blade is

necessary because the front structure of the engine must be able to withstand the large out of balance forces that would result from a fan blade failure. To achieve a sufficiently light solid fan blade, even with titanium, requires a short axial length (or chord). However, with this design, the special feature of a mid-span support ('snubber' or 'clapper') is required to prevent aerodynamic instability. This design concept has the disadvantage of the snubber being situated in the supersonic flow where pressure losses are greatest, resulting in inefficiency and a reduction in airflow. This disadvantage has been overcome with the introduction of the Rolls-Royce designed wide chord fan blade; stability is provided by the increased chord of the blade thus avoiding the need for snubbers. The weight is maintained at a low level by fabricating the blade from skins of titanium incorporating a honeycomb core.

Centrifugal impeller material requirements are similar to those for the axial compressor rotors. Titanium is thus normally specified though aluminium may still be employed on the largest low pressure ratio designs where robust sections give adequate ingestion capability and temperatures are acceptably low.

Compressor Thermodynamics:

The thermodynamic process in a gas generator begins with the mechanical compression of air in the compressor. As the compressor discharge contains higher energy gas, that is, the compressed air, it requires *external power* to operate. The power comes from the turbine via a shaft, in case of an operating gas turbine engine. Other sources of external power may be used to *start* the engine, which are in the form of electric motor, air turbine, and hydraulic starters. The flow of air in a compressor is considered to be an essentially adiabatic process, which suggests that only a *negligible* amount of heat transfer takes place between the air inside and the ambient air outside the engine. Therefore, even in a real compressor analysis, we will still treat the flow as adiabatic. Perhaps a more physical argument in favor of neglecting the heat transfer in a compressor can be made by examining the order of magnitude of the energy transfer sources in a compressor. The power delivered to the medium in a compressor is achieved by one or more rows of rotating blades (called rotors) attached to one or more spinning shafts (typically referred to as *spools*). Each rotor blade, which changes the *spin* (or swirl) of a medium, will experience a counter torque as a reaction to its own action on the fluid. If we denote the rotor torque as τ, then the power delivered to the medium by the rotor spinning at the angular speed ω follows Newtonian mechanics, that is,

$$\wp = \tau \cdot \omega \qquad (4.7)$$

Atypical axial-flow compressor contains hundreds of rotor blades (distributed over several stages), which interact with the medium according to the above equation. Therefore, the rate of mechanical energy transfer in a typical modern compressor is usually measured in mega-Watt (MW) and is several orders of magnitude larger than heat transfer through the compressor wall. Symbolically, we may present this as

$$\wp_c \ggg \dot{Q}_w \qquad (4.8)$$

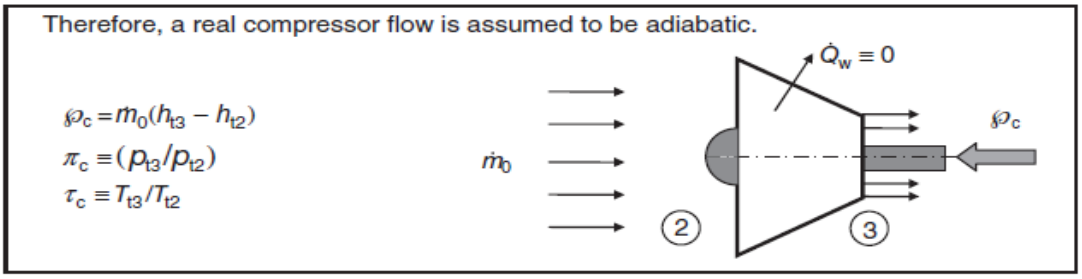

As a real process, however, the presence of wall friction acting on the medium through the boundary layer and shock waves caused by the relative supersonic flow through compressor blades will render the process irreversible. Therefore, the sources of irreversibility in a compressor are due to the viscosity of the medium and its consequences (boundary layer formation, wakes, vortex shedding) and the shock formation in relative supersonic passages.

The measure of irreversibility in a compressor may be thermodynamically defined through some form of compressor efficiency. There are two methods of compressor efficiency definitions. These are _ compressor adiabatic efficiency η_c

_ compressor polytropic efficiency e_c.

■ **FIGURE 4.6** **Enthalpy–entropy (h–s) diagram of an actual and ideal compression process (note Δs_c)**

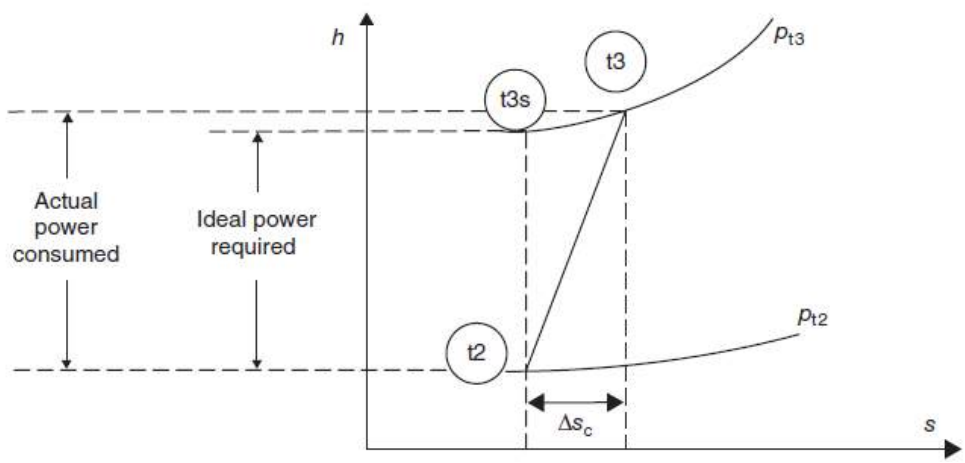

To define the compressor adiabatic efficiency η_c, we depict a "real" compression process on an h–s diagram, as shown in Figure 4.6 and compare it to an ideal, that is, isentropic process. The state "t_2" represents the *total* (or stagnation) state of the gas entering the compressor, typically designated by p_{t2} and T_{t2}. An actual flow in a compressor will follow the solid line from "t_2" to "t_3", thereby experiencing an entropy rise in the process, Δs_c. The actual total state of the gas is designated by "t_3" in Figure 4.6. The ratio p_{t3}/p_{t2} is known as the compressor pressure ratio, with a shorthand notation πc. The compressor total temperature ratio is depicted by, the shorthand notation, $\tau_c \equiv T_{t3}/T_{t2}$. Since the state "$t_3$" is the actual state of the gas at the exit of the compressor and is not achieved via an isentropic process, we cannot expect the isentropic relation between τc and π_c, to hold, that is,

$$\tau_c \neq \pi_c^{\frac{\gamma-1}{\gamma}} \qquad \textbf{(4.9)}$$

It can be seen from Figure 4.6 that the actual τ_c is larger than the ideal, that is, isentropic τ_c, which is denoted by the end state T_{t3s}. This fact actually helps with the exponent memorization in

a real compression process. The compressor adiabatic efficiency is the ratio of the ideal power required to the power consumed by the compressor, that is,

$$\eta_c \equiv \frac{h_{t3s} - h_{t2}}{h_{t3} - h_{t2}} = \frac{\Delta h_{t,\text{isentropic}}}{\Delta h_{t,\text{actual}}} \qquad \textbf{(4.10)}$$

The numerator in Equation 4.10 is the power-per-unit mass flowrate in an *ideal compressor* and the denominator is the power-per-unit mass flow rate in the actual compressor. If we divide the numerator and denominator of Equation 4.10 by h_{t2}, we get

$$\eta_c = \frac{T_{t3s}/T_{t2} - 1}{T_{t3}/T_{t2} - 1} \qquad \textbf{(4.11)}$$

Since the thermodynamic states "t_{3s}" and "t_2" are on the same isentrope, the temperature and pressure ratios are then related via the isentropic formula, that is,

$$\frac{T_{t3s}}{T_{t2}} = \left(\frac{p_{t3s}}{p_{t2}}\right)^{\frac{\gamma-1}{\gamma}} = \left(\frac{p_{t3}}{p_{t2}}\right)^{\frac{\gamma-1}{\gamma}} = \pi_c^{\frac{\gamma-1}{\gamma}} \qquad \textbf{(4.12)}$$

Therefore, compressor adiabatic efficiency may be expressed in terms of compressor pressure and temperature ratios as

$$\eta_c = \frac{\pi_c^{\frac{\gamma-1}{\gamma}} - 1}{\tau_c - 1} \qquad \textbf{(4.13)}$$

Equation 4.13 involves three parameters, η_c, π_c, and τ_c. It can be used to calculate τ_c for a given compressor pressure ratio and adiabatic efficiency. As compressor pressure ratio and efficiency are typically known and assumed quantities in a gas turbine cycle analysis, the only unknown in Equation 4.13 is τ_c. A second efficiency parameter in a compressor is *polytropic efficiency* e_c. As might be expected, compressor adiabatic and polytropic efficiencies are related. The definition of compressor polytropic efficiency is

$$e_c \equiv \frac{dh_{ts}}{dh_t} \qquad \textbf{(4.14)}$$

It is interesting to compare the definition of compressor adiabatic efficiency, involving finite jumps (Δh_t), and the polytropic efficiency, which takes infinitesimal steps (dh_t). The conclusion can be reached that the polytropic efficiency is actually the adiabatic efficiency of a compressor with *small* pressure ratio. Consequently, compressor polytropic efficiency is also called *small stage efficiency*. From the combined first and second law of thermodynamics, we have

$$T_t ds = dh_t - \frac{dp_t}{\rho_t} \qquad \textbf{(4.15)}$$

We deduce that for an isentropic process, that is, $ds = 0$, $dh_t = dh_{ts}$ and, therefore,

$$dh_{ts} = \frac{dp_t}{\rho_t} \qquad \textbf{(4.16)}$$

If we substitute Equation 4.16 in 4.14 and replace density with pressure and temperature from the perfect gas law, we get

$$e_c = \frac{\dfrac{dp_t}{p_t}}{\dfrac{dh_t}{RT_t}} = \frac{\dfrac{dp_t}{p_t}}{\dfrac{C_p dT_t}{RT_t}} = \frac{\dfrac{dp_t}{p_t}}{\dfrac{\gamma}{\gamma-1}\dfrac{dT_t}{T_t}} \tag{4.17}$$

$$\frac{dp_t}{p_t} = \frac{\gamma e_c}{\gamma - 1}\frac{dT_t}{T_t} \tag{4.18}$$

which can now be integrated between the inlet and exit of the compressor to yield

$$\frac{p_{t3}}{p_{t2}} = \pi_c = \left(\frac{T_{t3}}{T_{t2}}\right)^{\frac{\gamma e_c}{\gamma-1}} = (\tau_c)^{\frac{\gamma e_c}{\gamma-1}} \tag{4.19}$$

To express the compressor total temperature ratio in terms of compressor pressure ratio and polytropic efficiency, Equation 4.19 can be rewritten as

$$\tau_c = \pi_c^{\frac{\gamma-1}{\gamma e_c}} \tag{4.20}$$

The presence of e_c in the denominator of the above exponent (Equation 4.20) causes the exponent of π_c to be greater than its isentropic exponent (which is $(\gamma - 1)/\gamma$), therefore,

$$\tau_{c,\text{real}} > \tau_{c,\text{isentropic}} \quad \text{or} \quad T_{t3} > T_{t3s} \tag{4.21}$$

as noted earlier (Figure 4.6). The physical argument for higher actual T_t than the isentropic T_t (to achieve the same compressor pressure ratio) can be made on the grounds that *lost work* to overcome the irreversibility in the real process (friction, shock) is converted into heat, a higher exit T_t is reached in a real machine due to dissipation. On the contrary, for a given compressor pressure ratio π_c, an ideal compressor consumes less power than an actual compressor (the factor being η_c, as defined earlier). Again, the absence of dissipative mechanisms, leading to lost work, is cited as the reason for a reversible flow machine to require less power to run. Now, to relate the two types of compressor efficiency description, e_c and η_c, we may substitute Equation 4.20 into Equation 4.13, to get

$$\eta_c = \frac{\pi_c^{\frac{\gamma-1}{\gamma}} - 1}{\tau_c - 1} = \frac{\pi_c^{\frac{\gamma-1}{\gamma}} - 1}{\pi_c^{\frac{\gamma-1}{\gamma e_c}} - 1} \tag{4.22}$$

Equation 4.22 is plotted in Figure 4.7. The compressor adiabatic efficiency η_c is a function of compressor pressure ratio, while the polytropic efficiency is independent of it. Consequently, in a cycle analysis, we usually assume the polytropic efficiency e_c as the figure of merit for a compressor (and turbine) and then we can maintain e_c as constant in our engine off-design analysis. Typical values for the polytropic efficiency in modern compressors are in the range 88–92%. So far, we have studied the thermodynamics of the mechanical compression through the stagnation states of the working medium. It is also instructive to examine the static states of the gas in a compressor as well. The mental connection between these states will help us with the fluid dynamics of the compressors. Figure 4.8 is basically an elaborate version of the earlier Figure 4.6, to which we have added the static states of the gas at the inlet and exit of the

compressor. These states, that is, the local stagnation and static states, when plotted on the *h*–*s* diagram, are distanced from each other only by the amount of local (specific) kinetic energy $V^2/2$ and on the same isentrope. The flow velocity at the compressor inlet, V_2, is nearly the same as the fluid velocity at the compressor exit, V_3, by design. This explains why the vertical gap shown in Figure 4.8, between the static and stagnation states at 2 and 3 is nearly the same, that is,

$$V_2^2/2 \approx V_3^2/2 \qquad (4.23)$$

This design philosophy, that is, $V_2 = V_3$, is a part of the so-called constant through flow assumption often used in compressor aerodynamics.

■ **FIGURE 4.7**
Variation of compressor adiabatic efficiency with the pressure ratio and polytropic efficiency

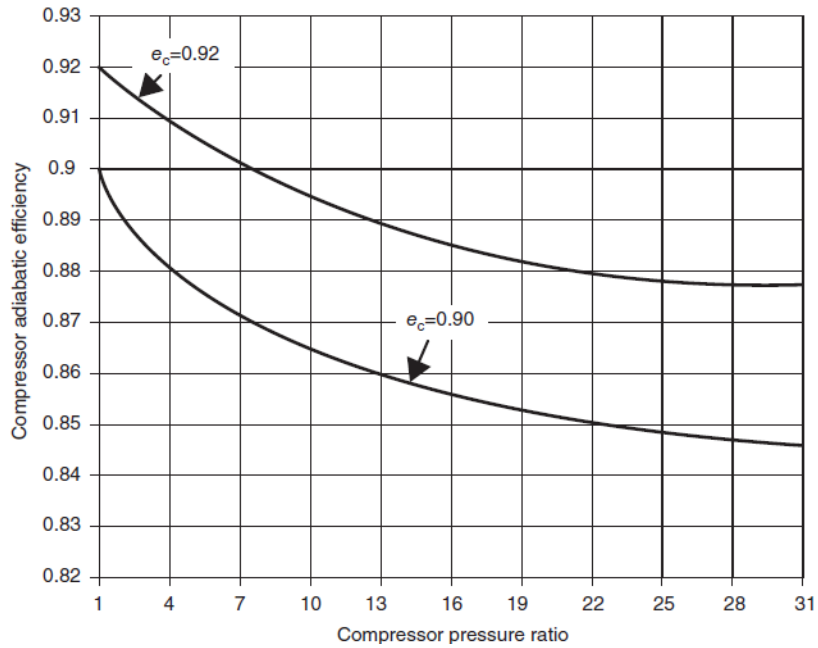

■ **FIGURE 4.8**
Static and stagnation states at the compressor inlet and exit on an *h*–*s* diagram

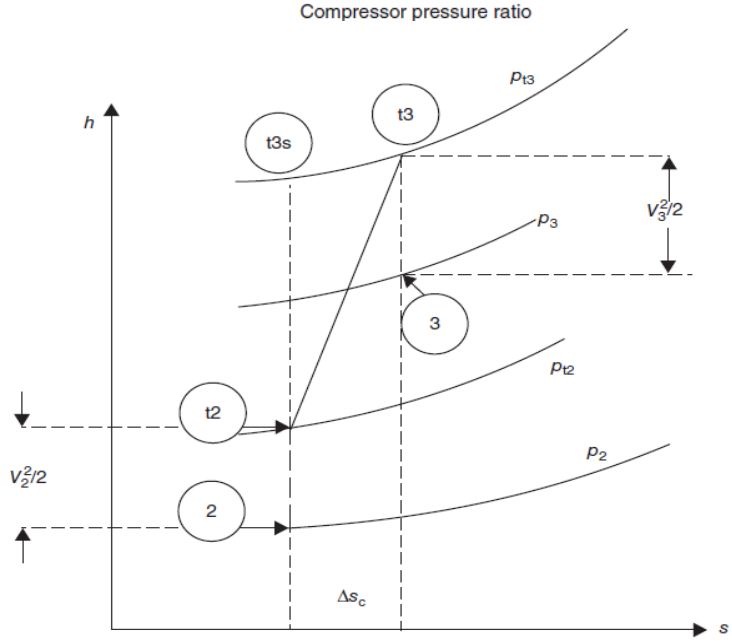

Numerical Example:

A multistage axial-flow compressor has a mass flow rate of 50 kg/s and a total pressure ratio of 35. The compressor polytropic efficiency is $e_c = 0.90$. The inlet flow condition to the compressor is described by $T_{t2} = 288$ K and $p_{t2} = 100$ kPa. Assuming the flow in the compressor is adiabatic, and constant gas properties throughout the compressor are assumed, i.e., $\gamma = 1.4$ and $c_p = 1004$ J/kg · K, calculate

(a) compressor exit total temperature T_{t3} in K

(b) compressor adiabatic efficiency η_c

(c) compressor shaft power $\wp_c$ in MW

Solution:

Following Equation 4.20, we relate compressor total temperature and pressure ratio via polytropic efficiency,

$$\tau_c = \pi_c^{\frac{\gamma-1}{\gamma \cdot e_c}} = (35)^{0.31746} \cong 3.0916$$

Therefore, the exit total temperature is $T_{t3} = 3.0916\ T_{t2} = 3.0916(288\text{ K}) \cong 890.4$ K.

Compressor adiabatic efficiency is related to the polytropic efficiency and compressor pressure ratio, via Equation 4.13

$$\eta_c = \frac{\pi_c^{\frac{\gamma-1}{\gamma}} - 1}{\tau_c - 1} = \frac{35^{0.2857} - 1}{3.0916 - 1} \approx 0.8422$$

Therefore, compressor adiabatic efficiency is $\eta_c \cong 84.22\%$.

Compressor shaft power is proportional to the mass flow rate (i.e., the size of the compressor) as well as the total enthalpy rise across the compressor, according to

$$\begin{aligned}\wp_c &= \dot{m}(h_{t3} - h_{t2}) = \dot{m}c_p(T_{t3} - T_{t2}) \\ &= (50\,\text{kg/s})(1004\,\text{J/kg}\cdot\text{K})(890.4 - 288)\,\text{K} \\ &\approx 30.24\,\text{MW}\end{aligned}$$

Therefore the shaft power delivered to the compressor is $\wp_c \approx 30.24$ MW

Combustion Chamber

The combustion chamber has the difficult task of burning large quantities of fuel, supplied through the fuel spray nozzles, with extensive volumes of air, supplied by the compressor, and releasing the heat in such a manner that the air is expanded and accelerated to give a smooth stream of uniformly heated gas at all conditions required by the turbine. This task must be accomplished with the minimum loss in pressure and with the maximum heat release for the limited space available. The amount of fuel added to the air will depend upon the temperature rise required. However, the maximum temperature is limited to within the range of 850 to 1700 deg. C. by the materials from which the turbine blades and nozzles are made. The air has already been heated to between 200 and 550 deg. C. by the work done during compression, giving a temperature rise requirement of 650 to 1150 deg. C. from the combustion process. Since the gas temperature required at the turbine varies with engine thrust, and in the case of the turbo-propeller engine upon the power required, the combustion chamber must also be capable of maintaining stable and efficient combustion over a wide range of engine operating conditions.

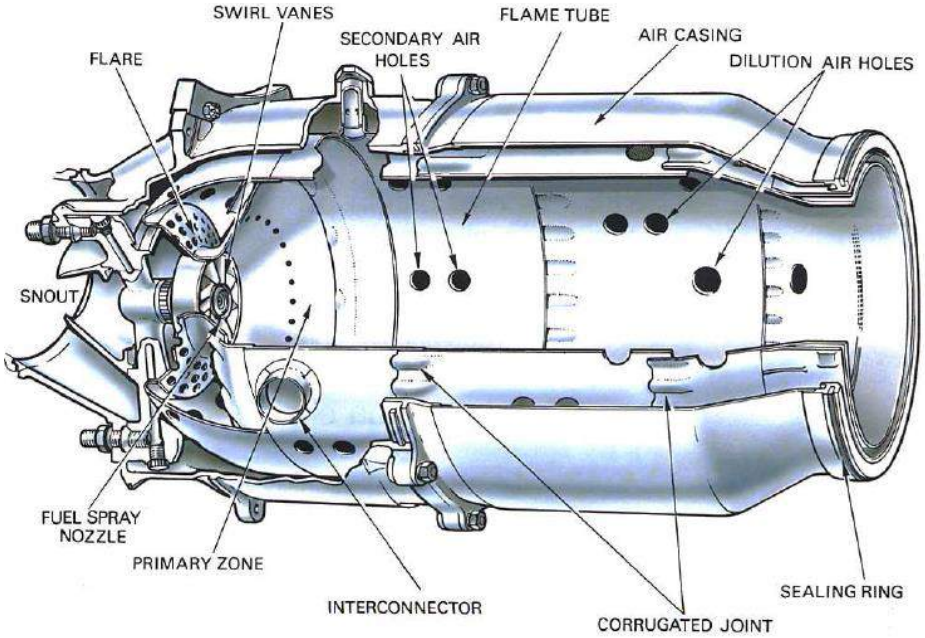

Fig. 4-1 An early combustion chamber.

Efficient combustion has become increasingly important because of the rapid rise in commercial aircraft traffic and the consequent increase in atmospheric pollution, which is seen by the general public as exhaust smoke.

Combustion Process

Air from the engine compressor enters the combustion chamber at a velocity up to 500 feet per second, but because at this velocity the air speed is far too high for combustion, the first thing that the chamber must do is to diffuse it, i.e. decelerate it and raise its static pressure. Since the speed of burning kerosine at normal mixture ratios is only a few feet per second, any fuel lit even in the diffused air stream, which now has a velocity of about 80 feet per second, would be blown away. A region of low axial velocity has therefore to be created in the chamber, so that the flame will remain alight throughout the range of engine operating conditions. In normal operation, the

overall air/fuel ratio of a combustion chamber can vary between 45:1 and 130:1, However, kerosine will only burn efficiently at, or close to, a ratio of 15:1, so the fuel must be burned with only part of the air entering the chamber, in what is called a primary combustion zone. This is achieved by means of a flame tube (combustion liner) that has various devices for metering the airflow distribution along the chamber. Approximately 20 per cent of the air mass flow is taken in by the snout or entry section. Immediately downstream of the snout are swirl vanes and a perforated flare, through which air passes into the primary combustion zone. The swirling air induces a flow upstream of the centre of the flame tube and promotes the desired recirculation. The air not picked up by the snout flows into the annular space between the flame tube and the air casing. Through the wall of the flame tube body, adjacent to the combustion zone, are a selected number of secondary holes through which a further 20 per cent of the main flow of air passes into the primary zone. The air from the swirl vanes and that from the secondary air holes interacts and creates a region of
low velocity recirculation. This takes the form of a toroidal vortex, similar to a smoke ring, which has the effect of stabilizing and anchoring the flame. The recirculating gases hasten the burning of freshly injected fuel droplets by rapidly bringing them to ignition temperature.

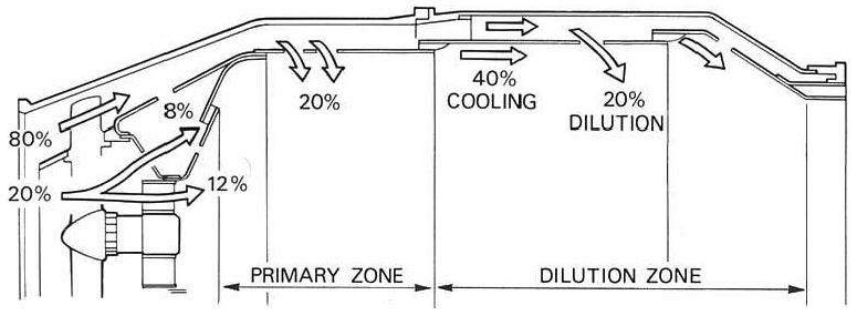

Fig. 4-2 Apportioning the airflow.

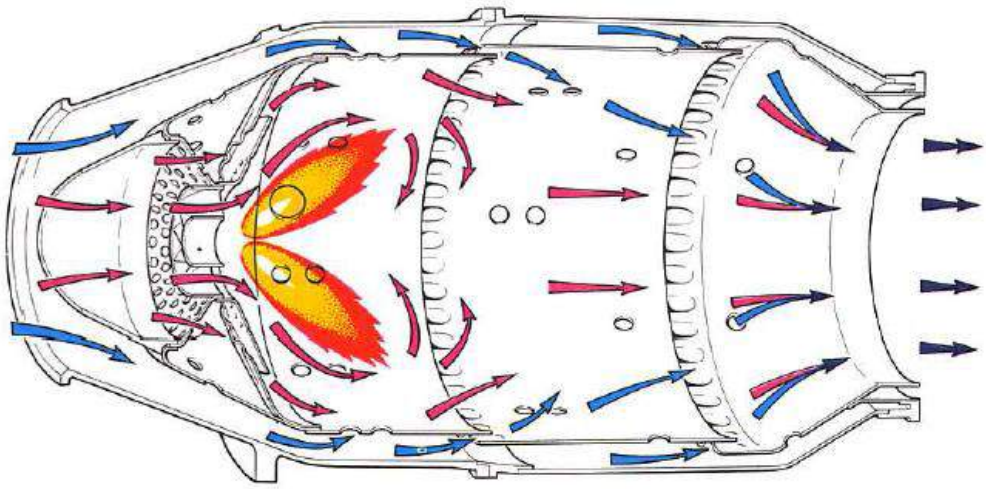

Fig. 4-3 Flame stabilizing and general airflow pattern.

It is arranged that the conical fuel spray from the nozzle intersects the recirculation vortex at its centre. This action, together with the general turbulence in the primary zone, greatly assists in breaking up the fuel and mixing it with the incoming air. The temperature of the gases released by combustion is about 1,800 to 2,000 deg. C., which is far too hot for entry to the nozzle guide vanes of the turbine. The air not used for combustion, which amounts to about 60 per cent of the total airflow, is therefore introduced progressively into the flame tube. Approximately a third of this is used to lower the gas temperature in the dilution zone before it enters the turbine and the remainder is used for cooling the walls of the flame tube. This is achieved by a film of cooling air flowing along the inside surface of the flame tube wall, insulating it from the hot combustion gases. A recent development allows cooling air to enter a network of passages within the flame tube wall before exiting to form an insulating film of air, this can reduce the required wall cooling airflow by up to 50 per cent. Combustion should be completed before the dilution air enters the flame tube, otherwise the incoming air will cool the flame and incomplete combustion will result.

An electric spark from an igniter plug initiates combustion and the flame is then self sustained. The design of a combustion chamber and the method of adding the fuel may vary considerably, but the airflow distribution used to effect and maintain combustion is always very similar to that described.

TYPES OF COMBUSTION CHAMBER

There are three main types of combustion chamber in use for gas turbine engines. These are the multiple chamber, the tubo-annular chamber and the annular chamber.

Multiple combustion chamber

This type of combustion chamber is used on centrifugal compressor engines and the earlier types of axial flow compressor engines. It is a direct development of the early type of Whittle combustion chamber. The major difference is that the Whittle chamber had a reverse flow as illustrated in fig. 4-6 but, as this created a considerable pressure loss, the straight-through multiple chamber was developed by Joseph Lucas Limited.

The chambers are disposed around the engine (fig. 4-7) and compressor delivery air is directed by ducts to pass into the individual chambers. Each chamber has an inner flame tube around which there is an air casing. The air passes through the flame tube snout and also between the tube and the outer casing. The separate flame tubes are all interconnected. This allows each tube to operate at the same pressure and also allows combustion to propagate around the flame tubes during engine starting. However there occurs the problem of flame propagation and light round. These type of combustion chamber are easy to be tested in lab as a single can be dissembled from the assembly. Some of the limitations of this type of combustion chamber are, that they are not efficient in terms of use of space. They are comparatively heavy and they do not transfer mechanical forces to the body.

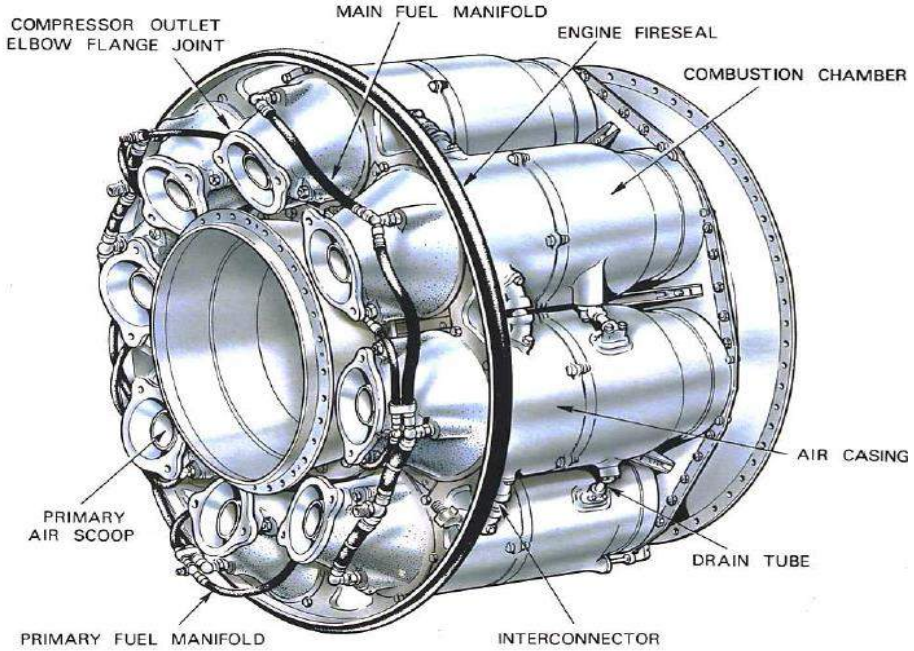

Fig. 4-7 Multiple combustion chambers.

Tubo-annular combustion chamber

It is also known as a *'can-annular'* system. The tubo-annular combustion chamber bridges the evolutionary gap between the multiple and annular types. A number of flame tubes are fitted inside a common air casing. The airflow is similar to that already described. This arrangement combines the ease of overhaul and testing of the multiple system with the compactness of the annular system.

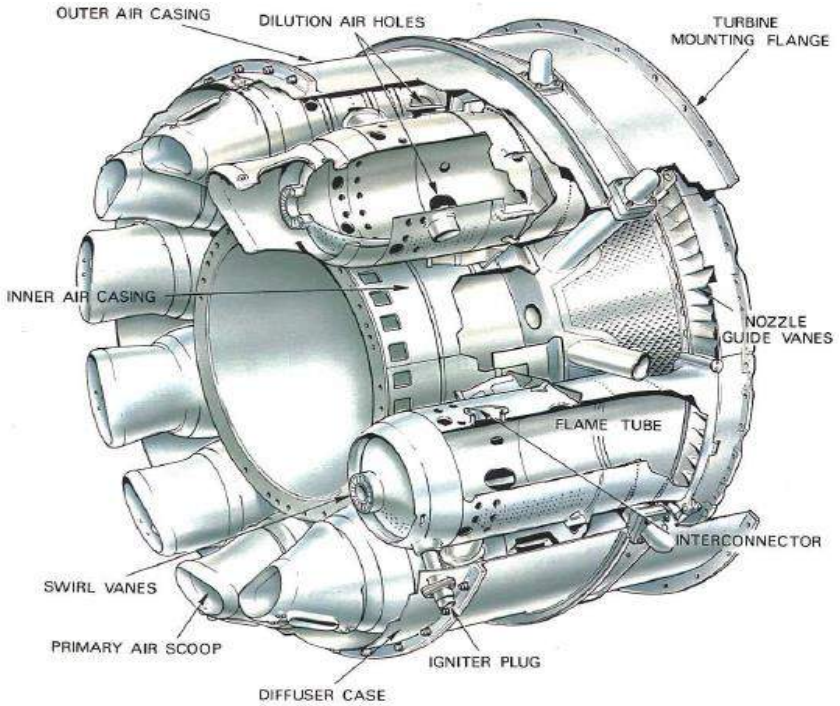

Fig. 4-8 Tubo-annular combustion chamber.

Annular combustion chamber

This type of combustion chamber consists of a single flame tube, completely annular in form, which is contained in an inner and outer casing. The airflow through the flame tube is similar to that already described, the chamber being open at the front to the compressor and at the rear to the turbine nozzles. The main advantage of the annular chamber is that, for the same power output, the length of the chamber is only 75 per cent of that of a tubo-annular system of the same diameter, resulting in considerable saving of weight and production cost. Another advantage is the elimination of combustion propagation problems from chamber to chamber. In comparison with a tubo-annular combustion system, the wall area of a comparable annular chamber is much less; consequently the amount of cooling air required to prevent the burning of the flame tube wall is less, by approximately 15 per cent, This reduction in cooling air raises the combustion efficiency to virtually eliminate unburnt fuel, and oxidizes the carbon monoxide to non-toxic carbon dioxide, thus reducing air pollution. The introduction of the air spray type fuel spray nozzle to this type of combustion chamber also greatly improves the preparation of fuel for combustion by aerating the over-rich pockets of fuel vapours close to the spray nozzle; this results in a large reduction in initial carbon formation.

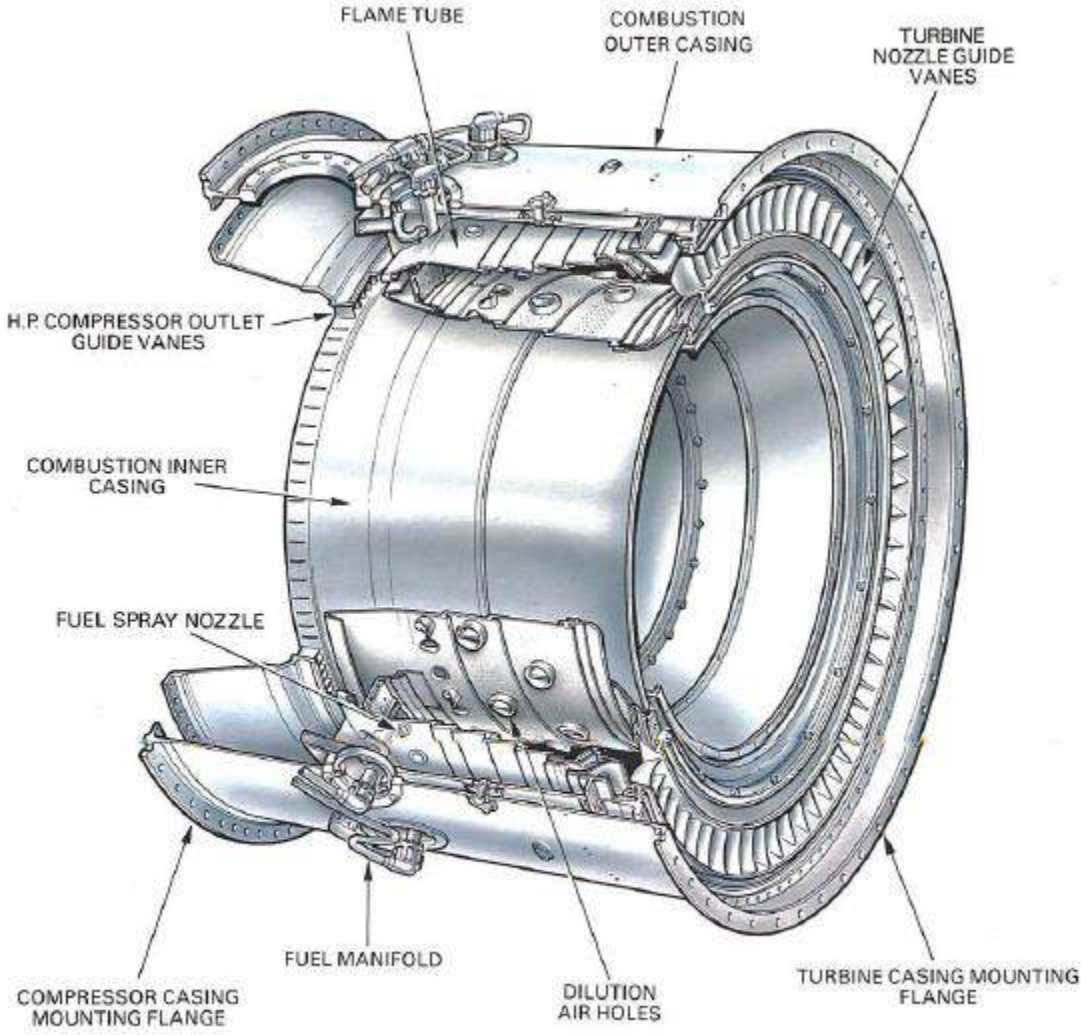

Fig. 4-9 Annular combustion chamber.

Combustion Chamber Thermodynamics

In the combustor, the air is mixed with the fuel and a chemical reaction ensues which is *exothermic*, that is, it results in a heat release. The ideal burner is considered to behave like a reversible heater, which in the combustion context, means very low burning, $M_b \approx 0$, and with no friction acting on its walls. Under such circumstances, the total pressure remains conserved.

In a real combustor, due to wall friction, turbulent mixing and chemical reaction at finite Mach number, the total pressure drops, that is,

$$\pi_b = \frac{p_{t4}}{p_{t3}} < 1 \quad \text{“}\textit{real}\text{ combustion chamber”} \qquad \textbf{(4.24)}$$

$$\pi_b = 1 \quad \text{“}\textit{ideal}\text{ combustion chamber”} \qquad \textbf{(4.25)}$$

Kerrebrock gives an approximate expression for π_b in terms of the average Mach number of the gas in the burner, M_b, as

$$\pi_b \approx 1 - \varepsilon \frac{\gamma}{2} M_b^2 \quad \text{where} \quad 1 < \varepsilon < 2 \qquad \textbf{(4.26)}$$

The total pressure loss in a burner is then proportional to the average dynamic pressure of the gases inside the burner, that is, $\propto \gamma / 2M^2_b$, where the proportionality coefficient is ε. Assuming an average Mach number of gases of 0.2 and $\varepsilon = 2$, we get $\pi_b \approx 0.95$ (for a $\gamma \approx 1.33$). This formula is obviously not valid for supersonic combustion throughflows, rather it points out the merits of *slow* combustion in a conventional burner. A schematic diagram of a combustion chamber, and its essential components, is shown in below.

■ **FIGURE 4.9**
Components of a conventional combustion chamber and the first turbine stage

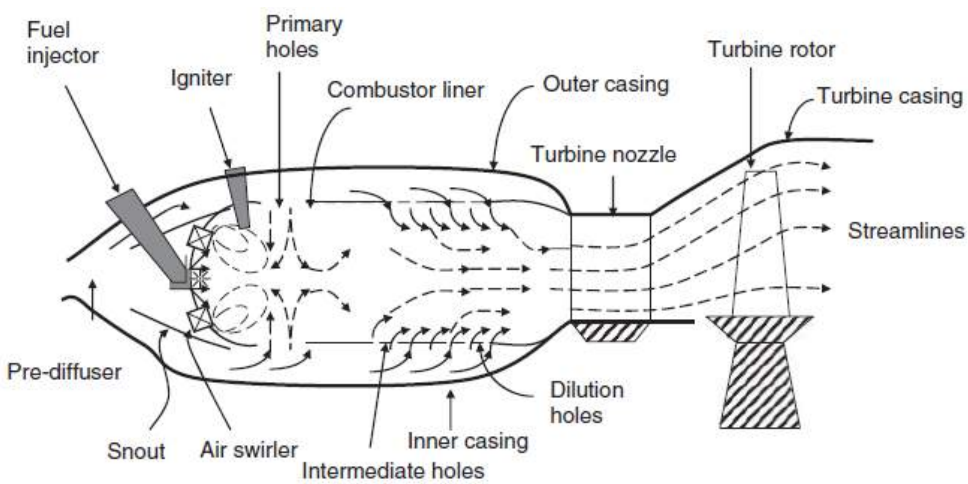

A preliminary discussion of the components of the combustion chamber is useful at this time. The inlet diffuser decelerates the compressor discharge flow to a Mach number of about 0.2–0.3. The low-speed flow will provide an efficient burning environment in the combustor. Mixing improvement with the fuel in the combustor primary zone is achieved via the air swirler. A recirculation zone is created that provides the necessary stability in the primary combustion zone. To create a fuel-rich environment in the primary zone to sustain combustion, a large percentage of air is diverted around a dome-like structure. The airflow that has bypassed the burner primary zone will enter the combustor as the cooling flow through a series of cooling holes (as shown). The fuel-air mixture is ignited in the combustor primary zone via an igniter properly positioned in the dome area. For the purposes of *cycle analysis*, a combustor flow is analyzed only at its

inlet and outlet. Thus, we will not consider the details of combustion processes such as atomization, vaporization, mixing, chemical reaction, and dilution in the cycle analysis phase. Also, we do not consider pollutant formation and the means of reducing it in this chapter. We will address these issues in a later chapter dealing with combustor flow and design considerations. Obviously, with the details of flow and reaction omitted, we need to make assumptions regarding the loss of total pressure and burner efficiency in the cycle analysis only.

■ FIGURE 4.10
Block diagram of a burner with mass and energy balance

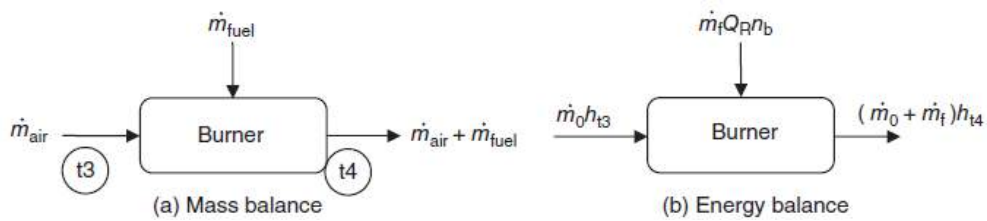

A block diagram representation of a combustor, useful in cycle analysis, is shown in Figure 4.10. Figures 4.10a and 4.10b are the steady-state mass and the energy balance applied to the combustion chamber, that is,

$$\dot{m}_4 = \dot{m}_0 + \dot{m}_f = \dot{m}_0(1 + f) \qquad \textbf{(4.27)}$$

Where f is the fuel-air ratio. Using the energy balance in Figure 4.10b gives

$$\dot{m}_0 h_{t3} + \dot{m}_f Q_R \eta_b = \left(\dot{m}_0 + \dot{m}_f\right) h_{t4} = \dot{m}_0(1 + f) h_{t4} \qquad \textbf{(4.28)}$$

The fuel is characterized by its *energy content per unit mass*, that is, the amount of thermal energy inherent in the fuel, capable of being released in a chemical reaction. This parameter is heat of reaction and is given the symbol QR. The unit for this parameter is energy/mass, which in the metric system is kJ/kg and in the British system of units is BTU/lbm. In an actual combustion chamber, primarily due to volume limitations, the entirety of the QR cannot be realized. The fraction that can be realized is called *burner efficiency* and is given the symbol η_b. Therefore,

$$\eta_b \equiv \frac{Q_{R,Actual}}{Q_{R,Ideal}} \qquad \textbf{(4.29)}$$

The ideal heat of reaction, or heating value of typical hydrocarbon fuels, to be used in our cycle analysis is

$$Q_R = 42{,}000 \text{ kJ/kg} \qquad \textbf{(4.30a)}$$

However, the most energetic fuel is the hydrogen, which is capable of releasing roughly three times the energy of typical hydrocarbon fuels per unit mass, that is,

$$Q_R = 127{,}500 \text{ kJ/kg} \qquad \textbf{(4.30c)}$$

Typically in modern gas turbine engines, the burner efficiency can be as high as 98–99%. In a cycle analysis, we need to make assumptions about the loss parameters in every component, which in a combustion chamber are $\pi_b \prec 1$ and $\eta_b \prec 1$. The real and ideal combustion process can be depicted on a *T–s* diagram, which later will be used to perform cycle analysis. Figure 4.11 shows the burner thermodynamic process on a *T–s* diagram.

The isobars p_{t3} and p_{t4} drawn at the entrance and exit of the combustor in Figure 4.11, clearly show a total pressure drop in the burner, Δp_t, burner. The maximum temperature limit T_{t4} is governed by the level of cooling technology, material selection, and the protective thermal coating used in the turbine. Typical current values for the maximum T_{t4} are about 3200–3,600 ◦R or 1775–2,000 K. Another burner parameter is the temperature rise ΔT_t across the combustion chamber, as shown in Figure 4.11. The thermal power invested in the engine (by the fuel) is proportional to the temperature rise across the combustor, that is, it is nearly equal to

$m_0 c_p(\Delta T_t)$burner. The application of energy balance across the burner, that is, Equation 4.28, will yield the fuel-to-air ratio f as the only unknown parameter. To derive an expression for the fuel-to-air ratio, we will divide Equation 4.28 by $\dot{m}_0$, the air mass flow rate, to get

$$h_{t3} + fQ_R\eta_b = (1+f)h_{t4} \qquad \textbf{(4.31)}$$

■ **FIGURE 4.11**
Actual flow process in a burner (note total pressure loss Δp_t across the burner)

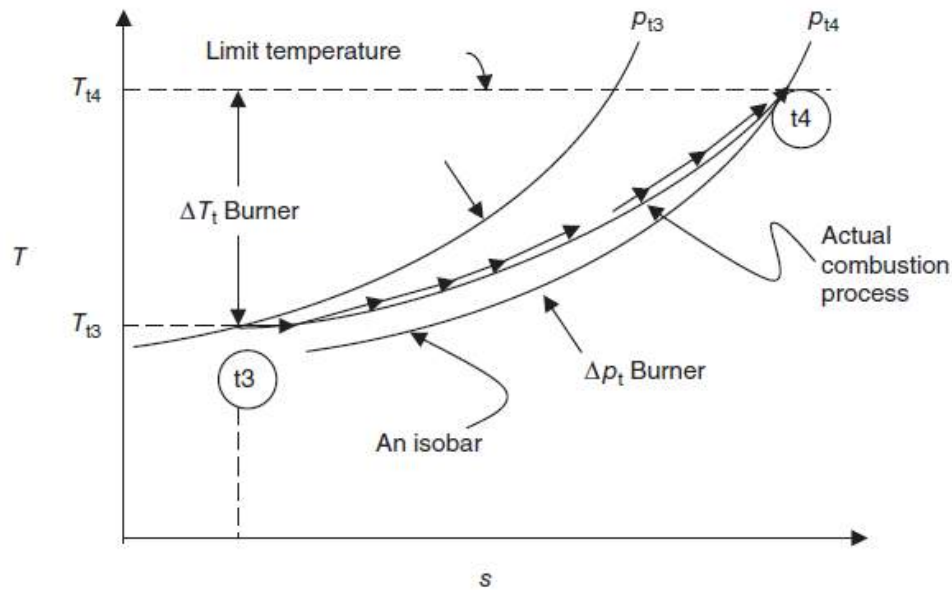

The unknown parameter f can be isolated and expressed as

$$f = \frac{h_{t4} - h_{t3}}{Q_R\eta_b - h_{t4}} \qquad \textbf{(4.32)}$$

Knowing the fuel property Q_R, assuming burner efficiency η_b, and having specified a turbine inlet temperature T_{t4}, the denominator of Equation 4.32 is fully known. The compressor discharge temperature T_{t3} is established via compressor pressure ratio, efficiency, and inlet condition, as described in the compressor section and in Equation 4.19, which renders the numerator of Equation 4.32 fully known as well. Therefore, application of energy balance to a burner usually results in the establishment of fuel-to-air ratio parameter f. It is customary to express Equation 4.32 in terms of non-dimensional parameters,
by dividing each term in the numerator and denominator by the flight static enthalpy h_0 to get

$$f = \frac{\dfrac{h_{t4}}{h_0} - \dfrac{h_{t3}}{h_0}}{\dfrac{Q_R\eta_b}{h_0} - \dfrac{h_{t4}}{h_0}} = \frac{\tau_\lambda - \tau_r\tau_c}{\dfrac{Q_R\eta_b}{h_0} - \tau_\lambda} \qquad \textbf{(4.33)}$$

where we recognize the product $\tau_r\,\tau_c$ as h_{t3}/h_0, and τ_λ as the cycle thermal limit parameter h_{t4}/h_0.

Numerical Example:

A gas turbine combustor has inlet condition T_{t3} = 800 K, p_{t3} = 2 Mpa, air mass flow rate of 50 kg/s, γ_3 = 1.4, c_{p3} =1004 J/kg · K. A hydrocarbon fuel with ideal heating value Q_R = 42,000 kJ/kg is injected in the combustor at a rate of 1 kg/s. The burner efficiency is η_b = 0.995 and the total pressure at the combustor exit is 96% of the inlet total pressure, i.e., combustion causes a 4% loss in total pressure. The gas properties at the combustor exit are γ_4 = 1.33 and c_{p4} = 1156 J/kg · K. Calculate

(a) fuel-to-air ratio f

(b) combustor exit temperature T_{t4} in K and p_{t4} in MPa

Solution:

The air and fuel flow rates are specified at 50 and 1 kg/s, respectively, in the problem, therefore, f = 1/50 = 0.02 or 2%.

We calculate combustor exit temperature by energy balance,

$$\dot{m}_0 h_{t3} + \dot{m}_f Q_R \eta_b = (\dot{m}_0 + \dot{m}_f) h_{t4} = \dot{m}_0 (1+f) h_{t4}$$

Therefore

$$h_{t3} + f Q_R \eta_b = (1+f) h_{t4}$$

$$T_{t4} = \frac{(c_{p3}/c_{p4}) T_{t3} + f Q_R \eta_b / c_{p4}}{1+f}$$

$$= \frac{(1004/1156)\,800\,\text{K} + 0.02\,(42000\,\text{kJ/kg})\,(0.995)\,/1.156\,\text{kJ/kg}\cdot\text{K}}{1.02}$$

Therefore, combustor exit temperature is $T_{t4} \cong 1390$ K and $p_{t4} = 0.96(2\text{ MPa}) = 1.92$ MPa

Chemical Reaction and Flame Temperature

First, we define a series of terms that describe a chemical reaction, such as exothermic or endothermic. Let us assume the following chemical reaction:

$$a\text{A} + b\text{B} \rightarrow c\text{C} + d\text{D}$$

If the reaction proceeds from the *reactants* A and B to the *products* C and D and the reaction produces heat as a result, we call such reactions as *exothermic*. If the opposite occurs, that is, if the reactants would not naturally react without an initial external heat input (stimulus), then such reactions are called *endothermic.* An example of an exothermic reaction is the combustion of hydrocarbon fuels and air. An example of an endothermic reaction is the phase transformation of water from liquid to vapor that requires a heat input. Our interest in chemical reaction lies primarily in the study of combustion and hence exothermic processes. In gas turbine engines, the reactants are typically hydrocarbon fuels and air. In a liquid propellant chemical rocket, the reactants are typically highly energetic fuels, such as hydrogen, and an oxidizer, such as oxygen. Let us consider octane (C_8H_{18}) as a typical hydrocarbon fuel in a gas turbine engine. Let us also describe air (by lumping argon into the nitrogen molecule) as being approximately composed of

$$\text{Air} \cong \text{O}_2 + \frac{79}{21}\text{N}_2 \cong \text{O}_2 + 3.76\,\text{N}_2 \qquad \textbf{(7.28)}$$

Now, we define a *unique* mass ratio between the fuel and oxidizer, which results in the *complete combustion* of the fuel and a *stable* product composition. This unique ratio is called the *stoichiometric* ratio and now we apply it to the combustion of octane and air, as an example.

$$\text{C}_8\text{H}_{18} + \frac{25}{2}\left(\text{O}_2 + 3.76\,\text{N}_2\right) \rightarrow 8\text{CO}_2 + 9\text{H}_2\text{O} + \frac{25}{2}(3.76)\text{N}_2 \qquad \textbf{(7.29)}$$

We took a mole of octane and brought in 25/2 moles of O_2 and (3.76) (25/2) moles of N_2. Note that the need for 25/2 came from turning "C_8 " of octane into "8 CO_2" and the "H_{18}" of octane into "9 H_2O," therefore 16 + 9 = 25 oxygen atoms were needed for the complete combustion (which also means complete *oxidation)* of one mole of octane. As noted, this *unique* proportion of fuel to oxidizer results in neither excess oxygen nor any excess fuel. Any more fuel would result in unburned fuel in the products of combustion and any more air would result in excess oxygen in the products of combustion. The nitrogen (molecule) (N_2) is treated as remaining unreacted (or *inert* in chemical terms) in the combustion process. Now, the stoichiometric fuel-to-air ratio for the combustion of octane in air is

$$f_{\text{stoich}} \equiv \frac{\text{mass}_{\text{fuel}}}{\text{mass}_{\text{oxidizer}}} = \frac{\dot{m}_{\text{f}}}{\dot{m}_{\text{air}}} \approx \frac{8(12)+18(1)}{\frac{25}{2}[32+3.76(28)]} \cong \frac{114}{1716} \cong 0.0667 \qquad \textbf{(7.30)}$$

Therefore, we say that the stoichiometric ratio for hydrocarbon fuels and air is about 6.7%. This is a number to remember. If we use proportionately less fuel than the stoichiometric ratio, the combustion is said to be on a *fuel lean* basis and the opposite is called a *fuel rich* combustion. A parameter that describes the fuel lean or rich condition of a combustor is called the *equivalence ratio* ϕ, which is defined as

$$\phi \equiv \frac{f}{f_{\text{stoich}}} \quad \text{Equivalence ratio definition} \qquad \textbf{(7.31)}$$

■ FIGURE 7.2 Flame temperature dependence on the equivalence ratio showing T_{max} at $\phi \cong 1$

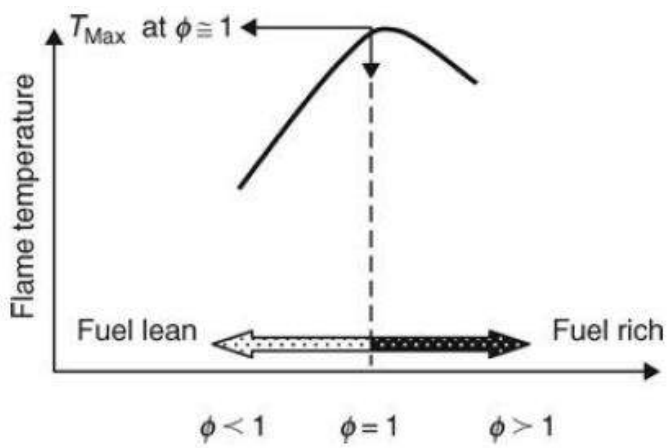

Consequently,

$\phi \succ 1$ A fuel rich combustion **(7.32)**

$\phi = 1$ Stoichiometric combustion **(7.33)**

$\phi \prec 1$ A fuel lean combustion **(7.34)**

It will be demonstrated in this chapter that the highest combustion temperature is achieved very near the stoichiometric ratio (proportion of the fuel to the oxidizer). This fact, which is depicted in Figure 7.2, should also be stored in memory as a useful concept. For many fuels, the maximum temperature, that is, the adiabatic flame temperature, occurs at the equivalence ratio between 1 and 1.1, since the product-specific heat is reduced with a slightly fuel rich mixture ratio.

Now, assuming that we know the composition of the products in a chemical reaction, that is, the constituents of the product and their number of moles, the fundamental question that remains is the product's temperature. How do we arrive at the product's temperature? If we treat the combustor as a black box, where the reactants enter the box at certain temperature, say T_1, and the products leave the box at another temperature, say T_2, and we can describe the heat transfer through the sides of the box, that is, the heat exchange with the surrounding, as say Q, we can use the law of conservation of energy to write:

$$Q_{\text{external}} = \sum H_{\text{Products}} - \sum H_{\text{Reactants}} \qquad \textbf{(7.35)}$$

Where H is the *absolute* enthalpy and Q is the *external* heat interaction with the combustion chamber. Remember *absolute enthalpy* from thermodynamics that was defined as the sum of heat of formation of the substance at the reference temperature (298.16 K) and what was called the *sensible enthalpy*, which raised the enthalpy of the substance from the reference temperature to the desired temperature. Absolute enthalpy H may be written as the product of mass and the specific absolute enthalpy for a substance. The mass may be expressed as the product of the number of moles and the molecular weight of the substance. Now, for a perfect gas, if we incorporate all of the above concepts, the absolute enthalpy may be written as

$$H = m \cdot h = n \cdot MW \cdot h = n \cdot MW \left[\int_{T_f}^{T} c_p dT + \Delta h_f^0 \right] \qquad \textbf{(7.36)}$$

■ **FIGURE 7.3**
Combustion chamber is depicted at its boundaries, through energy exchange

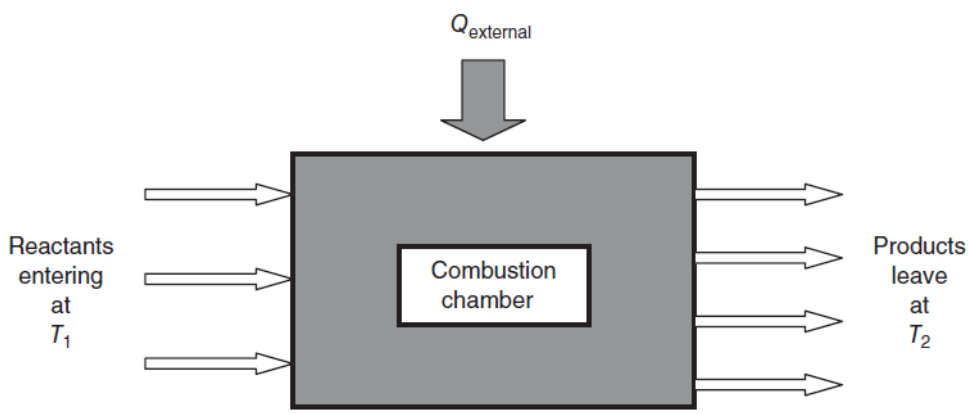

where T_f is the reference temperature, $\Delta h0f$ is the standard heat of formation of the substance at the reference temperature per unit mass at the pressure of 1 bar. The subscript "f" refers to the reference temperature and the superscript "0" refers to the standard state of the chemical compound at the pressure of 1 bar. We define the product of the molecular weight and the specific heat at constant pressure (that appears above) as the *molar specific heat*, and give it a special symbol, namely, the c_p with a bar, that is, let

$$\bar{c}_p \equiv MW \cdot c_p \qquad \textbf{(7.37)}$$

We also define the product of the molecular weight and the heat of formation per unit mass of a substance, as the *molar* heat of formation, and give it a special symbol (with a bar to identify the molar), as $\Delta\bar{h}^0_f$

$$\Delta\bar{h}^0_f \equiv MW \cdot \Delta h^0_f \qquad (7.39)$$

The molar heat of formation is the evolved heat in forming *one mole* of the substance from its elements in their standard states at constant temperature of T_f = 298.16 K and the constant pressure of p_f = 1 bar. Imagine a reaction chamber, where the basic elements of a chemical compound, at their standard state, enter at a reference temperature T_f at the pressure of 1 bar and the compound is then formed in the reaction chamber. Now, in order to maintain the temperature of the compound at the reference temperature, we need to interact with the reaction chamber through heat transfer to or from the box. The heat of formation of a chemical compound is the amount of heat exchange to (positive) or from (negative) a reaction chamber, which forms the chemical compound from its constituents, and maintains a constant (known as reference) temperature. The heat of formation of all naturally occurring elements is then, by definition, zero. The reference temperature is 298.16 K, which corresponds to a standard room temperature of 25◦C (77◦F) and the reference pressure of 1 bar is the standard atmospheric pressure (also very close to 1 atm). This process can be schematically shown in Figure 7.4.

■ FIGURE 7.4 **Definition sketch for the *heat of formation* of (one mole of) a chemical compound in an isothermal process (p = 1 bar)**

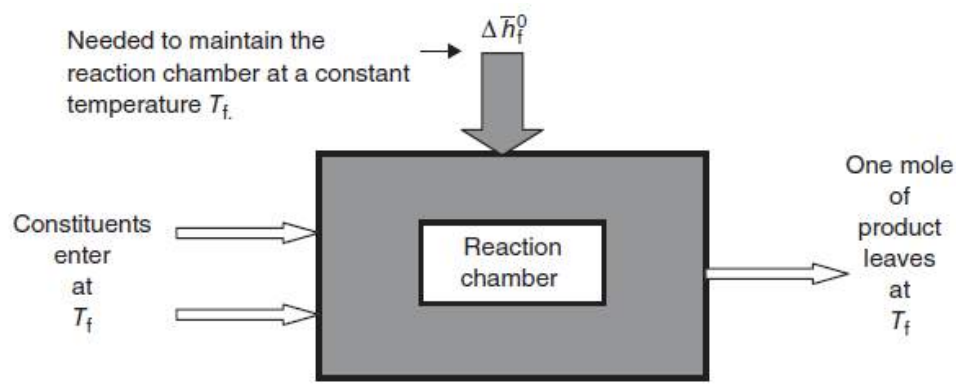

The exothermic reactions from basic elements to form one mole of a chemical compound then lead to a negative heat of formation, because we need to extract heat from the reaction chamber in order to maintain a constant temperature. The opposite is true for endothermic reactions to form a compound. These concepts are best learned through a series of examples. The heat of formation of carbon dioxide can be found from the following isothermal reaction at 1 bar:

$$C_{(s)} + O_{2(g)} \xrightarrow{298.16\ K} CO_{2(g)} - 393{,}522\ kJ/kmol$$

Therefore, $CO_2(g)$, carbon dioxide (gaseous), has a standard heat of formation of Δh^0_f=−393,522 kJ/kmol.We note that in the previous reaction the carbon enters the reaction as a solid and the oxygen as a gas, that is, the standard states of carbon and oxygen, to form one mole of carbon dioxide (in gaseous form).

$$C_{(s)} + \frac{1}{2}O_{2(g)} \xrightarrow{298.16\ K} CO_{(g)} - 110{,}530\ kJ/kmol$$

The following four reactions serve as additional examples on the standard heat of formation.

$$\frac{1}{2}O_{2(g)} \xrightarrow{298.16\ K} O + 249{,}170\ kJ/kmol \Rightarrow \left(\Delta\bar{h}_f^0\right)_O = +249{,}170\ kJ/kmol$$

$$\frac{1}{2}H_{2(g)} \xrightarrow{298.16\ K} H + 217{,}999\ kJ/kmol \Rightarrow \left(\Delta\bar{h}_f^0\right)_H = +217{,}999\ kJ/kmol$$

$$8C_{(s)} + 9H_2 \xrightarrow{298.16\ K} C_8H_{18(g)} - 208{,}447\ kJ/kmol \Rightarrow \left(\Delta\bar{h}_f^0\right)_{C_8H_{18(g)}} = -208{,}447\ kJ/kmol$$

$$8C_{(s)} + 9H_2 \xrightarrow{298.16\ K} C_8H_{18(l)} - 249{,}930\ kJ/kmol \Rightarrow \left(\Delta\bar{h}_f^0\right)_{C_8H_{18(l)}} = -249{,}930\ kJ/kmol$$

The energy balance equation across the burner (Equation 7.35) may now be expressed on a molar basis, to include the complete enthalpy expression. This will account for the reactants entering the combustion chamber at other than reference temperature, namely, T_1, and the products of combustion leave the chamber at another temperature, namely, T_2, as follows:

$$Q_{\text{external}} = \sum_j \left[n_j \cdot \bar{c}_{pj}\left(T_2 - T_f\right)_j\right]_{\text{Products}} - \sum_i \left[n_i \cdot \bar{c}_{pi}\left(T_1 - T_f\right)_i\right]_{\text{Reactants}} + \Delta H_{\text{RPf}} \tag{7.41}$$

where "*P*" and "*R*" stand for products and reactants, respectively, and the last term defined as

$$\Delta H_{\text{RPf}} = \sum_j \left[n_j \Delta\bar{h}_{fj}^0\right]_{\text{Products}} - \sum_i \left[n_i \Delta\bar{h}_{fi}^0\right]_{\text{Reactants}} \tag{7.42}$$

is the difference between the standard heats of formation of all the product constituents and the reactant constituents, at the reference temperature at the pressure of 1 bar. This quantity is also called *heat of reaction* with a symbol Q_R. Therefore, heat of reaction in a combustion process is defined as

$$Q_R \equiv \sum_P n_j \Delta\bar{h}_{fj}^0 - \sum_R n_i \Delta\bar{h}_{fi}^0 \tag{7.43}$$

We can specialize the concept of the *heat of reaction* to combustion of a fuel in pure oxygen O_2. This will be the basis for the definition of the fuel heating value. Assuming that the fuel and the gaseous oxygen, that is, O_2 (g), enter the combustion chamber at the reference temperature of 298.16 K and a complete combustion takes place, the heat release per unit mass of the fuel, which will return the products of combustion to the reference temperature, is called the *heating value* of the fuel. In simple terms, substitute T_f for T_1 and T_2 in Equation 7.41, which will force the summations over the products and the reactants to zero, and note that

$$Q = Q_R = \sum_P n_j \Delta\bar{h}_{f_j}^0 - \sum_R n_i \Delta\bar{h}_{fi}^0 \tag{7.44}$$

Although the negative sign on the summations of Equation 7.43 or 7.44 shows the necessity of *removing* a quantity of heat from the combustion chamber in order to maintain an isothermal environment, it is customary to report the fuel heating value as a positive quantity. Hence, we define

$$\text{Fuel heating value} = -Q_R \tag{7.45}$$

Now, depending on the state of water in the products of combustion, that is, as a liquid or vapor, the fuel heating value is referred to as higher heating value (HHV) or lower heating value (LHV), respectively. Since the difference between the higher and lower heating values depends on the energy spent in vaporizing the condensed water in the products of combustion, the following energy balance relates the two heating values:

$$\mathrm{HHV} = \mathrm{LHV} + \frac{m_{\mathrm{H_2O}}}{m_{\mathrm{fuel}}} h_{\mathrm{lg}} \qquad \textbf{(7.46)}$$

where the last term h_{lg} is the latent heat of vaporization for water at 25◦C, which is 2443 kJ/kg. Now, let us put these concepts to work and obtain a fuel heating value based on the standard heats of formation and the water/fuel mass fraction and the latent heat of vaporization of water.

Applying Equation 7.41, to a chemical reaction with a known product composition and a known heat exchange characteristics through the walls of the combustor, $Q_{external}$, will result in the calculation of the exit temperature of the products of combustion, T_2. A reference boundary condition on the combustion chamber is the adiabatic assumption of zero heat exchange with the environment, that is, $Q_{external} \equiv 0$, which leads to a unique exit temperature value, known as the *adiabatic flame temperature* T_{af}. In addition, there are polynomial expressions that are developed for the molar specific heats of various chemical compounds, such as the sample produced in Table 7.2, which provide the remaining input to the enthalpy balance equation across the combustor, that is, Equation 7.41. As the polynomial expressions for specific heat are in temperature, and we do not a priori know the temperature of the products of combustion, the process of selecting a suitable molar specific heat is iterative. Otherwise an *average* specific heat may be assumed, over the expected temperature range. Also note that in a fuel-rich combustion, $\phi \succ 1$, the heat of reaction remains the same as that of stoichiometric reaction, whereas the flame temperature will be reduced as the heat of reaction is now used to raise the temperature of additional fuel.

■ FIGURE 7.6 Adiabatic flame temperature of Jet A fuel combustion in air at 800 K initial temperature and 25 atm pressure. Source: Blazowski 1985. Reproduced with permission from AIAA

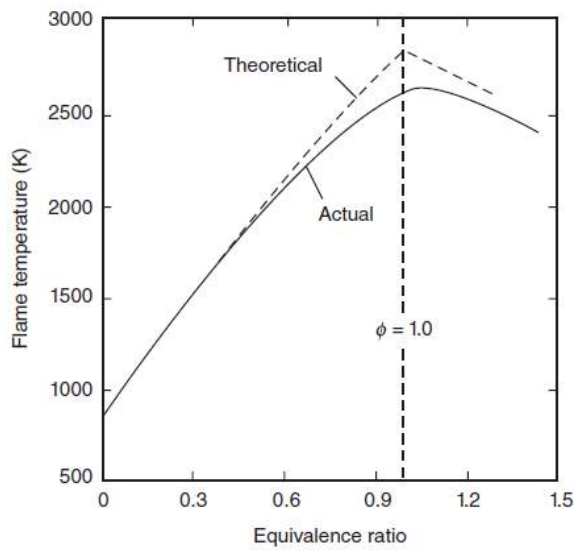

The adiabatic flame temperature as a function of equivalence ratio for the Jet A fuel combustion in air at 800 K initial temperature and 25 atm initial pressure is shown in Figure 7.6 (from Blazowski, 1985). There are several noteworthy features in Figure 7.6 that are instructive to our study. First, the initial temperature and pressure were chosen to represent the combustion chamber inlet conditions in a modern aircraft gas turbine engine. Second, the *actual* flame temperature that allows for dissociation falls below the theoretical predictions (of a complete combustion). The difference between the actual curve and theoretical predictions starts around an equivalence ratio of ~0.4–0.5, which points to a flame temperature of ~1650–1750 K, where dissociation reactions begin. Interestingly, a combustion chamber in a modern aircraft gas turbine engine operates in the 0.4–0.5 range of the equivalence ratio, which corresponds to a

fuel-to-air ratio of ~2.5–3.5%. Third, although the figure caption identifies the initial temperature at 800 K, we could have discerned this fact from the flame temperature at zero equivalence ratio on the graph, that is, no combustion. Fourth, as noted earlier, the maximum flame temperature occurs at an equivalence ratio slightly greater than 1 (~1. 1). Also, note that the burner exit (or flame) temperature is a double-valued function of equivalence ratio, or fuel-to-air ratio, that is, we can reach a burner exit temperature from either the fuel-lean or the fuel-rich side of the stoichiometric point. The effect of initial air temperature on the stoichiometric flame temperature of a Jet A fuel combustion in air is shown in Figure 7.7a. Comparing the slope of the flame temperature rise with inlet temperature to a slope = 1.0 line drawn in Figure 7.7a for reference, we note that only ~1/2 of the inlet temperature rise appears as the rise in the final flame temperature. This behavior corresponds to higher molar concentrations of dissociated species that appear with higher temperatures. Consequently, a 100 K increase in the inlet air temperature for this reaction results in ~50 K final flame temperature rise. The effect of the combustion pressure on the stoichiometric flame temperature of Jet A fuel is shown in Figure 7.7b. The increasing pressure leads to a rise in the stoichiometric flame temperature. The increase is due to a suppressed dissociation levels with pressure. We observed that a lower mixture pressure promoted nitrogen dissociation and it was suppressed with an increasing mixture pressure.

■ FIGURE 7.7 **Effect of inlet temperature and pressure on the stoichiometric flame temperature of a Jet-A fuel combustion in air. Source: Blazowski 1985. Reproduced with permission from AIAA**

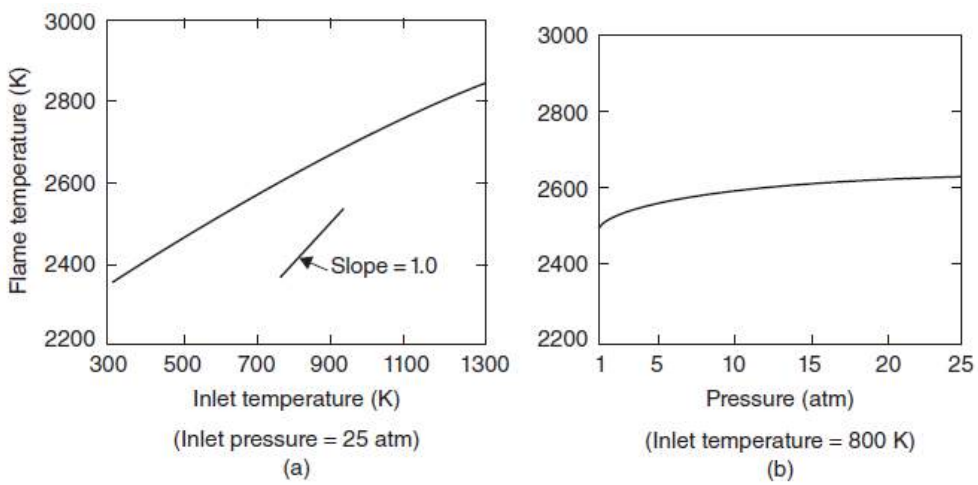

It is instructive to examine the effect of oxidizer, as in pure oxygen or air, on the combustion of various fuels and the impact of the oxidizer on the stoichiometric flame temperature. For this purpose, Table 7.4 is reproduced from Glassman (1987) that examines the maximum temperature at equivalence ratios near stoichiometric of various fuels reacting with air or pure oxygen. Moreover, the effect of pressure on combustion temperature is reported for methane, similar to Figure 7.7b. Combustion of hydrogen in air results in a stoichiometric flame temperature of ~2400 K at 1 atm pressure. The flame temperature for the combustion of hydrogen with pure oxygen is ~3080 K, at 1 atm pressure. Air contains nitrogen (~78% by volume), which for the most part is inert and does not react with the fuel or oxidizer. Also, the fuel heating value remains the same whether the oxidizer is oxygen or air. For the same energy release (per unit mass of the fuel), there are more reactants in air that do not participate in the combustion but need to be heated to the final temperature. Consequently, the flame temperature will be lower when a fuel reacts with air as opposed to pure oxygen.

Now to the effect of pressure on combustion, we note that methane reacts with air at 1 atm pressure and reaches a maximum flame temperature of 2210 K. If we increase the combustion pressure to 20 atm, the flame temperature increases to ~2270 K. This is a rather minor increase in temperature, which is caused by a decrease in the dissociation levels of the products of combustion with pressure. At this temperature, the dissociation levels were small and hence a suppressed level of dissociation did not cause a pronounced effect in final temperature. To ascertain this point, we examine the combustion of methane with pure oxygen, which reaches a flame temperature of ~3030 K at 1 atm pressure. The flame temperature rises to ~3460 K when methane reacts with pure oxygen at 20 atm pressure. At the temperature of 3030 K, the level of dissociation is much higher, hence the effect of pressure on suppressing the product dissociation is more pronounced and leads to a flame temperature of ~3460 K.

Ignition and Relight Envelope

As noted earlier, the pressure dependence of the reaction rate coefficient may cause a relight problem at high altitude. A relight zone is plotted in Figure 7.8 in an altitude– Mach number plot (i.e., flight envelope) for the combustion of a typical hydrocarbon fuel in air (Henderson and Blazowski, 1989).We note that below 0.2 atm pressure, combustor relight is not possible at standard temperature, due to low reaction rate.

■ FIGURE 7.8
The typical ignition/relight envelope shows relight capability in the shaded zone. Source: Henderson and Blazowski 1989. Reproduced with permission from AIAA

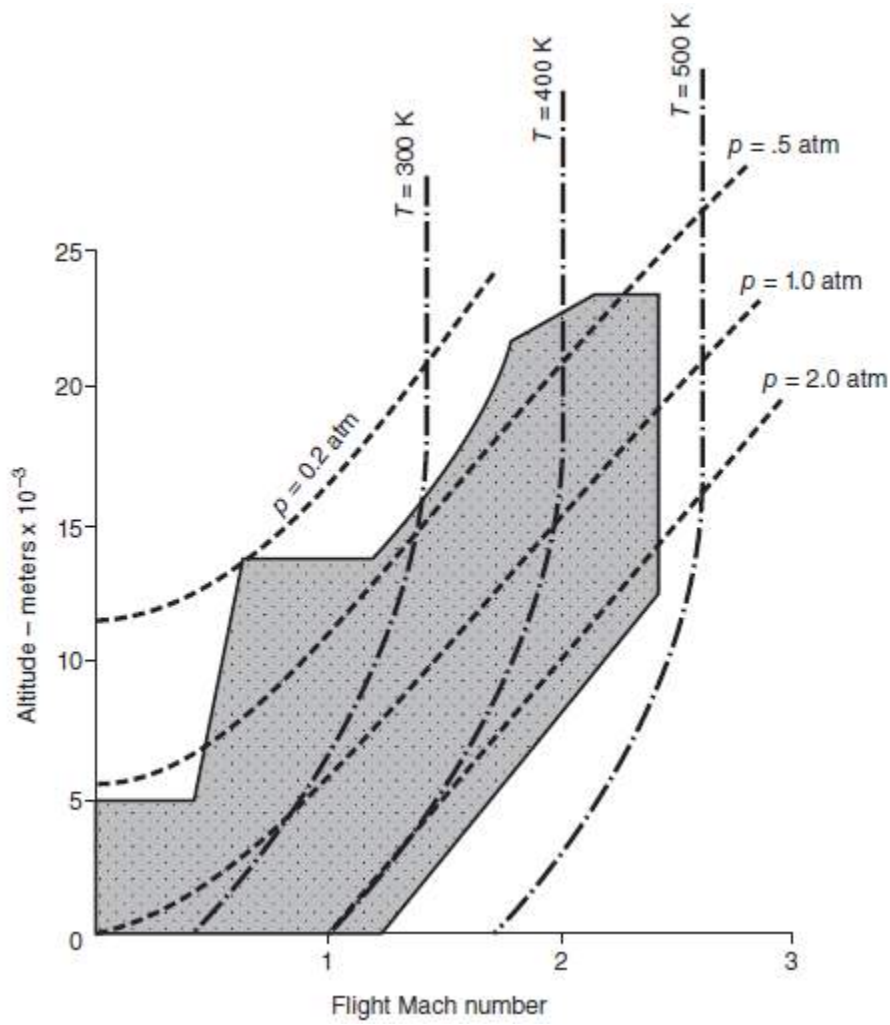

Flame Stability

Combustion stability means smooth burning and the ability of the flame to remain alight over a wide operating range. For any particular type of combustion chamber there is both a rich and weak limit to the air/fuel ratio, beyond which the flame is extinguished. An extinction is most likely to occur in flight during a glide or dive with the engine idling, when there is a high airflow and only a small fuel flow, i.e. a very weak mixture strength. The range of air/fuel ratio between the rich and weak limits is reduced with an increase of air velocity, and if the air mass flow is increased beyond a certain value, flame extinction occurs. A typical stability loop is illustrated in fig. 7.16 The operating range defined by the stability loop must obviously cover the air/fuel ratios and mass flow of the combustion chamber. The ignition process has weak and rich limits similar to those shown for stability in fig. 7.16. The ignition loop, however, lies within the stability loop since it is more difficult to establish combustion under 'cold' conditions than to maintain normal burning.

■ FIGURE 7.16 A typical stability loop for a combustor at $p_3 =$ constant. Source: Lefebvre 1983. Reproduced with permission from Taylor and Francis Group LLC, a division of Informa plc

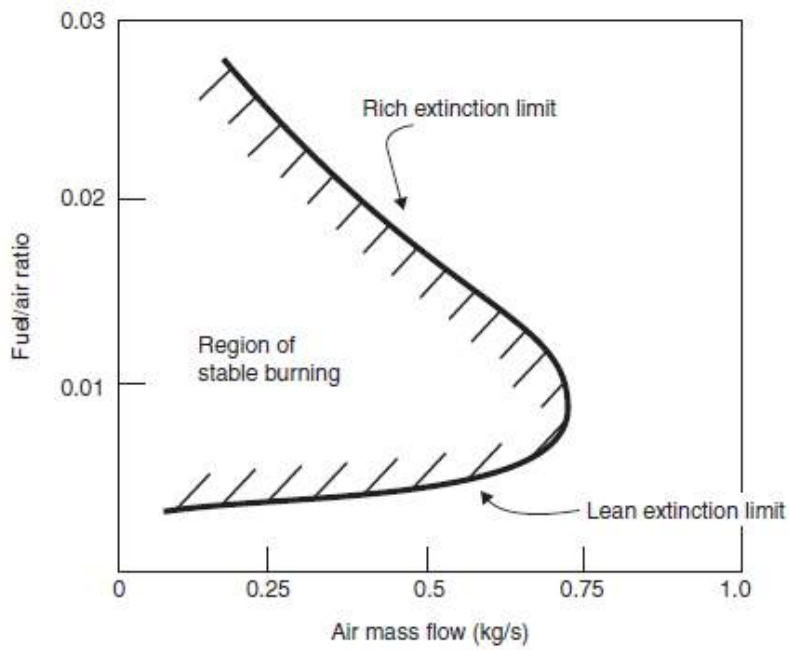

The lower branch of the stability loop is the lean extinction limit and the upper branch is the rich extinction limit of combustion chamber. The maximum blowout speed occurs at the maximum flame speed, which is usually near the stoichiometric mixture ratio. The effect of pressure on the lean stability limit is negligible and widens the rich stability limit with the increase in pressure. A recirculation zone in the burner (with a backward flow) is needed to stabilize a premixed flame. In studying swirling jets, we learn that when the ratio of jet angular momentum to jet axial thrust times jet diameter exceeds ~0.5, a recirculatory flow in the core of the swirling jet is established. This is known as a vortex breakdown.

Combustion efficiency

Combustion efficiency measures the actual rate of heat release in a burner and compares it with the theoretical heat release rate possible. The theoretical heat of reaction of the fuel assumes a complete combustion with no unburned hydrocarbon fuel and no dissociation of the products of combustion. The actual heat release is affected by the quality of fuel atomization, vaporization, mixing, ignition, chemical kinetics, flame stabilization, intermediate air flow, liner cooling, and, in general, the aerodynamics of the combustor. Here a variety of timescales as in residence time,

chemical reaction/reaction rate timescales, spontaneous ignition delay time that includes vaporization timescale, among other time constants enter the real combustion problem. The unburned hydrocarbon (UHC) and carbon monoxide (CO) that contribute to combustor inefficiency are also among the combustion-generated pollutants. The allowable levels of these pollutants in aircraft gas turbine engine emissions, regulated by the U.S. Environmental Protection Agency (EPA), place a 99% combustion efficiency demand on the combustor. For a gas turbine combustor, when chemical kinetics is the limiting factor in combustor performance, Lefebvre (1959, 1966) introduces a combustor loading parameter (CLP) θ, which correlates well with combustion efficiency. parameter is defined as

$$\mathrm{CLP} = \theta = \frac{p_{t3}^{1.75} A_{\mathrm{ref}} H \cdot e^{\frac{T_{t3}}{b}}}{\dot{m}_3} \qquad \textbf{(7.113)}$$

The combustor inlet pressure, temperature, and mass flow rate are pt3, Tt3, and $\dot{m}$ 3, respectively, maximum cross-sectional area of the burner is defined as Aref, the combustor height is$H$and b is a reaction rate parameter. The dependence of the reaction rate parameter b on the primary zone equivalence ratio ϕ is estimated by Herbert (1957) to be

$$b = 382\left(\sqrt{2} \pm \ln\frac{\phi}{1.03}\right) \quad [(+)\text{ for } \phi < 1.03, (-)\text{ for } \phi > 1.03] \qquad \textbf{(7.114)}$$

The lowest combustion efficiency is, of course, zero in the flameout limit. This could happen at a high altitude when the low combustor pressure in essence slows the reaction rate to a halt. The combustion efficiency of most gas turbine engines at sea-level take-off conditions is almost 100 per cent, reducing to 98 per cent at altitude cruise conditions

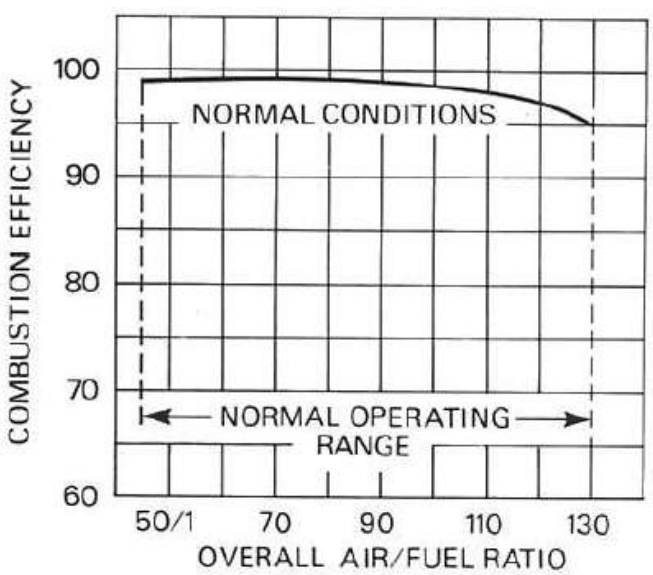

Fig. 4-10 Combustion efficiency and air/fuel ratio.

Combustion intensity

The heat released by a combustion chamber or any other heat generating unit is dependent on the volume of the combustion area. Thus, to obtain the required high power output, a comparatively small and compact gas turbine combustion chamber must release heat at exceptionally high rates. It is often desirable to express the heat intensity as Burning strength Q_{vf}. It is used to measure heat released per hour per unit volume under unit pressure.

$$Q_{vf} = \frac{3600\eta_b \dot{m}_f LHV}{p_{t2} V_f}$$

Combustion Emission

The unwanted pollutants which are found in the exhaust gases are created within the combustion chamber. There are four main pollutants which are legislatively controlled; unburnt hydrocarbons (unburnt fuel), smoke (carbon particles), carbon monoxide and oxides of nitrogen. The principal conditions which affect the formation of pollutants are pressure, temperature and time. In the fuel rich regions of the primary zone, the hydrocarbons are converted into carbon monoxide and smoke, Fresh dilution air can be used to oxidize the carbon monoxide and smoke into non-toxic carbon dioxide within the dilution zone. Unburnt hydrocarbons can also be reduced in this zone by continuing the combustion process to ensure complete combustion. Oxides of nitrogen are formed under the same conditions as those required for the suppression of the other pollutants, Therefore, it is desirable to cool the flame as quickly as possible and to reduce the time available for combustion. This conflict of conditions requires a compromise to be made, but continuing improvements in combustor design and performance has led to a substantially ’cleaner’ combustion process.

Turbine

The turbine has the task of providing the power to drive the compressor and accessories and, in the case of engines which do not make use solely of a jet for propulsion, of providing shaft power for a propeller or rotor. It does this by extracting energy from the hot gases released from the combustion system and expanding them to a lower pressure and temperature. High stresses are involved in this process, and for efficient operation, the turbine blade tips may rotate at speeds over 1,500 feet per second, The continuous flow of gas to which the turbine is exposed may have an entry temperature between 850 and 1,700 deg. C. and may reach a velocity of over 2,500 feet per second in parts of the turbine. To produce the driving torque, the turbine may consist of several stages each employing one row of stationary nozzle guide vanes and one row of moving blades. The number of stages depends upon the relationship between the power required from the gas flow, the rotational speed at which it must be produced and the diameter of turbine permitted. The number of shafts, and therefore turbines, varies with the type of engine; high compression ratio engines usually have two shafts, driving high and low pressure compressors (fig, 5-2). On high by-pass ratio fan engines that feature an intermediate pressure system, another turbine may be interposed between the high and low pressure turbines, thus forming a triple-spool system (fig, 5-3). On some engines, driving torque is derived from a free-power turbine (fig. 5-4). This method allows the turbine to run at its optimum speed because it is mechanically independent of other turbine and compressor shafts.

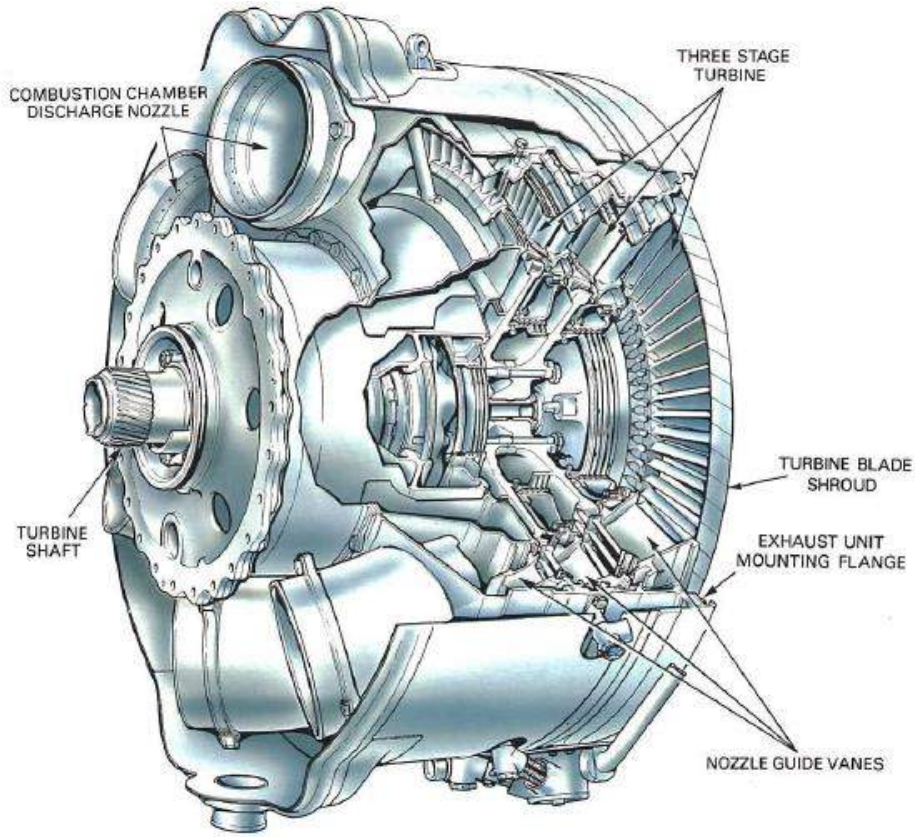

Fig. 5-1 A triple-stage turbine with single shaft system.

The mean blade speed of a turbine has considerable effect on the maximum efficiency possible for a given stage output. For a given output the gas velocities, deflections, and hence losses, are reduced in proportion to the square of higher mean blade speeds. Stress in the turbine disc increases as the square of the speed, therefore to maintain the same stress level at higher speed the sectional thickness, hence the weight, must be increased disproportionately. For this reason, the final design is a compromise between efficiency and weight. Engines operating at higher turbine inlet temperatures are thermally more efficient and have an improved power to weight ratio. By-pass engines have a better propulsive efficiency and thus can have a smaller turbine for a given thrust. The design of the nozzle guide vane and turbine blade passages is based broadly on aerodynamic considerations, and to obtain optimum efficiency, compatible with compressor and combustion design, the nozzle guide vanes and turbine blades are of a basic aerofoil shape. There are three types of turbine; impulse, reaction and a combination of the two known as impulse-reaction. In the impulse type the total pressure drop across each stage occurs in the fixed nozzle guide vanes which, because of their convergent shape, increase the gas velocity whilst reducing the pressure. The gas is directed onto the turbine blades which experience an impulse force caused by the impact of the gas on the blades. In the reaction type the fixed nozzle guide vanes are designed to alter the gas flow direction without changing the pressure. The converging

blade passages experience a reaction force resulting from the expansion and acceleration of the gas. Normally gas turbine engines do not use pure impulse or pure reaction turbine blades but the impulse-reaction combination. The proportion of each principle incorporated in the design of a turbine is largely dependent on the type of engine in which the turbine is to operate, but in general it is about 50 per cent impulse and 50 per cent reaction. Impulse-type turbines are used for cartridge and air starters.

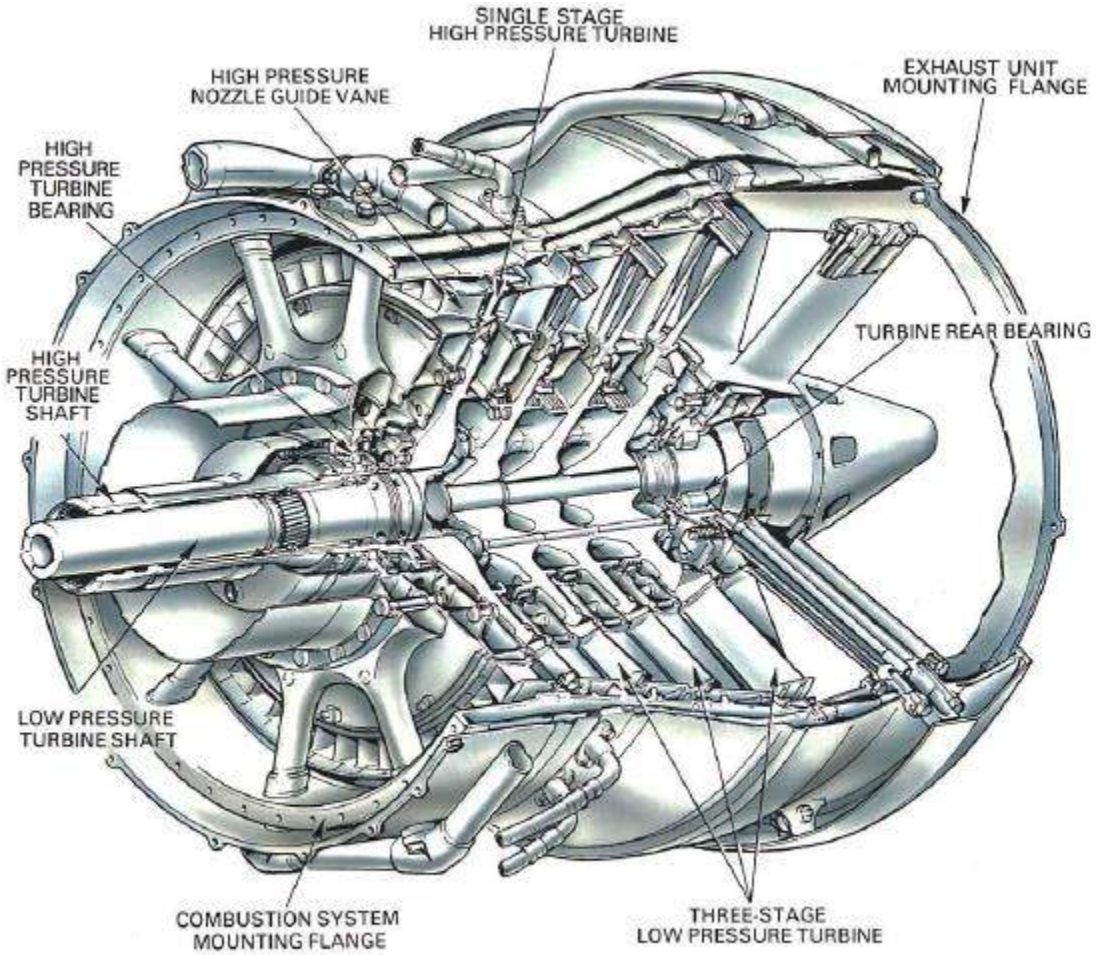

Fig. 5-2 A twin turbine and shaft arrangement.

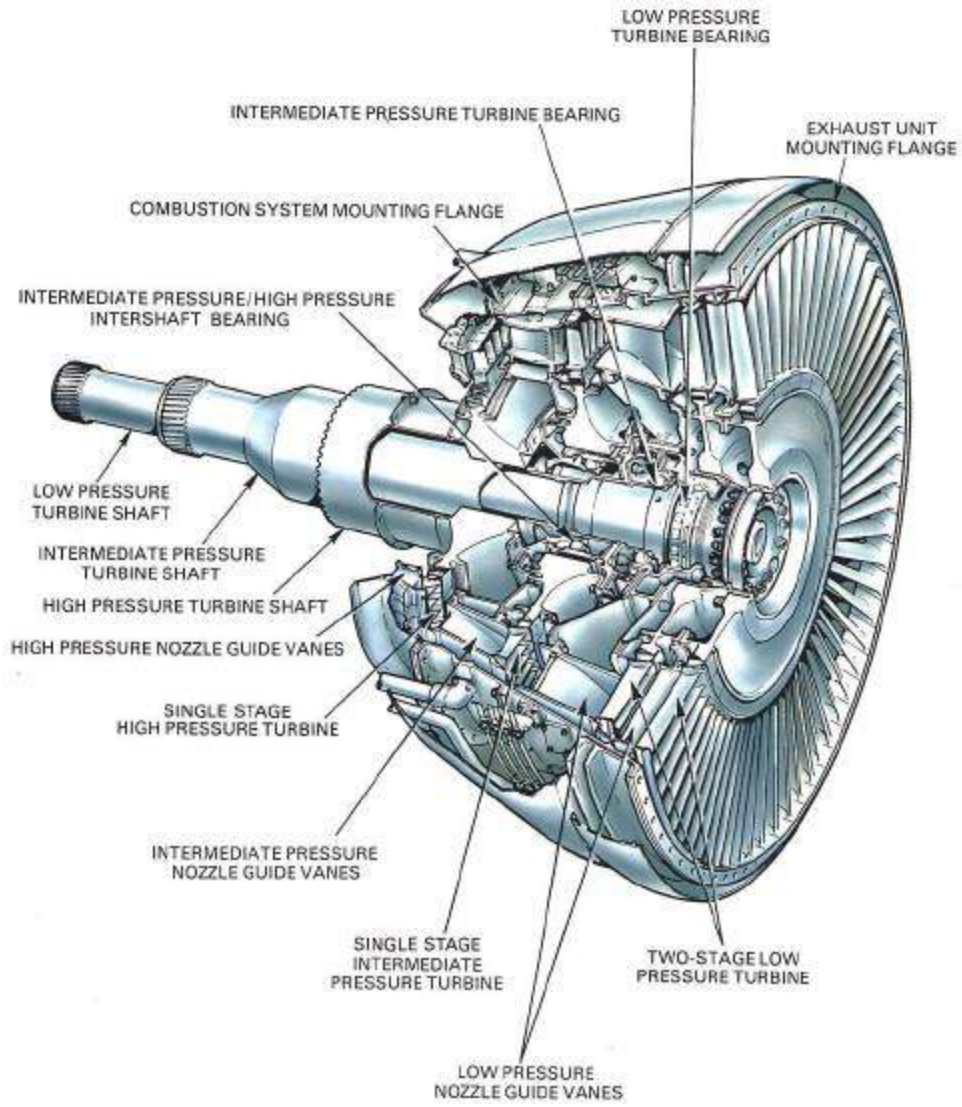

Fig. 5-3 A triple turbine and shaft arrangement.

ENERGY TRANSFER FROM GAS FLOW TO TURBINE

When the gas is expanded by the combustion process, it forces its way into the discharge nozzles of the turbine where, because of their convergent shape, it is accelerated to about the speed of sound which, at the gas temperature, is about 2,500 feet per second. At the same time the gas flow is given a 'spin' or 'whirl' in the direction of rotation of the turbine blades by the nozzle guide vanes. On impact with the blades and during the subsequent reaction through the blades, energy is absorbed, causing the turbine to rotate at high speed and so provide the power for driving the turbine shaft and compressor.

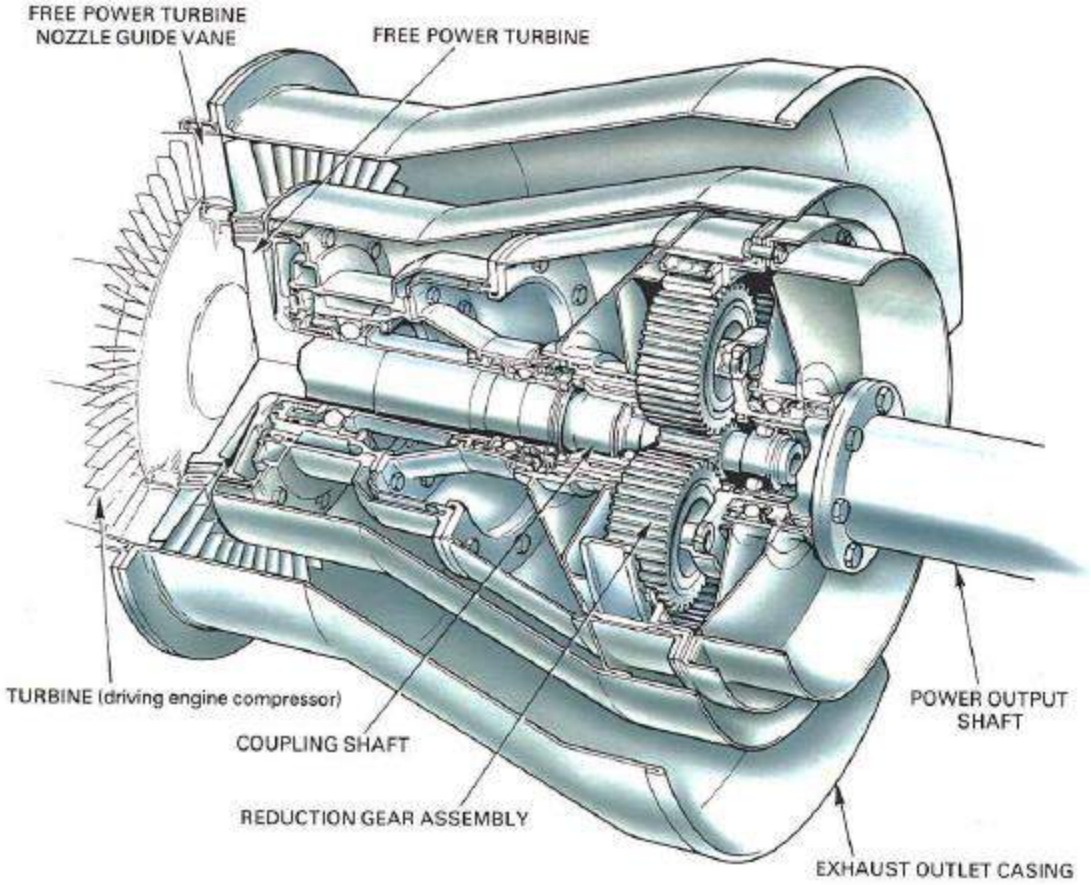

Fig. 5-4 A typical free power turbine.

The torque or turning power applied to the turbine is governed by the rate of gas flow and the energy change of the gas between the inlet and the outlet of the turbine blades, The design of the turbine is such that the whirl will be removed from the gas stream so that the flow at exit from the turbine will be substantially 'straightened out' to give an axial flow into the exhaust system. Excessive residual whirl reduces the efficiency of the exhaust system and also tends to produce jet pipe vibration which has a detrimental effect on the exhaust cone supports and struts. It will be seen that the nozzle guide vanes and blades of the turbine are 'twisted', the blades having a stagger angle that is greater at the tip than at the root (fig. 5-6). The reason for the twist is to make the gas flow from the combustion system do equal work at all positions along the length of the blade and to ensure that the flow enters the exhaust system with a uniform axial velocity. This results in certain changes in velocity, pressure and temperature occurring through the turbine, as shown diagrammatically in fig. 5-7. The 'degree of reaction' varies from root to tip, being least at the root and highest at the tip, with the mean section having the chosen value of about 50 per cent. The losses which prevent the turbine from being 100 per cent efficient are due to a number of reasons. A typical uncooled three-stage turbine would suffer a 3.5 per cent loss because of aerodynamic losses in the turbine blades. A further 4.5 per cent loss would be incurred by aerodynamic losses in the nozzle guide vanes, gas leakage over the turbine blade tips and exhaust system losses; these losses are of approximately equal proportions. The total losses result in an overall efficiency of approximately 92 per cent.

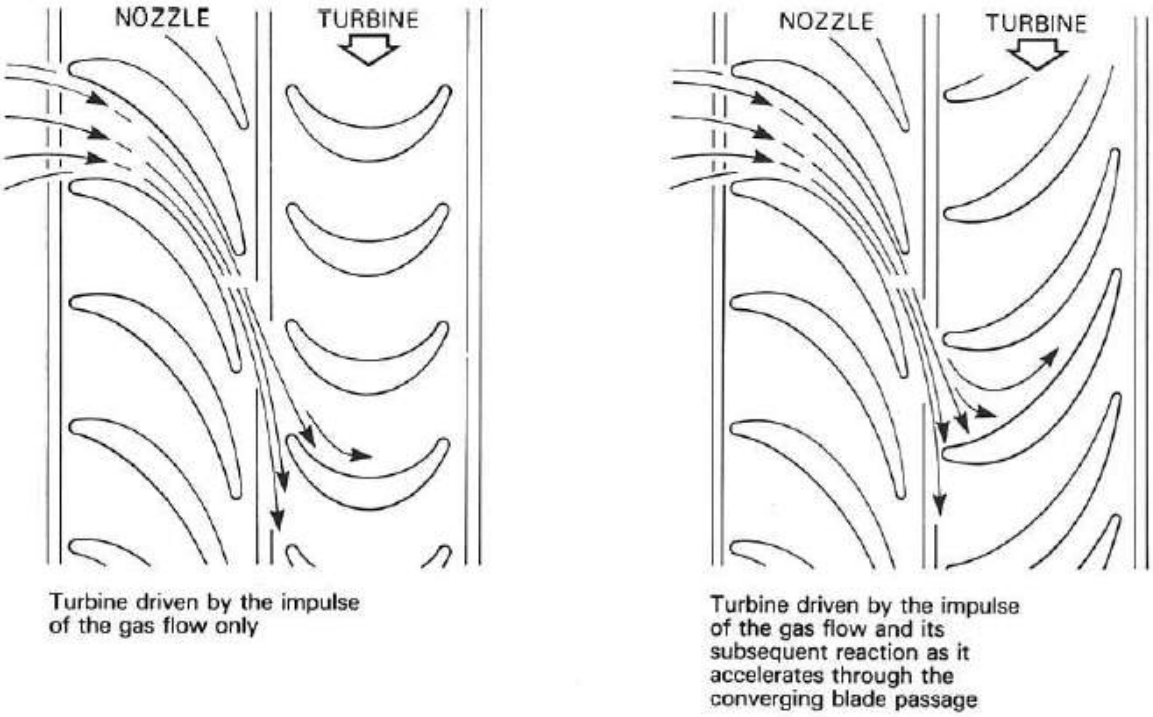

Fig. 5-5 Comparison between a pure Impulse turbine and an impulse/reaction turbine.

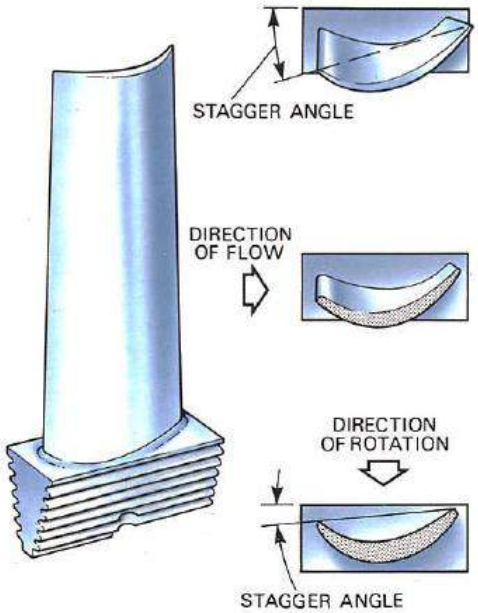

Fig. 5-6 A typical turbine blade showing twisted contour.

CONSTRUCTION

The basic components of the turbine are the combustion discharge nozzles, the nozzle guide vanes, the turbine discs and the turbine blades. The rotating assembly is carried on bearings mounted in the turbine casing and the turbine shaft may be common to the compressor shaft or connected to it by a self-aligning coupling.

Nozzle guide vanes

The nozzle guide vanes are of an aerofoil shape with the passage between adjacent vanes forming a convergent duct. The vanes are located (fig. 5-8) in the turbine casing in a manner that allows for expansion.

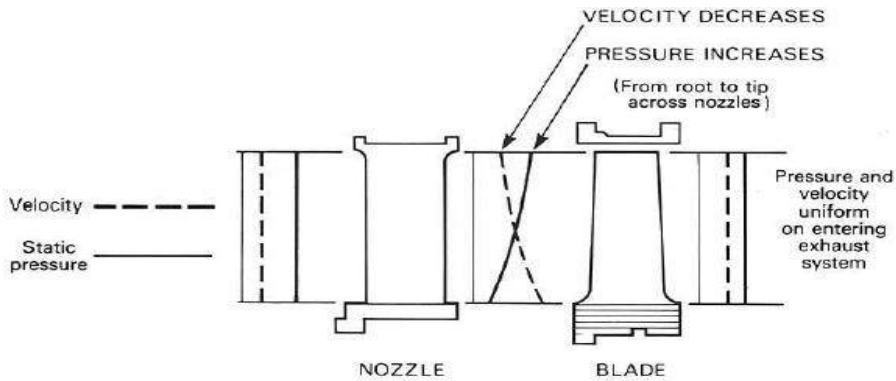

Fig. 5-7 Gas flow pattern through nozzle and blade.

The nozzle guide vanes are usually of hollow form and may be cooled by passing compressor delivery air through them to reduce the effects of high thermal stresses and gas loads. Turbine discs are usually manufactured from a machined forging with an integral shaft or with a flange onto which the shaft may be bolted. The disc also has, around its perimeter, provision for the attachment of the turbine blades. To limit the effect of heat conduction from the turbine blades to the disc a flow of cooling air is passed across both sides of each disc.

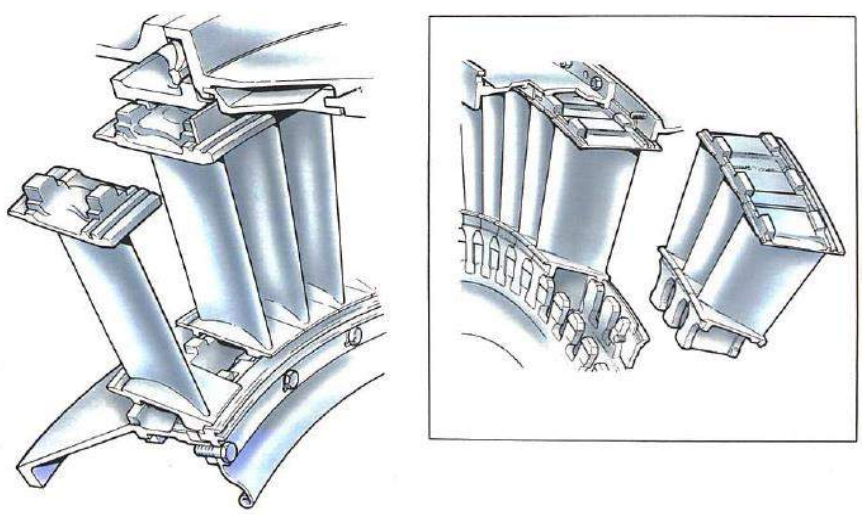

Fig. 5-8 Typical nozzle guide vanes showing their shape and location.

Turbine Blades

The turbine blades are of an aerofoil shape, designed to provide passages between adjacent blades that give a steady acceleration of the flow up to the 'throat', where the area is smallest and the velocity reaches that required at exit to produce the required degree of reaction. The actual area of each blade cross-section is fixed by the permitted stress in the material used and by the size of any holes which may be required for cooling purposes. High efficiency demands thin trailing edges to the sections, but a compromise has to be made so as to prevent the blades cracking due to the temperature changes during engine operation. The method of attaching the blades to the turbine disc is of considerable importance, since the stress in the disc around the fixing or in the blade root has an important bearing on the limiting rim speed. The blades on the early Whittle engine were attached by the de Laval bulb root fixing, but this design was soon superseded by the 'fir-tree' fixing that is now used in the majority of gas turbine engines. This type of fixing involves very accurate machining to ensure that the loading is shared by all the serrations. The blade is free in the serrations when the turbine is stationary and is stiffened in the root by centrifugal loading when the turbine is rotating. Various methods of blade attachment are shown in fig. 5-9; however, the B.M.W. hollow blade and the de Laval bulb root types are not now generally used on gas turbine engines.

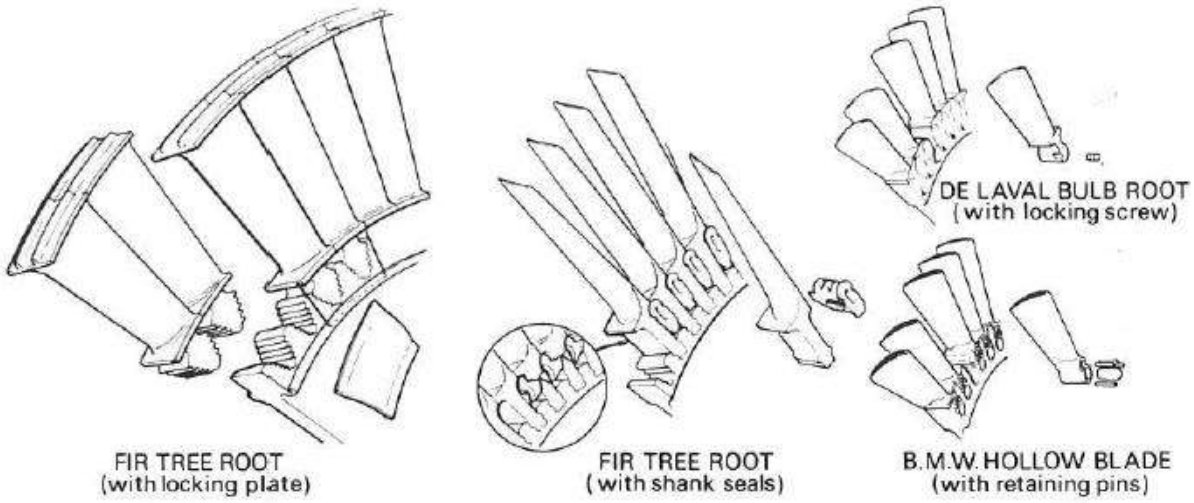

Fig. 5-9 Various methods of attaching blades to turbine discs.

A gap exists between the blade tips and casing, which varies in size due to the different rates of expansion and contraction. To reduce the loss of efficiency through gas leakage across the blade tips, a shroud is often fitted as shown in fig. 5-1. This is made up by a small segment at the tip of each blade which forms a peripheral ring around the blade tips. An abradable lining in the casing may also be used to reduce gas leakage. Active Clearance Control (A.C.C.) is a more effective method of maintaining minimum tip clearance throughout the flight cycle. Air from the compressor is used to cool the turbine casing and when used with shroudless turbine blades, enables higher temperatures and speeds to be used.

MATERIALS

Among the obstacles in the way of using higher turbine entry temperatures have always been the effects of these temperatures on the nozzle guide vanes and turbine blades. The high speed of rotation which imparts tensile stress to the turbine disc and blades is also a limiting factor.

Nozzle guide vanes

Due to their static condition, the nozzle guide vanes do not endure the same rotational stresses as the turbine blades. Therefore, heat resistance is the property most required. Nickel alloys are used, although cooling is required to prevent melting. Ceramic coatings can enhance the heat resisting properties and, for the same set of conditions, reduce the amount of cooling air required, thus improving engine efficiency.

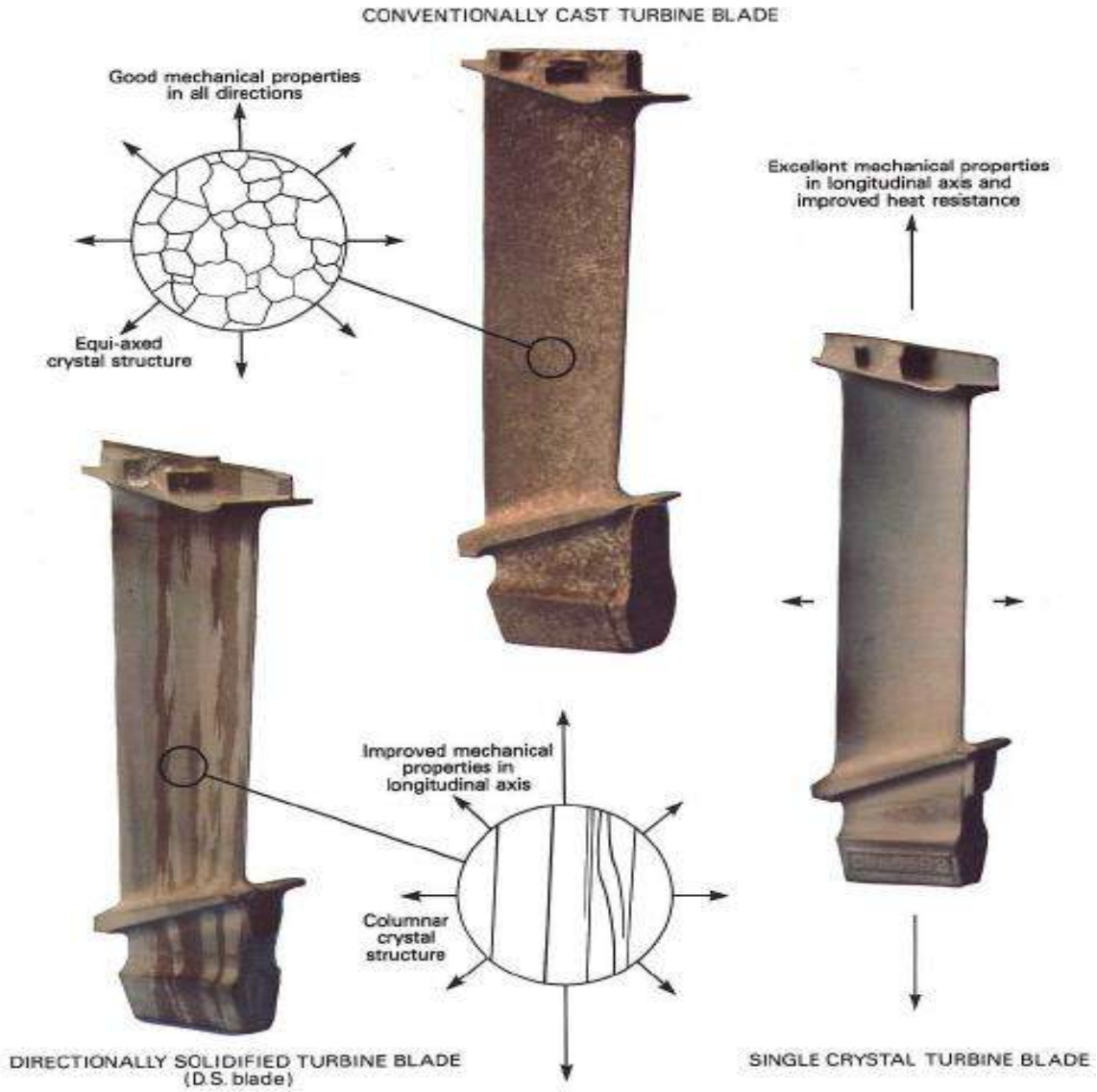

Fig. 5-11 Section through a dual alloy disc.

Turbine discs

A turbine disc has to rotate at high speed in a relatively cool environment and is subjected to large rotational stresses. The limiting factor which affects the useful disc life is its resistance to fatigue cracking. In the past, turbine disc have been made in ferritic and austenitic steels but nickel based alloys are currently used. Increasing the alloying elements in nickel extend the life limits of a disc by increasing fatigue resistance. Alternatively, expensive powder metallurgy discs, which offer an additional 10% in strength, allow faster rotational speeds to be achieved.

Turbine blades

A brief mention of some of the points to be considered in connection with turbine blade design will give an idea of the importance of the correct choice of blade material. The blades, while glowing red-hot, must be strong enough to carry the centrifugal loads due to rotation at high speed. A small turbine blade weighing only two ounces may exert a load of over two tons at top speed and it must withstand the high bending loads applied by the gas to produce the many thousands of turbine horsepower necessary to drive the compressor. Turbine blades must also be resistant to fatigue and thermal shock, so that they will not fail under the influence of high frequency fluctuations in the gas conditions, and they must also be resistant to corrosion and oxidization. In spite of all these demands, the blades must be made in a material that can be accurately formed and machined by current manufacturing methods.

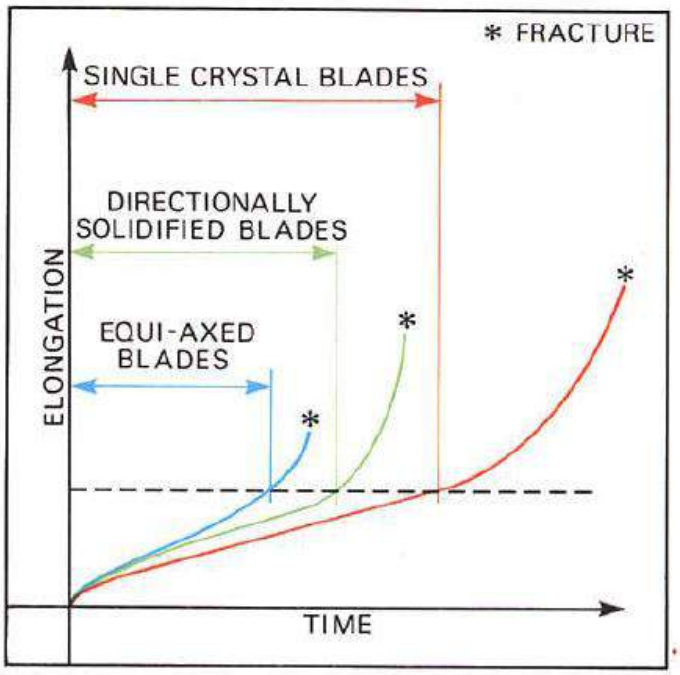

Fig. 5-13 Comparison of turbine blade life properties.

From the foregoing, it follows that for a particular blade material and an acceptable safe life there is an associated maximum permissible turbine entry temperature and a corresponding maximum engine power. It is not surprising, therefore, that metallurgists and designers are constantly searching for better turbine blade materials and improved methods of blade cooling. Over a period of operational time the turbine blades slowly grow in length. This phenomenon is

known as ’creep’ and there is a finite useful life limit before failure occurs. The early materials used were high temperature steel forgings, but these were rapidly replaced by cast nickel base alloys which give better creep and fatigue properties. Close examination of a conventional turbine blade reveals a myriad of crystals that lie in all directions (equi-axed). Improved service life can be obtained by aligning the crystals to form columns along the blade length, produced by a method known as ’Directional Solidification’. A further advance of this technique is to make the blade out of a single crystal, Examples of these structures are shown in fig. 5-12. Each method extends the useful creep life of the blade (fig. 5-13) and in the case of the single crystal blade, the operating temperature can be substantially increased. A non-metal based turbine blade can be manufactured from reinforced ceramics. Their initial production application is likely to be for small high speed turbines which have very high turbine entry temperatures.

Turbine Thermodynamics

The high pressure and temperature gas that leaves the combustor is directed into a turbine. The turbine may be thought of as a *valve* because on one side it has a high-pressure gas and on the other side it has a low-pressure gas of the exhaust nozzle or the tailpipe. Therefore, the first *valve*, that is, the throttle station, in a gas turbine engine is at the turbine. The throat of an exhaust nozzle in a supersonic aircraft is the second and final throttle station in an engine. Thus, the flow process in a turbine (and exhaust nozzle) involves significant (static) pressure drop and, in harmony with it, the (static) temperature drop, which is called *flow expansion*. The flow expansion produces the necessary power for the compressor and the propulsive power for the aircraft. The turbine is connected to the compressor via a common shaft, which provides the shaft power to the compressor (Figure 4.12). In drawing an analogy, we can think of the expansion process in a gas turbine engine as the counterpart of *power stroke* in an intermittent combustion engine. However, in a turbine, the power transmittal is continuous.

Due to high temperatures of the combustor exit flow, the first few stages of the turbine, that is, the high-pressure turbine (HPT), need to be cooled. The coolant is the air bleed from the compressor, which may be bled from different compression stages, for example, between the low- and high-pressure compressor and at the compressor exit. It has been customary, however, to analyze an *uncooled* turbine in the preliminary cycle analysis, followed by an analysis of the cycle with cooling effects in the turbine and the exhaust nozzle. Other cooling media, such as water, have been used in stationary gas turbine power plants. However, in the design-to-weight environment of an aircraft carrying extra water to cool the turbine blades is not feasible. A cooling solution, which uses the engine cryogenic fuel, such as hydrogen or methane, as the coolant to cool the engine and aircraft components is called *regenerative cooling* and has proven its effectiveness in liquid propellant chemical rocket engines for decades. Areal flow process in an uncooled turbine involves irreversibilities such as frictional losses in the boundary layer, tip clearance flows, and shock losses in transonic turbine stages. The viscous dominated losses, that is, boundary layer separation, reattachment, and tip vortex flows, are concentrated near the end walls, thus a special attention in turbine flow optimization is made on the *end-wall* regions. We will address the end wall losses and treatments in the turbomachinery chapters. Another source of irreversibility in a real turbine flow is related to the cooling losses. Coolant is typically injected from the blade attachment (to the hub or casing) into the blade, which provides internal convective cooling and usually external film cooling on the blades. The turbulent mixing associated with the coolant stream and the hot gases is the primary mechanism for (the turbine stage) cooling losses. We will examine the question of turbine cooling and cycle thermal

efficiency later in this chapter. The thermodynamic process for an uncooled turbine flow may be shown in an *h–s* diagram (Figure 4.13). The actual expansion process in the turbine is depicted by the solid line connecting the total (or stagnation) states t4 and t5 (Figure 4.13). The isentropically reached exit state t5s represents the ideal, loss-free flow expansion in the turbine to the same backpressure *p*t5. The relative height, on the enthalpy scale in Figure 4.13, between the inlet total and outlet total condition of the turbine represents the power production

■ FIGURE 4.13
Expansion process in an uncooled turbine (note the entropy rise across the turbine, Δs_t)

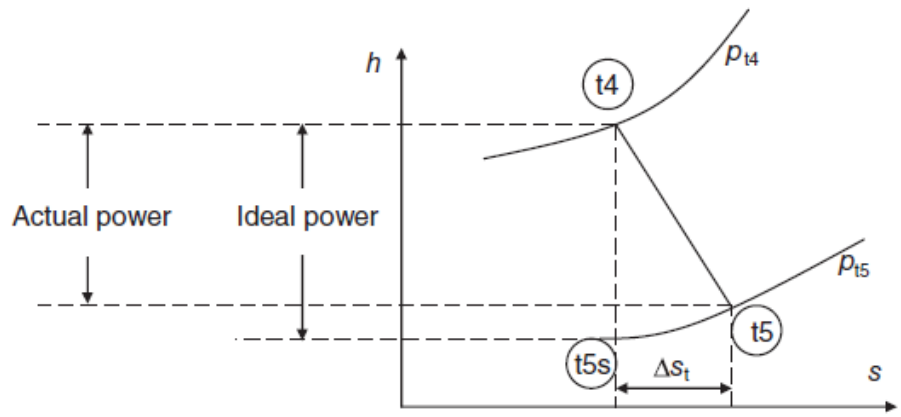

potential (i.e., ideal) and the actual power produced in a turbine. The ratio of these two heights is called the turbine adiabatic efficiency η_t, that is,

$$\wp_{t,actual} = \dot{m}_t(h_{t4} - h_{t5}) = \dot{m}_t \Delta h_{t,actual} \quad \textbf{(4.34)}$$

$$\wp_{t,ideal} = \dot{m}_t(h_{t4} - h_{t5s}) = \dot{m}_t \Delta h_{t,isentropic} \quad \textbf{(4.35)}$$

$$\eta_t \equiv \frac{h_{t4} - h_{t5}}{h_{t4} - h_{t5s}} = \frac{\Delta h_{t,actual}}{\Delta h_{t,isentropic}} \quad \textbf{(4.36)}$$

In Equations 4.34 and 4.35, the turbine mass flow rate is identified as m_t, which accounts for the air and fuel mass flow rate that emerge from the combustor and expand through the turbine, that is,

$$\dot{m}_t = \dot{m}_0 + \dot{m}_f = (1 + f)\dot{m}_0 \quad \textbf{(4.37)}$$

The numerator in Equation 4.36 is the actual power produced in a *real uncooled turbine*, and the denominator is the *ideal* power that in a reversible and adiabatic turbine could be produced. If we divide the numerator and denominator of Equation 4.36 by h_{t4}, we get

$$\eta_t = \frac{1 - T_{t5}/T_{t4}}{1 - T_{t5s}/T_{t4}} \quad \textbf{(4.38)}$$

Since the thermodynamic states "t_{5s}" and "t_4" are on the same isentrope, the temperature and pressure ratios are then related via the isentropic formula, that is,

$$\frac{T_{t5s}}{T_{t4}} = \left(\frac{p_{t5s}}{p_{t4}}\right)^{\frac{\gamma-1}{\gamma}} = \left(\frac{p_{t5}}{p_{t4}}\right)^{\frac{\gamma-1}{\gamma}} = \pi_t^{\frac{\gamma-1}{\gamma}} \quad \textbf{(4.39)}$$

Therefore, turbine adiabatic efficiency may be expressed in terms of the turbine total pressure and temperature ratios as

$$\eta_t = \frac{1 - \tau_t}{1 - \pi_t^{\frac{\gamma-1}{\gamma}}} \quad \textbf{(4.40)}$$

We may also define a *small-stage* efficiency for a turbine, as we did in a compressor, and call it the turbine polytropic efficiency e_t. For a small expansion, representing a small stage, we can replace the finite jumps, that is, Δs, with incremental step *d* in Equation 4.36 and write

$$e_t \equiv \frac{dh_t}{dh_{ts}} = \frac{dh_t}{\frac{dp_t}{\rho_t}} \qquad \textbf{(4.41)}$$

Expressing enthalpy in terms of temperature and specific heat at constant pressure as $dh_t = c_p dT_t$, which is suitable for a perfect gas, and simplifying Equation 4.41 similar to the compressor section, we get

$$\tau_t = \pi_t^{\frac{(\gamma-1)e_t}{\gamma}} \quad \text{or} \quad \pi_t = \tau_t^{\frac{\gamma}{(\gamma-1)e_t}} \qquad \textbf{(4.42)}$$

$$\tau_t \equiv T_{t5}/T_{t4} \qquad \textbf{(4.43)}$$

$$\pi_t \equiv p_{t5}/p_{t4} \qquad \textbf{(4.44)}$$

■ **FIGURE 4.14**
Variation of turbine adiabatic efficiency η_t with the inverse of turbine expansion ratio $1/\tau_t$

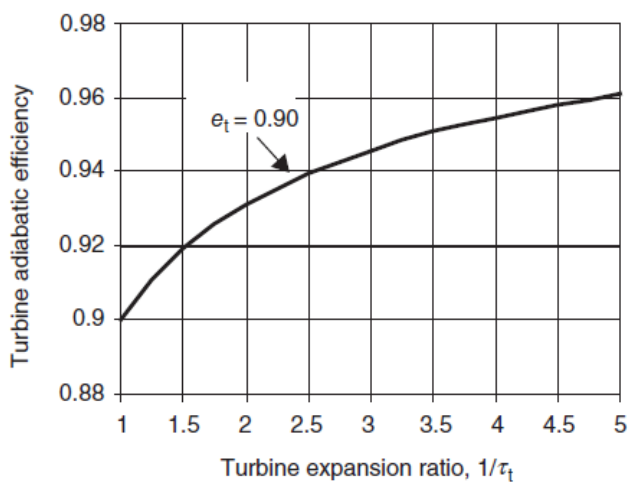

We note that in Equation 4.42, in the limit of e_t approaching 1, that is, isentropic expansion, we will recover the isentropic relationship between the temperature and pressure ratio, as expected. Replacing π_t in Equation 4.39 by its equivalent expression (from Equation 4.42), we derive a relation between the two types of turbine efficiencies, η_t and e_t, as

$$\eta_t = \frac{1-\tau_t}{1-\tau_t^{1/e_t}} \qquad \textbf{(4.45)}$$

Equation 4.45 is plotted in Figure 4.14. For a small-stage efficiency of 90%, that is, $e_t = 0.90$, the turbine adiabatic efficiency η_t grows with the inverse of turbine expansion parameter $1/\tau_t$. This may initially defy logic that how is it possible to become more efficient if we *add* more stages to the turbine? Wouldn't it add to losses? The opposite of this trend occurred in the compressor, that is, compressor adiabatic efficiency for a finite size compressor *was* lower than the efficiency of a small-stage compressor (Figure 4.7). The explanation is that the energy transfer occurs from the fluid to the rotor in the turbine; therefore, more stages offer more opportunities to convert fluid energy into shaft power. The opposite happens in a compressor, that is, the compressor stages *consume* power, which means that the additional stages add losses to the process. In simple terms, the turbine stages may be thought of as *opportunities* and compressor stages as the *burden*.

The temperature ratio parameter τ_t across the turbine is established via a power balance between the turbine, compressor, and other shaft power extraction (e.g., electric generator) on the gas generator. Let us first consider the power balance between the turbine and compressor in its simplest form and then try to build on the added parameters. Ideally, the compressor absorbs all the turbine shaft power, that is,

$$\wp_t = \wp_c \qquad \textbf{(4.46a)}$$

$$\dot{m}_0(1+f)(h_{t4} - h_{t5}) = \dot{m}_0(h_{t3} - h_{t2}) \qquad \textbf{(4.46b)}$$

which simplifies to the following non-dimensional form

$$(1+f)\tau_\lambda(1-\tau_t) = \tau_r(\tau_c - 1) \qquad \textbf{(4.46c)}$$

The only unknown in the above equation is τ_t, as all other parameters either flow from upstream components, for example, the combustor will provide f, the compressor produces τ_c, and so on, or are design parameters such as τ_λ or τ_r. Hence, the turbine expansion parameter τ_t can be written as

$$\tau_t = 1 - \frac{\tau_r(\tau_c - 1)}{(1+f)\tau_\lambda} \qquad \textbf{(4.46d)}$$

Next, we consider the practical issue of hydrodynamic (frictional) losses in (radial) bearings holding the shaft in place and provide dynamic stability under operating conditions to the rotating assemblies of turbine and compressor. Therefore, a small fraction of the turbine power output is dissipated through viscous losses in the bearings, that is,

$$\wp_t = \wp_c + \Delta\wp_{\text{bearings}} \qquad \textbf{(4.47)}$$

where $\Delta\wp_{\text{bearings}}$ is the power loss due to bearings. In addition, an aircraft has electrical power needs for its flight control system and other aircraft subsystems, which requires tapping into the turbine shaft power. Consequently, the power balance between the compressor and turbine should account for the electrical power extraction, which usually accompanies the gas generator, that is,

$$\wp_t = \wp_c + \Delta\wp_{\text{bearing}} + \Delta\wp_{\text{electric generator}} \qquad \textbf{(4.48a)}$$

$$\wp_c = \wp_t - \Delta\wp_{\text{bearing}} - \Delta\wp_{\text{electric generator}} \qquad \textbf{(4.48b)}$$

In a simple cycle analysis, it is customary to lump all power dissipation and power extraction terms into a single *mechanical efficiency* parameter η_m that is multiplied by the turbine shaft power, to derive the compressor shaft power, that is,

$$\wp_c = \eta_m \wp_t \qquad \textbf{(4.49)}$$

where η_m is the mechanical efficiency parameter that needs to be specified a'priori, for example, $\eta_m = 0.95$

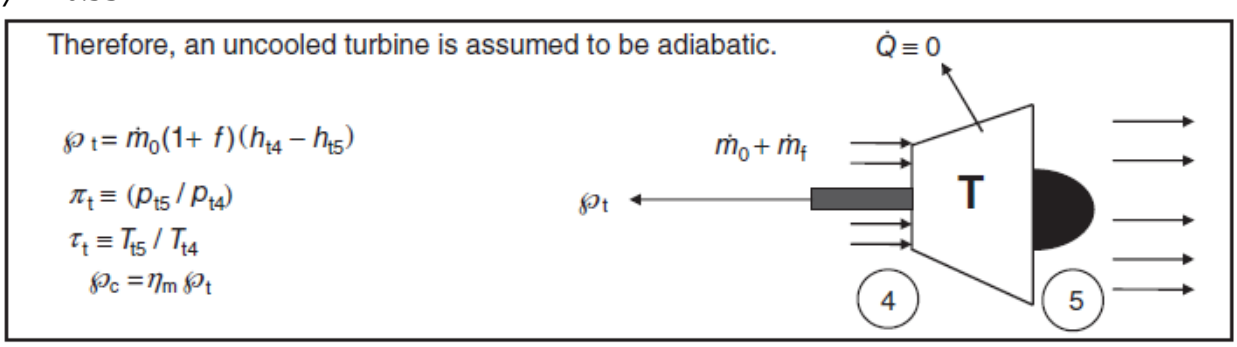

Turbine Cooling

An important consideration at the design stage of a gas turbine engine is the need to ensure that certain parts of the engine, and in some instances certain accessories, do not absorb heat to the extent that is detrimental to their safe operation. The principal areas which require air cooling are the combustor and turbine. Cooling air is used to control the temperature of the compressor shafts and discs by either cooling or heating them. This ensures an even temperature distribution and therefore improves engine efficiency by controlling thermal growth and thus maintaining minimum blade tip and seal clearances.

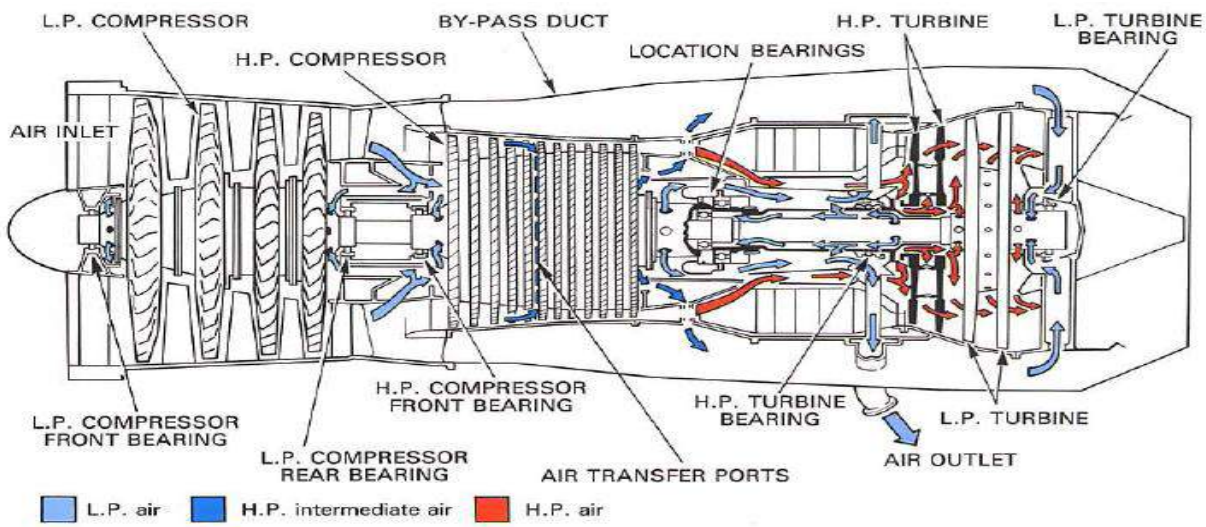

Fig. 9-1 General internal airflow pattern.

High thermal efficiency is dependent upon high turbine entry temperature, which is limited by the turbine blade and nozzle guide vane materials. Continuous cooling of these components allows their environmental operating temperature to exceed the material's melting point without affecting the blade and vane integrity. Heat conduction from the turbine blades to the turbine disc requires the discs to be cooled and thus prevent thermal fatigue and uncontrolled expansion and contraction rates.

An air cooled high pressure nozzle guide vane and turbine blade arrangement illustrating the cooling airflow is shown in fig. 9-2. Turbine vane and turbine blade life depends not only on their form but also on the method of cooling, therefore the flow design of the internal passages is important. There have been numerous methods of turbine vane and turbine blade cooling which have been used throughout the history of gas turbines. Generally, single pass internal (convection) cooling was of great practical benefit but development has lead to multipass internal cooling of blades, impingement cooling of vanes with external air film cooling of both vanes and blades.

The 'pre-swirl nozzles' reduce the temperature and pressure of the cooling air fed to the disc for blade cooling. The nozzles also impart a substantial whirl velocity to assist efficient entry of the air into the rotating cooling passages. Cooling air for the turbine discs enters the annular spaces between the discs and flows outwards over the disc faces. Flow is controlled by interstage seals and, on completion of the cooling function, the air is expelled into the main gas stream.

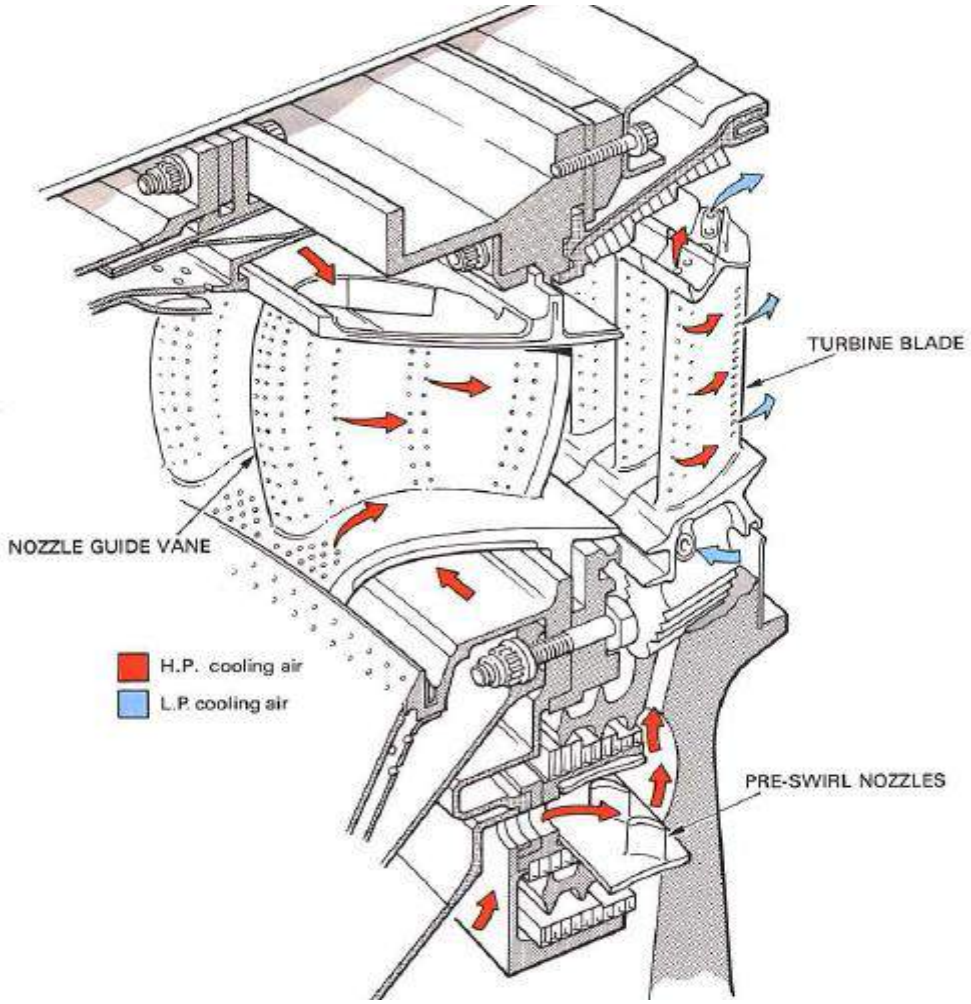

To cool the high-pressure turbine stages, a small fraction of compressor air can be diverted from various stages of the compression. Engine cooling is essentially a *pressure driven* process, which calls for a pressure scheduling of the coolant to achieve the highest cooling efficiency. For example, to cool the first nozzle and the first rotor in a turbine,

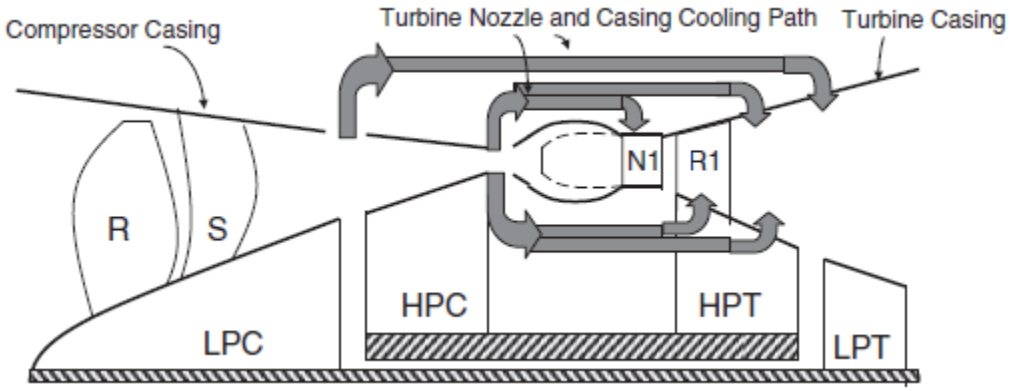

we need to tap the compressor exit air, as it has the *right* pressure. Earlier stages of the compressor have not yet developed the necessary pressure to overcome downstream pressure in

the high-pressure end of a turbine. To cool the medium-pressure turbine stages, we need to divert compressor air from the medium-pressure compressor. We could use higher pressure compressor exit air as well but the extra compression work we spent compressing the gas to the exit condition is essentially a wasted effort, that is, energy loss for the cycle. Therefore, the problem of *pressure matching* between the coolant stream and the hot gas in a turbine is real and significant. The consequence of a mismatch is either inadequate cooling flow in a turbine blade with even a possibility of a *reverse flow* of hot gases into the cooling channels or the need for excessive throttling of the coolant stream and associated cycle losses. Figure above shows possible coolant extraction in the compressor for turbine cooling. We can simplify the investigation of the thermodynamics of cooled turbine stages significantly by assuming that each blade row coolant is discharged at the blade row exit, that is, trailing edge ejection. This simplifies the thermodynamics as we consider *dumping* the entire coolant used in a given blade row at the trailing edge of the blades and then apply conservation laws to the coolant–hot gas mixing process. This approach avoids the discrete coolant–hot gas mixing, which may be distributed over the suction and pressure surfaces of the blade row, as in film-cooled blades. Application of the energy equation to the coolant–hot gas mixing process will result in a lower mixed-out temperature for the hot gas. Consequently, the hot gas stream will experience a reduced entropy state after mixing with the coolant. In return, the coolant stream, which is heated by the hot gas, will experience an entropy rise, which according to the second law of thermodynamics is greater than the entropy reduction in the hot gas stream. The expansion process in a turbine with two cooled stages followed by an uncooled low-pressure turbine is depicted in an *h–s* diagram in Figure 4.16.

■ FIGURE 4.16
***h–s* diagram for a turbine expansion with two cooled stages followed by an uncooled LPT (blade row exit mixing with the coolant is indicated by a negative Δ*s* and a temperature drop)**

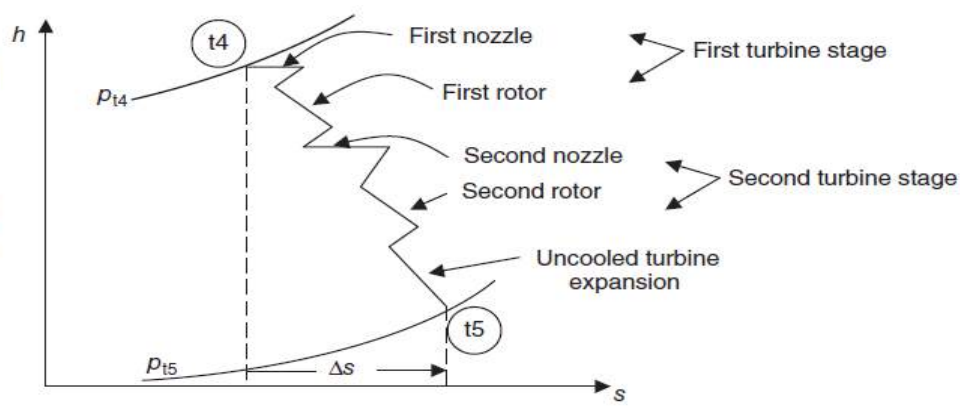

The mixing process at the exit of each blade row is identified with negative entropy production, and the cooling path is roughly drawn in as a nearly constant pressure process. In contrast, the coolant stream will undergo a heating process from the blade and then through mixing with the hot gases in the turbine. The thermodynamic state of the coolant is shown in Figure 4.16. The *h–s* diagram for the hot gas (shown in Figure 4.16) shows a constant h_t process for the first and second turbine nozzle. Constant total enthalpy indicates an adiabatic process with no mechanical energy exchange. These two criteria are met in an uncooled turbine nozzle, which is stationary and consequently exchanges no mechanical energy with the fluid. Across the nozzle, due to frictional and shock losses, a total pressure drop is indicated in Figure 4.16. Regarding the blade cooling, however, we will introduce the entire blade row coolant at the blade row exit, as suggested earlier. The cooling process results in a lower total temperature of the mixture of hot and cold gas, as well as a total pressure drop due to turbulent mixing of the two streams. This

process can be seen in Figure 4.17. The drop of total enthalpy across the rotor is proportional to the shaft power production by the rotor blade row. This shaft power may be written as

$$\wp_{\text{rotor}} = \tau_{\text{rotor}}\omega = \dot{m}_{\text{rotor}}\Delta h_{\text{t}} \qquad \textbf{(4.50)}$$

The product of rotor torque τ and the angular speed ω of the rotor is the shaft power `a la Newton. The irreversibility in the flow through the rotor is shown via a process involving entropy rise across the rotor in Figure 4.16. Again the flow expansion after the rotor is cooled off by the blade row coolant, which is injected at the blade row trailing edge and the process continues. To establish the mixed-out state of the coolant and the hot gas, we will apply the conservation principles, as noted earlier. The law of conservation of energy applied to a coolant stream of $\dot{m}_c$ mass flow rate carrying a total enthalpy of $h_{t,c}$ mixing with a hot gas stream of $\dot{m}_g$ with a total enthalpy of $h_{t,g}$ is written as

$$\dot{m}_{\text{c}}h_{\text{t,c}} + \dot{m}_{\text{g}}h_{\text{t,g}} = (\dot{m}_{\text{c}} + \dot{m}_{\text{g}})h_{\text{t,mixed-out}} \qquad \textbf{(4.51)}$$

■ **FIGURE 4.17**
***h–s* diagram of the coolant stream, first inside the blade then mixing with the hot turbine gas**

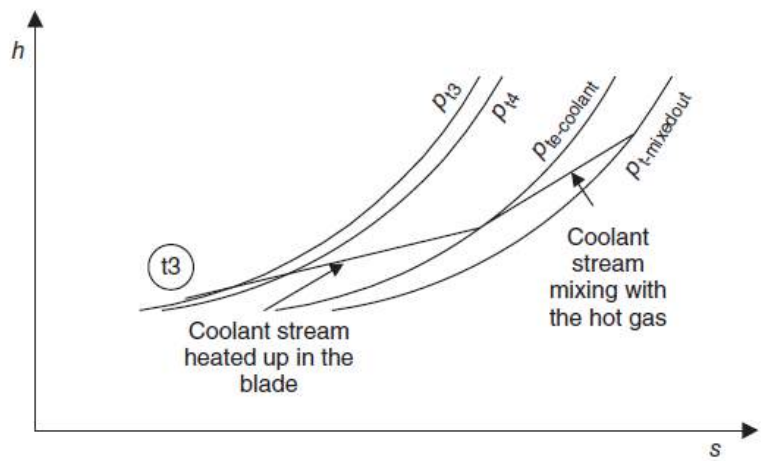

where the only unknown is the mixed-out enthalpy state of the coolant-hot gas mixture, $h_{t,mixed-out}$. We can express the above equation in nondimensional form by dividing bothsides by $\dot{m}_g h_{t,g}$, to get

$$\frac{h_{\text{t,mixed-out}}}{h_{\text{t,g}}} = \frac{1 + \dfrac{\dot{m}_{\text{c}}}{\dot{m}_{\text{g}}}\dfrac{h_{\text{t,c}}}{h_{\text{t,g}}}}{1 + \dfrac{\dot{m}_{\text{c}}}{\dot{m}_{\text{g}}}} \approx \left(1 - \frac{\dot{m}_{\text{c}}}{\dot{m}_{\text{g}}}\right)\left(1 + \frac{\dot{m}_{\text{c}}}{\dot{m}_{\text{g}}}\frac{h_{\text{t,c}}}{h_{\text{t,g}}}\right) \qquad \textbf{(4.52)}$$

In Equation 4.52, two non -dimensional parameters emerge that basically govern the energetics of a hot and a cold mixture. These parameters are

- $\dfrac{\dot{m}_{\text{c}}}{\dot{m}_{\text{g}}}$ the coolant mass fraction (typically $\ll 1$)
- $\dfrac{h_{\text{t,c}}}{h_{\text{t,g}}}$ cold-to-hot total enthalpy ratio.

We have also used a mathematical approximation in Equation 4.52, in the form of binomial expansion:

$$\frac{1}{1+\varepsilon} \approx 1 - \varepsilon \qquad \textbf{(4.53)}$$

where $\varepsilon \prec\prec 1$ and the largest neglected term in the series is $O(\varepsilon^2)$. The coolant stream experiences a total pressure drop in the cooling channels of the blade as a result of frictional

losses and a total pressure drop as a result of turbulent mixing with the hot gas. The enthalpy-entropy diagram representing a coolant stream is depicted in Figure 4.17.

Numerical Example:

Consider an uncooled gas turbine with its inlet condition the same as the exit condition of the combustor described in example before. The turbine adiabatic efficiency is 88%. The turbine produces a shaft power to drive the compressor and other accessories at $\wp_t$ = 45 MW. Assuming that the gas properties in the turbine are the same as the burner exit in Example before, calculate

(a) turbine exit total temperature T_{t5} in K

(b) turbine polytropic efficiency, e_t

© turbine exit total pressure p_{t5} in kPa

(d) turbine shaft power $\wp_t$ based on turbine expansion ΔT_t

Solution:

The turbine shaft power is proportional to the mass flow rate through the turbine, which from Example 4.3 is 51 kg/s (50 for air and 1 for fuel flow rate), as well the total enthalpy drop, i.e.,

$$\wp_t = \dot{m}_t(h_{t4} - h_{t5})$$

Therefore, we isolate h_{t5} from above equation to get

$$\begin{aligned} h_{t5} &= h_{t4} - \wp_t/\dot{m}_t = c_{p4}T_{t4} - 35 \times 10^6/51 \\ &= 1.156\,\text{kJ/kg}\cdot\text{K}\,(1390\,\text{K}) \\ &\quad - 45{,}000\,\text{kW}/51\,\text{kg/s} \approx 724.5\,\text{kJ/kg} \end{aligned}$$

$$\begin{aligned} T_{t5} &= h_{t5}/c_{p5} \\ &= (724.5\,\text{kJ/kg})/(1.156\,\text{kJ/kg}\cdot\text{K}) \approx 626.7\,\text{K} \end{aligned}$$

Turbine polytropic efficiency e_t may be related to its adiabatic efficiency and τ_t via equation

$$\eta_t = \frac{1 - \tau_t}{1 - \tau_t^{1/e_t}}$$

The turbine expansion parameter τ_t = 626.7/1390 = 0.4509; and if we isolate e_t from above equation we get

$$\begin{aligned} e_t &= \ln(\tau_t)/\ln[1 - (1 - \tau_t)/\eta_t] \\ &= \ln(0.4509)/\ln[1 - 0.5491/0.88] \cong 0.8144 \end{aligned}$$

We know that turbine pressure and temperature ratios are related by the polytropic efficiency via

$$\pi_t = \tau_t^{\frac{\gamma}{(\gamma-1)e_t}} = (0.4509)^{\frac{1.33}{0.33(0.8144)}} \cong 0.01941$$

The turbine exit total pressure is therefore $p_{t4} \cdot \pi_t$. We had found p_{t4} = 1.92 MPa in Example 4.3, therefore,

$$p_{t5} = 0.01941(1.92\,\text{MPa}) = 37.26\,\text{kPa}$$

The turbine shaft power is the product of the turbine mass flow rate and the total enthalpy drop across the turbine, i.e.,

$$\begin{aligned} \wp_t &= \dot{m}_t c_{pt}(T_{t4} - T_{t5}) \\ &= 51\,\text{kg/s}\,(1156\,\text{J/kg}\cdot\text{K})(1390 - 626.7)\,\text{K} \cong 45\,\text{MW} \end{aligned}$$

Chapter Four
Gas Turbine Nozzles

The gas turbine nozzles are discussed in details in this chapter as they need special considerations and an introduction to compressible fluid flows. A sound knowledge of compressible fluid flows in a duct is required to go through this chapter.

Nozzles and Types:

A nozzle is a duct by flowing through which the velocity of fluid increases at an expense of pressure drop. A duct which decreases the velocity of a fluid may be either a nozzle or a diffuser depending upon the end conditions across it. Many engineering applications require a jet of high velocity and this objective is efficiently achieved with a nozzle. In turbo machines (Steam and Gas turbines) the high speed stream of fluid is directed on the curved blades and the kinetic energy is transformed into mechanical work. In rocket motors and jet propulsion, the thrust produced by the jet provides the propulsive effort. In flow measurement, the differential pressure drop is correlated to velocity to find the discharge. Other applications of nozzles are the injectors for pumping feed water into the boiler and the ejectors for removing air from the condensers.

Fluid enters the nozzle at high pressure and expands to lower a pressure maintained by some means at the exit.

a. Converging Nozzle: If the cross-section of the nozzle decreases continuously from the entrance to exit, it is called a converging nozzle.

b. Diverging Nozzle: If the cross-section of the nozzle increases continuously from the entrance to the exit, it is called the diverging nozzle.

c. Converging-Diverging Nozzle: If the cross-section of the nozzle first decreases and then increases, it is called convergent-divergent nozzle.

Speed of Sound & Mach Number

Sound waves are infinitesimal pressure waves propagating in a medium. The propagation of sound waves, or acoustic waves, is reversible and adiabatic, hence isentropic. Since sound propagates through collision of fluid molecules, the speed of sound is higher in liquids than gas. The derivation of the speed of sound is very simple and instructive. Assume a plane sound wave propagates in a medium at rest with speed u. The fluid behind the wave is infinitesimally set in motion at the speed du with an infinitesimal change of pressure, temperature, and density. The fluid ahead of the wave is at rest and yet unaffected by the approaching wave. A schematic drawing of this wave and fluid properties are shown in Figure 2.2. By switching observers from the gas at rest to an observer that moves with the wave at the wave speed u, we change the unsteady wave propagation problem into a steady one. This is known as the Lorentz transformation. The transformed problem is shown in Figure 2.3. The fluid static properties, pressure, density, and temperature are independent of the motion of an observer; hence they remain unaffected by the observer transformation. We may now apply steady conservation principles to a control volume, as shown in Figure 2.3. The control volume is a box with its sides parallel to the flow, an inlet and an exit area normal to the flow. We may choose the entrance and exit areas of the box to be unity. The continuity demands

$$\rho u = (\rho + d\rho)(u + du) \qquad (2.56)$$

■ **FIGURE 2.2**
Propagation of a plane acoustic wave in a gas at rest (an unsteady but isentropic problem)

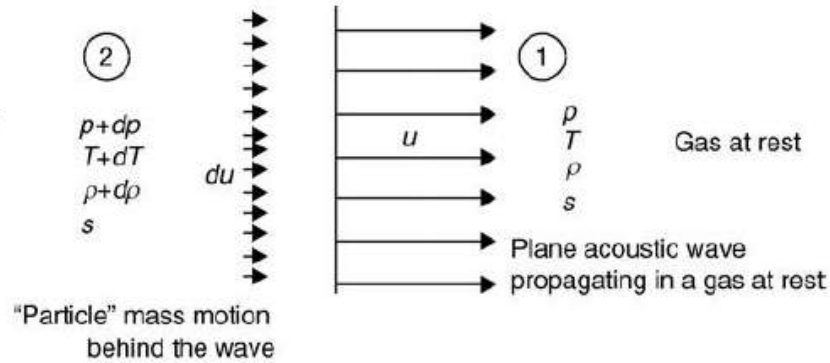

■ **FIGURE 2.3**
Flow as seen by an observer fixed at the wave (a steady problem)

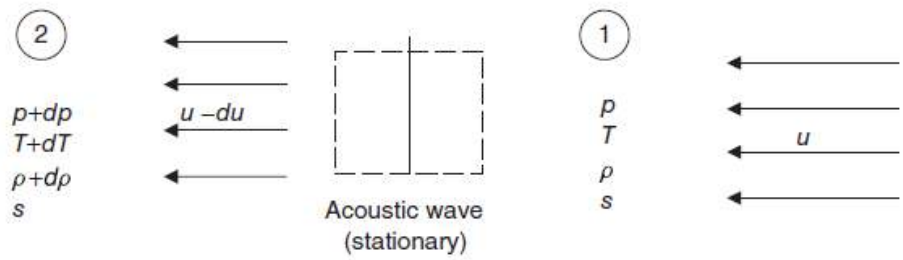

which simplifies to

$$\rho du = -u d\rho \qquad \textbf{(2.57)}$$

The momentum equation for this one-dimensional wave problem is

$$(\rho u)(u + du) - (\rho u)u = p - (p + dp) \qquad \textbf{(2.58)}$$

The change of momentum from inlet to exit is shown on the LHS of Equation 2.58. The first parenthesis of each momentum term is the mass flow rate, which is multiplied by the respective flows speeds at the exit and inlet. The driving forces on the RHS of Equation 2.58 are the pressure-area terms in the direction and opposite to the fluid motion, acting on areas that were chosen to be unity. The momentum equation simplifies to

$$\rho u du = dp \qquad \textbf{(2.59)}$$

Now, let us substitute the continuity equation (2.57) in the momentum equation (2.59), to get an expression for the square of the acoustic wave propagation in terms of pressure and density changes that occur as a result of wave propagation in a medium at rest

$$u^2 d\rho = dp \qquad \textbf{(2.60)}$$

$$u^2 = \frac{dp}{d\rho} = \left(\frac{\partial p}{\partial \rho}\right)_s \qquad \textbf{(2.61)}$$

Since, for isentropic flow, $p = \text{const} \cdot \rho$, Equation 2.61 reduces to

$$u^2 = \frac{\gamma p}{\rho} = \gamma R T \qquad \textbf{(2.62)}$$

We replaced the ratio of pressure to density by RT from the perfect gas law in Equation 2.62. The symbol we use in this book for the speed of sound is "a," hence, local speed of sound in a gas is

$$a = \sqrt{\frac{\gamma p}{\rho}} = \sqrt{\gamma R T} = \sqrt{(\gamma - 1) c_p T} \qquad \textbf{(2.63)}$$

The speed of sound is a *local* parameter, which depends on the local absolute temperature of the gas. Its value changes with gas temperature, hence it drops when fluid accelerates (or *expands*) and increases when gas decelerates (or *compresses*). The speed of sound in air at standard sea

level conditions is ~340 m/s or ~1100 ft/s. The type of gas also affects the speed of propagation of sound through its molecular weight. We may observe this behavior by the following substitution:

$$a = \sqrt{\gamma RT} = \sqrt{\gamma \left(\frac{\overline{R}}{MW}\right) T} \qquad \textbf{(2.64)}$$

A light gas, like hydrogen (H_2) with a molecular weight of 2, causes an acoustic wave to propagate *faster* than a heavier gas, such as air with (a mean) molecular weight of 29. If we substitute these molecular weights in Equation 2.64, we note that sound propagates in gaseous hydrogen *nearly four times faster* than air. Since both hydrogen and air are diatomic gases, the ratio of specific heats remains (nearly) the same for both gases at the same temperature. The equation for the speed of propagation of sound that we derived is for a gas at rest. Let us superimpose a uniform collective gas speed in a particular direction to the wave front, then the wave propagates as the vector sum of the two, namely, V+a waves. For waves propagating normal to a gas flow, we get either ($V + a$) or ($V - a$) as the propagation speed of sound. It is the ($V - a$) behavior that is of interest here. In case the flow is sonic, then ($a - a = 0$), which will not allow the sound to travel upstream and hence creates a zone of silence upstream of the disturbance. In case the flow speed is even faster than the local speed of sound, that is, known as supersonic flow, the acoustic wave will be confined to a cone. These two behaviors for small disturbances are shown in Figure 2.4.

■ FIGURE 2.4
Acoustic wave propagation in sonic and supersonic flows (or the case of a moving source)

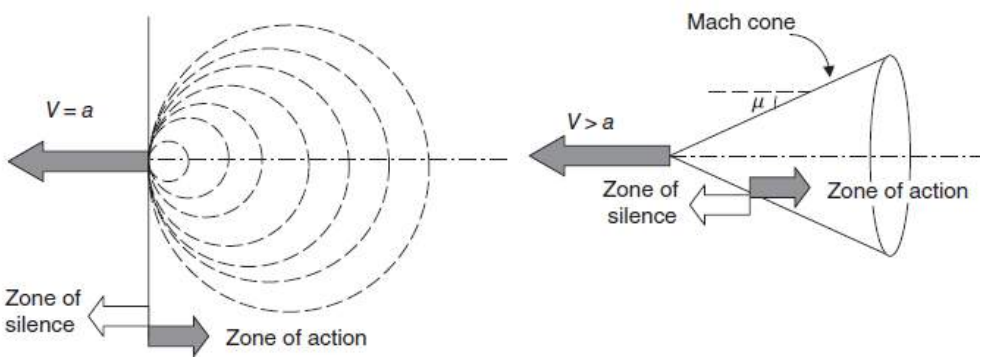

■ FIGURE 2.5
Wave front created by a *small disturbance* moving at a supersonic speed

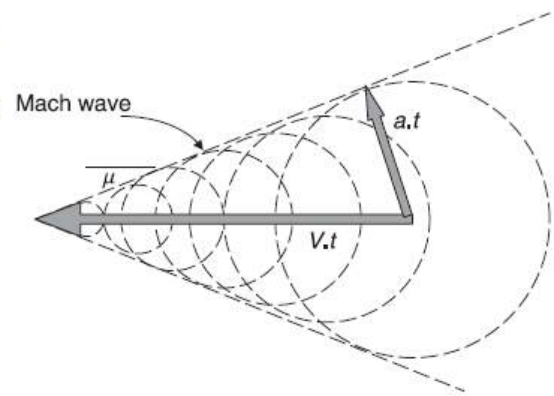

The ratio of local gas speed to the speed of sound is called Mach number, *M*

$$M \equiv \frac{V}{a} \qquad (2.65)$$

The envelope of the waves that create the zones of action and silence is the Mach wave. It makes a local wave angle with respect to the flow μ, which from the geometry of wave propagation, as shown in Figure 2.5, is

$$\mu = \sin^{-1}\left(\frac{a \cdot t}{V \cdot t}\right) = \sin^{-1}\left(\frac{1}{M}\right) \qquad (2.66)$$

Stagnation State

We define the stagnation state of a gas as the state reached in decelerating a flow to rest reversibly and adiabatically and without any external work. Thus, the stagnation state is reached isentropically. This state is also referred to as the *total* state of the gas. The symbols for the stagnation state in this book use a subscript "t" for total. The total pressure is p_t, the total temperature is T_t, and the total density is ρ_t. Since the stagnation state is reached isentropically, the static and total entropy of the gas are the same, that is, $s_t = s$. Based on the definition of stagnation state, the total energy of the gas does not change in the deceleration process, hence the stagnation enthalpy h_t takes on the form

$$h_t \equiv h + \frac{V^2}{2} \qquad (2.52)$$

which we defined earlier in this chapter. Assuming a *calorically perfect gas*, we may simplify the total enthalpy relation 2.52 by dividing through by c_p to get an expression for total temperature according to

$$T_t = T + \frac{V^2}{2c_p} \quad \text{(valid for a calorically perfect gas)} \qquad (2.67)$$

This equation is very useful in converting the local static temperature and gas speed into the local stagnation temperature. To non-dimensionalize Equation 2.67, we divide both sides by the static temperature, that is,

$$\frac{T_t}{T} = 1 + \frac{V^2}{2c_pT} \qquad (2.68)$$

The denominator of the kinetic energy term on the RHS is proportional to the square of the local speed of sound a^2 according to Eq 2.63, which simplifies to

$$\frac{T_t}{T} = 1 + \left(\frac{\gamma - 1}{2}\right)\frac{V^2}{a^2} = 1 + \left(\frac{\gamma - 1}{2}\right)M^2 \qquad (2.69)$$

Therefore to arrive at the stagnation temperature of the gas, we need to have its static temperature as well as either the gas speed V or the local Mach number of the gas M to substitute in Equations 2.68 or 2.69, respectively. The ratio of stagnation to static temperature of a (calorically perfect) gas is a unique function of local Mach number, according to Equation 2.69. We may also use a spreadsheet tabulation of this function for later use for any gas characterized by its ratio of specific heats γ. From isentropic relations between the pressure and temperature ratio that we derived earlier based on Gibbs equation of thermodynamics, we may now relate the ratio of stagnation to static pressure and the local Mach number via

$$\frac{p_t}{p} = \left(\frac{T_t}{T}\right)^{\frac{\gamma}{\gamma-1}} = \left[1 + \left(\frac{\gamma - 1}{2}\right)M^2\right]^{\frac{\gamma}{\gamma-1}} \quad \text{(valid for a calorically perfect gas)} \qquad (2.70)$$

We used the isentropic relation between the stagnation and static states based on the definition of the stagnation state that is reached isentropically. Also, the stagnation density is higher than the static density according to

$$\frac{\rho_t}{\rho} = \left(\frac{p_t}{P}\right)^{\frac{1}{\gamma}} = \left[1 + \left(\frac{\gamma - 1}{2}\right) M^2\right]^{\frac{1}{\gamma - 1}} \quad \text{(Valid for a calorically perfect gas)} \qquad (2.71)$$

We note that the ratio of stagnation-to-static state of a gas is totally described by the local Mach number and the type of gas γ. The tabulation of these functions, that is, p_t/p, T_t/T, and ρ_t/ρ are made in isentropic tables for a gas described by its ratio of specific heats γ. Figure 2.6 shows the variation of the stagnation state with Mach number for a diatomic gas, such as air ($\gamma = 1.4$). The least variation is noted for the stagnation temperature, followed by the density and pressure. To graph these variations (up to Mach 6), we had to use a logarithmic scale, as the total pressure rise with Mach number reaches above one thousand (times the static pressure) while the stagnation temperature stays below ten (times the static temperature). We may examine higher Mach numbers in Figure 2.7. The assumption in arriving at the stagnation state properties relative to the static properties was *a calorically perfect gas*. The impact of high-speed flight on the atmosphere is to cause molecular dissociation, followed by ionization of the oxygen and nitrogen molecules. A host of other chemical reactions takes place, which result in a violation of our initial assumption. In reality, both the specific heats (c_p and c_v) are functions of temperature as well as the pressure at hypersonic Mach numbers, that is, $M > 5$. There are two lessons to be learned here.

■ FIGURE 2.6
Variation of the stagnation state with Mach number for a diatomic gas, $\gamma = 1.4$ (For a calorically perfect gas, i.e., c_p, c_v, and γ are constants)

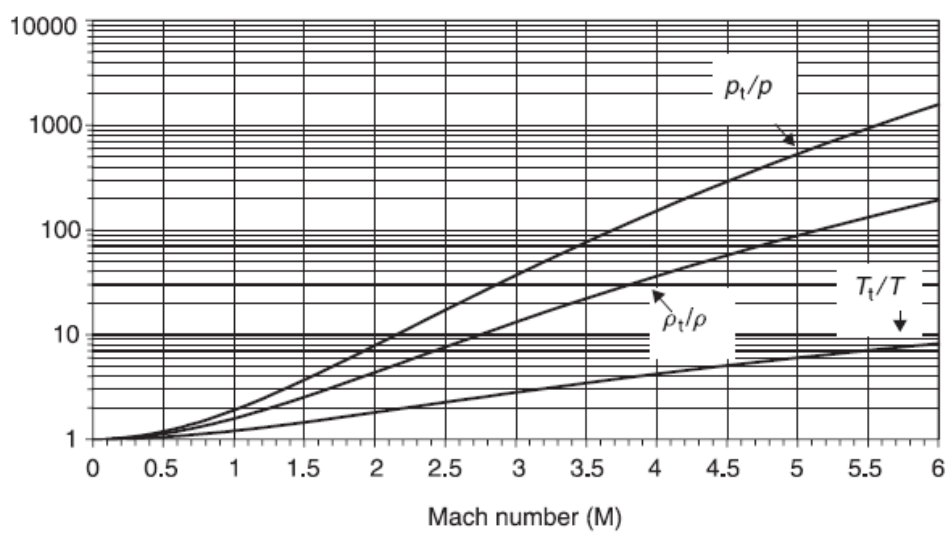

Although the pressure ratio (p_t/p) is relieved through real gas effects due to a high-speed flight, it still remains high. Consequently, the high-speed flight has to be scheduled at a high altitude where the static pressure is low. For example, the static pressure at 25 km is only ~2.5% and at 50 km altitude is 0.07% of the sea level pressure. To identify the local static and stagnation states of a gas in a Mollier (h–s) diagram is important in studying propulsion. We use the stagnation enthalpy definition to identify the local stagnation properties of a gas, for example, we start with the static state and then build up a kinetic energy, as in Figure 2.8. We may also apply the Gibbs equation to the stagnation state of the gas to get

$$\Delta s = c_p \ell n(T_{t2}/T_{t1}) - R\ell n(p_{t2}/p_{t1}) \qquad \textbf{(2.72)}$$

For adiabatic flows the first term on the RHS identically vanishes, since the total temperature remains constant. Hence, the total pressure for adiabatic flows with losses, for example, due to frictional losses, always decreases, since the entropy change has to be positive. The exponential relationship between the total pressure ratio and the entropy rise in an adiabatic flow is very useful to propulsion studies and we write it in Equation 2.73

$$p_{t2}/p_{t1} = e^{-\frac{\Delta s}{R}} \qquad \textbf{(2.73)}$$

All adiabatic flows with loss result in a drop of total pressure. For example, in a supersonic inlet with shocks and frictional losses in the boundary layer, we encounter a total pressure loss. Since, the total pressure is now cast as a measure of loss via Equation 2.73, it serves as a commodity that propulsion engineers try to preserve as much as possible. The *T*–*s* diagram of an adiabatic flow with loss is shown in Figure 2.9.

■ FIGURE 2.7 **Variation of stagnation state of gas with flight Mach number for $\gamma = 1.4$ (for a *calorically perfect gas*)**

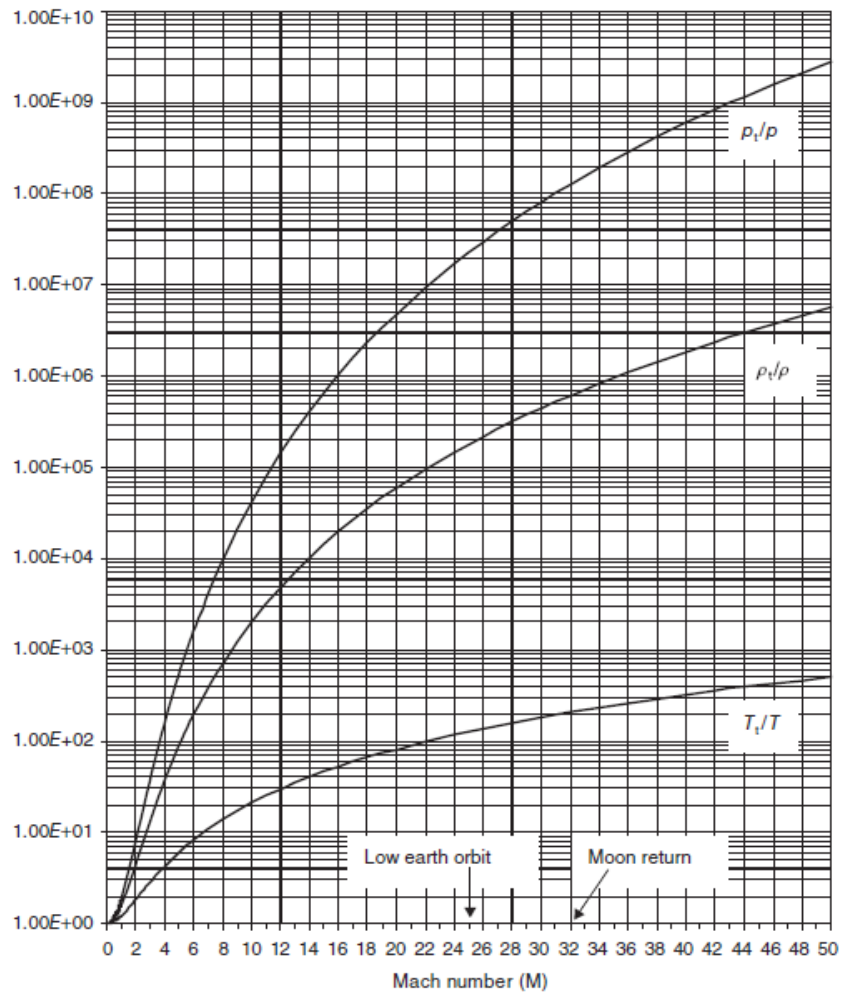

■ **FIGURE 2.8**
Stagnation and static states of a gas in motion shown on an *h–s* diagram

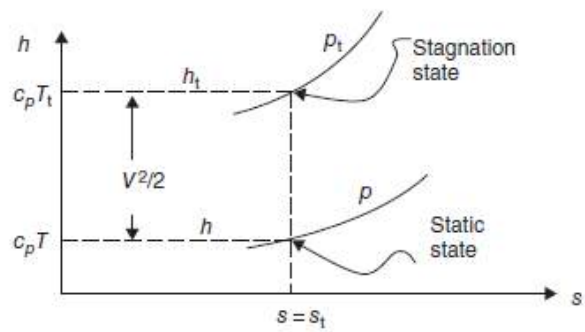

■ **FIGURE 2.9**
Adiabatic flow that shows total pressure loss Δp_t, e.g., flows containing shocks

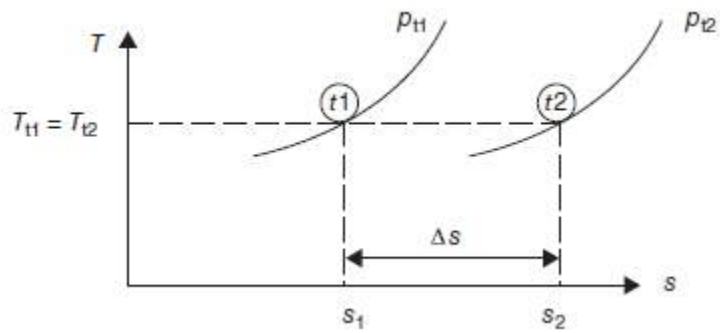

One Dimensional Steady flow

In duct flows with area variations, such as a diffuser or a nozzle, where the boundary layers are completely attached, the streamwise variation of flow variables dominate the lateral variations. In essence, the flow behaves as a uniform flow with pressure gradient in a variable-area duct. A schematic drawing of a duct with area variation is shown in Figure 2.10. The primary flow direction is labeled as "*x*" and the lateral direction is "*y*." Although the flow next to the wall assumes the same slope as the wall, the cross-sectional flow properties are based on uniform parallel flow at the cross-section. The flow area at a cross-section enters the conservation laws, but the variation in the cross-section from the centerline to the wall is neglected.

■ **FIGURE 2.10**
Schematic drawing of a variable-area duct with attached boundary layers

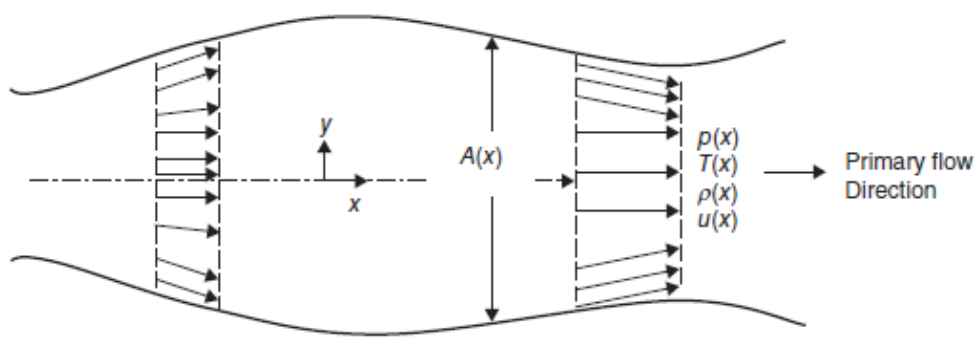

To develop the quasi-one-dimensional flow equations in a variable-area duct with inviscid fluid, we examine a slice, known as a *slab*, of the flow and apply the Taylor series approximation to the two sides of the slab. Figure 2.11 shows a thin slice of a duct flow with streamwise length *dx* separating the two sides of the slab. We assume general parameters on one side and step in the *x*-direction using the Taylor series approximation of an analytical function expanded in the neighborhood of a point. Since the step size *dx* is small, we may truncate the infinite Taylor series after the first derivative.

■ **FIGURE 2.11** ***Slab*** **of inviscid fluid in a variable-area duct (walls exert pressure on the fluid)**

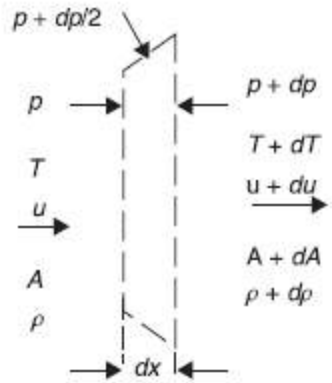

Note that the walls exert one-half of the incremental pressure ($dp/2$) over the upstream pressure p, since we take only one-half the step size ($dx/2$) to reach its center. Now, let us apply the conservation principles to this thin slice of the flow. Continuity demands

$$\rho u A = (\rho + d\rho)(u + du)(A + dA) \qquad \textbf{(2.74)}$$

Ignoring higher order terms involving the products of two small parameters, such as $du \cdot dA$, we get

$$\rho u dA + u A d\rho + \rho A du = 0 \qquad \textbf{(2.75)}$$

Now dividing both sides by a nonzero constant, namely puA, we get the continuity equation in differential form

$$\frac{dA}{A} + \frac{d\rho}{\rho} + \frac{du}{u} = 0 \qquad \textbf{(2.76)}$$

This is also known as the *logarithmic derivative* of the local mass flow rate, puA = constant. Since we use the logarithmic derivative often in our analysis, let us examine it now. From the continuity equation

$$\rho u A = \text{Constant} \qquad \textbf{(2.77)}$$

We take the natural logarithm of both sides, to get the sum

$$\ell n(\rho) + \ell n(u) + \ell n(A) = \text{Constant} \qquad \textbf{(2.78)}$$

Now, if we take the differential of both sides we get Equation 2.76, which is called the logarithmic derivative of the continuity equation.

The momentum balance in the streamwise direction gives

$$(\rho u A)(u + du) - (\rho u A) u = pA - (p + dp)(A + dA) + (p + dp/2)\, dA \qquad \textbf{(2.79)}$$

The first term on the LHS is the rate of momentum out of the slab, which is the mass flow rate times the velocity out of the box. The second term on the LHS is the rate of momentum into the box. The first term on the LHS is the pressure force pushing the fluid out. The second term on the LHS is the pressure force in the opposite direction to the flow, hence negative. The last term on the LHS is the pressure force contribution of the walls. First, we note that its direction is in the flow direction, hence positive. Second, we note that the projection of the sidewalls in the flow direction is dA, which serves as the *effective* area for the wall pressure to push the fluid out of the box. We may simplify this equation by canceling terms and neglecting higher order quantities to get

$$\rho u A du = -A dp \qquad \textbf{(2.80)}$$

The flow area term is cancelled from Equation 2.80 (as expected) to yield

$$\rho u du = -dp \qquad (2.81)$$

The energy equation for an adiabatic (non heat-conducting) flow with no shaft work is the statement of conservation of total enthalpy, which differentiates into

$$dh_t = dh + udu = 0 \qquad (2.82)$$

The equation of state for a perfect gas may be written in logarithmic derivative form as

$$dp/p = d\rho/\rho + dT/T \qquad (2.83)$$

Also, as we stipulated an isentropic flow through the duct, that is, $ds = 0$, the pressure– density relationship follows the isentropic rule, namely $p/\rho\gamma$ = constant, which has the following logarithmic derivative:

$$\frac{dp}{p} - \gamma\frac{d\rho}{\rho} = 0 \qquad (2.84)$$

The set of governing equations for an isentropic flow through a duct of variable area are summarized as:

$$d\rho/\rho + du/u + dA/A = 0$$
$$\rho u du = -dp$$
$$dh + udu = 0$$
$$dp/p = d\rho/\rho + dT/T$$

The unknowns are the pressure p, density ρ, temperature T, and velocity u. The enthalpy for a perfect gas follows $dh = c_p dT$, hence we need to know the specific heat at constant pressure of the gas as well. The entropy remains constant, hence the static pressure is related to the speed of sound and density according to:

$$p = \rho a^2/\gamma \qquad (2.85)$$

Area Mach Number Relationship

Let us divide the momentum equation by $d\rho$, to get

$$\frac{\rho}{d\rho}udu = -\frac{dp}{d\rho} = -a^2 \qquad (2.86)$$

which yields

$$\frac{d\rho}{\rho} = -\frac{udu}{a^2} \qquad (2.87)$$

Now, let us substitute the density ratio in the continuity equation to relate the area variation to Mach number according to

$$-\frac{udu}{a^2} + \frac{du}{u} + \frac{dA}{A} = 0 \qquad (2.88a)$$

This simplifies to

$$(M^2 - 1)\frac{du}{u} = \frac{dA}{A} \qquad (2.88b)$$

■ **FIGURE 2.12**
Area variations for a subsonic diffuser and a nozzle

(a) A subsonic diffuser ($dA/dx > 0$) (b) A subsonic nozzle ($dA/dx < 0$)

■ **FIGURE 2.13**
Area variations for a supersonic diffuser and nozzle

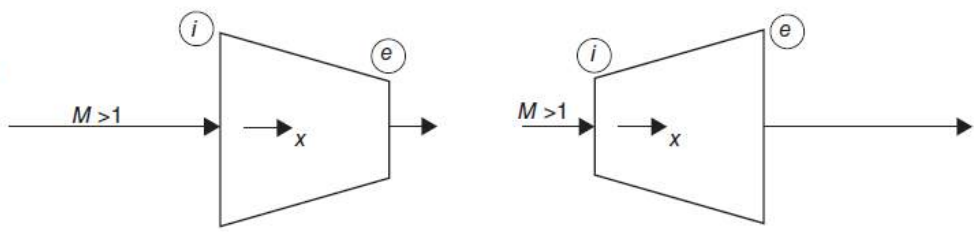

(a) A supersonic diffuser ($dA/dx < 0$) (b) A supersonic nozzle ($dA/dx > 0$)

This equation relates area variation to speed variation for the subsonic and supersonic flows. Assuming a subsonic flow, the parenthesis involving Mach number becomes a negative quantity. Hence, an area increase in a duct, that is, $dA > 0$, results in $du < 0$, to make the signs of both sides of Equation 2.88b consistent. A negative du means flow deceleration. Hence, a subsonic diffuser requires a duct with $dA/dx > 0$. A subsonic nozzle with $du > 0$ demands $dA < 0$. These two duct geometries for a subsonic flow are shown in Figure 2.12. For a supersonic flow, the parenthesis that involves Mach number in Equation 2.88b is positive. Hence, an area increase results in flow acceleration and vice versa. These geometric relationships between area variation and flow speed for supersonic flow are shown in Figure 2.13. We note that the geometric requirements for a desired fluid acceleration or deceleration in a duct are opposite to each other in subsonic and supersonic flow regimes. This dual behavior is seen repeatedly in aerodynamics.

Sonic Throat

A unique flow condition separates the subsonic from supersonic flow. It is the sonic flow that marks the boundary between the two flows. In a subsonic flow, we learned that area reduction accelerates the gas and, ultimately, could reach a sonic state at the exit of the subsonic nozzle. A sonic flow may accelerate to supersonic Mach numbers if the area of the duct increases in the streamwise direction. This initial contraction and later expansion of the duct is capable of accelerating a subsonic flow to supersonic exit flow. This is called a convergent–divergent duct, with an internal throat, that is, the sonic throat. Conversely, a convergent–divergent duct with a supersonic entrance condition has the capability of decelerating the flow to subsonic exit conditions through a sonic throat. These duct geometries are shown in Figure 2.14.

■ **FIGURE 2.14** **Convergent–divergent duct with an internal sonic throat**

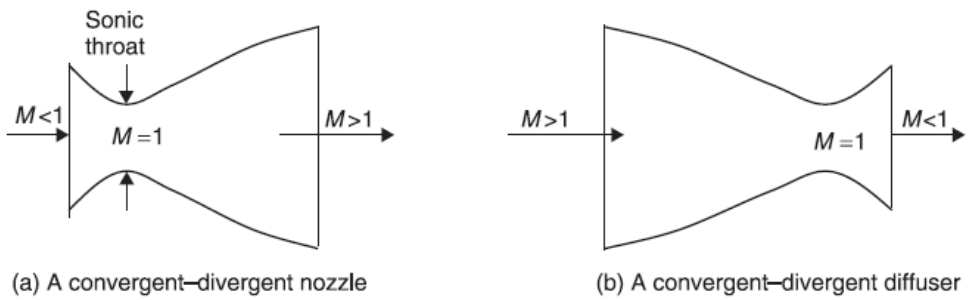

(a) A convergent–divergent nozzle (b) A convergent–divergent diffuser

The sonic state where the gas speed and the local speed of sound are equal is distinguished with a asterisk and also called critical properties. For example, the pressure at the sonic point is $p*$ and the temperature is $T*$, the speed of sound is $a*$, and so on. Since the flow is isentropic throughout the duct, the stagnation pressure remains constant and as a consequence of adiabatic duct flow the stagnation temperature remains constant. By writing the stagnation temperature in terms of the local static temperature and local Mach number, we may relate the local static temperature to sonic temperature according to

$$T_t = T\left[1 + \left(\frac{\gamma - 1}{2}\right)M^2\right] = T^*\left[1 + \left(\frac{\gamma - 1}{2}\right)(1)\right] = T^*\left(\frac{\gamma + 1}{2}\right) \qquad \textbf{(2.89)}$$

Taken in ratio, the above equation yields

$$\frac{T}{T^*} = \frac{\dfrac{\gamma + 1}{2}}{1 + \left(\dfrac{\gamma - 1}{2}\right)M^2} \qquad \textbf{(2.90)}$$

We may apply the isentropic relationship between temperature ratio and pressure ratio (Equation 2.24) to get an expression for $p/p*$.

$$\frac{p}{p^*} = \left[\frac{\dfrac{\gamma + 1}{2}}{1 + \left(\dfrac{\gamma - 1}{2}\right)M^2}\right]^{\frac{\gamma}{\gamma-1}} \qquad \textbf{(2.91)}$$

From perfect gas law and the two expressions for temperature and pressure ratio, (2.90) and (2.91), we get an expression for the density ratio

$$\frac{\rho}{\rho^*} = \frac{p}{p^*}\bigg/\frac{T}{T^*} = \left[\frac{\dfrac{\gamma + 1}{2}}{1 + \left(\dfrac{\gamma - 1}{2}\right)M^2}\right]^{\frac{1}{\gamma-1}} \qquad \textbf{(2.92)}$$

The above expressions for the sonic ratios describe the properties of a section of the duct where flow Mach number is M to the flow properties at the sonic point. The mass flow rate balance between any section of the duct and the sonic throat yields an expression for the area ratio $A/A*$. First, let us write the continuity equation for a uniform flow in terms of the total gas properties, p_t and T_t.

$$\dot{m} = \rho AV = \frac{\gamma p}{a^2}AV = \frac{\gamma pAM}{a} = \sqrt{\frac{\gamma}{R}}\frac{p}{\sqrt{T}}AM \qquad \textbf{(2.93a)}$$

We replaced the density with speed of sound and pressure to get Equation 2.93a. Now, we may substitute the total pressure and temperature for the static pressure and temperature of Equation 2.93a and their respective functions of Mach number to get Equation 2.93b.

$$\dot{m} = \sqrt{\frac{\gamma}{R}}\frac{p_t}{\sqrt{T_t}}A \cdot M\left(\frac{1}{1+\frac{\gamma-1}{2}M^2}\right)^{\frac{\gamma+1}{2(\gamma-1)}} \qquad \textbf{(2.93b)}$$

According to Equation 2.93b, we need the local flow area A, the local Mach number M, the local total pressure and temperature pt and Tt, respectively, and the type of gas, γ, R, to calculate the mass flow rate. The total temperature remains constant in adiabatic flows with no shaft work and the total pressure remains constant for isentropic flows with no shaft work, hence they are convenient parameters in Equation 2.93b. Since the mass flow rate between any two sections of a duct in steady flow has to be equal, Equation 2.93b is a Mach number–area relationship. We use the sonic flow area $A*$, with $M = 1$, to express a non-dimensional area ratio.

$$\frac{A}{A^*} = \frac{1}{M}\left(\frac{1+\frac{\gamma-1}{2}M^2}{\frac{\gamma+1}{2}}\right)^{\frac{\gamma+1}{2(\gamma-1)}} \qquad \textbf{(2.94)}$$

We may tabulate the functions $p/p*$, $T/T*$, and $A/A*$ in addition to p_t/p, T_t/T in an isentropic table for a specific gas, that is, γ = constant. Figure 2.15 shows the isentropic flow parameters as a function of Mach number for a diatomic gas, such as air. At the minimum-area section, the ratio of mass flow rate to the cross-sectional area becomes maximum. Therefore, to demonstrate that $M = 1$ maximizes the mass flow per unit area, we differentiate the following equation and set it equal to zero,

$$\frac{\dot{m}}{A} = const \cdot M \cdot \left(\frac{1}{1+\frac{\gamma-1}{2}M^2}\right)^{\frac{\gamma+1}{2(\gamma-1)}}$$

$$\frac{d}{dM}\left(\frac{\dot{m}}{A}\right) = const \cdot \left[\left(\frac{1}{1+\frac{\gamma-1}{2}M^2}\right)^{\frac{\gamma+1}{2(\gamma-1)}} + M\left(\frac{-(\gamma+1)}{2(\gamma-1)}\right)((\gamma-1)M)\left(\frac{1}{1+\frac{\gamma-1}{2}M^2}\right)^{\frac{\gamma+1}{2(\gamma-1)}+1}\right] = 0 \qquad \textbf{(2.95)}$$

■ **FIGURE 2.15**
Isentropic flow parameters for a diatomic (calorically perfect) gas, $\gamma = 1.4$

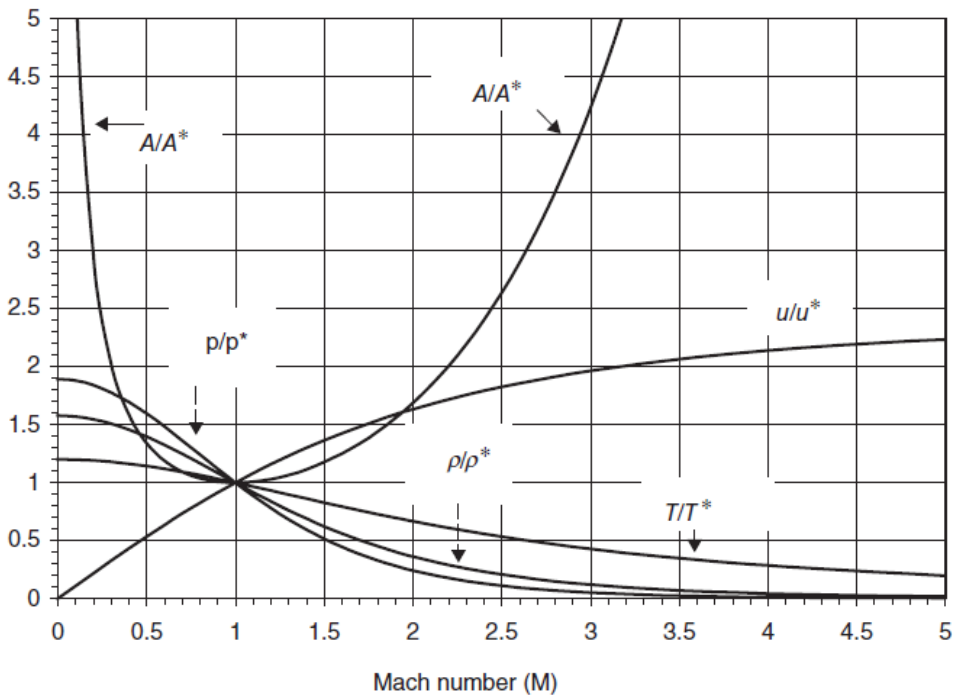

After some minor simplifications we get

$$1 - \left(\frac{\gamma+1}{2}M^2\right) \Big/ \left(1 + \frac{\gamma-1}{2}M^2\right) = 0 \qquad \textbf{(2.96)}$$

Equation 2.96 is identically satisfied by $M = 1$. We may also demonstrate this principle graphically by plotting the function *f(M)* (from Equation 2.93b):

$$f(M) = M \Big/ \left(1 + \frac{\gamma-1}{2}M^2\right)^{\frac{\gamma+1}{2(\gamma-1)}} \qquad \textbf{(2.97)}$$

Figure 2.16 is a graph of the non-dimensional mass flow rate per unit area, that is, Equation 2.97

■ **FIGURE 2.16**
Nondimensional mass flow parameter variation with Mach number shows a sonic condition at the minimum-area section, i.e., the throat

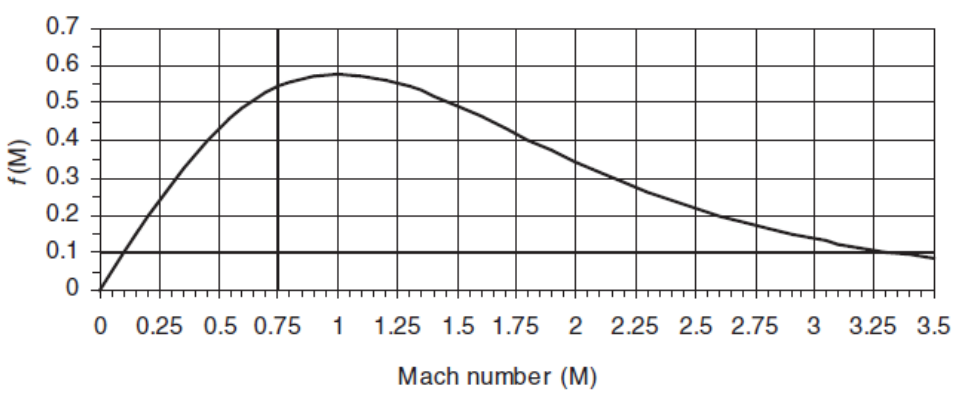

Exhaust/ Nozzle system of Gas Turbine Engine

Aero gas turbine engines have an exhaust system which passes the turbine discharge gases to atmosphere at a velocity, and in the required direction, to provide the resultant thrust. The velocity and pressure of the exhaust gases create the thrust in the turbo-jet engine but in the turbopropeller engine only a small amount of thrust is contributed by the exhaust gases, because most of the energy has been absorbed by the turbine for driving the propeller. The design of the exhaust system therefore, exerts a considerable influence on the performance of the engine. The areas of the jet pipe and propelling or outlet nozzle affect the turbine entry temperature, the mass airflow and the velocity and pressure of the exhaust jet.

The temperature of the gas entering the exhaust system is between 550 and 850 deg. C. according to the type of engine and with the use of afterburning can be 1,500 deg. C. or higher. Therefore, it is necessary to use materials and a form of construction that will resist distortion and cracking, and prevent heat conduction to the aircraft structure. A basic exhaust system is shown in fig. 6-1. The use of a thrust reverser, noise suppressor and a two position propelling nozzle entails a more complicated system as shown in fig. 6-2. The low by-pass engine may also include a mixer unit (fig. 6-4) to encourage a thorough mixing of the hot and cold gas streams.

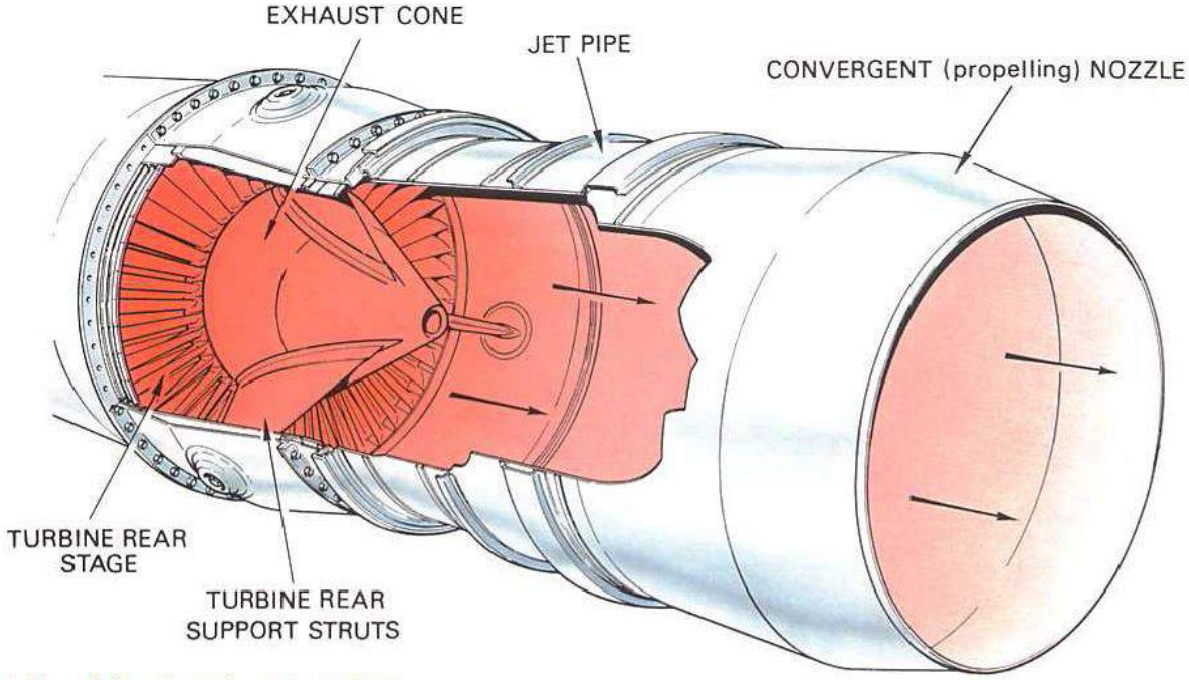

Fig. 6-1 A basic exhaust system.

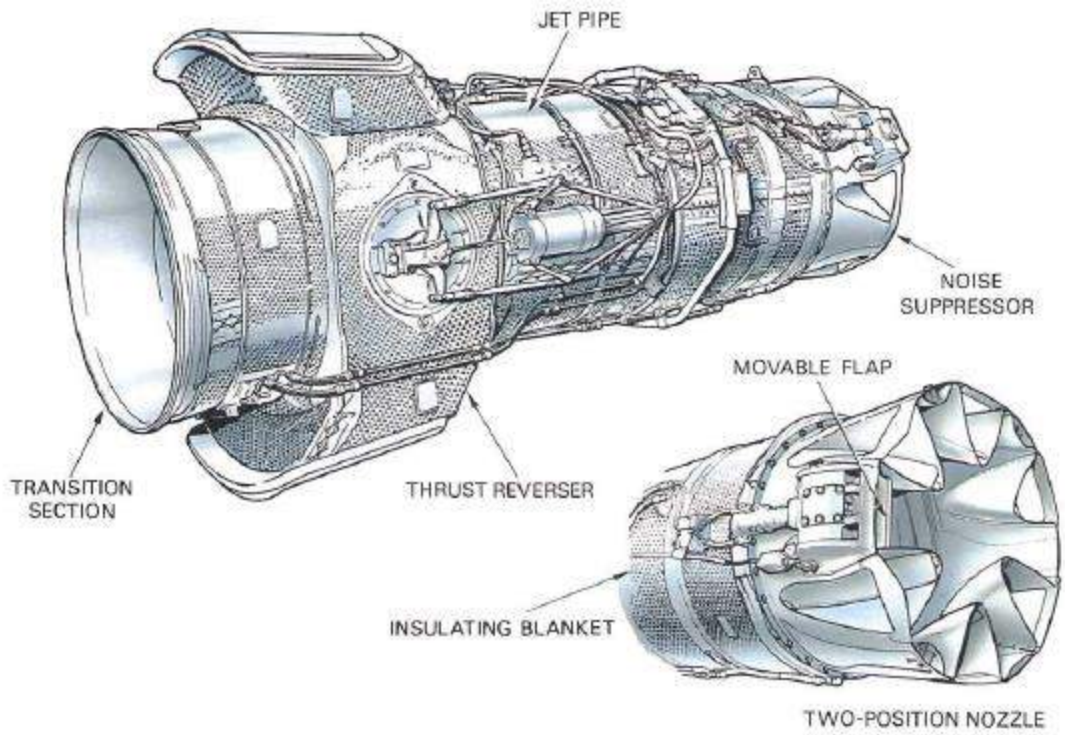

Fig. 6-2 Exhaust system with thrust reverser, noise suppressor and two position propelling nozzle.

Exhaust Gas Flow

Gas from the engine turbine enters the exhaust system at velocities from 750 to 1,200 feet per second, but, because velocities of this order produce high friction losses, the speed of flow is decreased by diffusion. This is accomplished by having an increasing passage area between the exhaust cone and the outer wall as shown in fig. 6-1. The cone also prevents the exhaust gases from flowing across the rear face of the turbine disc. It is usual to hold the velocity at the exhaust unit outlet to a Mach number of about 0.5, i.e. approximately 950 feet per second. Additional losses occur due to the residual whirl velocity in the gas stream from the turbine. To reduce these losses, the turbine rear struts in the exhaust unit are designed to straighten out the flow before the gases pass into the jet pipe. The exhaust gases pass to atmosphere through the propelling nozzle, which is a convergent duct, thus increasing the gas velocity. In a turbojet engine, the exit velocity of the exhaust gases is subsonic at low thrust conditions only.

During most operating conditions, the exit velocity reaches the speed of sound in relation to the exhaust gas temperature and the propelling nozzle is'choked'; that is, no further increase in velocity can be obtained unless the temperature is increased. As the upstream total pressure is increased above the value at which the propelling nozzle becomes 'choked', the static pressure of the gases at exit increases above atmospheric pressure. This pressure difference across the propelling nozzle gives what is known as 'pressure thrust' and is effective over the nozzle exit area. This is additional thrust to that obtained due to the momentum change of the gas stream.

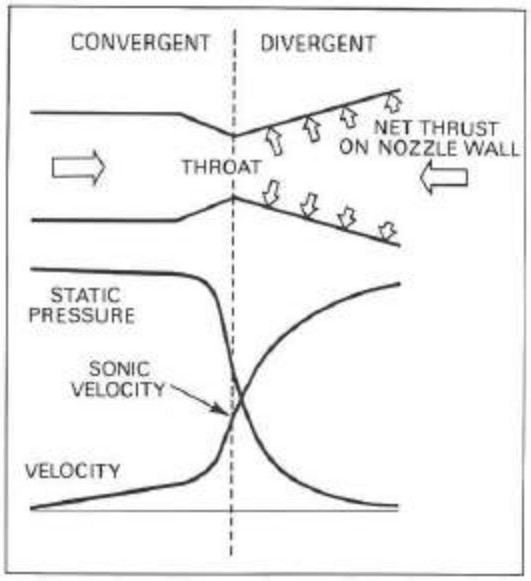

Fig. 6-3 Gas flow through a convergent-divergent nozzle.

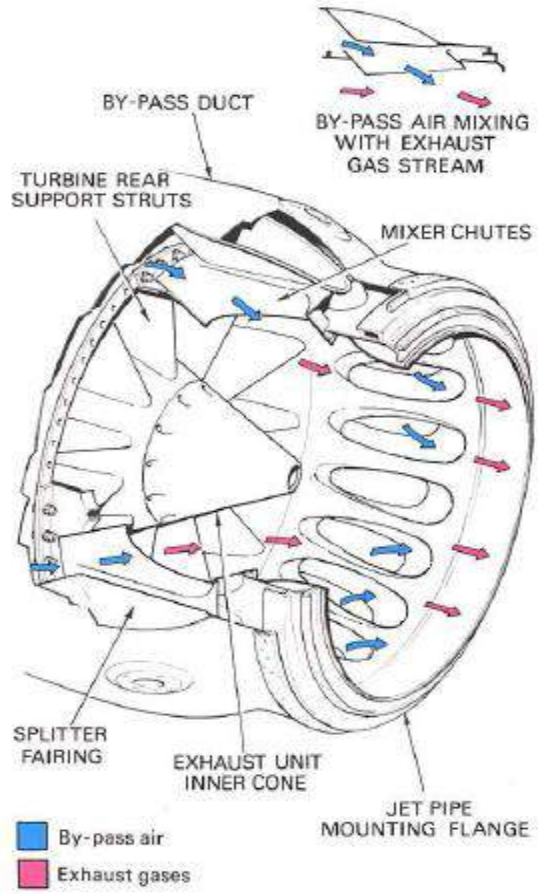

Fig. 6-4 A low by-pass air mixer unit.

With the convergent type of nozzle a wastage of energy occurs, since the gases leaving the exit do not expand rapidly enough to immediately achieve outside air pressure. Depending on the aircraft flight plan, some high pressure ratio engines can with advantage use a convergent-divergent nozzle to recover some of the wasted energy. This nozzle utilizes the pressure energy to obtain a further increase in gas velocity and, consequently, an increase in thrust. From the illustration (fig. 6-3), it will be seen that the convergent section exit now becomes the throat, with the exit proper now being at the end of the flared divergent section. When the gas enters the convergent section of the nozzle, the gas velocity increases with a corresponding fall in static pressure. The gas velocity at the throat corresponds to the local sonic velocity. As the gas leaves the restriction of the throat and flows into the divergent section, it progressively increases in velocity towards the exit. The reaction to this further increase in momentum is a pressure force acting on the inner wall of the nozzle. A component of this force acting parallel to the longitudinal axis of the nozzle produces the further increase in thrust.

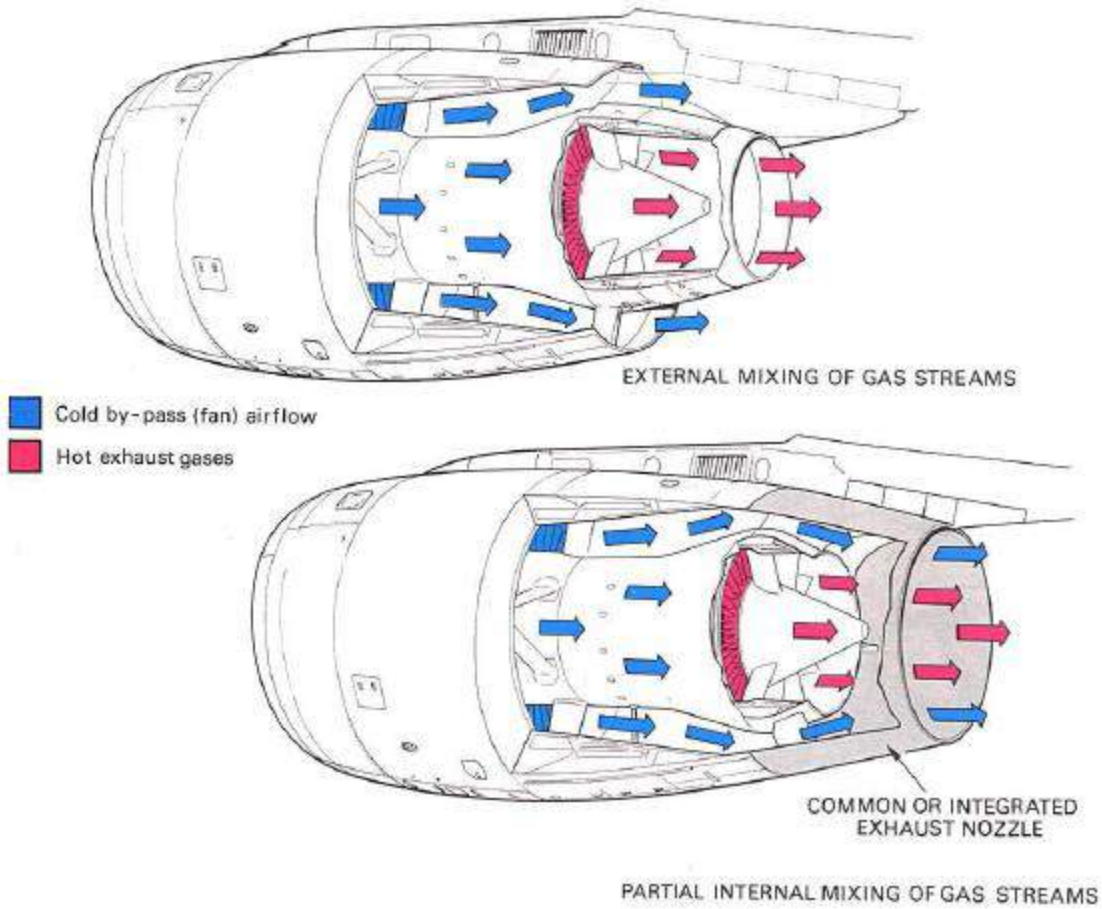

Fig. 6-5 High by-pass ratio engine exhaust systems.

The propelling nozzle size is extremely important and must be designed to obtain the correct balance of pressure, temperature and thrust. With a small nozzle these values increase, but there is a possibility of the engine surging, whereas with a large nozzle the values obtained are too low. A fixed area propelling nozzle is only efficient over a narrow range of engine operating conditions. To increase this range, a variable area nozzle may be used. This type of nozzle is usually automatically controlled and is designed to maintain the correct balance of pressure and temperature at all operating conditions. In practice, this system is seldom used as the performance gain is offset by the increase in weight. However, with afterburning a variable area nozzle is necessary. The by-pass engine has two gas streams to eject to atmosphere, the cool by-pass airflow and the hot turbine discharge gases.

In a low by-pass ratio engine, the two flows are combined by a mixer unit (fig. 6-4) which allows the by-pass air to flow into the turbine exhaust gas flow in a manner that ensures thorough mixing of the two streams. In high by-pass ratio engines, the two streams are usually exhausted separately. The hot and cold nozzles are co-axial and the area of each nozzle is designed to obtain maximum efficiency. However, an improvement can be made by combining the two gas flows within a common, or integrated, nozzle assembly. This partially mixes the gas flows prior to ejection to atmosphere. An example of both types of high by-pass exhaust system is shown in fig, 6-5.

Nozzle operating parameters/characteristics

Before going through this section, it is advisable to go through the thrust and operating characteristics of a jet engine as discussed in chapter six.

The nozzle parameter that is of utmost importance in *propulsion* is the gross thrust F_g. The expression we had for the gross thrust is

$$F_g = \dot{m}_9 V_9 + (p_9 - p_0)A_9 \qquad \textbf{(4.54)}$$

In this equation, the first term on the right-hand side is called the momentum thrust and the second term is called the pressure thrust. It is interesting to note that the nozzles produce a "signature," typically composed of infrared radiation, thermal plume, smoke, and acoustic signatures, which are key design features of a stealth aircraft exhaust system in *addition* to the main propulsion requirement of the gross thrust. As the fluid accelerates in a nozzle, the static pressure drops and hence *a favorable pressure gradient* environment is produced in the nozzle. This is in contrast to diffuser flows where an *adverse pressure gradient* environment prevails. Therefore, boundary layers are, by and large, well behaved in the nozzle and less cumbersome to treat than the inlet. For a subsonic exit Mach number, that is, $M_9 < 1$, the nozzle expansion

■ **FIGURE 4.18**
Schematic drawing of a subsonic nozzle with its static pressure distribution

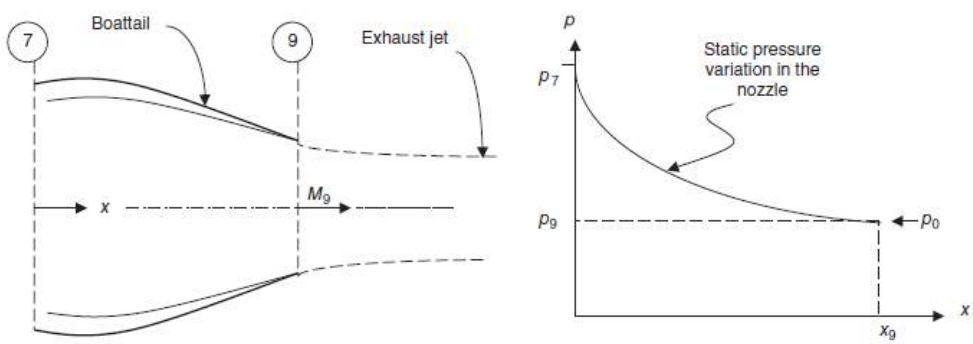

process will continue all the way to the ambient pressure p_0. This important result means that in subsonic streams, the static pressure inside and outside of the jet are the same. In fact, there is no mechanism for a pressure jump in a subsonic flow, which is in contrast to the supersonic flows where shock waves and expansion fans allow for static pressure discontinuity. We have depicted a convergent nozzle in Figure 4.18 with its exhaust stream (i.e., a jet) emerging in the ambient gas of static state (0). The outer shape of the nozzle is called a boattail, which affects the *installed performance* of the exhaust system. The external aerodynamics of the nozzle installation belongs to the propulsion system integration studies and does not usually enter the discussions of the *internal performance*, that is, the cycle analysis. However, we need to be aware that our decisions for the internal flow path optimization, for example, the nozzle exit-to-throat area ratio, could have adverse effects on the installed performance that may offset any gains that may have been accrued as a result of the internal optimization.

We have learned in aerodynamics that a convergent duct, as shown in Figure 4.18, causes flow acceleration in a subsonic stream to a maximum Mach number of 1, which can only be reached at the minimum area of the duct, namely at its exit. So we stipulate that for all subsonic jets, that is, $M_9 < 1$, there is a static pressure equilibrium in the exhaust stream and the ambient fluid, that is, $p_9 = p_0$. Let us think of this as the *Rule 1* in nozzle flow.

$$\boxed{\text{Rule 1}: \quad \text{If} \quad M_{\text{jet}} < 1, \quad \text{then} \quad p_{\text{jet}} = p_{\text{ambient}}}$$

The expression "jet" in the above rule should not be confusing to the reader, as it relates to the flow that emerges from the nozzle. In that context, M_{jet} is the same as M_9, and p ambient is the same as p_0. We recognize that not only it is entirely possible but also desirable for the sonic and supersonic jets to expand to the ambient static pressure as well.

Such nozzle flows are called *perfectly expanded*. Actually, the nozzle gross thrust can be maximized if the nozzle flow is perfectly expanded. We state this principle here without proof, but we will address it again, and actually prove it, in the next chapters. Let us think of this as the *Rule 2* in nozzle flow.

Rule 2 :	If $p_{jet} = p_{ambient}$
	then we have a perfectly expanded nozzle which results in $F_{g,max}$

Here, the stipulation is only on the *static pressure match* between the jet exit and the ambient static pressure and not *perfect flow* inside the nozzle. A real nozzle flow experiences total pressure loss due to viscous dissipation in the boundary layer as well as shock waves, and yet it is possible for it to *perfectly expand* the gas to the ambient condition. Remembering compressible duct flows in aerodynamics, we are reminded that the exit pressure p_9 is a direct function of the nozzle area ratio A_{exit}/A_{throat}, which in our notation becomes A_9/A_8, and the nozzle pressure ratio (NPR). Recalling the definition of NPR,

$$\text{NPR} \equiv \frac{p_{t7}}{p_0} \tag{4.55}$$

we will demonstrate a critical value of NPR will result in the choking condition at the nozzle throat, that is, $M_8 = 1.0$, when NPR $\geq$ (NPR)critical. Let us think of this as *Rule 3* in convergent or convergent-divergent nozzle aerodynamics. These rules do not apply if the divergent section of a C–D nozzle becomes a subsonic a diffuser.

Rule 3 :	If NPR $\geq (\text{NPR})_{\text{critical}}$
	then the nozzle throat velocity is sonic (i.e., choked), $M_8 = 1.0$

A schematic drawing of a convergent–divergent supersonic nozzle is shown in Figure 4.19. The nozzle throat becomes choked at a static pressure of about 50% of the nozzle total pressure, that is, $p_{throat} \sim 1/2\ p_{t7}$. This fact provides for an important *rule of thumb* in nozzle flows, which is definitely worth remembering. Let us consider this as *Rule 4*.

Rule 4 :	If $\dfrac{p_{t7}}{p_0} \geq \sim 2$ then the nozzle throat can be choked, i.e., $M_8 = 1.0$

For example, a passage (or a duct) connecting a pressure vessel of about 30 psia pressure to a room of about 15 psia pressure will experience sonic speed at its minimum (orifice) area. As with any rules of thumb, Rule 4 is stated as an *approximation* and the exact value of the critical nozzle pressure ratio depends on the nozzle expansion efficiency, that is, the extent of losses in the nozzle.

■ **FIGURE 4.19**
A choked convergent–divergent nozzle and the static pressure distribution along the nozzle axis

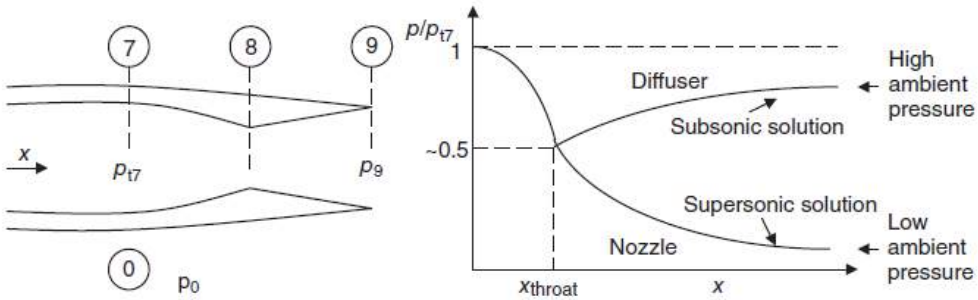

The two possible solutions in static pressure distribution along the nozzle axis are shown in Figure 4.19. One is a subsonic solution downstream of the nozzle throat and the second is a supersonic flow solution downstream of the throat. The subsonic solution is clearly a result of high backpressure, that is, p_0, and causes a flow deceleration on the divergent duct downstream of the throat. Therefore, the divergent portion of the duct is actually a *diffuser* and not a nozzle. The supersonic solution is a result of low backpressure and, therefore, the flow continues to expand (i.e., accelerates) beyond the throat to supersonic speeds at the exit. Also note that only a perfectly expanded nozzle flow is shown as the supersonic branch of the nozzle flow in Figure 4.19. For ambient pressures in between the two pressures shown in Figure 4.19, there are a host of shock solutions, which occur as an oblique shock at the lip or normal shock inside the nozzle.

The range of backpressures for a given nozzle area ratio, which lead to a normal shock solution inside the nozzle is shown in Figure 4.20. The jump in static pressure across a normal shock is shown as an abrupt (i.e., vertical) pressure rise in Figure 4.20, whereas in reality shocks have finite thickness, and, therefore, all the *jump* conditions are then *diffused* or *spread* over the scale of shock thickness. We note the diffusing nature of the flow, that is, the static pressure increasing, after the shock occurs inside the nozzle, which signifies a *diffuser environment* after the shock. For a lower range of backpressures, the oblique shock solution is possible, which indicate an oblique shock is hanging on the nozzle lip. Then we reach a unique nozzle pressure ratio, which leads to perfect expansion, as shown in Figure 4.19 and repeated in Figure 4.20. For all backpressures lower than the perfect expansion, we get the isentropic centered expansion fan solution. All these waves are the necessary mechanisms to satisfy the physical requirement of continuous static pressure across the slipstream in the jet exit flow. Let us call this important gas dynamic *boundary condition* as rule number 5 in nozzle flows. Note that this rule is not unlike the familiar Kutta condition in airfoil aerodynamics, where we prevented a static pressure jump at the sharp tailing edge of an airfoil.

To examine the efficiency of a nozzle in expanding the gas to an exit (static) pressure p_9, we create an enthalpy–entropy diagram, very similar to an inlet. In the inlet studies, we took the ambient static condition 0 and compressed it to the total intake exit condition t2. But since a nozzle may be treated as a reverse-flow diffuser (and vice versa), we take the nozzle inlet gas, at the total state t7, and expand it to the exit static condition 9. This process is shown in Figure 4.21. The analogy in the thermodynamic analysis of a nozzle and a diffuser is helpful in better learning both components. The actual nozzle expansion process is shown by a solid line connecting the gas total state t7 to the exit static state 9.

■ **FIGURE 4.20**
Schematic drawing of possible static pressure distributions inside a choked supersonic nozzle

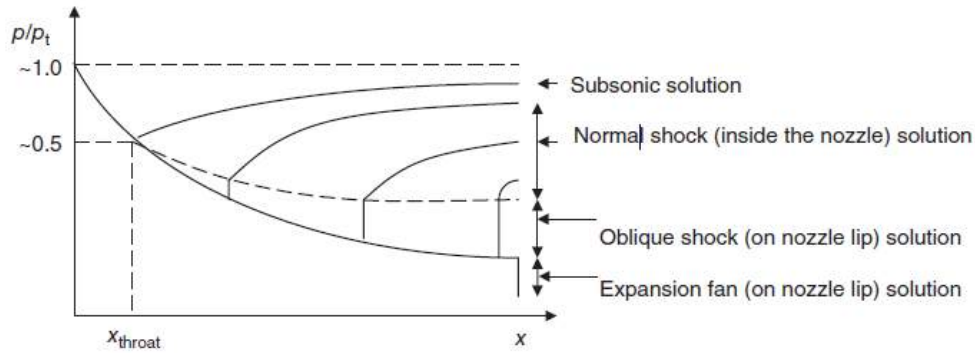

■ **FIGURE 4.21**
Enthalpy–entropy diagram of nozzle flow expansion

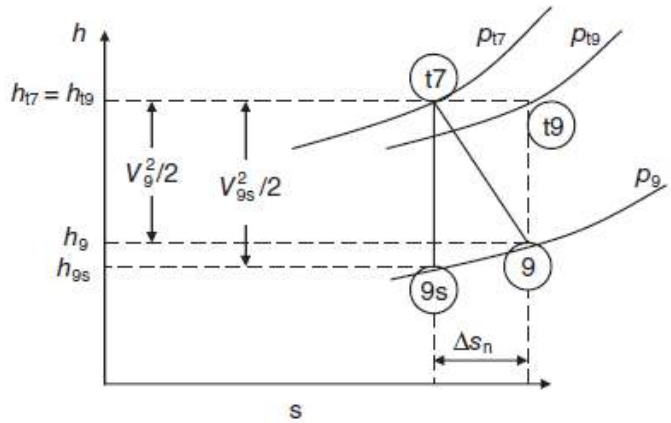

As the real nozzle flows may still be treated as adiabatic, the total enthalpy h_t, remains constant in a nozzle.

Rule 5 :	Static pressure must be continuous across the slipstream of a jet exhaust plume.

$$h_{t7} = h_{t9} \tag{4.56}$$

We remember that the inlet flow was also considered to be adiabatic. An ideal exit state 9s is reached isentropically from the total state t7 to the same exit pressure p_9, in Figure 4.21. The vertical gap between a total and static enthalpy states, in an h–s diagram, represents the kinetic energy of the gas, $V^2/2$, which is also shown in Figure 4.21. Due to frictional and shock losses in a nozzle, the flow will suffer a total pressure drop, that is,

$$p_{t9} < p_{t7} \tag{4.57}$$

as depicted in Figure 4.21. Again, this behavior is quite analogous to a diffuser. We can immediately define the total pressure ratio across a nozzle as its figure of merit, similar to the total pressure recovery of an inlet, namely,

$$\pi_n \equiv \frac{p_{t9}}{p_{t7}} \tag{4.58}$$

Now we can quantify the entropy rise in an adiabatic nozzle, as a result of total pressure losses, using the combined first and second law of thermodynamics,

$$\frac{\Delta s_n}{R} = -\ln \pi_n \qquad \textbf{(4.59)}$$

We may also define a nozzle adiabatic efficiency η_n very similar to the inlet adiabatic efficiency, as

$$\eta_n \equiv \frac{h_{t7} - h_9}{h_{t7} - h_{9s}} = \frac{V_9^2/2}{V_{9s}^2/2} \qquad \textbf{(4.60)}$$

Let us interpret the above definition in physical terms. The fraction of an ideal nozzle exit kinetic energy $V^2_{9s}/2$, which is realized in a real nozzle $V^2_9/2$, is called the nozzle adiabatic efficiency. The loss in total pressure in a nozzle manifests itself as a loss of kinetic energy. Consequently, the adiabatic efficiency η_n, which deals with the loss of kinetic energy in a nozzle, has to be related to the nozzle total pressure ratio π_n. Again, in a very similar manner as in the inlet, let us divide the numerator and denominator of Equation 4.60 by h_{t7}, to get

$$\eta_n = \frac{1 - \dfrac{h_9}{h_{t7}}}{1 - \dfrac{h_{9s}}{h_{t7}}} = \frac{1 - \dfrac{h_9}{h_{t7}}}{1 - \left(\dfrac{p_9}{p_{t7}}\right)^{\frac{\gamma-1}{\gamma}}} = \frac{1 - \left(\dfrac{p_9}{p_{t9}}\right)^{\frac{\gamma-1}{\gamma}}}{1 - \left(\dfrac{p_9}{p_{t7}}\right)^{\frac{\gamma-1}{\gamma}}} \qquad \textbf{(4.61)}$$

where we used $h_{t7} = h_{t9}$ in the numerator and the isentropic relation between the temperature and pressure ratios in both numerator and denominator. It is interesting to note that as the nozzle exit total pressure p_{t9} approaches the value of the nozzle inlet total pressure p_{t7}, the nozzle adiabatic efficiency will approach 1.We may treat Equation 4.61 as containing only one unknown and that is pt9. Therefore, for a given nozzle exit static pressure p_{t9} and the nozzle inlet total pressure p_{t7}, the nozzle adiabatic efficiency η_n will result in a knowledge of the total pressure at the exit of the nozzle, p_{t9}. Now, if we multiply the numerator and denominator of the right-hand side of Equation 4.61 by $(p_{t7}/p_9)^{(\gamma-1)/\gamma}$, we will reach our goal of relating the two figures of merit in a nozzle, that is,

$$\eta_n = \frac{\left(\dfrac{p_{t7}}{p_9}\right)^{\frac{\gamma-1}{\gamma}} - \pi_n^{-\frac{\gamma-1}{\gamma}}}{\left(\dfrac{p_{t7}}{p_9}\right)^{\frac{\gamma-1}{\gamma}} - 1} \qquad \textbf{(4.62)}$$

There are three parameters in Equation 4.62. The two figures of merit, ηn and πn, and the ratio of nozzle inlet total pressure to the nozzle exit static pressure, p_{t7}/p_9. The last parameter is a known quantity, as we know the nozzle inlet total pressure pt7 from the upstream component analysis (in a turbojet, it is the turbine, $p_{t7} = p_{t5}$), and the nozzle exit pressure p_9 is a direct function of the nozzle area ratio A_9/A_8. To express Equation 4.62 in terms of the NPR, we may split p_{t7}/p_9 into

$$\frac{p_{t7}}{p_9} = \frac{p_{t7}}{p_0}\frac{p_0}{p_9} = \text{NPR} \cdot \left(\frac{p_0}{p_9}\right) \qquad \textbf{(4.63)}$$

Now, substituting the above expression in Equation 4.62, we get

$$\eta_n = \frac{\left\{\mathrm{NPR}\left(\frac{p_0}{p_9}\right)\right\}^{\frac{\gamma-1}{\gamma}} - \pi_n^{-\frac{\gamma-1}{\gamma}}}{\left\{\mathrm{NPR}\left(\frac{p_0}{p_9}\right)\right\}^{\frac{\gamma-1}{\gamma}} - 1} \tag{4.64}$$

■ **FIGURE 4.22**
Two figures of merit in a nozzle plotted as a function of NPR ($\gamma = 1.33$)

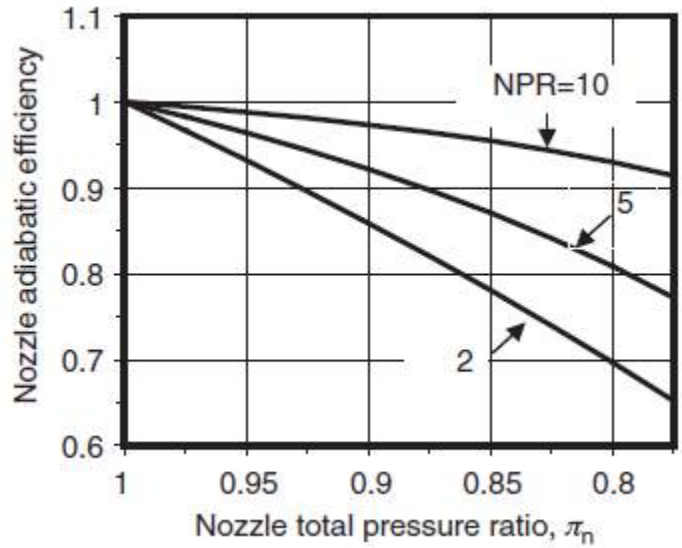

A plot of Equation 4.64 is shown in Figure 4.22 for a perfectly expanded nozzle, that is, $p_9 = p_0$. It is comforting to note that in Equation 4.64, the nozzle adiabatic efficiency will approach 1, as the nozzle total pressure ratio approaches 1. The parameter p_0/p_9 represents a measure of mismatch between the nozzle exit static pressure and the ambient static pressure. For $p_9 > p_0$, the flow is considered to be *under expanded*. For $p_9 < p_0$, the flow is defined as *over expanded*. In the under-expanded scenario, the nozzle area ratio is not adequate, that is, not large enough, to expand the gas to the desired ambient static pressure. In the over expanded nozzle flowcase, the nozzle area ratio is too large for perfect expansion. As noted earlier, a perfectly expanded nozzle will have $p_0 = p_9$, therefore, the above equation is further simplified to

$$\eta_n = \frac{\{\mathrm{NPR}\}^{\frac{\gamma-1}{\gamma}} - \pi_n^{-\frac{\gamma-1}{\gamma}}}{\{\mathrm{NPR}\}^{\frac{\gamma-1}{\gamma}} - 1} \tag{4.65}$$

for a perfectly expanded nozzle. It is instructive to show the three cases of nozzle expansion, that is, under-, over-, and perfectly expanded cases, on an *h–s* diagram (Figure 4.23). In Figure 4.23a, the nozzle area ratio is smaller than necessary for perfect expansion and that explains the high exit pressure p_9. However, an expansion fan at the nozzle exit plane will adjust the pressure down to the ambient level, after the jet leaves the nozzle, in accordance to Rule 5.

■ **FIGURE 4.23**
The *h–s* diagram for the three possible nozzle expansions

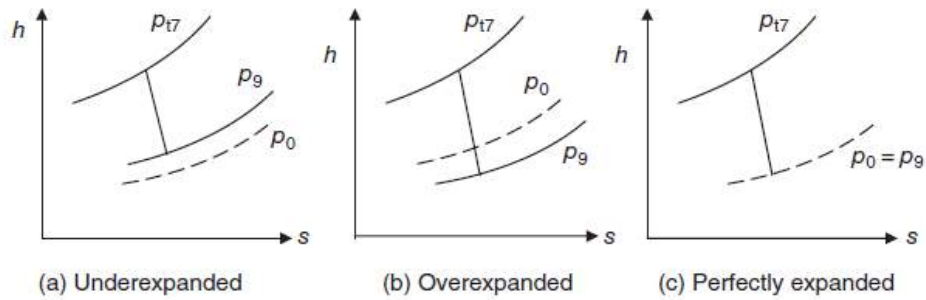

After all, the slipstream cannot take a (static) pressure jump. In Figure 4.23b, the nozzle area ratio is too large for this altitude, which explains a lower-than-ambient static pressure at the nozzle exit. To adjust the low exit pressure up to the ambient level, a shock wave is formed on the nozzle exit lip, which for mild overexpansion will be an oblique shock. Higher levels of over expansion will strengthen the shock to a normal position and, eventually, cause the shock to enter the nozzle. Figure 4.23c shows a perfect expansion scenario, which implies the nozzle area ratio is perfectly matched to the altitude requirements of ambient pressure. Again, as noted in Figure 4.23, all nozzle expansions are depicted as irreversible processes with an associated entropy rise; therefore, *perfect expansion* is not to be mistaken as *perfect (isentropic) flow*.

Numerical Example:
Consider a convergent–divergent nozzle with a pressure ratio NPR = 10. The gas properties are γ = 1.33 and c_p =1,156 J/kg ·K and remain constant in the nozzle. The nozzle adiabatic efficiency is η_n = 0.94. Calculate
(a) nozzle total pressure ratio π_n
(b) nozzle area ratio A_9/A_8 for a perfectly expanded nozzle
(c) nozzle exit Mach number M_9 (perfectly expanded)

Solution:
We may use Equation 4.64 that relates the figures of merit of a nozzle (η_n and π_n) with *NPR*,

$$\eta_n = \frac{\left\{\mathrm{NPR}\left(\frac{p_0}{p_9}\right)\right\}^{\frac{\gamma-1}{\gamma}} - \pi_n^{-\frac{\gamma-1}{\gamma}}}{\left\{\mathrm{NPR}\left(\frac{p_0}{p_9}\right)\right\}^{\frac{\gamma-1}{\gamma}} - 1}$$

For a perfectly expanded nozzle, $p_0 = p_9$, therefore, we get the following expression for π_n

$$\pi_n = \left[\mathrm{NPR}^{\frac{\gamma-1}{\gamma}} - \eta_n\left(\mathrm{NPR}^{\frac{\gamma-1}{\gamma}} - 1\right)\right]^{\frac{-\gamma}{\gamma-1}} \cong 0.8335$$

The entropy rise in an adiabatic nozzle is a function of the total pressure ratio π_n, according to (Equation 4.59)

$$\Delta s_n/R = -\ell n\pi_n \cong -\ell n(0.8335) \approx 0.1822$$

We can calculate the local Mach number M_9 if we know the total and static pressures p_{t9} and p_9 simultaneously. From the NPR and the total pressure ratio, we may write

$$p_{t9}/p_9 = (p_{t9}/p_{t7})(p_{t7}/p_0)(p_0/p_9) = 0.8335(10)(1) = 8.335$$

From the general expression for total pressure and Mach number

$$p_t/p = (1 + (\gamma - 1)M^2/2)^{\frac{\gamma}{\gamma-1}}$$

We can isolate Mach number as follows

$$M_9 = \sqrt{\frac{2}{\gamma - 1}\left[(p_{t9}/p_9)^{\frac{\gamma-1}{\gamma}} - 1\right]} = \sqrt{\frac{2}{0.33}\left[(8.335)^{0.3/1.33} - 1\right]} \cong 2.05$$

Using continuity, we calculate $A_9/A_8 \sim 1.8242$

Chapter Five
Jet Engines

Introduction

This chapter deals with the different methods of aircraft propulsion that uses jet propulsion principle. Jet engines can be broadly classified into two groups; air-breathing and non-air-breathing engines. The latter group explicitly deals with the pure rocket engines. However, with advancement in the propulsion techniques, a pure rocket engine is combined with different air-breathing engines to produce efficient engines for trans-atmospheric propulsion and space launch. We will discuss each of the following engines in detail in this chapter.

- Ramjet Engine,
- Pulsejets, Pulsed Detonation engines,
- Rocket engines and
- Hybrid engines and combined cycle engines.

The Ramjet Engine

The ramjet is a simple engine concept consisting of a diffuser (consisting of an inlet and an isolator), a burner (or combustion chamber) and a nozzle, shown in figure below. Because it diffuers from other airbreathing engines by having no moving or rotating parts, like a compressor in the turbojet, or a turbine, the ramjet is lighter and simpler than the turbojet.

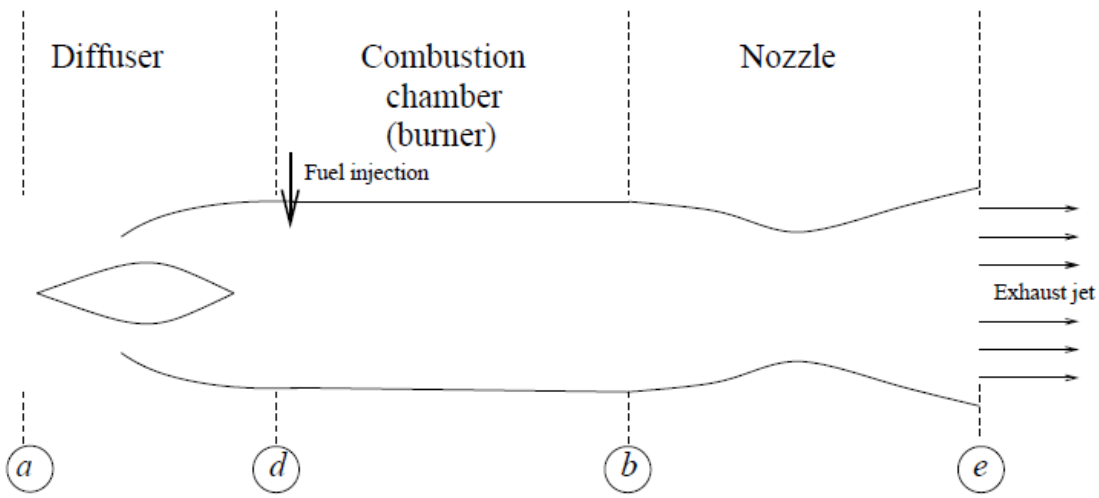

Figure 1: The ramjet.

The name ramjet comes from the way of air compression done by the inlet, which collects and compresses, or rams, the incoming air flow to the isolator and from there on to the combustor. By doing this, the air flow velocity decreases dramatically from supersonic to subsonic speeds by means of a normal shock system inside the isolator, and produces ram pressure and an increase in temperature of the air flow. In the fixed area combustor (consisting of a fuel injector and a flame holder), heat and mass is added, through injection, mixing and burning of fuel with the incoming air flow. And finally the nozzle converts a portion of the energy of the outgoing combustion flow to kinetic energy to produce thrust. This is done by accelerating the flow and the reaction to this acceleration produces the thrust, as is explained by Newton's Third Law. The thrust F can be seen as a mechanical force, which is defined as the change in momentum, which

is the mass flow rate m dot times the velocity u plus the pressure difference Δp times the exit area Ae:

$$F = \dot{m}_e u_e - \dot{m}_0 u_0 + (p_e - p_0) A_e \tag{1.1}$$

One of the characteristics of the ramjet is that the engine has two sections where the air flow has a velocity in the vicinity of Mach 1, which is also known as choked flow. When the flow is choked, it means that the mass flow rate has become independent of the pressure downstream, and only dependent on the pressure and temperature upstream. Before choking occurs, the flow is dependent on the downstream conditions. The flow is choked in the throat section, between the exit of the combustor and the nozzle, and generates a back pressure towards the entrance of the combustor. And for a ramjet to have subsonic combustion, it is therefore required to have a strong or normal shock system between the inlet and the combustor, reducing the flow velocity to below M = 1. The section where this shock system (further referred to as shock train) is located is called the isolator.

One major drawback of the ramjet is the lack of producing static thrust. A ramjet only produces thrust when the vehicle is moving and cannot produce thrust when the engine is stationary or static. Because of this, ramjets need other propulsion systems to accelerate the vehicle to a speed where the ramjet is able to produce thrust. Rockets for example could be used to accelerate ramjets to supersonic velocities.

Ideal Ramjet Performance

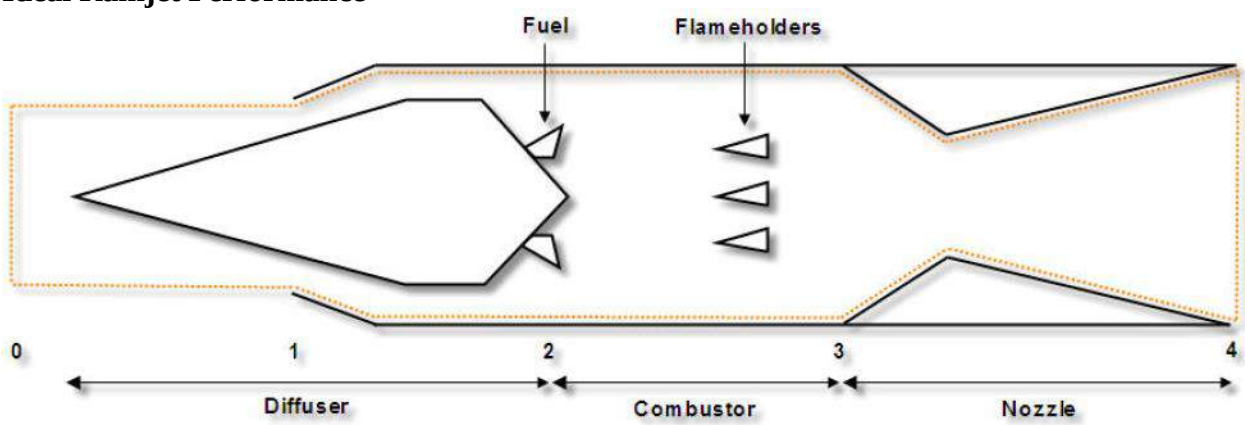

Figure 1.6: Ramjet schematic

The ideal theoretical performance of the subsonic ramjet can be shown by considering several ideal conditions and by using a control volume analysis schematically shown in figure 1.6. The performance itself is indicated by three characteristics: the total pressure loss, the entropy increase and the specific impulse. For the subsonic ramjet the thrust and specific impulse are sufficient here to indicate the performance. We will limit our discussions only to subsonic ramjets with an introduction to supersonic ramjet engines where the combustion occurs at supersonic speeds.

Between stations 0 and 2 isentropic (reversible and adiabatic) diffusion and compression with a decrease in Mach number ($M_2 << 1$). Here the station 1 is taken as the entrance of the internal inlet, station 0 is in fact the entrance of the external inlet. Between stations 2 and 3 there is constant pressure combustion, according to the ideal Brayton cycle. And between stations 3 and

4 ideal expansion through the nozzle ($p_4 = p_0$). There are no moving or rotating parts, so there are no mechanical losses to take into account. The working fluid inside the engine is air, which is assumed to behave as a perfect gas with constant specific heats.

Using equation (1.1) to calculate the thrust F, with ideal expansion:

$$F = \dot{m}(u_4 - u_0) \tag{1.2}$$

where u4 and u0 are the exit and inlet flow velocities. The thrust equation given in terms of non-dimensional parameters is:

$$\frac{F}{\dot{m}a_0} = \frac{u_4}{a_4}\frac{a_4}{a_0} - \frac{u_0}{a_0} \tag{1.3}$$

where a is the speed of sound. This results in

$$\frac{F}{\dot{m}a_0} = M_4\frac{a_4}{a_0} - M_0 = M_4\sqrt{\frac{T_4}{T_0}} - M_0 \tag{1.4}$$

Subsonic combustion ramjets have combustor flow velocities M_2 usually taken between 0.3 and 0.35, and for ideal performance analysis the pressure remains constant (Brayton cycle). The low velocity flow is necessary to keep the flame holders from blowing out, meaning the flames deattach from the flameholders. The conservation of momentum equation now becomes:

$$p_2A_2 + \rho_2u_2^2A_2 = p_3A_3 + \rho_3u_3^2A_3$$

$$A_2(1 + \gamma M_2^2) = A_3(1 + \gamma M_3^2)$$

where it can be seen that the flow velocity after combustion is larger then before combustion, but still smaller than unity $M_2 < M_3 << 1$. The ratio of the temperature at the inlet and the temperature at the exit is needed to find the thrust. Since both sections are isentropic and adiabatic compressed or expanded, the temperature ratio can be given by:

$$\frac{T_{t_4}}{T_{t0}} = \frac{T_{t_3}}{T_{t2}} = \tau_c \tag{1.5}$$

with τc the stagnation temperature ratio across the combustor. The thrust can now be written as:

$$\frac{F}{\dot{m}a_0} = M_0\left(\sqrt{\frac{T_{t_3}}{T_{t_2}}} - 1\right) = M_0(\sqrt{\tau_c} - 1) \tag{1.6}$$

It can be seen that a ramjet needs to move forward to develop thrust and is dependent on the ram compression of the incoming air flow. Efficient compression of the incoming flow requires high enough velocities. And equation (1.8) shows that the thrust performance of the ramjet depends on the stagnation temperature ratio between stations 2 and 3, the higher the ratio, the better the thrust performance (T_{t2} increases with increasing flight Mach number). This also shows the second disadvantage of the ramjet for using subsonic combustion, the static temperature at station 3 (the combustor) increases to very high values at higher mach numbers, which could be catastrophic to the material used inside the engine. For this reason, at higher Mach numbers, the high specific impulse through subsonic combustion loses its advantage due to the increasing static combustor temperature and supersonic combustion would then be more favorable.

At very high velocities the inlet efficiency η_R is usually taken kinetic energy efficiency ηKE, defined as:

$$\eta_{KE} = \left(\frac{u_{2,is}}{u_0}\right)^2 \tag{1.9}$$

Here u_2 is the velocity after isentropic compression. Rewriting eq.(1.2) with the kinetic energy efficiency:

$$\frac{F}{\dot{m}u_0} = \eta_{KE}^{\frac{1}{2}}\left(\frac{u_e}{u_{2,is}}\right) - 1 \tag{1.10}$$

Or, in terms of the specific thrust ψ

$$\Psi = \frac{F}{\dot{m}} = u_0\left[\eta_{KE}^{\frac{1}{2}}\left(\frac{T_{t_4}}{T_{t_0}}^{\frac{1}{2}}\right) - 1\right] \tag{1.11}$$

Also needed is the thrust specific fuel consumption TSFC and the specific impulse Isp. The TSFC is defined as the ratio between the fuel to air ratio f and the specific thrust:

$$TSFC = \frac{\dot{m}_f}{\dot{m}}\frac{1}{\Psi} \tag{1.12}$$

A low TSFC means a high efficiency and vice versa a high TSFC a low efficiency. The specific impulse is given as the specific thrust divided by the fuel to air ratio and the gravitational constant g:

$$I_{sp} = \frac{\Psi}{g\left(\frac{\dot{m}_f}{\dot{m}}\right)} \tag{1.13}$$

Using certain values for the flight Mach number M_0, the temperature and the velocity of sound in the stratosphere (T_0 = 216.7K and a_0 = 295m/s), and stoichiometric combustion of hydrogen (ER=1 and m_f /m = 0.0292), with a combustion heating value Hc=120 MJ/kg for hydrogen the temperature rise in the combustor can be determined and is found to be T_{t4} - T_{t2}=3490 K (de Wolf, 1993). In reality, because of real-gas effects, these temperatures will not be reached (de Wolf, 1995). The specific impulse and the specific thrust with stoichiometric combustion can be determined using the above mentioned values. It can be analytically determined that the maximum performance of a ramjet with hydrogen as fuel is around Mach 3 and continues to decrease with increasing flight Mach number.

Another approach to determine the performance of the ramjet is by looking at the structural limits of a ramjet. Structural limits are for instance the melting temperature or maximum internal pressure of a material or construction. A structural limit of the ramjet, in particular the ramjet combustor, is the combustor stagnation temperature T_{t3} for a chosen material, which is increased by the addition of fuel and the conversion of chemical energy into thermal energy during combustion. From literature several maximum temperatures are given, depending on the choice of material, ranging from 1600K to 2200K. With this we can determine the specific thrust of an ideal ramjet, assuming no losses in the inlet by using the following equation:

$$\frac{F}{\dot{m}_0} = a_0 M_0\left(\sqrt{\frac{T_{t_3}}{T_{t_2}}} - 1\right) = a_0 M_0\left(\sqrt{\frac{T_{t_4}}{T_{t_0}}} - 1\right) \tag{1.14}$$

Concept of Supersonic Combustion Ramjets (Scramjets)

The velocity of the oncoming air flow to the engine inlet can be represented as relative kinetic energy. When the air flow is decelerated within the inlet, the velocity and thus the kinetic energy decreases. Since the conservation of energy in a flow must hold, the missing kinetic energy will reappear as internal energy. This means that the more the air flow is decelerated to subsonic flow, the more internal energy appears inside the engine, resulting in a higher pressure, temperature and density of the air flow entering the combustor.

When the temperature is increased too much through combustion, dissociation of combustion products will occur. Dissociation is the separation of molecules into less complicated molecules, with accompanying absorption of energy. This means that much of the chemical energy of the fuel in dissociation products will not be usable but is lost, resulting in a decrease in generation of thrust. Because of this, the static temperature at the entrance of the combustion chamber has an upper limit. From literature, this limit for subsonic combustion is around 2000K, corresponding with an inlet Mach number of 6 to 7, depending on material choice, cooling, and the altitude of the engine. The stagnation temperature is given by:

$$\frac{T_t}{T} = 1 + \frac{\gamma - 1}{2} M^2 \qquad (1.15)$$

and with Tt2 = Tt0 the static entrance temperature T_2 can be found with:

$$T_2 = \frac{T_{t_0}}{1 + \frac{\gamma-1}{2} M_2^2} \qquad (1.16)$$

For subsonic combustion ramjets, an upper limit can be set for the velocity inside the combustion chamber, called the blow-off limit, which is the maximum velocity at which the flame remains attached to the flame holders. A higher Mach number will cause the flame to detach from the flame holders. From literature (de Wolf, 1994) this limit is a Mach number of M = 0.35. With this the static temperature T_2 at the entrance of the combustion chamber can be determined. But, when the airflow is not slowed down to a Mach number of below one, the flow at the entrance of the combustor remains supersonic and combustion changes from subsonic combustion to supersonic combustion. One of the important changes is the static temperature difference at the entrance of the combustor. Figure 1.11 shows combustor entrance static temperature levels (for divergent inlet entrance Mach numbers) versus the free stream flow Mach number and it can be seen that when the inlet entrance Mach number increases the slope of the combustor static entrance temperature decreases. Thus when the ramjet operates in the hypersonic regime it must operate with supersonic combustion and without normal shock waves to avoid reaching unnecessary high heat transfer and structural loads.

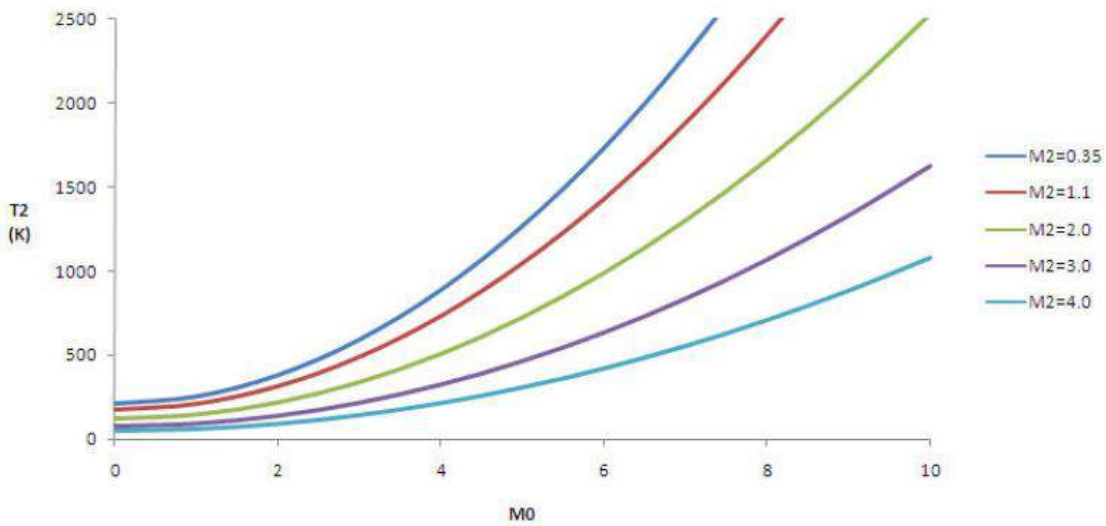

Figure 1.11: Ramjet combustor entrance temperature

Advantages

- No moving parts
- Light in weight
- Wide variety of fuels (hydrogen , hydrocarbons etc)

Disadvantages

- Cannot start of its own, requires a launching device to attain certain velocity. So a ramjet is equipped usually with a turbojet.
- High fuel consumption at low Mach no.
- Complicated Intake and Diffuser design and matching
- Combustion Instability/ requirements of flame holders
- Structural limits are for instance the melting temperature or maximum internal pressure of a material or construction determined by the combustor stagnation temperature Tt3 for a chosen material,

Intermittent combustion engines

This class engine contains the oldest type of reciprocating piston engines to the near recently developed pulsejets and pulse detonation engines (PDE), the latter ones working by jet propulsion technique. To study these variants of intermittent combustion engines, we first deal with the types of combustion and the difference between what is called the deflagration and detonation combustion.

Deflagration

Deflagration is the relatively gentle process of burning fuel rapidly with flames. One of the main characteristics of deflagration is that the flame travels at subsonic speeds i.e. $M<1$. The common type of combustion that we see in our daily lives, like fire, is infact deflagration. Deflagration is a characteristic of combustion in ramjet and turbojet engines with typical deflagrations propagation speeds on the order of 1-100 m/s. Across a deflagration wave traveling in a given direction, the pressure decreases while the volume increases i.e. $P_2<P_1$ and $v_2>v_1$. A deflagration wave is a slow propagating wave front with low-pressure ratio.

Detonation

Detonation, on the other hand, can be thought of as a violent reaction that travels at supersonic speeds M>1. Detonation produces a much higher amount of pressure compared to deflagration and the pressure ratio is quite high, in the order of 20 for a stoichiometric hydrogen fuel to air ratio, compared to that of deflagration waves. A typical detonation waves propagate at a velocity on the order of 2000 m/s i.e Mach number in the order of 4-8).Unlike deflagration waves, in detonation waves, the pressure increases while the volume decreases i.e. $P_2>P_1$ and $v_2<v_1$. In contrast to deflagration the combustion zone in detonation is very small. If the detonation propagates in a lean mixture, the combustion temperature is relatively low, so a low emission of NOx is expected (also due to a small residence time). Thus there is no necessity to add extra air before the turbine (in turbojet engines). In addition due to the detonative combustion the pressure in chamber is increased. So application of the detonation to jet engines offers significant improvement to its performance.

The Pulsejet Engine

Pulsejets are very simple devices and they have been flown long back, even during World War 2. Pulsejet actually operates under very simple principle that the flow which comes in, comes in through valves. However valveless pulsejets are under study and they dominate the traditional valved design in respect to weight and structural limitation of maintaining an efficient valve operation.

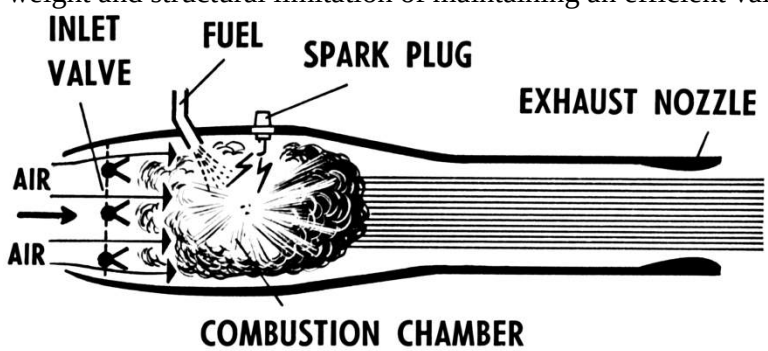

Working Cycle

Pulsejets work on the Humphrey cycle, a different cycle from that of Brayton Cycle in that the heat addition process (combustion) occurs at a constant volume rather than constant pressure. The combustion event begins when the combustion chamber pressure is above atmospheric and the temperature of the fuel/air mixture increases, due to mixing with residual products, to the auto ignition temperature. A compression wave is generated and combustion increases both temperature and pressure in the combustion chamber, driving the flow toward the exit and inlet at gradually increasing velocity. The relatively short combustion event ends and when the compression wave reaches either the pulsejet inlet or the exit, an expansion wave due to overexpansion travels back into the combustion chamber. Flow velocity reaches its positive maximum at the exit at this time. The expansion wave decreases the pressure in the exhaust tube and the combustion chamber to sub atmosphere, resulting in backflow at both the inlet and exit. The next charge of air enters into the chamber due to this backflow at the inlet. The mass addition increases the combustion chamber pressure. When the pressure in the combustion chamber approaches the atmosphere pressure, the next cycle begins. The combustion in a pulsejet engine occurs in a subsonic regime and hence is a deflagration wave. The cycle repeats around 40-45 times per second and generates a constant thrust.

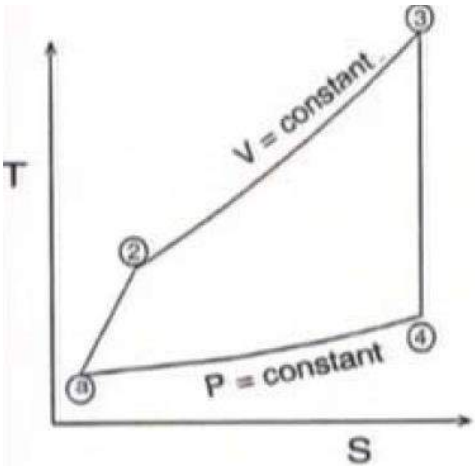

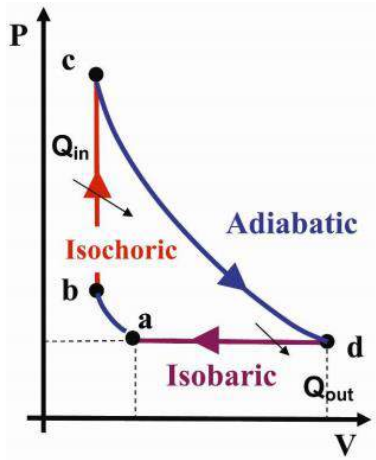

Advantages and Limitations

Pulse jets have been designed for helicopter rotor propulsion and some dispense with inlet valves by careful design of the ducting to control the changing pressures of the resonating cycle. The pulse jet is unsuitable as an aircraft power plant because it has a high fuel consumption and is unable to equal the performance of the modern gas turbine engine. Below listed are some of its advantages and limitations.

- High power to weight ratio
- Lower complexity for integrating into RC vehicles (no fuel pump system needed)
- temperamental to start

Limitations

- valves wear out, sometimes in seconds
- more difficult to build
- The fuel injection system, combustion chamber, and the inlet geometry must be carefully designed to create a fast mixing process and the necessary fluid dynamic and acoustic time scales to permit pulsejet operation.
- Another challenge is the heat loss to the walls due to the high surface-area-to volume ratio. Large thermal losses have a direct impact on overall combustor efficiency and they can increase kinetic times and narrow flammability limits through suppression of the reaction temperatures.
- For the oscillating combustion process to be self-sustaining, excessive heat loss, which lowers the temperature of the walls and the residual gas, must be prevented. is generated.

The Valveless Pulsejet Engine

Valveless pulsejet engines have no moving parts and use only their geometry to control the flow of exhaust out of the engine. Valveless pulsejets expel exhaust out of both the intakes and the exhaust, though most try to have the majority of exhaust go out of the longer tail pipe for more efficient propulsion. The valveless pulsejet operates on the same principle as the valved pulsejet, but the 'valve' is the engine's geometry. Fuel, as a gas or atomized liquid spray, is either mixed

with the air in the intake or directly injected into the combustion chamber. Starting the engine usually requires forced air and an ignition source, such as a spark plug, for the fuel-air mix. With modern manufactured engine designs, almost any design can be made to be self-starting by providing the engine with fuel and an ignition spark, starting the engine with no compressed air. Once running, the engine only requires input of fuel to maintain a self-sustaining combustion cycle.

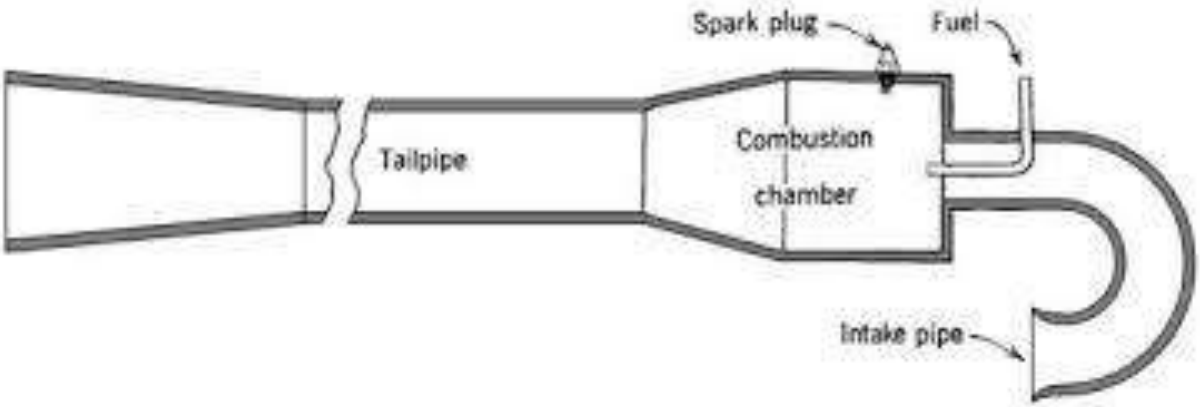

Working Principle

When the fuel-air mixture combusts in the chamber, the process generates a great amount of hot gas very quickly. This happens so fast that it resembles an explosion. The immediate, explosive rise in internal pressure first compresses the gas inside and then pushes it forcefully out of the chamber. Two powerful spurts of hot expanding gas are created – a big one that blows through the tailpipe and a smaller one blowing through the intake. Leaving the engine, the two jets exert a pulse of thrust – they push the engine in the opposite direction. As the gas expands and the combustion chamber empties, the pressure inside the engine drops. Due to inertia of the moving gas, this drop continues for some time even after the pressure falls back to atmospheric. The expansion stops only when the momentum of the gas pulse is completely spent. At that point, there is a partial vacuum inside the engine. The process now reverses itself. The outside (atmospheric) pressure is now higher than the pressure inside the engine and fresh air starts rushing into the ends of the two ports. At the intake side, it quickly passes through the short tube, enters the chamber and mixes with fuel. The tailpipe, however, is rather longer, so that the incoming air does not even get as far as the chamber before the engine is refilled and the pressure peaks. One of the prime reasons for the extra length of the tailpipe is to retain enough of the hot exhaust gas within the engine at the moment the suction starts. This gas is greatly rarified by the expansion, but the outside pressure will push it back and increase its density again. Back in the chamber, this remnant of previous combustion mixes vigorously with the fresh fuel/air mixture that enters from the other side. The heat of the chamber and the free radicals in the retained gas will cause ignition and the process will repeat itself. The spark plug shown on the picture is needed only at start-up. Once the engine fires, the retained hot gas provides self-ignition and the spark plug becomes unnecessary. Indeed, if spark ignition is left on, it can interfere with the

normal functioning of the engine. The sharp transition from the intake tract into the chamber is necessary to generate strong turbulence in the incoming air, so that it mixes with injected fuel properly. A gentler, more gradual entry would not generate the necessary swirling of gases. In addition, turbulence increases the intensity of combustion and the rate of the heat release.

Advantages

- Easy to start
- No moving parts, virtually no maintenance an unlimited run time
- Can run on almost anything that burns including waste material
- Extremely large throttle range

Limitations

- Difficult to design one with really good performance
- Harder to integrate into RC vehicles

Pulsed Detonation Engine (PDE)

PDEs are an extension of pulse-jet engines, they share many similarities. However, there is one important difference between them: PDEs detonate, rather than deflagrate, their fuel. PDE's are the efficient engine that is primarily used for high-speeds (potentially Mach 5), as well as high-altitudes. A pure PDE consists of detonation tube, an inlet, and a nozzle.

Working

Pulse Detonation Engine typically consists of a sufficiently long tube which is filled with fresh fuel-oxidizer mixtures and ignited by sufficiently strong energy source. Flame initiated by ignition must in relatively short time accelerate to detonation velocity, so the transition from deflagration to detonation must happen in relatively small distance. Detonative combustion produces high pressure which is converted to thrust. After all mixture is consumed by detonation, combustion products have to be evacuated from the tube and fresh mixture must be quickly resupplied, and the cycle is repeated. Typical frequency of such engine operation is usually in range of dozen Hertz. The PDE engine follows Humphrey Cycle as depicted in figure below.

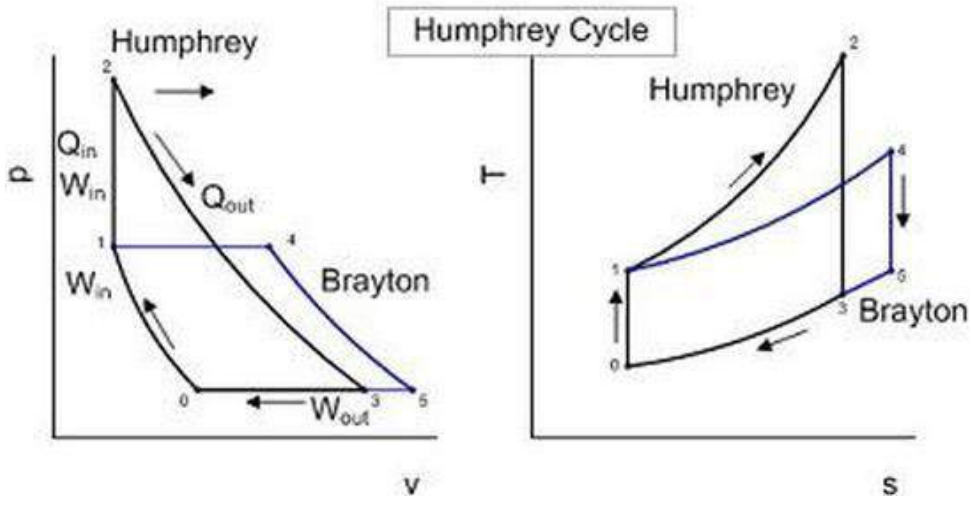

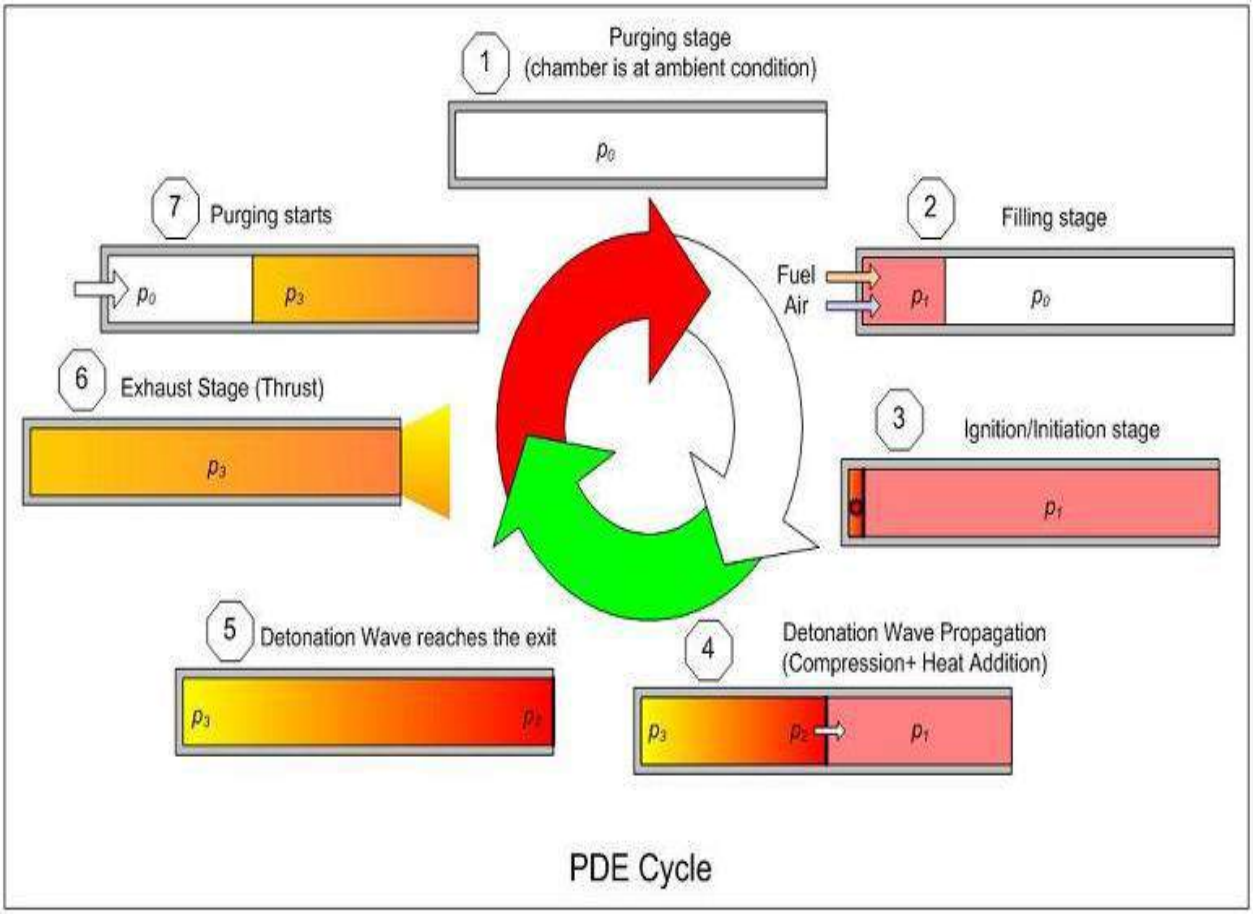

PDE can operate in wide flight Mach number, ranging from 0 and up to M4+, but the engine operates in a pulsed mode, so the thrust is varying in time and the detonation must be initiated each time. The system is complicated because fast purging and refilling are required. Also the engine is operating in the stoichiometric condition (due to necessity of fast initiation of detonation), and the frequency is relatively low. If the pulsed detonation could be applied for turbojet combustion chambers, it would be necessary to add an extra air to decrease the temperature before the first turbine stage. Also the production of NOx would be high.

A detonation may form via direct initiation or deflagration-to-detonation transition (DDT). The former mode is dependent upon an ignition source driving a blast wave of sufficient strength such that the ignitor is directly responsible for initiating the detonation. The latter case begins with a deflagration initiated by some relatively weak energy source which accelerates through interactions with its surroundings into a coupled shock wave-reaction zone structure characteristic of a detonation. Direct initiation by a concentrated source requires an extremely large energy deposition relative to deflagrative ignition. A deflagration can be ignited in a typical hydrocarbon mixture such as 1 bar stoichiometric propane-air with a 1 mJ spark, whereas direct initiation of a detonation in the same mixture requires an energy deposition of over 100 kJ. This six order of magnitude difference in ignition source energy is indicative of the general difficulty associated with employing direct initiation techniques in pulse detonation engines. On the other hand, after a small spark has created a deflagration, the transition process can take several meters or longer and a corresponding large amount of time. The key to detonation initiation schemes

applicable to pulse detonation engines is to significantly shorten the distance and time required for deflagration-to-detonation transition.

Applications

- Tactical missiles ‰
- Manned and unmanned tactical aircraft
- Decoys
- Subsonic/supersonic propulsion for hypersonic cruise
- Space launchers
- Space propulsion

Advantages

- Higher cycle efficiency
- Potentially lower SFC
- Simple architecture
- Lightweight, high T/W
- Compact
- Low cost to acquire and operate - few moving parts
- Broad operating range
- Easy integration to airframe

Limitations

- One of the factors affecting the practical implementation of PDEs is the difficulty in achieving consistent detonations within the combustion chamber, within a short tube length.
- Detonation is often difficult to initiate within fuel and air mixtures in shorter tubes, requiring the addition of large amounts of energy. DDT technique is adopted for the remedy.
- Engineering materials to withstand the immense pressures and thermal stresses caused by the blasts

Rocket Engine

A chemical rocket is a self-contained jet engine that carries both the fuel and oxidizer that are needed for combustion. The fuel and oxidizer are jointly called the *propellant.* Since the rocket carries its own oxidizer, it does not need an air inlet to provide oxygen for combustion, as in a gas turbine engine. It is this independence of rocket operation from atmospheric air that makes it a good candidate for space propulsion. The relative simplicity and manufacturing cost of a rocket engine as compared with an airbreathing jet engine have made rockets the propulsor of choice for low-cost weapons and aerospace vehicle boost applications. For example, the Space Shuttle uses two solid rocket boosters (known as SRBs) to help achieve liftoff and vehicle acceleration to orbit. The Space Shuttle also uses a liquid propellant rocket engine as its main engine, dubbed SSME or Space Shuttle Main Engine. Depending on the form of propellant that is used in combustion, a chemical rocket may be called a *liquid propellant*, a *solid propellant*, a *gaseous propellant* rocket or, if the fuel is in solid form and the oxidizer is in liquid (or gaseous) form, the rocket is called a *hybrid.* For a liquid propellant rocket, the fuel and oxidizer are stored in separate tanks in liquid form. The solid propellant rocket has the fuel and oxidizer in solid form, packed or cast in the rocket case, in the form of a paste. Since rockets operate on the principle of jet propulsion, which is achieved when a fluid is ejected through a nozzle at finite speed, the

fluid and the form of acceleration opens new categories of rocket propulsion devices. For example, if the fluid is made up of ions (of an atom, say cesium) that are accelerated in an electric field (in lieu of a nozzle), the rocket achieves a thrust and this class of rocket propulsion belongs to electric or ion propulsion.

For the case of fluid (like hydrogen) that is heated by a nuclear reactor before ejection through a nozzle, the category of engine is called a nuclear rocket propulsion device. For atmospheric applications that require stringent emissions standards, only the liquid and solid propellant rockets are suitable. These belong to the general category of *chemical rocket propulsion.* Forward (1995) presented intriguing advanced propulsion concepts (other than pure rockets) that are thought provoking and thus recommended for reading. The main drawback of rocket engines operating in the Earth's atmosphere is their high propellant consumption rate per unit thrust produced as compared to the fuel consumption rate in air-breathing engines. The figure of merit that compares rockets to air-breathing engines is the specific impulse *I*s (in seconds) that we defined in Chapter 6, repeated here for convenience:

$$I_s \equiv \frac{F}{\dot{m}_p g_0} \quad \text{(s)} \qquad (3.48)$$

Where

$$\dot{m}_p \equiv \dot{m}_f + \dot{m}_o \qquad (3.49)$$

The numerator in specific impulse is the net (uninstalled) thrust produced, which for an Air-breathing engine we derived to be (Equation 3.14)

$$F_n)_{\text{uninstalled}} = (\dot{m}_0 + \dot{m}_f)V_9 - \dot{m}_0 V_0 + (p_9 - p_0)A_9 \qquad (3.14)$$

Since, conventional rockets do not suffer from any ram drag, they produce thrust according to (Equation 3.46):

$$F_{\text{rocket}} = (\dot{m}_o + \dot{m}_f)V_9 + (p_9 - p_0)A_9 \qquad (3.46)$$

The denominator of specific impulse is the propellant weight flow rate for a rocket (i.e., the sum of oxidizer and fuel weight flow rates) and only the fuel weight flow rate for an air-breathing engine. The use of a more energetic fuel like hydrogen leads to directly higher specific impulse, since a smaller, that is, nearly two and half times lower, consumption of hydrogen is needed to achieve the same temperature in the combustor. Now, if we graph representative values for the specific impulse of typical air-breathing and rocket engines for a hydrocarbon and hydrogen fuel as a function of flight Mach number, we note the following important features:

- rocket-specific impulse is independent of vehicle speed, as it does not suffer from any ram drag penalty, nor is its combustion is affected by the stagnation temperature rise in intake
- the specific impulse for a chemical rocket is about 250–450 s
- the specific impulse for air-breathing engines is shifted upward when hydrogen is used as fuel in comparison to hydrocarbon fuels
- a gas turbine engine achieves takeoff thrust and the best low-speed performance, as depicted by a specific impulse of between ~4000 and 8000 s for a turbojet and higher than 10,000 s for a turbofan
- the specific impulse of gas turbine engines drop with flight Mach number
- the rapid fall of a gas turbine engine performance with forward speed is broken up if we switch to the ramjet family of air-breathing engines, for example, near Mach 3, a conventional ramjet starts to outperform a turbojet

- the rapid fall of a conventional ramjet engine performance with flight Mach number is halted if we switch to the supersonic combustion ramjet (or scramjet)
- the flight Mach number of ~6 is where scramjet outperforms other air-breathing engines
- deterioration of scramjet performance with forward speed is inevitable as the flight stagnation temperature increases and components losses mount
- although the upper operational Mach number of scramjets is unknown, it is suspected that for high flight Mach numbers, for example, Mach~10–15, scramjet performance may begin to fall below a chemical rocket.

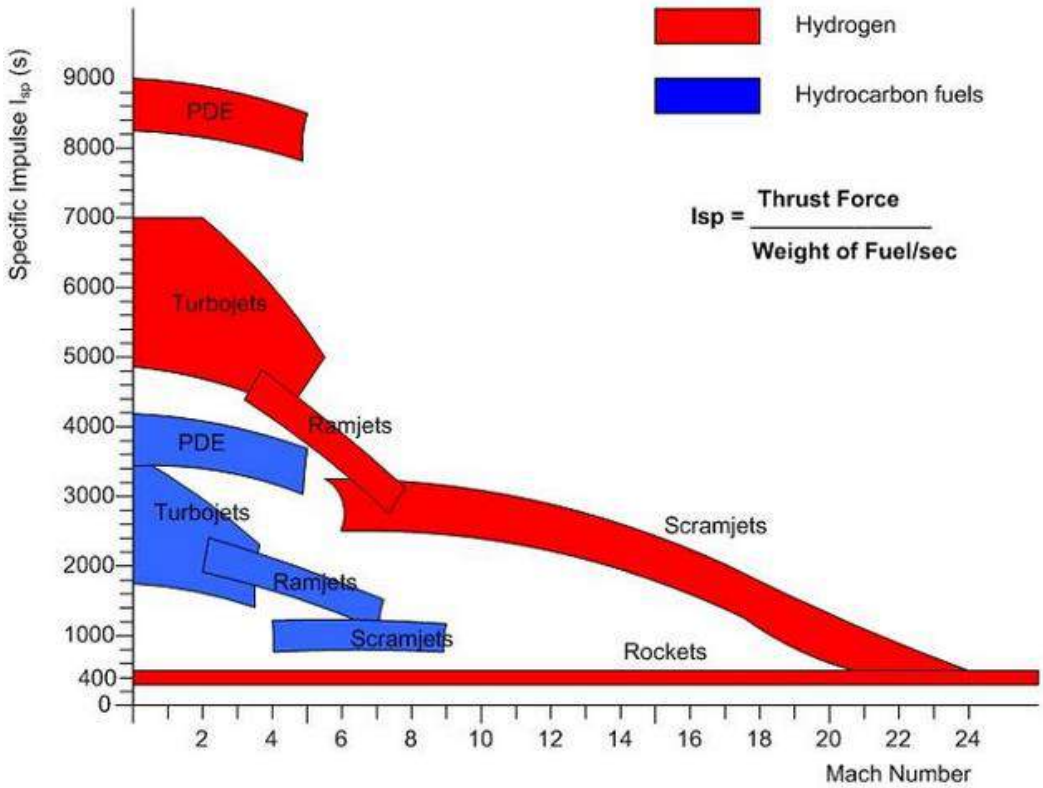

Chemical Rocket

Various components of a chemical rocket are shown in a schematic drawing in Figure 12.2. The example shown in Figure 12.2 uses liquid fuel and oxidizer as propellant. The fuel and oxidizer are stored in insulated tanks in liquid state to reduce the volumetric requirements of the propellant. The fuel and oxidizer pumps provide the propellant feed system into the combustion chamber. The pumps are driven by a turbine (not shown in the schematic drawing), therefore the name *turbopump* system. The propellant is fed into the combustion chamber through an injector plate. The pressure in the combustion chamber is ~20% lower than the feed pressure to avoid pressure oscillation instability known as chugging.

■ **FIGURE 12.2**
Schematic diagram of a (simplified) chemical rocket with liquid hydrogen as fuel and liquid oxygen (LO_2)as the oxidizer (with turbopump feed system)

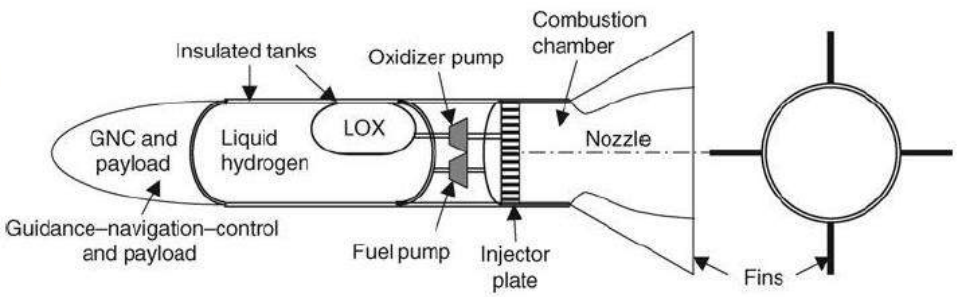

The combustion temperature is governed by the heat of reaction of the fuel and oxidizer. The products of combustion are then accelerated through an exhaust nozzle. The thrust may be controlled (to the point of shutting down and restarting) by the fuel and oxidizer pumps. The guidance, navigation, control, and payload are shown in the nose chamber. The fins provide aerodynamic control and stability of the rocket.

■ **FIGURE 12.3**
Schematic drawing of a solid-propellant chemical rocket with internal burning grain (grain designs referred to neutral, progressive, and regressive describe thrust-time behavior)

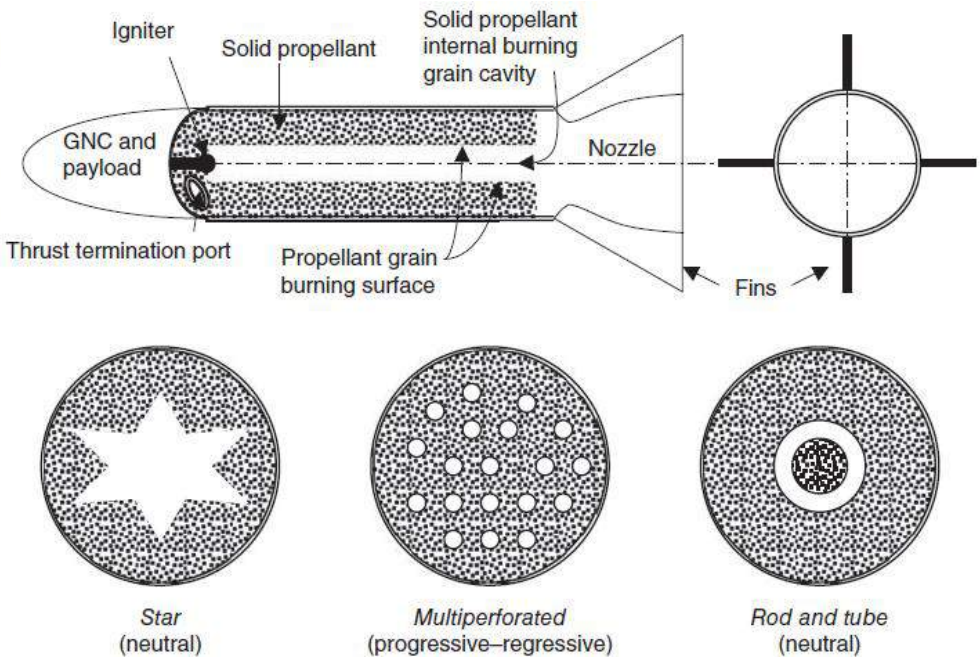

Elements of a solid rocket motor are shown in Figure 12.3. The propellant is in solid form and is called the grain or charge. Propellant is bonded to the rocket motor case, which typically has an internal burning grain cavity, as shown. The igniter initiates the burning of the solid grain. Once burning is initiated and hot gases are expelled through an exhaust nozzle, the thrust of the solid motor is established by the burning grain surface area and the propellant-burning rate. Since solid rocket motors have no pumps or valves to control the amount of propellant engaged in the combustion process, the thrust cannot be fully controlled. We can, however, terminate the operation of a solid rocket motor by opening thrust termination ports to cancel the thrust, as shown. A hybrid rocket typically uses a solid fuel and a liquid oxidizer, as shown in Figure 12.4. The oxidizer flow is regulated by the pressurized tank and a valve and injects the stream of oxidizer through a solid fuel port. The chemical reaction may be initiated by an igniter, similar to a solid propellant rocket motor. The hot combustion gases are expelled through the exhaust nozzle to produce thrust.

Application

- Launch engine
- Boost engines
- Space Maneuver Engines
- Attitude control Rockets

Concept of Hybrid Engines

A vehicle requires a flight Mach number of ~25 to achieve a circular low Earth orbit (LEO). The proof of that is very simple. On a circular orbit of radius r (which for LEO is ≥100 km above the Earth of ~6000 km radius), a vehicle of mass m experiences a centrifugal force of magnitude mV^2/r. The gravitational pull on the vehicle toward the Earth is *roughly* ~$mg0$. These two forces are in balance if the vehicle is to maintain its circular orbit, therefore,

$$V \approx \sqrt{rg_0} \approx \sqrt{6000\,\mathrm{km}\,(9.8\,\mathrm{m/s^2})} \approx 7668\,\mathrm{m/s}$$

Which for a speed of sound of ~300 m/s (at high altitude), we get a flight (or orbital) Mach number of ~25.5. The purpose of this simple demonstration was to get a *rough order of magnitude* for the Mach number required at LEO to maintain a circular orbit. We recognize that we made several approximations, for example, in the gravitational force on the vehicle when we applied $g0$ on the Earth's surface, instead of a reduced gravitational acceleration that corresponds to an altitude of 100 km, or when we did not account for any atmospheric drag at 100 km, or when we used an "average" Earth radius (of 6000 km) as in a homogeneous spherical earth.

To reach LEO and maintain a circular orbit, we need to fly about Mach 25. For a single-stage to orbit aircraft (what is known as SSTO), the engine(s) have to produce takeoff thrust, maintain climb rate, and acceleration until the vehicle has achieved Mach 25. If we wish to use the most efficient means of reaching Mach 25 from takeoff, we have to employ a variety of engines, as depicted by the specific impulse chart shown before. At takeoff, we could use a turbofan engine and gradually reduce its bypass ratio (as in a variable-bypass TF engine) with flight Mach number until it operates as a turbojet. Then, we should be able to shut down the gas generator all together near Mach 3 and switch over to a conventional (or subsonic combustion) ramjet for up to ~Mach 6. The scramjet is to take over beyond Mach 6 and accelerate the vehicle through Mach 10–15, depending on the hydrocarbon or hydrogen fuel, respectively. At these Mach numbers, we are still too slow to maintain a circular orbit at LEO. Therefore, chemical rocket engines have to be fired for the last leg of our launch, which should take the vehicle to Mach 25 and low Earth orbit. The main challenge for such a *combination propulsion system* (CPS) is complex system integration into a vehicle and the mechanical complexities involved in transition from one set or class of engines to another. The solution is, we develop a single engine having a combination of characteristics of different engines which we define as hybrid engine, or combined cycle engines, that operate with different cycle accordingly to different requirements. This class of engine is also commonly called *combined cycle propulsion system* (CCPS).

Combined Cycle Engine

An engine system whose main element is the ramjet/PDE engine (with subsonic and or supersonic combustion) that is boosted to ramjet/PDE takeover speed by means of turbo engine (turbo-accelerator) or rocket based system and that uses ramjet/PDE propulsion at the higher speeds within a single engine body are termed as combined cycle engine.

In other words, a CCPS is defined as a single propulsion system assembly that has multiple operating modes using the same propulsion subsystems (compressor, combustor, and nozzle) interchangeably throughout the flight. The first mode of operation is low speed subsystem from Mach 0 to 3, supersonic subsystem from Mach 3 to 5, hypersonic subsystem from Mach 5 to 10, and finally the rocket subsystem from Mach 10 to orbital velocity. The basic subsystems are

turbofan or turbojets, ramjets or pulsejets, and rockets. There are basically two different types of CCPS.

- Turbine Based Combined Cycle (TBCC)
- Rocket Based Combined Cycle (RBCC)

Turbine Based Combined Cycle

Turbine-based combined cycle engines operate by using a gas turbine propulsion cycle which transitions to a ramjet cycle; they bypass the turbomachinery at high Mach numbers, where pressures, temperatures, and flow velocities make such machinery impractical or redundant or both. Such a configuration by itself is not capable of orbital insertion because at some altitude the ramjet mode will lack the inlet mass flow to sustain thrust; however, TBCC engines hold strong promise for use with carrier vehicles or atmospheric ascent stages. Turbojet propulsion systems are generally limited to Mach 3 due to the rise in inlet temperature present at the compressor face; turbine engines are also in general more limited in altitude with respect to their ramjet counterparts as well. They provide more efficient operation, however, at lower altitudes and Mach numbers relative to ramjet-based engines. The limitation to lower Mach numbers and altitudes is not universal, especially if the ramjet mode is effective enough to compensate for the additional weight of the turbomachinery.

Turbine-based combined-cycle engines have seen actual flight time, a qualification which is not shared by RBCC engines. For example, the SR-71 J-58 engine is a turbine-based engine that operates in multiple cycles depending on the flight regime (with known cruise conditions of approximately Mach 3.2 at an altitude of 70,000 ft). Additionally, recent advanced hypersonic systems such as the Defense Advanced Research Projects Agency (DARPA) and USAF Force Application and Launch from the Continental United States (CONUS) (FALCON) Blackswift program have proposed using TBCC-class propulsion systems. Some turbine operation will most likely be required for a significant portion of the trajectory in order to provide system power for the operation of the vehicle. The RBCC engine, by comparison, cannot directly supply on-board power; thus, an additional auxiliary power unit or power supply would likely be necessary for such systems.

Rocket Based Combined Cycle

Rocket-based combined-cycle engines are syntheses of rocket and airbreathing propulsion systems that can operate in ejector (ducted rocket), ramjet, scramjet, and pure rocket modes. During operation in the ejector mode (suitable for ground launch), the thrust from the rocket engine is augmented by the entrained air from the ejector action of the rocket plumes flowing inside the airbreathing flowpath. The remaining three modes, listed in the order of their usually-designed phase of operation, are more well-known engine concepts, and are assumed to be largely self-explanatory. Rocket-based combined-cycle engines could be the first or intermediate stage in a multistage system for space launch. An RBCC-type engine operates in one or more airbreathing modes at altitudes low enough to provide adequate mass ingestion to use oxygen from the atmosphere, and then switches to pure rocket operation at higher altitudes and in space flight. The airbreathing mode allows the craft to avoid carrying the mass of the oxidizer that is required for ascent through the lower altitudes, and thus in theory realizes a significant propellant weight savings (and associated increased payload fraction) over pure rockets. The savings are estimated to be possibly as high as a factor of five to ten, although these claims are generally the result of modeling studies and are unverified by substantial flight data as of yet. The large savings in propellant mass are, however, counteracted by increased system dry mass.

Chapter Six
Gas Turbine Cycles of Aircraft Propulsion

Introduction

We will be discussing the various gas turbine engine variants in this chapter and their overall comparison based on engine performance characteristics. Shortly, we will be starting the engine performance characteristics basically used in the analysis and comparison of aircraft gas turbine and jet engines.

Thrust

Thrust is defined as the forward propelling force generated by the aircraft engine. We use a control volume analysis as shown in figure 3.5 to derive the thrust equation. The mass flow of air into the engine is denoted by m_0 and the intake velocity by V_0. This velocity is often taken as the aircraft flight speed. The exiting mass will be the sum of fuel and the air. i.e. m_0+m_f with a velocity V_9 through the nozzle.

■ **FIGURE 3.5**
Control volume and the mass flow rates in and out of its boundaries

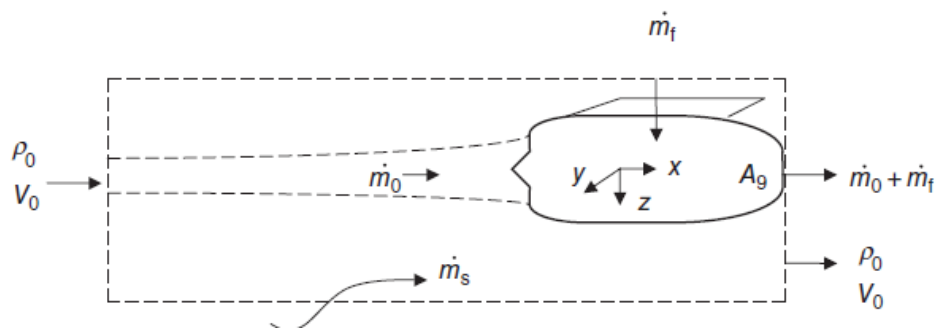

we have to use the momentum conservation principles, namely, we need to balance the fluid momentum in the *x*-direction and the resultant external forces *acting on the fluid* in the *x*-direction. Before doing that, we must establish the fluid flow rates in and out of the control volume. This is achieved by applying the law of conservation of mass to the control volume. In its simplest form, that is, steady flow case, we have

$$\sum \dot{m}_{\text{in}} = \sum \dot{m}_{\text{out}} \qquad \textbf{(3.3)}$$

Applying Equation 3.3 to the control volume surrounding our engine (Figure 3.5) gives the following bookkeeping expression on the mass flow rates in and out of the box, namely,

$$\rho_0 V_0 A + \dot{m}_s + \dot{m}_f = (\dot{m}_0 + \dot{m}_f) + \rho_0 V_0 (A - A_9) \qquad \textbf{(3.4)}$$

which simplifies to:

$$\dot{m}_s = \dot{m}_0 - \rho_0 V_0 A_9 \qquad \textbf{(3.5)}$$

Now, we are ready to apply the momentum balance to the fluid entering and leaving our control volume. Again assuming steady, uniform flow, we may use the simplest form of the momentum equation, that is,

$$\sum (\dot{m} V_x)_{\text{out}} - \sum (\dot{m} V_x)_{\text{in}} = \sum (F_x)_{\text{fluid}} \qquad \textbf{(3.6)}$$

which states that the difference between the fluid (time rate of change of) momentum out of the box and into the box is equal to the net forces acting on the fluid in the *x*-direction on the boundaries and within the box. Now, let us spell out each of the contributions to the momentum balance of Equation 3.6, that is,

$$\sum(\dot{m}V_x)_{\text{out}} = (\dot{m}_0 + \dot{m}_f)V_9 + [\rho_0 V_0(A - A_9)]V_0 \tag{3.7}$$

$$\sum(\dot{m}V_x)_{\text{in}} = (\rho_0 V_0 A)V_0 + \dot{m}_s V_0 \tag{3.8}$$

$$\sum(F_x)_{\text{fluid}} = (-F)_{\text{fluid}} - (p_9 - p_0)A_9 \tag{3.9}$$

Substituting Equations 3.7, 3.8, and 3.9 into Equation 3.6 and for $\dot{m}$s from Equation 3.5, we get

$$\begin{aligned}(\dot{m}_0 + \dot{m}_f)V_9 + \rho_0 V_0(A - A_9)V_0 - \rho_0 V_0 A V_0 - (\dot{m}_0 - \rho_0 V_0 A_9)V_0 \\ = (-F_x)_{\text{fluid}} - (p_9 - p_0)A_9\end{aligned} \tag{3.10}$$

which simplifies to

$$(\dot{m}_0 + \dot{m}_f)V_9 - \dot{m}_0 V_0 = (-F_x)_{\text{fluid}} - (p_9 - p_0)A_9 \tag{3.11}$$

Now, through the action–reaction principle of the Newtonian mechanics, we know that an equal and opposite axial force is exerted on the engine, by the fluid, that is,

$$-F_x)_{\text{fluid}} = F_x)_{\text{pylon}} = F_x)_{\text{engine}} \tag{3.12}$$

Therefore, calling the axial force of the engine "thrust," or simply F, we get the following expression for the engine thrust

$$F = (\dot{m}_0 + \dot{m}_f)V_9 - \dot{m}_0 V_0 + (p_9 - p_0)A_9 \tag{3.13}$$

This expression for the thrust is referred to as the "net uninstalled thrust" and sometimes a subscript "n" is placed on F to signify the "net" thrust. Therefore, the thrust expression of Equation 3.13 is better written as

$$\boxed{F_n)_{\text{uninstalled}} = (\dot{m}_0 + \dot{m}_f)V_9 - \dot{m}_0 V_0 + (p_9 - p_0)A_9} \tag{3.14}$$

Now, we attribute a physical meaning to the three terms on the right-hand side (RHS) of Equation 3.14, which contribute to the engine net (uninstalled) thrust. We first note that the RHS of Equation 3.14 is composed of two momentum terms and one pressure–area term. The first momentum term is the exhaust momentum through the nozzle contributing positively to the engine thrust. The second momentum term is the inlet momentum, which contributes negatively to the engine thrust in effect it represents a drag term. This drag term is called "ram drag," or simply the penalty of bringing air in the engine with a finite momentum. As we have a positive forward thrust if the exhaust were backwards, we add a negative term for intaking the air with certain intake velocity. It is often given the symbol of Dram and expressed as

$$\boxed{D_{\text{ram}} = \dot{m}_0 V_0} \tag{3.15}$$

The last term in Equation 3.14 is a pressure–area term, which acts over the nozzle exit plane, that is, area A_9, and will contribute to the engine thrust only if there is an imbalance of static pressure between the ambient and the exhaust jet. As we remember from our aerodynamic studies, a nozzle with a subsonic jet will always expand the gases to the same static pressure as the ambient condition, and a sonic or supersonic exhaust jet may or may not have the same static pressure in

its exit plane as the ambient static pressure. Depending on the "mismatch" of the static pressures, we categorized the nozzle flow as

if $p_9 < p_0$, the nozzle is *overexpanded* which can happen in supersonic jets only (i.e., in convergent–divergent nozzles with area ratio *larger* than needed for perfect expansion)

if $p_9 = p_0$, the nozzle is *perfectly expanded* which is the case for *all subsonic jets* and sometimes in sonic or supersonic jets (i.e., with the "right" nozzle area ratio)

if $p_9 > p_0$, the nozzle is *underexpanded* which can happen in sonic or supersonic jets only (i.e., with inadequate nozzle area ratio)

Examining the various contributions from Equation 3.14 to the net engine (uninstalled) thrust, we note that the thrust is the difference between the nozzle contributions (both momentum and pressure–area terms) and the inlet contribution (the momentum term). The nozzle contribution to thrust is called *gross thrust* and is given a symbol F_g, that is,

$$F_g \equiv (\dot{m}_0 + \dot{m}_f)V_9 + (p_9 - p_0)A_9 \qquad \textbf{(3.16)}$$

and, as explained earlier, the inlet contribution was negative and was called "ram drag" Dram, therefore

$$F_n)_{\text{uninstalled}} = F_g - D_{\text{ram}} \qquad \textbf{(3.17)}$$

Now, we can generalize the result expressed in Equation 3.17 to aircraft engines with more than a single stream, as, for example, the turbofan engine with separate exhausts. This task is very simple as we account for all gross thrusts produced by all the exhaust nozzles and subtract all the ram drag produced by all the air inlets to arrive at the engine uninstalled thrust, that is,

$$F_n)_{\text{uninstalled}} = \sum (F_g)_{\text{nozzles}} - \sum (D_{\text{ram}})_{\text{inlets}} \qquad \textbf{(3.18)}$$

Another way of looking at this is to balance the momentum of the exhaust stream and the inlet momentum with the pressure thrust at the nozzle exit planes and the net uninstalled thrust of the engine. In a turbofan engine, the captured airflow is typically divided into a "core" flow, where the combustion takes place, and a fan flow, where the so-called "bypass" stream of air is compressed through a fan and later expelled through a fan exhaust nozzle. This type of arrangement, that is, bypass configuration, leads to a higher overall efficiency of the engine and lower fuel consumption. A schematic drawing of the engine is shown in Figure 3.6. In this example, the inlet consists of a single (or dual) stream, and the exhaust streams are split into a primary and a fan nozzle. We may readily write the uninstalled thrust produced by the engine following the momentum principle, namely,

$$F_n)_{\text{uninstalled}} = \dot{m}_9 V_9 + \dot{m}_{19} V_{19} + (p_9 - p_0)A_9 + (p_{19} - p_0)A_{19} - \dot{m}_0 V_0 \qquad \textbf{(3.19)}$$

■ FIGURE 3.6
Schematic drawing of a turbofan engine with separate exhausts

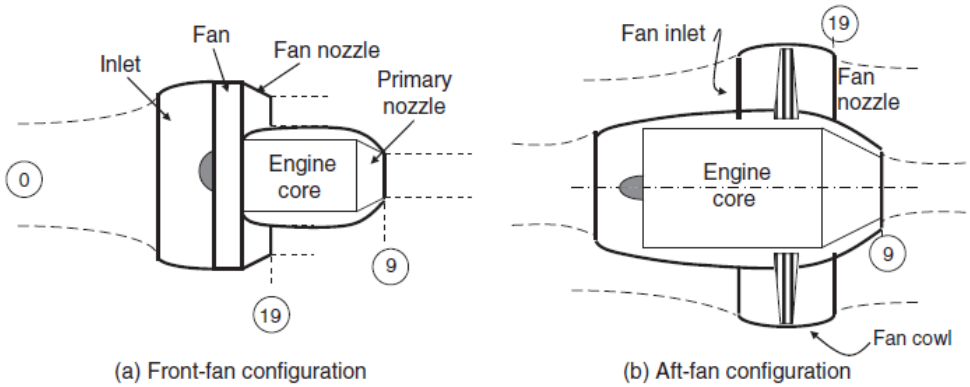

The first four terms account for the momentum and pressure thrusts of the two nozzles (what is known as gross thrust) and the last term represents the inlet ram drag.

Take-off Thrust

At takeoff, the air speed $V0$ ("flight" speed) is often ignored in the thrust calculation, therefore the ram drag contribution to engine thrust is neglected, that is,

$$F_{\text{takeoff}} \approx F_{\text{g}} = (\dot{m}_0 + \dot{m}_{\text{f}})V_9 + (p_9 - p_0)A_9 \qquad \textbf{(3.20)}$$

For a perfectly expanded nozzle, the pressure thrust term vanishes to give

$$F_{\text{takeoff}} \approx (\dot{m}_0 + \dot{m}_{\text{f}})V_9 \approx \dot{m}_0 V_9 \qquad \textbf{(3.21)}$$

Therefore, the takeoff thrust is proportional to the captured airflow.

Installed Thrust

As indicated by the description of the terms "installed thrust" and "uninstalled thrust," they refer to the *actual propulsive force* transmitted to the aircraft by the engine and the thrust produced by the engine if it had zero external losses, respectively. Therefore, for the installed thrust, we need to account for the installation losses to the thrust such as the nacelle skin friction and pressure drags that are to be included in the propulsion side of the drag bookkeeping. On the contrary, the pylon and the engine installation that affects the wing aerodynamics (in podded nacelle, wing-mounted configurations), namely by altering its "clean" drag polar characteristics, causes an "interference" drag that is accounted for in the aircraft drag polar. In the study of propulsion, we often concentrate on the engine "internal" performance, that is, the uninstalled characteristics, rather than the installed performance because the external drag of the engine installation depends not only on the engine nacelle geometry but also on the engine–airframe integration. Therefore, accurate installation drag accounting will require computational fluid dynamics (CFD) analysis and wind tunnel testing at various flight Mach numbers and engine *throttle settings*. In its simplest form, we can relate the installed and uninstalled thrust according to

$$F_{\text{installed}} = F_{\text{uninstalled}} - D_{\text{nacelle}} \qquad \textbf{(3.22)}$$

Rocket Thrust

We may think of the rocket thrust as a special case of an airbreathing engine with a "sealed inlet" ! It is simply too tempting to ignore this special case of jet propulsion with no inlet penalty. The thrust produced by a rocket engine amounts to only the *gross thrust* produced by an airbreathing

engine. We remember that the gross thrust was the *nozzle* contribution to thrust, which a rocket also possesses to accelerate the combustion gas. The air intake system is missing in a rocket, and therefore the inlet ram drag contribution is also absent from the rocket thrust equation. Consequently, we can express the rocket thrust as

$$F_{\text{rocket}} = (\dot{m}_{\text{ox}} + \dot{m}_{\text{f}})V_9 + (p_9 - p_0)A_9 \qquad \textbf{(3.46)}$$

It is interesting to note that the rocket thrust is independent of flight speed V_0, as Equation 3.46 does not explicitly involve V_0. However, if the flight trajectory has a vertical component to it, then the ambient pressure p_0 changes with altitude, and therefore the pressure thrust term of Equation 3.46 will then affect the thrust magnitude. For example, the space shuttle main engine produces about 25% more thrust in "vacuum" than at sea level, mainly due to the pressure thrust difference between sea level p_0 of 14.7 psia (or 1 atm) and p_0 of zero corresponding to "vacuum" in near earth orbit. Again, for the net propulsive force acting on the rocket, we need to account for the vehicle external drag. Although, the Equation 3.46 is not explicitly referred to as "uninstalled" thrust in rocket propulsion literature, the reader should view it as the *internal performance* of a rocket engine. The external aerodynamic analysis will produce control forces and vehicle external drag contributions.

Specific Thrust

The size of the air intake system is a design parameter that establishes the flow rate of air, $\dot{m}_0$. Accordingly, the fuel pump is responsible for setting the fuel flow rate in the engine, $\dot{m}_{\text{f}}$. Therefore, in producing thrust in a "macroengine," the engine size seems to be a "scaleable" parameter. The only exception in scaling the jet engines is the "microengines" where the component losses do not scale. In general, the magnitude of the thrust produced is directly proportional to the mass flow rates of the fluid flow through the engine. Then, it is logical to study thrust per unit mass flow rate as a figure of merit of a candidate propulsion system. In case of an airbreathing engine, the ratio of thrust to air mass flow rate is called *specific thrust* and is considered to be an engine performance parameter, that is,

Airbreathing engine performance parameter # 1:

$\dfrac{F}{\dot{m}_0}$ "specific thrust" with a metric unit of [N · s/kg] and a British unit of [lbf · s/lbm]

The target for this parameter, that is, specific thrust, in a cycle analysis is usually to be maximized, that is, to produce thrust with the least quantity of air flow rate, or equivalently to produce thrust with a minimum of engine frontal area. However, with subsonic cruise Mach numbers, the drag penalty for engine frontal area is far less severe than their counterparts in supersonic flight. Consequently, the specific thrust as a figure of merit in a commercial transport aircraft (e.g., Boeing 777 or Airbus A-340) takes a back seat to the lower fuel consumption achieved in a very large bypass ratio turbofan engine at subsonic speeds. As noted, specific thrust is a dimensional quantity with the unit of force per unit mass flow rate. A non-dimensional form of the specific thrust, which is useful for graphing purposes and engine comparisons, is

$$\text{Nondimensional specific thrust} \equiv \frac{F}{\dot{m}_0 a_0} \qquad \textbf{(3.47)}$$

where a_0 is the ambient speed of sound taken as the reference velocity.

Specific Fuel Consumption (SFC) and Specific Impulse

The ability to produce thrust with a minimum of fuel expenditure is another parameter that is considered to be a performance parameter in an engine. In the commercial world, for example, the airline business, specific fuel consumption represents perhaps the most important parameter of the engine. After all, the money spent on fuel is a major expenditure in operating an airline, for example. However, the reader is quickly reminded of the unspoken parameters of *reliability and maintainability* that have a direct impact on the cost of operating commercial engines and, therefore, they are at least as important, if not more important, as the engine-specific fuel consumption. In the military world, the engine fuel consumption parameter takes a decidedly secondary role to other aircraft performance parameters, such as stealth, agility, maneuverability, and survivability. For an airbreathing engine, the ratio of fuel flow rate per unit thrust force produced is called thrust-specific fuel consumption (TSFC), or sometimes just the specific fuel consumption (sfc) and is defined as

Airbreathing engine performance parameter # 2:

$\frac{\dot{m}_f}{F}$ "thrust-specific fuel consumption"

(TSFC) with a metric unit of [mg/s/N] and a British unit of : [lbm/h/lbf]

The target for this parameter, that is, TSFC, in a cycle analysis is to be minimized, that is, to produce thrust with a minimum of fuel expenditure. This parameter, too, is dimensional. For a rocket, on the contrary, the oxidizer as well as the fuel both contribute to the "expenditure" in the engine to produce thrust, and as such the oxidizer flow rate $\dot{m}_{ox}$ needs to be accounted for as well. The word "propellant" is used to reflect the combination of oxidizer and fuel in a liquid propellant rocket engine or a solid propellant rocket motor. It is customary to define a corresponding performance parameter in a rocket as thrust per unit propellant weight flow rate. This parameter is called *specific impulse I*s, that is,

$$I_s \equiv \frac{F}{\dot{m}_p g_0} \qquad \textbf{(3.48)}$$

Where

$$\dot{m}_p \equiv \dot{m}_f + \dot{m}_{ox} \qquad \textbf{(3.49)}$$

and $g0$ is the gravitational acceleration on the surface of the earth, that is 9.8 m/s^2 or 32.2 ft/s^2.The dimension of $\dot{m}_p g_0$ in the denominator of Equation 3.48 is then the *weight flow rate* of the propellant based on earth's gravity, or force per unit time. Consequently, the dimension of specific impulse is "Force/Force/second" which simplifies to just the "second." All propulsors, rockets, and airbreathers, then could be compared using a unifying figure of merit, namely their specific impulse in seconds. An added benefit of the specific impulse is that regardless of the units of measurement used in the analysis, that is, either metric or the British on both sides of the Atlantic, specific impulse comes out as seconds in both systems. The use of specific impulse as a unifying figure of merit is further justified in the twenty-first century as we attempt to commercialize space with potentially reusable rocket-based combined cycle (RBCC) power plants in propelling a variety of single-stage-to-orbit (SSTO) vehicles. To study advanced propulsion concepts where the mission calls for multimode propulsion units, as in air-ducted

rockets, ramjets, and scramjets, all combined into a single "package," the use of specific impulse becomes even more obvious. In summary,

$$\text{Specific impulse}: I_s \equiv \frac{F}{\dot{m}_f g_0}[\text{s}] \quad \text{for an airbreathing engine}$$

$$\text{Specific impulse}: I_s \equiv \frac{F}{\dot{m}_p g_0}[\text{s}] \quad \text{for a rocket}$$

An important goal in an engine cycle design is to maximize this parameter, that is, the ability to produce thrust with the least amount of fuel or propellant consumption in the engine.

Thermal Efficiency

The ability of an engine to convert the thermal energy inherent in the fuel (which is unleashed in a chemical reaction) to a net kinetic energy gain of the working medium is called the engine thermal efficiency, η_{th}. Symbolically, thermal efficiency is expressed as

$$\eta_{th} \equiv \frac{\Delta K\dot{E}}{\mathcal{P}_{thermal}} = \frac{\dot{m}_9 \frac{V_9^2}{2} - \dot{m}_0 \frac{V_0^2}{2}}{\dot{m}_f Q_R} = \frac{(\dot{m}_0 + \dot{m}_f)V_9^2 - \dot{m}_0 V_0^2}{2\dot{m}_f Q_R} \qquad \textbf{(3.50)}$$

where $\dot{m}$ signifies mass flow rate corresponding to stations 0 and 9, subscript "f" signifies fuel, and Q_R is the fuel heating value. The unit of QR is energy per unit mass of the fuel (e.g., kJ/kg or BTU/lbm) and is tabulated as a fuel property. Equation 3.50 compares the *mechanical power* production in the engine to the *thermal power* investment in the engine. Figure 3.19 is a definition sketch, which is a useful tool to help remember thermal efficiency definition, as it graphically depicts the energy sources in an airbreathing engine. The rate of thermal energy consumption in the engine and the rate of mechanical power production by the engine are not equal.

■ **FIGURE 3.19**
Thermal power input and the mechanical power production (output)

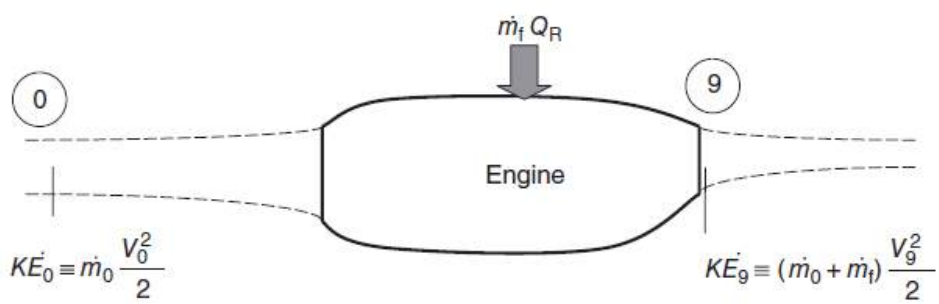

Yet, we are not violating the law of conservation of energy. The thermal energy production in an engine is not actually "lost," as it shows up in the hot jet exhaust stream, rather this energy is "wasted" and we were unable to convert it to a "useful" power. It is important to know, that is, to quantify, this inefficiency in our engine.

Propulsive Efficiency

The fraction of the net mechanical output of the engine which is converted into thrust power is called the propulsive efficiency. The net mechanical output of the engine is $\Delta \dot{KE}$ for perfectly

expanded nozzle and the thrust power is $F \cdot V_0$, therefore, the propulsive efficiency is defined as their ratio:

$$\eta_p \equiv \frac{F \cdot V_0}{\Delta K\dot{E}} \tag{3.53}$$

Although the thrust power represented by $F \cdot V_0$ in Equation 3.53 is based on the *installed* thrust, for simplicity, it is often taken as the uninstalled thrust power to highlight a very important, and at first astonishing, result about the propulsive efficiency. Now, let us substitute the uninstalled thrust of a perfectly expanded jet in the above definition to get

$$\eta_p \approx \frac{[(\dot{m}_0 + \dot{m}_f)V_9 - \dot{m}_0 V_0]V_0}{(\dot{m}_0 + \dot{m}_f)\frac{V_9^2}{2} - \dot{m}_0\frac{V_0^2}{2}} \tag{3.54}$$

We recognize that the fuel flow rate is but a small fraction (~ 2%) of the air flow rate and thus can be ignored relative to the air flow rate; thus Equation 3.54 can be simplified to

$$\eta_p \approx \frac{(V_9 - V_0)V_0}{\frac{1}{2}(V_9^2 - V_0^2)} = \frac{2V_0}{V_9 + V_0} = \frac{2}{1 + \frac{V_9}{V_0}} \tag{3.55}$$

We further note that 100% propulsive efficiency (within the context of approximation presented in the derivation) is mathematically possible and will be achieved by engines whose exhaust velocity is as fast as the flight velocity, that is, $V_9 = V_0$. But a practical question poses itself, "how can we produce thrust in an airbreathing jet engine if the jet velocity is not *faster* than the flight velocity?" The short answer is that we cannot! Therefore, we conclude that some overspeeding in the jet, compared with flight speed, is definitely needed to produce reaction thrust in an airbreathing jet engine. Therefore for practical reasons, a 100% propulsive efficiency is not possible, just as the thermal efficiency of 100% was not possible. However, the smaller the increment of velocity rises across the engine, the higher its propulsive efficiency will be. In order to achieve a small velocity increment across a gas turbine engine for a given fuel flow rate, we need to drain the thermal energy in the combustion gas further and convert it to additional shaft power that in turn can act on a larger mass flow rate of air, in a secondary or a bypass stream, for example, a fan or a propeller, to produce the desired level of thrust.

Engine Overall Efficiency

The product of the engine thermal and propulsive efficiency is called the engine overall Efficiency

$$\eta_0 \equiv \eta_{th} \cdot \eta_p = \frac{\Delta K\dot{E}}{\dot{m}_f Q_R}\frac{F \cdot V_0}{\Delta K\dot{E}} = \frac{F \cdot V_0}{\dot{m}_f Q_R} \tag{3.59}$$

The overall efficiency of an aircraft engine is therefore the fraction of the fuel thermal power that is converted into the thrust power of the aircraft. Again a useful output is compared with the input investment in this efficiency definition.

Variation of the basic Gas Turbine Engine

We will limit our discussions to following different variants of Gas Turbine Engines.

a. Turbojet Engine
b. Turbofan Engine
c. Turbo Prop Engine
d. Turbo Shaft Engine

The Turbojet Engine

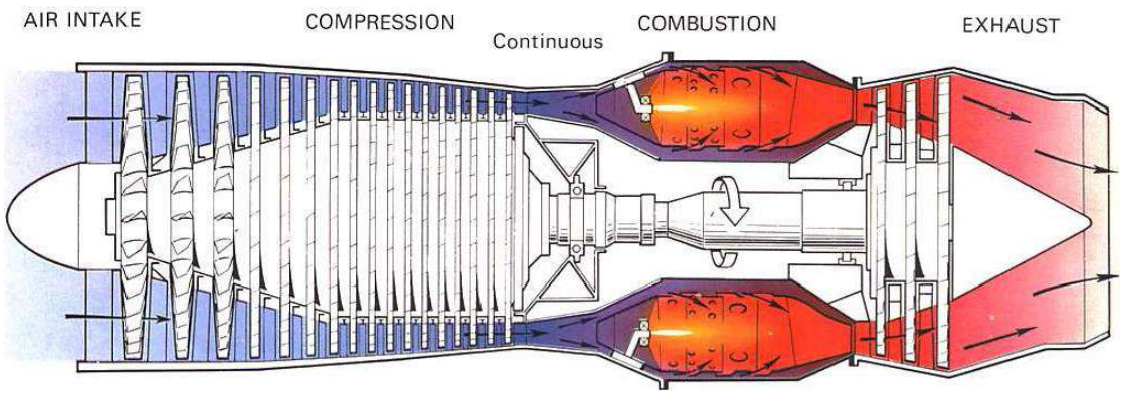

A turbojet engine is the simplest variant of a gas turbine engine which consists of an intake module, compressor, combustor, turbines and exhaust system. In most of the cases, a pure turbojet is augmented by an afterburner. We have already discussed these components in detail in chapter three. We will now move onto the performance parameters of a pure turbojet engine.

Thermal Efficiency of Turbo jet Engine

An ideal turbojet engine (with the components of inlet, gas generator, and the nozzle) is the same as an ideal Brayton cycle that we learned in thermodynamics. We remember the Brayton cycle efficiency as

$$\eta_{th} = 1 - \frac{T_0}{T_3} \qquad (4.66)$$

where T_3 is the compressor discharge temperature and $T0$ is the inlet temperature, we note that the Brayton cycle thermal efficiency improves with increasing $T3$.We can recast Equation 4.66 in terms of the compressor pressure ratio and the ram temperature ratio, as follows:

$$\eta_{th} = 1 - \frac{1}{\frac{T_3}{T_0}} = 1 - \frac{1}{\frac{T_{t3}}{T_{t2}}\frac{T_{t2}}{T_0}} = 1 - \frac{1}{\tau_c \tau_r} = 1 - \frac{1}{\pi_c^{\frac{\gamma-1}{\gamma}}\left(1 + \frac{\gamma-1}{2}M_0^2\right)} \qquad (4.67)$$

From Equation 4.67, we note that for a given flight Mach number M_0, that is, for a constant *ram* temperature ratio τ_r, the cycle thermal efficiency increases with the compressor temperature ratio τ_c. However, the higher the cycle pressure ratio, the higher the compressor discharge temperature will be, which implies the following attributes for the high-pressure compressor:

_ using turbine material in HPC
_ cooling needs of the HPC (potentially regenerative fuel cooling)
_ narrow passage (vanishing flow annulus) in HPC with large secondary flow losses.

■ **FIGURE 4.24**
Simple Brayton cycle with increasing cycle pressure ratio

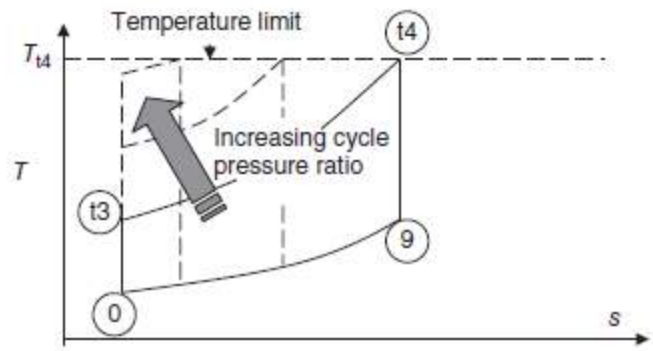

Furthermore, for a constant turbine inlet temperature T_{t4}, the cycle work output w cycle will eventually vanish in the limit of $T_{t3} = T_{t4}$. It is also interesting to note the emergence of Carnot-looking cycles with successively higher cycle pressure ratios (Figure 4.24). We remember from basic thermodynamics that a Carnot cycle operating between the temperature limits T_0 and T_4 will attain a thermal efficiency of

$$\eta_{\text{th-Carnot}} = 1 - \frac{T_0}{T_4} \tag{4.68}$$

which is the highest thermal efficiency of any heat engine operating between the temperature limits T_0 and T_4. The technology limit on compressor discharge temperature is shown in Figure 4.24 for the standard sea level condition at takeoff, that is, $M_0 \approx 0$. The information presented in Figure 4.25 identifies a limitation on the compressor pressure ratio π_c. Based on the practical limits of the compressor materials and potential cooling requirements, a compressor pressure ratio of ~40–45 seems to represent the upper limit of the current technology for the subsonic commercial aircraft gas turbine engines.

■ **FIGURE 4.25**
Influence of compressor pressure ratio on the discharge temperature T_{t3} ($M_0 = 0$, standard sea level condition)

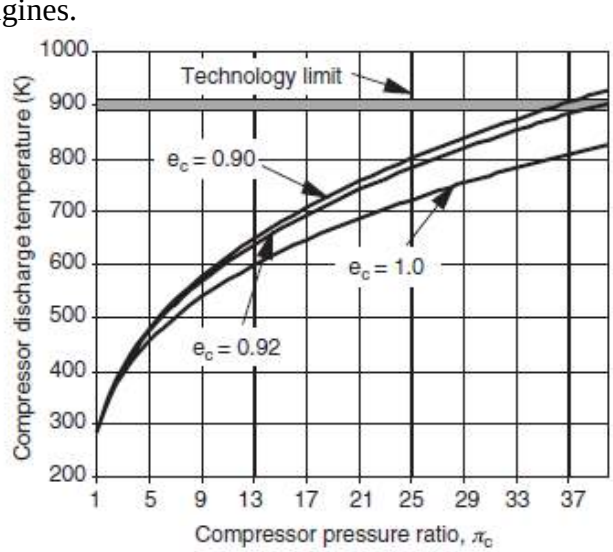

The useful portion of Equation 4.67 is repeated here for the purpose of discussion.

$$\eta_{\text{th}} = 1 - \frac{1}{\pi_c^{\frac{\gamma-1}{\gamma}}\left(1 + \frac{\gamma-1}{2}M_0^2\right)} \tag{4.67}$$

Propulsive Efficiency of a Turbojet Engine

The fraction of the net kinetic power created by the engine, which is converted into thrust power delivered to the vehicle, is called the propulsive efficiency of the engine. Symbolically, we may represent this as

$$\eta_p \equiv \frac{F \cdot V_0}{\Delta \dot{KE}} = \frac{F \cdot V_0}{\dot{m}_9 \frac{V_9^2}{2} - \dot{m}_0 \frac{V_0^2}{2}} \qquad (4.85)$$

For the thrust power expression in the numerator, we have an option of using the net *uninstalled* thrust, or include the effect of installations on the thrust and calculate the *installed* thrust power. The latter is more difficult, as it includes the throttle-dependent inlet and exhaust system drag and the engine-airframe integration. In order to simplify the calculations, the general form of the net uninstalled thrust is

$$F_{n_{uninstalled}} = \dot{m}_9 V_9 - \dot{m}_0 V_0 + (p_9 - p_0) A_9 \qquad (4.86)$$

However, if we assume a perfectly expanded nozzle, then the pressure thrust, that is, the last term in Equation 4.86, vanishes identically. Furthermore, if we neglect the small contribution of the fuel flow rate in the exhaust momentum term, the mass flow rate in the exit plane is nearly equated to the air mass flow rate, therefore,

$$F_{n_{uninstalled}} \approx \dot{m}_0 (V_9 - V_0) \qquad (4.87)$$

Now, if we substitute Equation 4.87 into Equation 4.85 and simplify, we get

$$\eta_p \cong \frac{2(V_9 - V_0)V_0}{V_9^2 - V_0^2} \cong \frac{2V_0}{V_9 + V_0} \cong \frac{2}{1 + (V_9/V_0)} \qquad (4.88)$$

in terms of only one variable, V_9/V_0, which is the ratio of the (exhaust) jet speed to the flight speed of the aircraft. The propulsive efficiency of an airbreathing aircraft engine drops inversely proportional to this velocity ratio. Also, we note that, in the limit of this velocity ratio approaching 1, the propulsive efficiency reaches 100%, that is, for $V_9/V_0 = 1$, then $\eta_p \approx 100\%$. The dilemma here is that an engine, which operates near 100% propulsive efficiency, that is, $V_9 = V_0$, cannot produce significant momentum thrust! The solution seems to be an engine that captures, that is, interacts with, large quantities of air and only imparts a small velocity jump to the flow. A turboprop or a large bypass ratio turbofan engine fit this description. The point is made, however, that for improved propulsive efficiency, the ratio of exhaust stream to flight speed needs to be slightly larger than 1. A plot of Equation 4.88 is a useful reminder of this fact and hence is shown in Figure 4.32.

■ **FIGURE 4.32**
Propulsive efficiency variation with the velocity ratio V_9/V_0

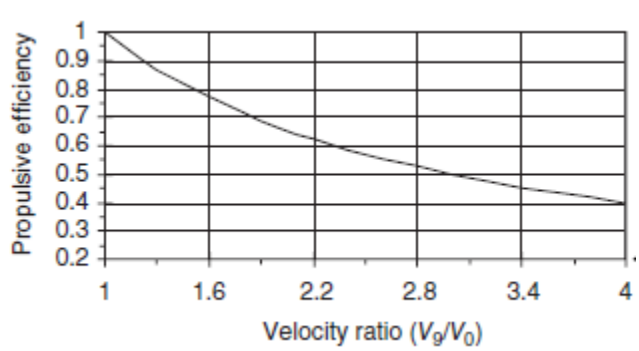

Overall Efficiency of a Turbojet Engine

The overall efficiency of a turbojet engine is defined as the product of the thermal and the propulsive efficiency of the engine, namely,

$$\eta_o \equiv \eta_{th} \cdot \eta_p = \frac{F \cdot V_0}{\dot{m}_f Q_R} \qquad (4.89)$$

which states that the fraction of thermal power invested in the engine by the fuel, which is converted into thrust power, is called the engine overall efficiency. The above equation for the overall efficiency, Equation 4.89, can be expressed in terms of specific thrust by dividing the numerator and denominator by the air mass flow rate through the engine, that is,

$$\eta_o = \frac{(F/\dot{m}_0)V_0}{fQ_R} \qquad (4.90)$$

Turbofan Engine

To create a turbofan engine, a basic gas generator is followed by an additional turbine stage(s), which tap into the exhaust stream thermal energy to provide shaft power to a fan. This arrangement of multiple loading demands on the turbine stages leads to a multiple shaft arrangement, referred to as *spools*. The fan stages and potentially several (low-pressure) compressor stages may be driven by a shaft, which is connected to the low-pressure turbine. The high-pressure compressor stages are driven by the high-pressure turbine stage(s). The rotational speeds of the two shafts are called N1 and N2, respectively, for the low- and high-pressure spools. An additional two new parameters enter our gas turbine vocabulary when we consider turbofan engines. The first is the *bypass ratio* and the second is the *fan pressure ratio*. The ratio of the flow rate in the fan *bypass duct* to that of the gas generator (i.e., the *core*) is called the bypass ratio α.

■ **FIGURE 4.39**
Schematic drawing of a separate-exhaust turbofan engine with two spools

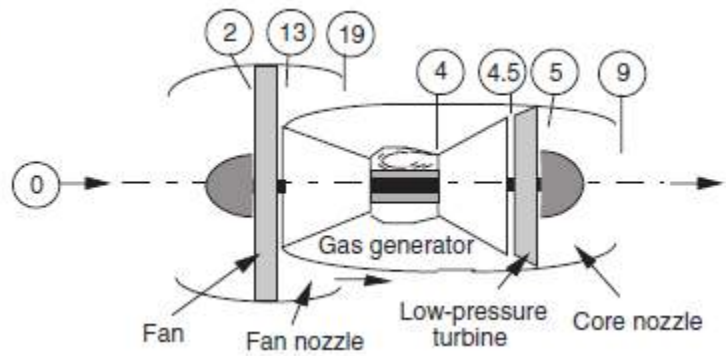

The fan pressure ratio is the ratio of total pressure at the fan exit to that of the fan inlet. It is given a symbol πf

$$\alpha \equiv \dot{m}_{\text{fan-bypass}}/\dot{m}_{\text{core}} \qquad (4.121)$$

$$\pi_f \equiv p_{t13}/p_{t2} \qquad (4.122)$$

The principle behind the turbofan concept comes from sharing the power with a larger mass flow rate of air at a smaller velocity increment pays dividend at low-speed flight. As we have seen earlier, the smaller the velocity increment across the engine, the higher the propulsive efficiency will be. This principle is Mach number independent; however, for supersonic flight the *installation drag* of large bypass ratio turbofan engines becomes excessive and, consequently, *small-frontal-area engines* are more suitable to high-speed flight. The fan exhaust stream may be

separate from the so-called *core* stream, which is then referred to as *separate exhaust turbofan engine*. Figure 4.39 shows the schematic drawing of a two-spool, separate-exhaust turbofan engine. Note that the gas generator is still the heart of this engine.

It is possible to extend the fan duct and provide mixing of the fan and the core stream in a common exhaust nozzle. The weight penalty of the long-duct turbofan engine needs to be assessed against the thrust enhancement potential of mixing a cold and hot stream in a mixer before the exhaust nozzle. The schematic drawing of this configuration is shown in Figure 4.40.

■ FIGURE 4.40
Schematic of a long-duct turbofan engine with a mixer

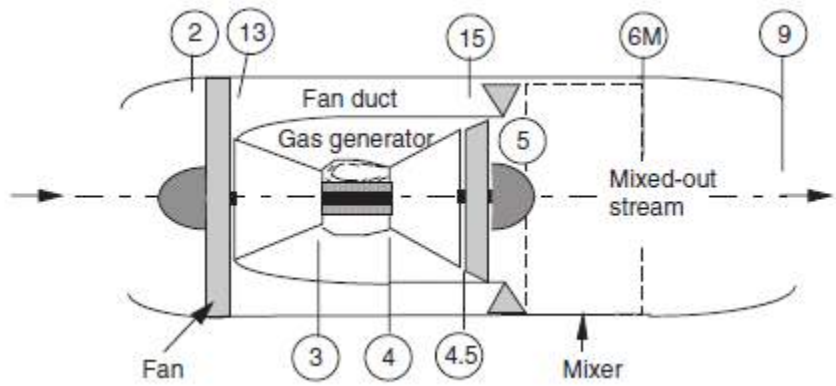

Fan Adiabatic efficiency

The fan should be treated the same way as a compressor. This short answer should suffice and it enables us to proceed with the analysis of a turbofan engine for now. As in a compressor, a fan is characterized by its pressure ratio and efficiency. We may define, in an analogous manner to the compressor, an adiabatic fan efficiency η_f or a fan polytropic efficiency e_f. Let us depict the fan compression process on an h–s diagram, as in Figure 4.41.

■ FIGURE 4.41
***h–s* diagram representing the flow process in an (adiabatic) fan**

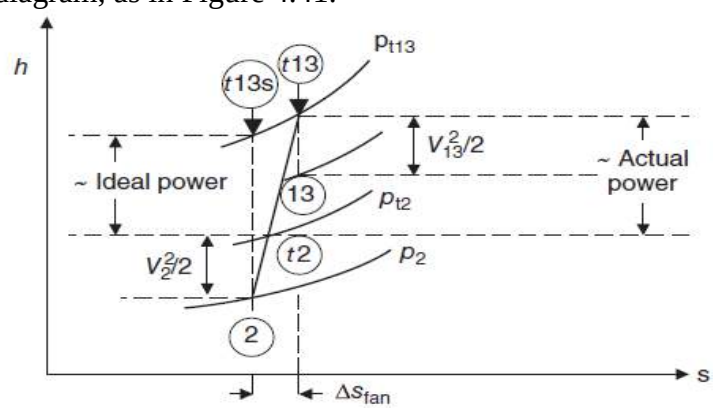

The fan adiabatic efficiency is defined as

$$\eta_f \equiv \frac{h_{t13s} - h_{t2}}{h_{t13} - h_{t2}} = \frac{\Delta h_{t,\,\text{isentropic}}}{\Delta h_{t,\,\text{actual}}} = \frac{\text{ideal power}}{\text{actual power}} \qquad \textbf{(4.123)}$$

Upon dividing the numerator and denominator of Equation 4.123 by h_{t2}, we get

$$\eta_f = \frac{T_{t13s}/T_{t2} - 1}{T_{t13}/T_{t2} - 1} = \frac{\pi_f^{\frac{\gamma-1}{\gamma}} - 1}{\tau_f - 1} \qquad \textbf{(4.124)}$$

which relates the fan pressure and temperature ratio through adiabatic fan efficiency, that is,

$$\tau_f = 1 + \frac{1}{\eta_f}\left(\pi_f^{\frac{\gamma-1}{\gamma}} - 1\right) \qquad \textbf{(4.125)}$$

$$\pi_f = \{1 + \eta_f(\tau_f - 1)\}^{\frac{\gamma}{\gamma-1}} \qquad \textbf{(4.126)}$$

Except for the subscript "*f*," the above expressions for the fan are identical to those we derived for the compressor (Equation 4.13, for example). The power balance between the turbine and compressor now includes the fan, that is, we have to write

$$\eta_m \dot{m}_0(1+f)(h_{t4} - h_{t5}) = \dot{m}_0(h_{t3} - h_{t2}) + \alpha\dot{m}_0(h_{t13} - h_{t2}) \qquad \textbf{(4.127)}$$

From the power balance equation (4.127), the core mass flow rate $\dot{m}_0$ cancels out and if we divide both sides by flight static enthalpy h_0 to non-dimensionalize the equation, we get

$$\eta_m(1+f)\frac{h_{t4}}{h_0}(1-\tau_t) = \frac{h_{t2}}{h_0}[(\tau_c - 1) + \alpha(\tau_f - 1)] \qquad \textbf{(4.128)}$$

We recognize the ratio of total enthalpy at the turbine inlet to the flight static enthalpy as τ_λ and the ratio h_{t2}/h_0 as τ_r, and we proceed to isolate τ_t and express it in terms of all the known quantities, namely

$$\tau_t = 1 - \frac{\tau_r[(\tau_c - 1) + \alpha(\tau_f - 1)]}{\eta_m(1+f)\tau_\lambda} \qquad \textbf{(4.129)}$$

$$f = \frac{\tau_\lambda - \tau_r\tau_c}{\dfrac{Q_R\eta_b}{h_0} - \tau_\lambda} \qquad \textbf{(4.130)}$$

Thermal Efficiency of Turbofan Engine

The ideal cycle thermal efficiency η_{th} is unaffected by the placement of a fan stage in a gas generator where the fan discharge is then expanded in a nozzle. The reason is that the power utilized to compress the gas in the fan is balanced by the power turbine and, therefore, the net energy exchange in the bypass duct comes from the balance of the fan inlet and the fan nozzle. A perfectly expanded nozzle will recover the kinetic energy exchange of the inlet diffuser, and thus the ideal thermal efficiency of a turbofan engine is unaffected.

Therefore, the thermal efficiency of an ideal turbofan engine is identical to a turbojet engine with the same cycle pressure ratio, hence

$$\eta_{th} = 1 - \frac{1}{\tau_r\tau_c} = 1 - \frac{1}{\left(1 + \frac{\gamma-1}{2}M_0^2\right)\pi_c^{\frac{\gamma-1}{\gamma}}} \qquad \textbf{(4.137)}$$

For the real, that is, non-ideal, turbofan engine, we start from the definition of thermal efficiency:

$$\eta_{th} \equiv \frac{\Delta KE}{\dot{m}_f Q_R} = \frac{\alpha\dot{m}_0\frac{V_{19}^2}{2} + (1+f)\dot{m}_0\frac{V_9^2}{2} - (1+\alpha)\dot{m}_0\frac{V_0^2}{2}}{\dot{m}_f Q_R} \qquad \textbf{(4.138a)}$$

$$= \frac{\alpha V_{19}^2 + (1+f)V_9^2 - (1+\alpha)V_0^2}{2fQ_R} = \frac{(1+f)V_9^2 - V_0^2}{2fQ_R} + \alpha\frac{V_{19}^2 - V_0^2}{2fQ_R}$$

The right-hand side of Equation 4.138a identifies the bypass ratio, the two exhaust velocities, the fuel-to-air ratio, the fuel heating value, and the burner efficiency as the parameters in a turbofan engine that affect the thermal efficiency of the engine. The typical unknowns, however, for the

design point analysis of a turbofan engine with a given bypass ratio and a fuel type, are the two nozzle exhaust velocities and the combustor fuel-to-air ratio. We note from the last equality in Equation 4.138a that all the bypass contribution to engine cycle thermal efficiency is lumped in the last term and the core contribution is in the first term. Ideally, the lower kinetic energy of the core due to power drainage of the fan, that is, the first term, appears as the kinetic energy rise in the bypass stream, that is, the second term. Therefore, the thermal efficiency of a turbofan engine is ideally unaffected by the magnitude of the bypass stream.

Equation 4.138a is correct for a turbofan engine with perfectly expanded nozzles. In the case that the exhaust nozzles are not perfectly expanded, we have to use *effective exhaust speeds* $V_{19\text{eff}}$ and $V_{9\text{eff}}$ in place of actual exit velocities V_{19} and V_9.We define the nozzle effective exhaust speed as

$$V_{19\text{eff}} \equiv \frac{F_{\text{g-fan}}}{\dot{m}_{19}} \qquad \textbf{(4.138b)}$$

$$V_{9\text{eff}} \equiv \frac{F_{\text{g-core}}}{\dot{m}_{9}} \qquad \textbf{(4.138c)}$$

Propulsive Efficiency of a Turbofan Engine.

The propulsive efficiency of a turbofan engine, in contrast to the thermal efficiency of such engines, is a strong function of the engine bypass ratio. Starting from the definition of propulsive efficiency

$$\eta_{\text{p}} \equiv \frac{F_{\text{n}}V_0}{\Delta K\dot{E}} = \frac{[(1+f)V_9 + \alpha V_{19} - (1+\alpha)V_0 + (p_9 - p_0)A_9 + (p_{19} - p_0)A_{19}]V_0}{(1+f)\dfrac{V_{9\text{eff}}^2}{2} + \alpha\dfrac{V_{19\text{eff}}^2}{2} - (1+\alpha)\dfrac{V_0^2}{2}} \qquad \textbf{(4.139)}$$

and assuming the nozzles are perfectly expanded and the fuel-to-air ratio f is negligible compared to 1, the above equation may be further simplified to

$$\eta_{\text{p}} \approx \frac{2V_0[V_9 + \alpha V_{19} - (1+\alpha)V_0]}{V_9^2 + \alpha V_{19}^2 - (1+\alpha)V_0^2} \qquad \textbf{(4.140)}$$

Let us recast Equation 4.140 in terms of nondimensional velocity ratios V_9/V_0 and V_{19}/V_0, by dividing the numerator and denominator of Equation 4.140 by the square of the flight velocity V^2_0 to get

$$\eta_{\text{p}} \approx \frac{2\left[\left(\dfrac{V_9}{V_0}\right) + \alpha\left(\dfrac{V_{19}}{V_0}\right) - (1+\alpha)\right]}{\left(\dfrac{V_9}{V_0}\right)^2 + \alpha\left(\dfrac{V_{19}}{V_0}\right)^2 - (1+\alpha)} \qquad \textbf{(4.141)}$$

In a turbofan engine, the propulsive efficiency seems to be influenced by three parameters, as shown in Equation 4.141, the bypass ratio α, the primary jet-to-flight velocity ratio V_9/V_0, and the fan jet-to-flight velocity ratio V_{19}/V_0. In the case that the fan nozzle velocity and the primary nozzle velocity are equal, Equation 4.141 reduces to the familiar expression we derived earlier for a turbojet, namely,

$$\eta_{\text{p}} \approx 2/(1 + V_9/V_0) \qquad \textbf{(4.142)}$$

which interestingly does not explicitly depend on the bypass ratio α! The effect of bypass ratio is implicit, however, in the exhaust velocity reduction that appears in the denominator of Equation

4.142. Again as noted earlier, if the nozzles are not perfectly expanded, we have to use the effective exhaust speeds instead of the "actual" velocities.

The Turbo Prop Engine

The turbine in the gas generator provides the shaft power to the compressor. However, we recognize that the gas in station 5 is still highly energetic (i.e., high p_t and T_t) and capable of producing shaft power, similar to a turbofan engine. Once this shaft power is produced in a follow-on turbine stage that is called "power" or "free" turbine, we can supply the shaft power to a propeller. A schematic drawing of this arrangement is shown in Figure 4.51.

■ FIGURE 4.51
Schematic drawing of a turboprop engine with station numbers identified

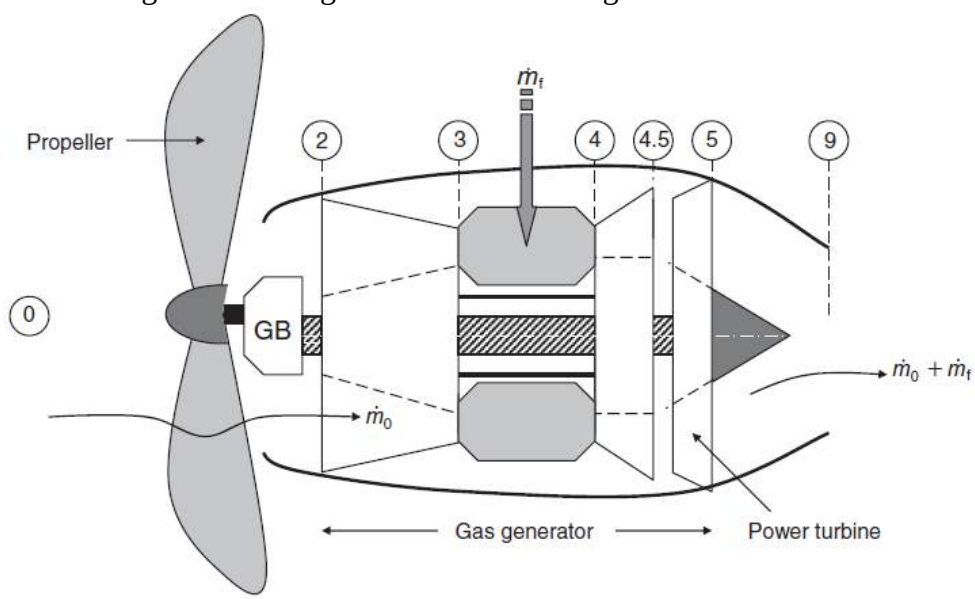

The attractiveness of a turbopropeller engine as compared with a turbofan engine lies in its ability to offer a very large bypass ratio, which may be between 30 and 100. The large bypass ratio, by necessity, will then cut back on the exhaust velocities of the propulsor, thereby attaining higher propulsive efficiencies for the engine. The high propulsive efficiency, however, comes at a price. The limitation on the tip Mach number of a rotating propeller, say to less than 1.3, leads to a cruise Mach number in the 0.7–0.8 range for advanced turboprops and to 0.4–0.6 for conventional propellers. We do not have *this limitation* on cruise Mach number in a turbofan engine. Also, the large diameter of the propeller often requires a reduction gearbox that adds to the engine weight and system complexity with its attendant reliability and maintainability issues.
We will limit our discussion only to the performance parameters of turboprop engine. The propeller theory however is not included in this chapter.

Efficiency

The propeller efficiency is different from the propulsive efficiency which can be oftenly mistaken. The propeller efficiency is defined as the fraction of propeller shaft power that is converted to the propeller thrust power.

$$\eta_{\text{prop}} \equiv \frac{F_{\text{prop}} V_0}{\mathscr{P}_{\text{p}}} \qquad \textbf{(4.212)}$$

By applying propulsive efficiency definition to the stream tube upstream and downstream of the propeller, we get:

$$\eta_p \equiv \frac{F_{prop} V_0}{\dot{m}_p \left(\frac{V_1^2}{2} - \frac{V_0^2}{2} \right)} \approx \frac{2V_0}{V_0 + V_1} \qquad \textbf{(4.213)}$$

We note that the propeller and propulsive efficiencies in Equations 4.212 and 4.213 are related to each other and indeed propulsive efficiency is the ideal limit of the propeller efficiency, since

$$\eta_{prop} \equiv \frac{F_{prop} V_0}{\mathscr{P}_p} = \left[\frac{F_{prop} V_0}{\dot{m}_p \left(\frac{V_1^2}{2} - \frac{V_0^2}{2} \right)} \right] \left[\frac{\dot{m}_p \left(\frac{V_1^2}{2} - \frac{V_0^2}{2} \right)}{\mathscr{P}_p} \right] = \eta_p \eta_L \qquad \textbf{(4.214)}$$

Where

$$\eta_L \equiv \frac{\dot{m}_p \left(\frac{V_1^2}{2} - \frac{V_0^2}{2} \right)}{\mathscr{P}_p} \qquad \textbf{(4.215)}$$

In Equation 4.215, η_L, is the efficiency of propeller in converting its shaft power into stream kinetic power. Since propulsive efficiency (Equation 4.213) is the maximum, or the limit, efficiency of a propeller, it is often times calculated and reported as the "ideal" propeller efficiency.

We can also perform analysis from a different perspective which is described in following paragraphs.

From the standpoint of power, the low-pressure turbine power is supplied to a gearbox, which somewhat diminishes it in its frictional loss mechanism in the gearing and then delivers the remaining power to the propeller.We will call the fractional delivery of shaft power through the gearbox, the *gearbox efficiency* η_{gb}, which symbolically is defined as

$$\eta_{gb} \equiv \mathscr{P}_{prop} / (\mathscr{P}_{LPT})_{gb} \qquad \textbf{(4.221)}$$

where the numerator is the power supplied to the propeller and the denominator is the shaft power provided by the power turbine to the gearbox. Also, we define the fraction of *propeller shaft power* that is converted in the *propeller thrust power* as the *propeller efficiency* η_{prop} as

$$\eta_{prop} \equiv F_{prop} \cdot V_0 / \mathscr{P}_{prop} \qquad \textbf{(4.222)}$$

Now, let us examine the overall thrust picture of a turboprop engine. We recognize that the propeller and the engine core both contribute to thrust production. We can express this fact as

$$F_{total} = F_{prop} + F_{core} \qquad \textbf{(4.223)}$$

The contribution of the engine core to the overall thrust, which we have called as the *core thrust*, takes on the familiar form of the gross thrust of the nozzle minus the ram drag of the air flow rate that enters the engine, that is,

$$F_{core} = (\dot{m}_0 + \dot{m}_f) V_9 - \dot{m}_0 V_0 + (p_9 - p_0) A_9 \qquad \textbf{(4.224)}$$

The pressure thrust contribution of the nozzle, that is, the last term in Equation 4.224, for a turboprop engine is often zero due to perfectly expended exhaust, that is, $p_9 = p_0$. So, for all practical purposes, the engine core of a turboprop produces a thrust based solely on the momentum balance between the exhaust and the intake of the engine, namely,

$$F_{core} \cong (\dot{m}_0 + \dot{m}_f) V_9 - \dot{m}_0 V_0 \qquad \textbf{(4.225)}$$

We can define the thermal efficiency of a turboprop engine as

$$\eta_{th} \equiv \frac{\wp_{prop} + \wp_{core}}{\dot{m}_f Q_R} = \frac{\left(\frac{\wp_{prop}}{\dot{m}_0} + \frac{\wp_{core}}{\dot{m}_0}\right)}{f Q_R} \qquad \textbf{(4.242)}$$

The propulsive efficiency η_p may be defined as

$$\eta_p \equiv \frac{F_{total} \cdot V_0}{\wp_{prop} + \wp_{core}} = \frac{\frac{F_{total}}{\dot{m}_0} \cdot V_0}{\left(\frac{\wp_{prop}}{\dot{m}_0} + \frac{\wp_{core}}{\dot{m}_0}\right)} \qquad \textbf{(4.243)}$$

Construction variation of Turboprop engine

There are two types of turboprop engine

- Direct-drive turboprop, and
- Free-turbine turboprop

With the direct-drive system, the propeller is connected to a shaft and turbine and the speed of the propeller is modified through a reduction gear mechanism.

In the free-turbine system, the propeller is connected to a power turbine which "floats" in the high pressure exhaust gases in the turbine section.

The free-turbine provides easier maintenance as the power section is not physically connected to the core turbine, but are less powerful by weight and less fuel efficient when compared to direct-drive turboprops

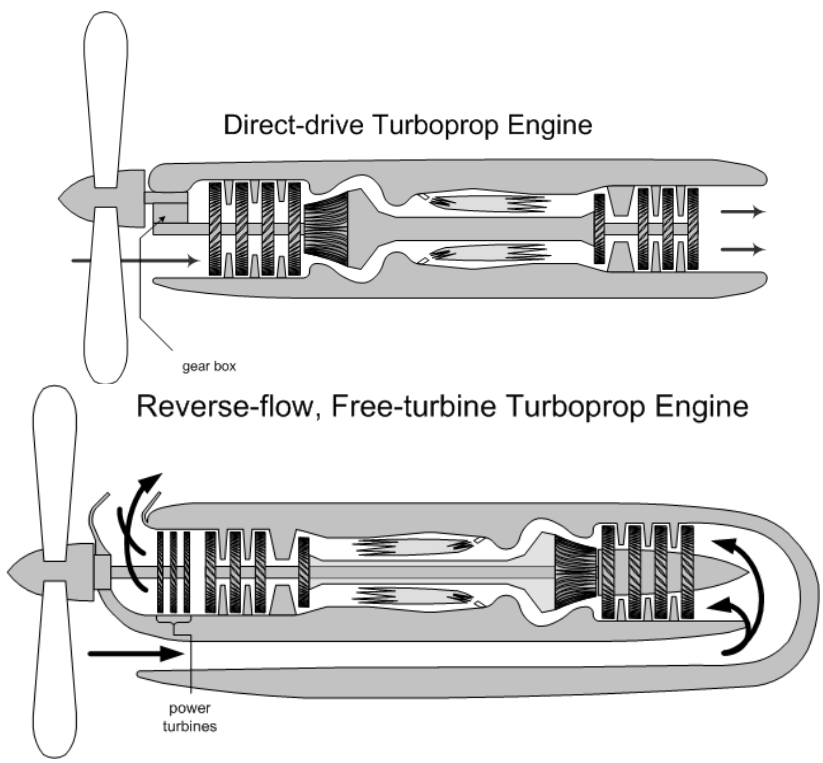

Turbo shaft Engine

A gas-turbine engine that delivers power through a shaft to operate something other than a propeller, e.g. rotor in a rotorcraft, is referred to as a turboshaft engine. The output shaft may be

coupled directly to the engine turbine, or the shaft may be driven by a turbine of its own (free turbine) located in the exhaust stream. As mentioned with the turboprop, the free turbine rotates independently. This principle is used extensively in current production of turboshaft engines. The turboshaft engine's output is measured in horsepower instead of thrust because the power output is a turning shaft.

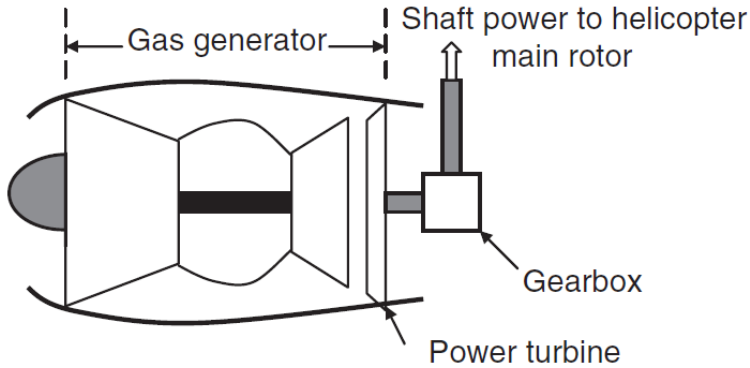

The thermal efficiency of a cycle that produces a shaft power can therefore be written as

$$\eta_{th} = \frac{\wp_{shaft} + \Delta K\dot{E}}{\dot{m}_f Q_R} \qquad (3.51)$$

In turboprops and turboshaft engines, the mechanical output of the engine is dominated by the shaft power; therefore, in the definition of the thermal efficiency of such cycles the rate of kinetic energy increase is neglected, that is,

$$\eta_{th} \equiv \frac{\wp_s}{\dot{m}_f Q_R} \quad \text{in turboprop and turboshaft engines} \qquad (3.52)$$

The propulsive efficiency of a turboshaft engine does not have any significance. However it can be calculated similarly as turbojet engine.

Comparison of Propulsive efficiency of different engines at different Mach no

Aircrafts designed to operate at sea level speeds below approximately 400 m.p.h. it is more effective to absorb the power developed in the jet engine by gearing it to a propeller instead of using it directly in the form of a pure jet stream. The disadvantage of the propeller at the higher aircraft speeds is its rapid fall off in efficiency, due to shock waves created around the propeller as the blade tip speed approaches Mach 1.0. Advanced propeller technology, however, has produced a multi-bladed, swept back design capable of turning with tip speeds in excess of Mach 1.0 without loss of propeller efficiency. By using this design of propeller in a contra-rotating configuration, thereby reducing swirl losses, a 'prop-fan' engine, with very good propulsive efficiency capable of operating efficiently at aircraft speeds in excess of 500 m.p.h. at sea level, can be produced.

To obtain good propulsive efficiencies without the use of a complex propeller system, the by-pass principle is used in various forms. With this principle, some part of the total output is provided by a jet stream other than that which passes through the engine cycle and this is energized by a fan or a varying number of LP. compressor stages. This bypass air is used to lower the mean jet temperature and velocity either by exhausting through a separate propelling nozzle, or by mixing with the turbine stream to exhaust through a common nozzle. These methods, we have already discussed in preceding chapters.

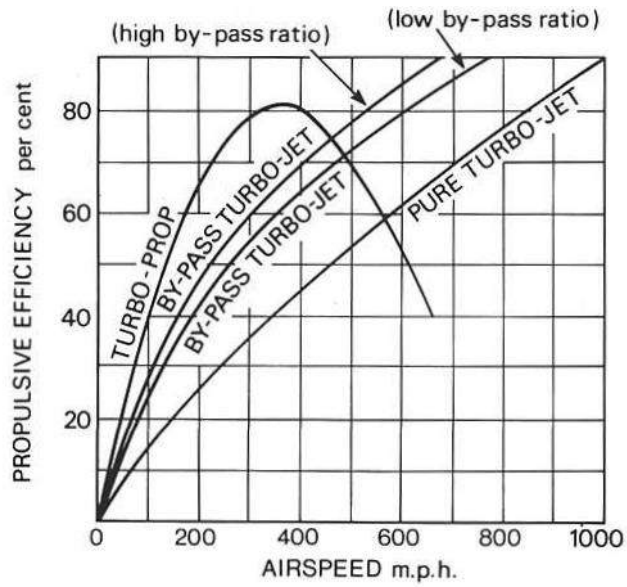

Fig. 21-9 Propulsive efficiencies and aircraft speed

Numerical

An airbreathing engine flies at Mach M_0 = 2.0 at an altitude where the ambient temperature is T_0 =−50 ^{0}C and ambient pressure is p_0 = 10 kPa. The airflow rate to the engine is 25 kg/s. The fuel flow rate is 3% of airflow rate and has a heating value of 42,800 kJ/kg. Assuming the exhaust speed is V_9 = 1050 m/s, and the nozzle is perfectly expanded, i.e., $p_9 = p_0$, calculate

(a) ram drag in kN
(b) gross thrust in kN
(c) net (uninstalled) thrust in kN
(d) thrust-specific fuel consumption in kg/h/N
(e) engine thermal efficiency η_{th}
(f) propulsive efficiency η_p
(g) engine overall efficiency η_o

A turbojet engine is shown in cruise condition. The flight condition is known to be: M_0 = 2.0, p_0 = 20 kPa, T_0 = −35◦C with γ = 1.4 and R = 287 J/kg.K. The air mass flow rate into the engine is known to be $\dot{m}_0$ = 110 kg⁄s. The fuel flow rate to the combustor is $\dot{m}_f$ = 4.2 kg⁄s with heating value Q_R = 42,800 kJ/kg. If the nozzle is perfectly expanded and the exhaust velocity is V_9 = 1,200 m/s, calculate:

(a) Ram drag, D_{ram}, in kN and lbf
(b) Gross thrust, F_g, in kN and lbf
(c) Net un-installed thrust in kN
(d) TSFC in mg/s/N and lbm/hr/lbf
(e) Engine thermal efficiency, η_{th}
(f) Propulsive efficiency, η_p